

INFORMATION TO USERS

This manuscript has been reproduced from the microfilm master. UMI films the text directly from the original or copy submitted. Thus, some thesis and dissertation copies are in typewriter face, while others may be from any type of computer printer.

The quality of this reproduction is dependent upon the quality of the copy submitted. Broken or indistinct print, colored or poor quality illustrations and photographs, print bleedthrough, substandard margins, and improper alignment can adversely affect reproduction.

In the unlikely event that the author did not send UMI a complete manuscript and there are missing pages, these will be noted. Also, if unauthorized copyright material had to be removed, a note will indicate the deletion.

Oversize materials (e.g., maps, drawings, charts) are reproduced by sectioning the original, beginning at the upper left-hand corner and continuing from left to right in equal sections with small overlaps. Each original is also photographed in one exposure and is included in reduced form at the back of the book.

Photographs included in the original manuscript have been reproduced xerographically in this copy. Higher quality 6" x 9" black and white photographic prints are available for any photographs or illustrations appearing in this copy for an additional charge. Contact UMI directly to order.

UMI

A Bell & Howell Information Company
300 North Zeeb Road, Ann Arbor MI 48106-1346 USA
313/761-4700 800/521-0600



University of Alberta

**Behavior of Lightly Prestressed Members
with Unbonded Tendons**

by

Yehia Mohamad Dahir



**A Thesis submitted to the Faculty of Graduate Studies and Research in partial
fulfillment of the requirements for the degree of Master of Science**

in

Structural Engineering

Department of Civil & Environmental Engineering

Edmonton, Alberta

Fall 1997



National Library
of Canada

Acquisitions and
Bibliographic Services

395 Wellington Street
Ottawa ON K1A 0N4
Canada

Bibliothèque nationale
du Canada

Acquisitions et
services bibliographiques

395, rue Wellington
Ottawa ON K1A 0N4
Canada

Your file Votre référence

Our file Notre référence

The author has granted a non-exclusive licence allowing the National Library of Canada to reproduce, loan, distribute or sell copies of this thesis in microform, paper or electronic formats.

L'auteur a accordé une licence non exclusive permettant à la Bibliothèque nationale du Canada de reproduire, prêter, distribuer ou vendre des copies de cette thèse sous la forme de microfiche/film, de reproduction sur papier ou sur format électronique.

The author retains ownership of the copyright in this thesis. Neither the thesis nor substantial extracts from it may be printed or otherwise reproduced without the author's permission.

L'auteur conserve la propriété du droit d'auteur qui protège cette thèse. Ni la thèse ni des extraits substantiels de celle-ci ne doivent être imprimés ou autrement reproduits sans son autorisation.

0-612-22589-5

Canada

University of Alberta

Library Release Form

Name of the Author:

Yehia Mohamad Daher

Title of Thesis:

Behavior of Lightly Prestressed

Members with Unbonded Tendons

Degree:

Master of Science

Year this Degree Granted:

1997

Permission is hereby granted to the University of Alberta Library to reproduce single copies of this thesis and to lend or sell such copies for private, scholarly, or scientific research purposes only.

The author reserves all other publication and other rights in association with the copyright in the thesis, and except as herein before provided, neither the thesis nor any substantial portion thereof may be printed or otherwise reproduced in any material from whatever without the author's prior written permission.


4022 - 32nd Avenue
Leduc, Alberta
Canada
T9E 6C9

Dated: Sept. 1 1997

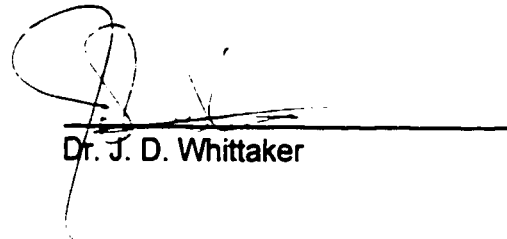
University of Alberta

Faculty of Graduate Studies and Research

The undersigned certify that they have read, and recommended to the Faculty of Graduate Studies and Research for acceptance, a thesis entitled BEHAVIOR OF LIGHTLY PRESTRESSED MEMBERS WITH UNBONDED TENDONS submitted by YEHIA MOHAMAD DAHER in partial fulfillment of the requirements for the degree of Master of Science in Structural Engineering.


Dr. D. M. Rogowsky, Supervisor


Dr. S. D. B. Alexander


Dr. J. D. Whittaker

Dated: August 29, 1997

ABSTRACT

This thesis presents an experimental investigation into the flexural behavior of lightly prestressed concrete members. While the results are applicable for new construction with high strength concrete, they are particularly valuable for the assessment of existing structures which due to corrosion has less effective reinforcement than required in current codes.

Test results of nine unbonded prestressed concrete beams and two ordinary reinforced concrete beams of rectangular cross-section, having a span to depth ratio of 14.25 are described. The effects of bonded reinforcement ratios ranging between 0% and 0.2% were investigated. Ductile behavior was achieved with less than half of the minimum bonded reinforcement required by CSA A23.3-94. The effects of concrete strength ranging from 50 MPa and 120 MPa were investigated. It was found that greater concrete strengths required more minimum reinforcement to insure ductile behavior.

A rational model that permits one to predict the entire load deflection response of unbonded prestressed members was developed. Based on experimental test results from this program and other investigators, a general equation for predicting tendon stress at ultimate is proposed.

ACKNOWLEDGMENTS

The author wishes to express his sincere gratitude and indebtedness to his research supervisor, Professor David M. Rogowsky, for his invaluable and brilliant guidance, interest and encouragement throughout this study. Professor Rogowsky's valuable comments, suggestions during the research program and his effort in reviewing the manuscript are greatly appreciated.

The technical assistance of L. Burden and R. Helfrich from the I.F. Morrison Structural Laboratory, University of Alberta, throughout the experimental program is acknowledged and appreciated.

The cement and admixture donations by Inland Cement, Lafarge Canada Inc., and Master Builders Technologies Ltd., as well as prestressing hardware donated by VSL Corporation are gratefully acknowledged.

This project was made possible through the financial assistant of the Natural Science and Engineering Research Council of Canada by a grant to Professor Rogowsky.

I greatly appreciate the patience and continuous support of my wife Andrea. This project could not have been completed without her understanding during the past two years. Her prayer and guidance gave me the strength to go on.

TABLE OF CONTENTS

CHAPTER 1 - INTRODUCTION	1
1.1 General	1
1.2 Objective and Scope	4
1.3 Organization of the Thesis	4
CHAPTER 2 - LITERATURE REVIEW	6
2.1 Introduction	6
2.2 Review of Existing Experimental Investigations Dealing With Flexural Behavior and Strength of Members Reinforced With Unbonded Tendons.	7
2.3 Code Requirements and Recommendations for Flexural Members With Unbonded Tendon.	18
2.3.1 Canadian Code Provisions.....	18
2.3.2 American Code Provisions and Recommendations.	22
2.4 Summary.....	24
CHAPTER 3 - EXPERIMENTAL PROGRAM	28
3.1 Introduction	28
3.2 Test Specimens	29
3.2.1 Beams Designation	29
3.2.2 Details of Specimens	29
3.3 Materials.....	30
3.3.1 Concrete	30
3.3.2 Prestressed Reinforcement.....	31
3.3.3 Nonprestressed Bonded Reinforcement	31
3.4 Fabrication	32
3.5 Prestressing	32
3.6 Test Set-up and Instrumentation	33
3.7 Test Procedure.....	35
3.7.1 Stroke Control Testing Procedure.....	35
3.7.2 Gravity Load Testing Procedure	35

3.8 Test Results	36
CHAPTER 4 - ANALYSIS	54
4.1 Introduction	54
4.2 Load-Deflection Relationship	55
4.3 Crack Patterns	60
4.4 Failure Modes	61
4.5 Extreme Compression Fiber Strain Measurements.....	62
4.6 Increase in Tendon Stress at Failure	63
4.7 Prediction of the Increase in Stress at Ultimate Using Collapse Mechanism.....	64
4.8 Prediction Model of Load-Deflection Relationship.....	66
4.9 Comparison of Test Results With the Current Codes.....	69
CHAPTER 5 - CONCLUSIONS	103
5.1 Summary.....	103
5.2 Conclusions.....	104
5.3 Recommendations for Future Research	106
APPENDIX A: Listing of Test Data.....	111
APPENDIX B: Complete Set of Predicted and Actual Load-Deflection Curves	148
APPENDIX C: Calculation Example of Load-Deflection Curve Prediction	163

LIST OF TABLES

Table	Page
2.1 Summary of Various Canadian Code Requirements for Members	
Reinforced with Unbonded Tendons.....	26
2.2 Summary of Various American Code Requirements for Members	
Reinforced with Unbonded Tendons.....	27
3.1 Specimen Properties	38
3.2 Concrete Mix Proportions	39
3.3 Concrete Strength	40
3.4 Reinforcement Properties	41
3.4 Test Results	42
4.1 Comparison of the Increase in Prestressing Steel Stress from	
Tests, CSA- A23.3, and ACI 318-95.	71
4.2 Comparison of Proposed Equations, CSA , and ACI for Increase in	
Prestressing Steel Stress at Ultimate.....	72
4.3 Comparison of Proposed Equations, CSA, and ACI for Ultimate	
Moment Capacity	74

LIST OF FIGURES

Number	Page
Fig. 3.1 Test Specimens.....	43
Fig. 3.2 Typical Stress-Strain Curve for 50 MPa Concrete	44
Fig. 3.3 Typical Stress-Strain Curve for 100 MPa Concrete.....	45
Fig. 3.4 Typical Stress-Strain Curve for Prestress Reinforcement	46
Fig. 3.5 Typical Stress-Strain Curve for Nonprestress Reinforcement ...	47
Fig. 3.6 View of Reinforcing Steel Cage in the Wooden Form	48
Fig. 3.7 Prestressing Set-up at Both Ends of the Beam	49
Fig. 3.8 Loading Frame for Stroke Controlled Test.....	50
Fig. 3.9 Loading Frame for Gravity Load Test	50
Fig. 3.10 Gravity Load Test Set-Up.....	51
Fig. 3.11 View of Gravity Loads Used in The Test.....	52
Fig. 3.12 Demec Gage Point Layout	53
Fig. 4.1 Idealized Member Response for Lightly Prestressed Unbonded Concrete Flexural Members.....	76
Fig. 4.2 Applied Load vs Deflection For Beams, R-1, R-2, and R-3	77
Fig. 4.3 Applied Load vs Deflection For Beams, R-4, and R-5	78
Fig. 4.4 Applied Load vs Deflection For Beams, R-2, and R-5	79
Fig. 4.5 Applied Load vs Deflection For Beams, R-3, and RH-3	80
Fig. 4.6 Applied Load vs Deflection For Beam, RH-1, and R3 [Ospina]... 81	81
Fig. 4.7 Applied Load vs Deflection For Beams, RH-2, RH-3 and, RH-4 .	82
Fig. 4.8 Applied Load vs Deflection For Beams, R-6, and RH-7	83
Fig. 4.9 Crack Patterns Developed in Test Beams.....	84
Fig. 4.10 Crack Development of Specimens R-3, and RH-1	86
Fig. 4.11 Failure Modes For All Test Specimens	87
Fig. 4.12 Variation in Concrete Compression Strain in the Top Fibers	93
Fig. 4.13 Applied Load vs Increase in Strand Stress R-1, R-2 and R-3	96

Fig. 4.14 Applied Load vs Increase in Strand Stress RH-2, RH-3 and RH-4	97
Fig. 4.15 Increase in Strand Stress vs Deflection	98
Fig. 4.16 The Sum of Crack Width vs Deflection	99
Fig. 4.17 Typical Collapse Mechanism for Unbonded Prestressed Beam	100
Fig. 4.18 Predicted Load vs Deflection Curve For Beam, R-1.....	101
Fig. 4.19 Predicted Load vs Deflection Curve For Beam, R-4.....	102
Appendix B: Actual and Predicted Load-Deflection Curves for all Beams.....	148

NOTATION

- a depth of equivalent rectangular stress block
- A area of that part of cross section between flexural tension face and centroid of gross section
- A_s area of nonprestressed bonded tension reinforcement
- A_p area of prestressing tendons in tension
- b width of the member
- c distance from extreme compression fiber to neutral axis calculated using factored material strengths and assuming a tendon force of $f_p A_p$
- c_y distance from extreme compression fiber to neutral axis calculated using factored material strengths and assuming a tendon force of $A_p f_{py}$
- d distance from extreme compression fiber to the centroid of longitudinal nonprestressed tension reinforcement, but need not be less than 0.8h for prestressed members
- d_p distance from the extreme compression fiber to the centroid of the prestressing tendons
- f'_c specified compressive strength of concrete
- $\sqrt{f'_c}$ square root of specified compressive strength of concrete
- f_{cr} modulus of rupture of concrete used in deflection and cracking moment calculations
- f_{pe} effective stress in prestressing tendons (after allowance for all prestress losses)
- f_{pr} stress in prestressing tendons at factored resistance
- f_{pu} tensile strength of prestressed reinforcement
- f_{py} yield strength of prestressed reinforcement

f_y	yield strength of nonprestressed tension reinforcement
h	overall height or thickness of member
I	moment of inertia of section about centroidal axis
l_1	length between the support and the first point load
l_e	length of tendon between anchors divided by the number of plastic hinges required to develop a failure mechanism in the span under consideration
L	span length
M_r	factored moment resistance
M_s	moment due to specified loads
M_d	moment due to dead loads
M_l	moment due to live loads
PPR	partial prestressing ratio, ratio of prestress force to total force in nonprestressed and prestressed reinforcement
α_1	ratio of average stress in rectangular compression stress block to the specified concrete strength
β_1	ratio of depth of rectangular compression stress block to the neutral axis depth
Δf_p	increase in tendon stress corresponding to a given applied load or deflection
Δf_{pr}	increase in tendon stress at ultimate
δ	deflection corresponding to a given applied load
δ_c	deflection corresponding to the cracking load
ϕ_c	resistance factor for concrete
ϕ_p	resistance factor for prestressed reinforcement
ϕ_s	resistance factor for nonprestressed reinforcement

λ factor to account for low density concrete

$$\rho = A_s/bd$$

$$\rho_p = A_p/bd_p$$

$$\rho' = A'_s/bd$$

$$\omega \text{ combined reinforcing index} = \rho_p f_{pe}/f'_c + \rho f_y/f'_c$$

$$\omega_p \text{ prestressed reinforcement reinforcing index} = \rho_p f_{pe}/f'_c$$

$$\omega_s \text{ nonprestressed reinforcement reinforcing index} = \rho f_y/f'_c$$

CHAPTER 1

INTRODUCTION

1.1 General

Unbonded post-tensioning is one of many types of prestressing in which strand, wires, or bars are tensioned after hardening of the concrete. The most commonly used type of unbonded tendon in building construction consists of a strand that is greased and placed inside a plastic sheath. The prestressing force is transferred to the concrete through the end anchorages, which are mechanical devices with bearing plates and wedge grips called chucks. This type of tendon is known as a "monostrand".

Unbonded post-tensioning has been used in Canada since the 1960's in cast-in-place construction. The advantages provided by post-tensioning include: reduced structural element dimensions, virtually crack-free members, control of deflection, longer spans, and improved economy. It is estimated that there are currently more than 1000 buildings in Canada with this type of reinforcement.

In recent years, the durability of monostrand structures has become an issue of concern. This issue is addressed by Schupack (1991), Kesner et al. (1996), and others. Some buildings have experienced corrosion and failure of the tendons. The loss in the effective prestress due to corrosion reduces the factor of safety and may make the structure "unsafe" under current code requirements. It

should be noted that code requirements are formulated for new construction rather than for evaluation of existing structures.

If the reinforcement is kept constant, but the concrete strength is increased, the member will behave as if it more lightly reinforced. The growing demands for high quality concrete and concrete structures with high durability have lead to the increased use of high strength concrete. Design codes and standards are usually conservative and tend to restrict the use of new material until substantial data and experience has been accumulated. The results of early research on conventional concrete are not necessarily applicable to high strength concrete because, in part, the high concrete strength tends to make members behave as if they are lightly reinforced.

There is a need to study the behavior of lightly prestressed members. This will assist in the assessment of deteriorating structures, and in the estimation of reinforcement required in new construction with high strength concrete.

Abeles (1981) introduced and developed the concept of partial prestressing. He recommended ten principles which are applicable not only to prestressed concrete, but to any endeavor that an engineer is called upon to undertake:

1. You cannot have everything. (Each solution has advantages and disadvantages that have to be tallied and traded off against each other.)
2. You cannot have something for nothing. (One has to pay in one way or another for something that is offered, as a "free gift" into the bargain, not without standing a solution being optimal for the problem.)

3. It is never too late. (e.g., to alter a design, to strengthen a structure before it collapses, or to adjust or even change principles previously employed in the light of increased knowledge and experience.)
4. There is no progress without considered risk. (While it is important to ensure sufficient safety, over-conservatism can never lead to increased understanding or novel structures.)
5. The proof of the pudding is in the eating. (This is in direct connection with the previous principle indicating the necessity of tests.)
6. Simplicity is always an advantage, but beware of oversimplification. (The latter may lead to theoretical calculations which are not always correct in practice, or to a failure to cover all conditions.)
7. Do not generalize, but rather qualify the specific circumstances. (Serious misunderstandings may be caused by unreserved generalizations.)
8. The important question is how good, not how cheap an item is. (A cheap price given by an inexperienced contractor usually results in bad work; similarly, cheap, unproved appliances may have to be replaced.)
9. We live and learn. (It is always possible to increase one's knowledge and experience.)
10. There is nothing completely new. (Nothing is achieved instantaneously, but only through step-by-step development.)

Engineers should follow these recommendations in their practical life in order to guarantee excellent performance and economy. This thesis will use these ten principles to create practical solutions.

1.2 Objective and Scope

The primary objective of this project is to study the behaviour of lightly prestressed members with unbonded tendons, and to estimate the minimum amount of nonprestressed bonded reinforcement required to produce ductile behavior. Both intermediate (50 MPa) and high strength (100 MPa) concrete are considered. The minimum bonded reinforcement requirements of A23.3 -94 (1994) and ACI 318-95 (1995) will be evaluated in the light of the research findings.

The scope of this investigation was limited to a review of the literature, and tests of 11 rectangular simply supported beams. The principle variables involved in this investigation were concrete strength, and the amount of prestressed unbonded and nonprestressed bonded reinforcement. An analytical model was developed and validated against the test results.

1.3 Organization of the Thesis

This thesis consists of five chapters and three appendices.

Chapter 2 presents a review of the literature on prestressed members with unbonded tendons.

In Chapter 3, the experimental phase of this study is described. Details of specimens, fabrication, material properties, instrumentation and testing procedure are provided. In addition, the test results are reported in this chapter.

Chapter 4 consists of an evaluation of the test results, and describes the development of a model that predicts the behaviour of the specimens. The analytical model explains the influence of each of the primary variables.

In Chapter 5, a summary of the significant results and conclusions, together with recommendations for future research are given.

In Appendix A, the test data are presented in tablular form. A complete set of actual and predicted load-deflection response curves is presented in Appendix B. Example calculations for predicting a load-deflection curve are presented in Appendix C.

CHAPTER 2

LITERATURE REVIEW

2.1 Introduction

This chapter reviews the technical literature regarding flexural members reinforced with unbonded tendons. Unbonded post-tensioning as we know it today is a relatively recent innovation. The relevant literature begins in 1960. First, experimental investigations and selected theoretical studies that deal with beams and one-way slabs are reviewed to establish the primary factors that influence flexural behavior. This is followed by a review of the requirements contained in design codes and guides to good practice that were used in Canada and The United States of America during the same period. Deficiencies in the codes and guides are summarized in the light of today's knowledge. The understanding of the deficiencies is useful when assessing existing structures because it identifies possible problems. Finally, the gaps and deficiencies in the experimental database that prevent updating of current code requirements are summarized. The most important gaps and deficiencies will be the focus of the experimental work contained in this thesis.

Where appropriate, equations are given in SI and customary American units. The notation follows A23.3-94 as much as possible.

2.2 Review of Existing Experimental Investigations Dealing With Flexural Behavior and Strength of Members Reinforced With Unbonded Tendons.

Warwaruk, Sozen and Siess (1962) tested a total of 82 simply supported beams. This discussion is limited to the 41 specimens that were reinforced with unbonded tendons. The beams had span-to-depth ratios ranging from 13.8 to 15.2. The main variables were the strength of concrete (10 MPa to 52 MPa), and the amount of unbonded reinforcement (0.183% to 0.979%). Some of the beams failed without large deflections ($\delta/L=1/274$) because the concrete compression zone crushed or spalled before the reinforcement yielded. One beam that was very lightly reinforced ($\rho=0$, $\rho_p=0.19\%$) also failed in a brittle manner because the cracking moment of the concrete was larger than the ultimate moment capacity of the section. This test highlighted the need for a minimum amount of bonded reinforcement to ensure ductile behavior. No loss of load capacity at the time of cracking was observed for any beam with bonded prestressed or non-prestressed reinforcement ($\rho = 0.22\%$). The stress in the unbonded reinforcement remained in the elastic range up to failure. Warwaruk et al. proposed the following equation for predicting the tendon stress at ultimate when $f_{pe} \geq 0.6f_{pu}$.

$$f_{pr} = f_{pe} + (30,000 - \frac{\rho_p}{f_c'} \times 10^{10}) \text{ psi} \quad (2.1a)$$

$$f_{pr} = f_{pe} + (207 - 4.76 \frac{\rho_p}{f_c'} \times 10^5) \text{ MPa} \quad (2.1b)$$

Burns and Pierce (1967) tested three beams that were continuous over two equal spans. The beams had a double-tee cross section and a span-to-depth ratios between 15 and 22. The main variables were the amounts of prestressed and nonprestressed reinforcement and the effective prestress f_{pe} . While the increase in tendon stress due to external loads was not reported, some of their observations and conclusion are of interest. Additional bonded reinforcement ($\rho' = 0.92\%$) in the compression zone led to additional rotational capacity of 21.7%, and a somewhat longer cracking zone near the interior support. If properly detailed to prevent shear failure, a continuous beam would develop "plastic hinges" at the points of peak moment before reaching ultimate load capacity.

Pannell (1969) carried out an experimental study to determine the effect of unbonded reinforcement ratio, span-to-depth ratio, and effective initial prestress (80%, 50%, and 30% of f_{pu}) on the ultimate flexural capacity. A total of 38 simply supported beams with unbonded tendons were tested in three sets having L/d of 27, 40, and 12 respectively. He concluded that the greatest ultimate capacity was obtained from beams with a moderately high unbonded prestressed steel ratio and the highest possible initial prestress. Specimens with a prestressed reinforcement index $\omega_p = \rho_p f_{pe} / f'_c$ of 0.12 exhibited a much greater capacity for plastic rotation than the beams with ω_p of 0.24. The range of increased rotational capacity was not reported. He also concluded that L/d should be considered in determining f_{pr} . Based on his experimental results, strain compatibility and equilibrium, he derived the following equation.

$$f_{pr} = f_{pe} + \frac{f'_c \left[\left(\frac{A_p f_{pe}}{bd_p f'_c} \right) + \lambda \right]}{\rho_p L + \frac{\lambda}{\alpha}} \quad (2.2)$$

$$\text{With } \lambda = \frac{\psi \rho_p \varepsilon_{cu} E_p d_p}{L f'_c} \quad (2.3)$$

Where:

ε_{cu} = the strain in the concrete top fiber at ultimate

$\psi = 10.5$

$\alpha = 0.85\beta_1$

β_1 = the stress block factor as defined by ACI 318-95

Rozvany and Woods (1969) studied the behavior of unbonded prestressed beams and slabs which exhibit a sudden drop in the load-deflection curve at flexural cracking. A theoretical explanation of this problem was given. Experimental verification was presented using the test results of 26 unbonded beams tested by Warwaruk et al. (1962) and 16 unbonded simply supported beams, having L/d of 24, subjected to a concentrated load at midspan. They found that sudden collapse could be avoided by making the average concrete stress due to prestressing greater than the modulus of rupture. This is not a very attractive solution since it requires a substantial amount of prestressed reinforcement.

Hemakon (1970) and Gebre-Michael (1970) reported test results from five one-way slabs continuous over two spans with $L/d=45.1$. The average initial

precompression in the concrete varied from 2.4 to 4.9 MPa. Primary variables were the amount of prestressed reinforcement ($\rho_p=0.253$ to 0.507%), and the pattern of loading (one-span loading versus two-span loading). Loading was by means of a single point load applied at a distance 0.4L away from the center support. They found that the values of Δf_{pr} for one-span loading were as much as fifty percent lower than for two-span loading. The value of Δf_{pr} varied inversely with the percentage of prestressed reinforcement and directly with the compressive strength of the concrete. They also found that the level of initial stress in the tendon did not affect the value of Δf_{pr} . It should be noted that the tendons never reached yield in any of their tests.

Chen (1971) tested two one-way slabs, with $L/d=30$, which were continuous over two equal spans and prestressed with unbonded tendons. The major variables in the test series were the pattern and sequence of loading (single span versus two-span loading), and the amounts of prestressed and non-prestressed reinforcement. He found that the values of Δf_{pr} for two-span loading were significantly higher than those for single span loading. For single span loading, the measured Δf_{pr} were higher than the values predicted by the 1963 ACI Code, but were in close agreement with the values predicted by the ACI 318-71 and A23.3-94. Bonded reinforcement ($\rho = 0.275\%$) served effectively in the distribution of cracks and enhanced the ultimate moment capacity of the member.

Mattock, Yamazaki and Kattula (1971) conducted an experimental study on three simply supported rectangular beams, three simply supported T-beams, and two T-beams continuous over two equal spans. The beams had a fixed span-to-depth ratio of 33.6, and were subjected to four loading points on each span in order to approximate a uniformly distributed load. The primary variables were the presence or absence of bond, the amount of prestressed unbonded reinforcement ($\rho_p = 0.551\%$) and nonprestressed bonded reinforcement ($\rho = 0.3$ to 0.56%). They found that f_{pr} for unbonded tendons as predicted by ACI 318-63 was approximately 30 percent less than that obtained from experiments. As the ratio $\omega_p = \rho_p f_{pe} / f'_c$ increased, the margin between predicted and observed f_{pr} decreased. They concluded that ACI 318-71 satisfactorily reflected the behavior of unbonded tendons for simply supported beams. Beams containing unbonded tendons and additional nonprestressed bonded reinforcement exhibited ductility and cracking patterns comparable to beams with bonded tendons. In continuous beams, compression reinforcement near the center support was required to allow complete redistribution of moment, and attainment of higher value of Δf_{pr} . A minimum 0.004A of nonprestressed tension reinforcement was recommended for beams when unbonded tendons are used. They showed that both the ACI 318-71 and the equation (2.1) proposed by Warwaruk et. al. (1962) were too conservative at low reinforcement ratios. They proposed the following equation:

$$f_{pr} = f_{pe} + \frac{1.4f'_c}{\rho_p} + 10,000 \text{ psi} \quad (2.4a)$$

$$f_{pr} = f_{pe} + \frac{1.4f'_c}{\rho_p} + 70 \text{ MPa} \quad (2.4b)$$

Tam and Pannell (1976) tested eight simply supported beams reinforced with unbonded tendons subjected to a single concentrated load at midspan. The main variables were: the amount of prestressed (0.51% to 1.02%) and non-prestressed reinforcement (0.58% to 1.67%); the span-to-depth ratio that ranged from 20 to 45, and the initial prestress that ranged from 650 to 950 MPa (approximately 0.4 to 0.6 of the ultimate tensile strength of the tendon). They observed that all beams developed fine cracks similar to those developed in beams containing prestressed bonded reinforcement. Based on their observations, they modified the prediction equation for f_{pr} presented by Pannell (Eq. 2.3) to account for the effect of nonprestressed reinforcement as follows.

$$f_{pr} = f_{pe} + \frac{f'_c \left[\left(\frac{A_p f_{pe}}{bd_p f'_c} \right) + \lambda - \left(\frac{A_s f_y}{bd_p f'_c} \right) \lambda \right]}{\rho_p \left[L + \frac{\lambda}{\alpha} \right] - \frac{\lambda}{\alpha + \lambda}} \quad (2.5)$$

Burns, Charney and Vines (1978) tested two half scale models of a prototype one-way slab, continuous over three equal spans, having a span-to-depth ratio of 44. The main variables were the amount of nonprestressed reinforcement (0 and 0.23%), tension stress in concrete at service load, the level of prestressing (average precompression in the concrete), and pattern of loading. The unbonded prestressed reinforcement ratios were 0.098% and 0.12%. They found that when determining f_{pr} one must consider the L/d ratio, the loading

arrangement, and consequent plastic hinge pattern at failure. They found a nearly linear relationship between tendon stress increase and deflection. At ultimate, the change in tendon stress for the case of two loaded spans was nearly double that of a single loaded span. The increase in tendon stress at ultimate did not reach the value predicted by ACI 318-77.

Cooke, Park and Yong (1981) tested nine simply supported fully prestressed one-way slabs with unbonded tendons to study the effect of the span-to-depth ratio and the amount of prestressing steel on the stress at ultimate in the unbonded tendons. The slabs were subdivided into three groups with L /d ratios of 20, 30, and 40, each group had a prestressing steel index $\omega_p = \rho_p f_{pe}/f'_c$ of 0.025, 0.125, and 0.25 respectively. They found that the equation for f_{pr} in unbonded tendons given in ACI 318-77 over estimated the stress in prestressing steel at low values of the reinforcing index ($\omega_p = 0.025$) by 2.4, 8.7, and 11.6 percent for slabs having L/d ratios of 20, 30, and 40, respectively. Their result showed that the equation proposed by Warwaruk, Sozen, and Siess (1962) and Pannell (1969) conservatively predict f_{pr} . Flexural instability (a large drop in stiffness at cracking), which occurs in members containing low amounts of prestressing steel can be prevented by using additional bonded nonprestressed reinforcement. They recommended that when ω_p is less than 0.11 bonded nonprestressed reinforcement should be present. They also recommended the use of ACI 318-63 Code equation for predicting the stress in unbonded tendons at ultimate.

Elzanaty and Nilson (1982) studied the effect of varying the amount of the initial prestressing force on the flexural strength of unbonded post-tensioned beams. They tested eight small-scale models in two series: under-reinforced (U series) and over-reinforced (O series). They concluded that beams of both series U and series O showed excellent ductility at failure ($\delta /L > 1/87$). They found that increasing the level of initial tendon stress increased the ultimate moment capacity especially in series O, since Δf_{pr} remained constant for all four beams of this series. Bonded reinforcement was effective in distributing the cracks. The ACI 318-77 equation for predicting f_{pr} was conservative for series O but unconservative for series U. They pointed out the need to change the provision of the ACI 318 for computing f_{pr} for unbonded tendons to include several factors such as the span-to-depth ratio, depth of the neutral axis, nonprestressed bonded reinforcement, and material properties of concrete and steel.

Trost, Cordes and Weller (1984) tested four beams continuous over two spans and having rectangular or T-shaped cross section with a span-to-depth ratio of 32. They concluded that the factors influencing the increase in stress in unbonded tendons at ultimate were the strength of concrete and the prestressing force applied to the member. They found that the span-to-depth ratio did not effect the value of Δf_{pr} . The presence of nonprestressed bonded reinforcement guaranteed satisfactory crack patterns and ductile behavior ($\delta/L > 1/48$). The change in tendon stress was proportional to the sum of the deflections at the critical sections.

Du and Tao (1985) carried out an experimental investigation to show the significance of non prestressed bonded reinforcement and its effect on the value of f_{pr} at ultimate. They tested 22 prestressed simply supported beams with unbonded tendons under third-point loading. The span-to-depth ratio was kept constant at 19.1, while the compressive strength of the concrete (33 MPa to 42 MPa), the unbonded prestressed reinforcement ($\rho_p = 0.11\% \text{ to } 0.45\%$) and bonded non prestressed reinforcement ($\rho = 0.39\% \text{ to } 2.01\%$) were varied. Based on their experimental observations, Du and Tao proposed an equation for predicting the stress at ultimate that accounts for the presence of non-prestressed reinforcement. In their discussion of that equation, they indicated that Δf_{pr} can be computed from the moment-curvature relationship, but they did not clarify the underlying assumptions used in their analysis and how the relation was obtained. They proposed the following equation to predict the stress in unbonded tendons at ultimate:

$$f_{pr} = f_{pe} + 114 - \frac{278.46}{bd_s f'_c} (A_s f_y + A_p f_{pe}) \text{ ksi} \quad (2.6a)$$

$$f_{pr} = f_{pe} + 786 - \frac{1920}{bd_s f'_c} (A_s f_y + A_p f_{pe}) \text{ MPa} \quad (2.6b)$$

provided that:

$$\omega = \left(\frac{A_s f_y + A_p f_{pe}}{bd f'_c} \right) \leq 0.3 \quad (2.7a)$$

$$0.55 f_{py} \leq f_{pe} \leq 0.65 f_{py} \quad \text{and} \quad f_{pr} \leq f_{py} \quad (2.7b)$$

Chouinard (1989) tested six prestressed simply supported concrete beams with unbonded tendons with third-point loading, and a span-to-depth ratio

of 15. The only variable was the amount of nonprestressed bonded reinforcement ($\rho = 0$ to 2.44%). Five of the beams were over-reinforced. It was observed that the addition of high amounts of nonprestressed bonded reinforcement reduced the value of f_{pr} . It should be noted that the beams failed when the compression zone capacity was exceeded (over-reinforced) rather than when the tensile reinforcement yielded. This explains the reduction in f_{pr} . Chouinard, observed that the strain distribution in the concrete at the level of the prestressing reinforcement was more uniformly distributed along the member and multiple fine cracks occurred when nonprestressed bonded reinforcement was present. For beams with no nonprestressed bonded reinforcement, the concrete strains were not uniform along the member. Very high concrete strains developed near the cracks in the midspan section where only one or two wide cracks formed. The extent of strain and cracking gave an indication of the spread of the plasticity zone along the beam top fiber.

Harajli and Kanj (1990) conducted an experimental and analytical investigation that included the testing of 26 prestressed simply supported concrete beams with unbonded tendons. The main variables were the reinforcing index, the span-to-depth ratio, and loading type (one or two concentrated loads). They concluded that the length of the plastic hinge at ultimate is as important as the effect of span-to-depth ratio on f_{pr} . The effect of loading type was found to be insignificant. They also concluded that the parameter ρ_p / f'_c which is the basis of Eq.(18-4) and (18-5) of ACI 318-83, is not a rational design parameter.

Chakrabarti, Whang, Brown, Arsal, and Amezeua (1993) investigated 33 beams with unbonded tendons. Four groups of beams were tested with the following variables studied: different combinations of prestressed and non-prestressed reinforcement, T-beams and rectangular beams, normal and high strength concrete, different initial stresses in the tendons, and high and low ratios of L/d. Based on test observations and load-deflection plots, they concluded that a very high value (1.00) of PPR ($PPR = A_p f_{pr} / (A_p f_{pr} + A_s f_y)$) caused sudden large cracking in the tension zone of the beam. A very high value (0.3) of $\omega = \rho_p f_{pe} / f'_c + \rho f_y / f'_c$ caused crushing of the compression zone of the specimens. In both T-beams and rectangular beams some improvement in strength and deflection control was observed with high-strength concrete when ω and PPR were maintained within an optimum range ($0.1 < \omega < 0.25$, and $0.25 < PPR < 0.70$). When L/d exceeded 35, post-cracking behavior and deflection control were greatly improved with a small amount of additional nonprestressed bonded reinforcement ($\rho = 0.22\%$). A further addition of nonprestressed bonded reinforcement improved the strength but did not improve the ductility or ultimate stress in the strand. For specimens with L/d > 35, Δf_{pr} was very low and almost half of that found in members with a small amount of nonprestressed bonded reinforcement. As the L/d ratio decreased the load carrying capacity of members with additional nonprestressed bonded reinforcement increased, but when there was no nonprestressed bonded reinforcement the L/d ratio did not seem to make a significant difference. The magnitude of the initial stress, f_{pe} , in the tendon did not have a pronounced effect on the overall beam behavior. However, as values

of f_{pe} increased, Δf_{pr} was reduced. It should be noted that all the members were over-reinforced so the conclusions are not necessarily applicable to typical members.

2.3 Code Requirements and Recommendations for Flexural Members With Unbonded Tendon

2.3.1 Canadian Code Provisions

The first Canadian code for the design of prestressed concrete appears to be A135 (1962).

The use of nonprestressed bonded reinforcement in conjunction with prestressed reinforcement was permitted in A135-1962. Bonded reinforcement was not required when there was no tensile stress in the precompressed tensile zone under service loads. An amount of nonprestressed reinforcement equal to 10 percent of tendons area was required when the tensile stress was less than or equal to $0.5 \sqrt{f_c}$. Statically determinate members with unbonded prestressing were required to have bonded nonprestressed reinforcement. The ultimate strength required was the greater of $1.8D + 1.8L$ or $1.2 D + 2.4 L$ with no strength reduction factors ϕ . This is significantly more capacity than required by current codes. The prediction equation for stress in tendon at ultimate was:

$f_{pr} = f_{pe} + 105$ MPa which is conservative for members with a span-to-depth ratio less than or equal to 40. The first version of A23.3 to include prestressed concrete members was A23.3-1973. Both A23.3-1973 and A23.3-M77

required a minimum amount of nonprestressed bonded reinforcement A_s in beams and one-way slabs equal to:

$$A_s = \frac{N_c}{0.5f_y} \quad (2.8a)$$

or

$$A_s = 0.004A \quad (2.8b)$$

which ever is larger, where:

A = area of that part of the cross-section between the flexural tension face and the center of gravity of the gross section

N_c = tensile force in the concrete under a load of $D+1.2L$

f_y should not exceed 400 MPa.,

The allowable concrete tensile stress under service loads was $0.5\sqrt{f'_c}$.

The ultimate strength required was $1.4D + 1.7L$ with a member strength reduction factor $\phi = 0.9$. The prediction equation for stress in a tendon at ultimate was changed to include f'_c and ρ_p as follows:

$$f_{pr} = f_{pe} + 70 + \frac{f'_c}{100\rho_p} \quad (2.9)$$

but not greater than $f_{pe} + 414$ MPa

This requirement remained in effect until A23.3-84 with permitted one to exceed the concrete tensile stress limit ($0.5\sqrt{f'_c}$) provided that analysis or tests demonstrate adequate fatigue resistance as well as adequate deflection and crack control under specified loads. In addition, A23.3-84 required a minimum area of bonded, nonprestressed reinforcement for beams and one-way slabs.

These minimum reinforcement requirements were 0.004A, for fully prestressed members i.e. tensile stress $\leq 0.5\sqrt{f'_c}$ MPa, and 0.005A for prestressed members were tensile stress $\geq 0.5\sqrt{f'_c}$ MPa. The ultimate strength required was 1.25D + 1.5L with material factors $\phi_c=0.6$, $\phi_s=0.85$, and $\phi_p=0.9$ for concrete, nonprestressed bonded reinforcement, and prestressed reinforcement respectively. The prediction equation for stress in a tendon at ultimate was changed to include the effect of nonprestressed bonded reinforcement and the number of plastic hinges in multiple continuous spans

$$f_{pr} = f_{pe} + \frac{5000}{l_e} (d_p - c_y) \text{ MPa} \quad (2.10)$$

The requirements of minimum nonprestressed bonded reinforcement for one-way slabs have been changed in the current CSA A23.3-94 to 0.003A and 0.004A for tensile stresses below and above $0.5\sqrt{f'_c}$ respectively. This amount of bonded flexural reinforcement must be distributed to provide adequate crack control.

The flexural strength requirement in the current code is that the factored flexural resistance, M_r , of the member must be equal or greater than the factored moment, M_f , due to external loads, $M_f = 1.25M_D + 1.5M_L$. The factored moment resistance, M_r , of the beam is provided by a couple consisting of a tensile force provided by the reinforcement (both prestressed and nonprestressed) and the compression force in the concrete near the top face of the beam.

$$M_r = \phi_p A_p f_{pr} (d_p - a/2) + \phi_s A_s f_y (d - a/2) + \phi' A'_s f_y (d' - a/2) \quad (2.11)$$

where:

$$a = \beta_1 c = (\phi_p A_p f_{pr} + \phi_s A_s f_y + \phi_s' A_s' f_y') / (\alpha_1 \phi_c f'_c b)$$

$\phi_c = 0.6$, $\phi_s = 0.85$, and $\phi_p = 0.90$ are the concrete, steel, and prestress material factors respectively.

$$\alpha_1 = 0.85 - 0.0015f'_c \geq 0.67 \quad (2.12a)$$

$$\beta_1 = 0.97 - 0.0025f'_c \geq 0.67 \quad (2.12b)$$

As well as providing adequate flexural capacity, the member must have sufficient ductility to provide warning of impending failure. The member will have a ductile response if it possesses adequate post-cracking capacity and if steel "yields" prior to crushing of the concrete. To ensure adequate post-cracking capacity, A135-1962 Code provisions required that the factored flexural resistance, M_r , be at least 20 percent greater than the cracking moment, M_{cr} . A23.3-84 waived this requirement if the factored flexural resistance of the section is one-third greater than M_r . These requirements exist in A23.3-94. To satisfy this requirement it may sometimes be necessary to add a minimum amount of non-prestressed reinforcement. To insure yield of reinforcement, the code requires that the depth of the compression zone, c , not exceed one-half of the section depth, h .

The prediction equation of the stress in the tendon at ultimate according to current provision of CSA A23.3-94 is:

$$f_{pr} = f_{pe} + \frac{8000}{l_e} (d_p - c_y) \text{ MPa} \quad (2.13)$$

$$f_{pr} \leq f_{py}$$

2.3.2 American Code Provisions and Recommendations

The first recommendations for prestressed concrete in the United States were published by ACI-ASCE committee 323 (1958). These recommendations permitted service load concrete tensile stresses of $0.5\sqrt{f'_c}$ with further provision that this tensile stress may be exceeded provided it is shown by tests that the structure will behave properly under service conditions and meet any necessary requirement for cracking load or temporary over load. The first code to appear was ACI 318-63. The ultimate strength required was $1.5D + 1.8L$ with a member strength reduction factor $\phi=0.9$. ACI 318-63 required the factored resistance be at least 1.2 times the cracking moment based on a modulus of rupture $f_r = 0.6\sqrt{f'_c}$. The prediction equation for stress in the tendon at ultimate was:

$$f_{pr} = f_{pe} + 105 \text{ MPa} \quad (2.14)$$

ACI-ASCE 423-69 recommended that an amount of bonded reinforcement $A_s = N_c / 0.5f_y$ must be provided for crack control.

ACI 318-71 permitted tensile stresses up to $1.0\sqrt{f'_c}$ provided that immediate and long-term deflections based on a cracked section and analysis were acceptable and provided that the concrete cover was increased by 50% for members exposed to earth, weather or corrosive environment. Because the tendons were unbonded, concern arose regarding the structural safety of such systems in the event of multiple tendon failures. To prevent such an occurrence, ACI 318-71 introduced provisions for minimum amounts of bonded nonprestressed reinforcement for structures using unbonded tendons. This

reinforcement was, and still is based on $0.004A$, where A is the area of that part of cross section between the flexural tension face and center of gravity of gross section. The ultimate strength required was and still is $1.4D + 1.7L$ with a member strength reduction factor $\phi=0.9$. The prediction equation for stress in the tendon at ultimate was:

$$f_{pr} = f_{pe} + 70 + \frac{f'_c}{100\rho_p} \quad (2.15)$$

but not greater than $f_{pe} + 414$ MPa.

In one-way slabs, economical use of the minimum bonded reinforcement leads to the use of design tensile stresses in the range of $0.75\sqrt{f'_c}$ to $1.0\sqrt{f'_c}$. ACI318-83 section 18.8.3 permits waiving of the requirement for factored resistance at least 1.2 times the cracking load for members with shear and flexural strength at least twice that required by section 9.2, i.e. $(2M_f, 2V_f)$. An upper limit for the minimum reinforcement of "at least one-third greater than required by analysis" has appeared in section 10.5 since ACI 318-63.

ACI-ASCE 423 (1983) recommended that Committee 318 waive the minimum reinforcement requirement of Section 18.8.3 (1.2 times the cracking load) for one-way slabs with unbonded tendons, considering the fact that unbonded tendons do not yield or rupture at cracking.

The current code requirements for strength and ductility is still the same as in ACI 318-83. The required strength according to the current ACI Code is expressed in terms of factored load or internal moment and forces. Factored moments are the loads specified in the general building code multiplied by

appropriate load factors, e.g. $M_r = 1.4M_o + 1.7M_u$ for dead and live load only. The ultimate moment resistance, is the nominal strength calculated in according with these provisions multiplied by a member performance factor $\phi = 0.90$.

$$M_r = \phi M_n = \phi \{ A_p f_{pr} (d_p - a/2) + A_s f_y (d - a/2) + A'_s f_y (d' - a/2) \} \quad (2.16)$$

where

$$a = \beta_1 c = (A_p f_{pr} + A_s f_y - A'_s f_y) / 0.85 f'_c b$$

$$f_{pr} = f_{pe} + 70 + \frac{f'_c}{\mu \rho_p} \text{ MPa} \quad (2.17)$$

for both provisions ACI 318-89 and ACI 318-95

where:

$$\mu = 100 \text{ for } L/d \leq 35, \text{ and } \mu = 300 \text{ for } L/d > 35.$$

2.4 Summary

The important points from this literature review can be summarized as follows:

1. There have been significant differences between codes at the ultimate limit state. See Tables 2.1 and 2.2.
2. There has been little difference between codes at the serviceability limit state. See Tables 2.1 and 2.2.
3. There have been significant differences between codes for ρ minimum.
4. Most research has been on heavily prestressed members.
5. There is little research on lightly prestressed members with unbonded tendons. Tests with less than minimum code reinforcement are required to

validate analytical models of deteriorated structures where prestress has been lost due to corrosion of tendons.

6. There is little research on high strength concrete members with unbonded tendons. More tests with concrete strength greater than 50 MPa are required to establish member behavior.
7. The parameters that effect the prestressing steel stress at ultimate as well as the actual behavior of the prestressed member are:
 - 1) Initial effective stress in the tendon immediately before testing. The greater the initial stress the greater the tendon stress at ultimate strength.
 - 2) Amount of prestressed reinforcement. It affects member strength and ductility.
 - 3) Span-to-depth ratio. Tendon stress at ultimate decreases as span-to-depth ratio increases.
 - 4) Amount of supplementary nonprestressed bonded reinforcement. It increases the strength, crack distribution, and member ductility.

While there are others, these are the most important parameters.

8. The ACI 318-95 equation for predicting f_{pr} is applicable for fully prestressed unbonded members, it does not account for most of the important parameters.
9. The CSA-A23.3-94 is the most comprehensive equation for f_{pr} , but it does not account for all parameters.
10. A more comprehensive analytical model that accounts for the four most important parameters is required.

Table 2.1: Summary of Various Provisions of Canadian Code Requirements for Members Reinforced With Unbonded Tendons

Title of the standard	A135 (1982)	A23.3-73	A23.3-M77	A23.3-M84	A23.3-94
Admissible stresses	<ul style="list-style-type: none"> • prestressing steel: <ul style="list-style-type: none"> -At stressing: $0.80 f_{pu}$ -Under service load: $0.60 f_{pu}$ • concrete: Admissible tensile stresses • concrete: Admissible tensile stresses -partially-prestressed : $0.5 \sqrt{f'_c}$ -fully-prestressed: $0.5 \sqrt{f'_c}$ -fully-prestressed: 0 	<ul style="list-style-type: none"> • prestressing steel: <ul style="list-style-type: none"> -At stressing: $0.80 f_{pu}$ -Under service load: $0.60 f_{pu}$ • concrete: Admissible tensile stresses -partially-prestressed : $0.5 \sqrt{f'_c}$ -fully-prestressed: $0.5 \sqrt{f'_c}$ 	<ul style="list-style-type: none"> • prestressing steel: <ul style="list-style-type: none"> -At stressing: $0.85 f_{pu}$ -Under service load: $0.74 f_{pu}$ • concrete: Admissible tensile stresses -partially-prestressed : $0.5 \sqrt{f'_c}$ -fully-prestressed: $0.5 \sqrt{f'_c}$ 	<ul style="list-style-type: none"> • prestressing steel: <ul style="list-style-type: none"> -At stressing: $0.80 f_{pu}$ -Under service load: $0.74 f_{pu}$ • concrete: Admissible tensile stresses -partially-prestressed : $0.5 \sqrt{f'_c}$ -fully-prestressed: $0.5 \sqrt{f'_c}$ 	<ul style="list-style-type: none"> • prestressing steel: <ul style="list-style-type: none"> -At stressing: $0.85 f_{pu}$ -Under service load: $0.74 f_{pu}$ • concrete: Admissible tensile stresses -partially-prestressed : $0.5 \sqrt{f'_c}$ -fully-prestressed: $0.5 \sqrt{f'_c}$
Ultimate limit state (MPa)	<ul style="list-style-type: none"> • Stress at ultimate <ul style="list-style-type: none"> $f_{pr} = f_{pe} + 105$ $f_{pe} \leq 0.6 f_{pu}$ $f_{pr} \leq f_{py}$ and $f_{pr} \leq f_{pe} + 414$ 	<ul style="list-style-type: none"> • Stress at ultimate <ul style="list-style-type: none"> $f_{pr} = f_{pe} + 70 + \frac{f_c}{100 p_p}$ $f_{pr} \leq f_{py}$ and $f_{pr} \leq f_{pe} + 414$ 	<ul style="list-style-type: none"> • Stress at ultimate <ul style="list-style-type: none"> $f_{pr} = f_{pe} + 70 + \frac{f_c}{100 p_p}$ $f_{pr} \leq f_{py}$ and $f_{pr} \leq f_{pe} + 414$ 	<ul style="list-style-type: none"> • Stress at ultimate <ul style="list-style-type: none"> $f_{pr} = f_{pe} + \frac{5,000}{l_e} (d_p - c_y)$ $f_{pr} \leq f_{py}$ 	<ul style="list-style-type: none"> • Stress at ultimate <ul style="list-style-type: none"> $f_{pr} = f_{pe} + \frac{8,000}{l_e} (d_p - c_y)$ $f_{pr} \leq f_{py}$
Resistance & load factors	$\phi = 1.0$ $1.8D+1.8L$ or $1.2D+2.4L$	$\phi = 0.90$ $1.4D+1.7L$	$\phi = 0.90$ $1.4D+1.7L$	$\phi = 0.9$, $\phi_t = 0.85$, $\phi_c = 0.80$ $1.25D+1.5L$	$\phi = 0.9$, $\phi_t = 0.85$, $\phi_c = 0.80$ $1.25D+1.5L$
Minimum bonded reinforcement	<ul style="list-style-type: none"> -partially-prestressed : $0.1 A_b$ -fully-prestressed : 0 .. 	<ul style="list-style-type: none"> $\frac{N_c}{A_b}$, where is larger $0.04A$ 	<ul style="list-style-type: none"> -partially-prestressed : $0.005 A$ -fully-prestressed: $0.004 A$ 	<ul style="list-style-type: none"> for beams -partially-prestressed : $0.005 A$ -fully-prestressed: $0.004 A$ for one-way slab $0.004 A$ and $0.003 A$ respectively 	<ul style="list-style-type: none"> for beams -partially-prestressed : $0.005 A$ -fully-prestressed: $0.004 A$ for one-way slab $0.004 A$ and $0.003 A$ respectively

Note:

A_b : area of unbonded prestressed steel

N_c : tensile force in the concrete under load of $D+1.2L$

A_b is the area of that part of the cross section between flexural tension face and centroid of gross section

*stress after transfer limited to $0.70 f_{pu}$ at anchorages and couplers

.. bonded reinforcement required for determinate members

Table 2.2: Summary of Various Provisions of American Code Requirements for Members Reinforced With Unbonded Tendons

Title of the standard	ACI 318-63	ACI 318-71	ACI 318-83	ACI 318-89	ACI 318-95
Admissible stresses	<ul style="list-style-type: none"> • prestressing steel: <ul style="list-style-type: none"> -At stressing: $0.80 f_{pu}$ -Under service load: $0.70 f_{pu}$ • concrete: Admissible tensile stresses <ul style="list-style-type: none"> -fully-prestressed: $0.5 \sqrt{f'_c}$ -partially-prestressed: $0.5 \sqrt{f'_c}$ 	<ul style="list-style-type: none"> • prestressing steel: <ul style="list-style-type: none"> -At stressing: $0.94 f_{py}$ and $\leq 0.80 f_{pu}$ -Under service load: $0.70 f_{pu}$ • concrete: Admissible tensile stresses <ul style="list-style-type: none"> -$0.5 \sqrt{f'_c}$ -$1.0 \sqrt{f'_c} \dots$ 	<ul style="list-style-type: none"> • prestressing steel: <ul style="list-style-type: none"> -At stressing: $0.94 f_{py}$ and $\leq 0.80 f_{pu}$ -Under service load: $0.70 f_{pu}$ • concrete: Admissible tensile stresses <ul style="list-style-type: none"> -$0.5 \sqrt{f'_c}$ -$1.0 \sqrt{f'_c} \dots$ 	<ul style="list-style-type: none"> • prestressing steel: <ul style="list-style-type: none"> -At stressing: $0.94 f_{py}$ and $\leq 0.80 f_{pu}$ -Under service load: $0.74 f_{pu}$ • concrete: Admissible tensile stresses <ul style="list-style-type: none"> -$0.5 \sqrt{f'_c}$ -$1.0 \sqrt{f'_c} \dots$ 	<ul style="list-style-type: none"> • prestressing steel: <ul style="list-style-type: none"> -At stressing: $0.94 f_{py}$ and $\leq 0.80 f_{pu}$ -Under service load: $0.74 f_{pu}$ • concrete: Admissible tensile stresses <ul style="list-style-type: none"> -$0.5 \sqrt{f'_c}$ -$1.0 \sqrt{f'_c} \dots$
Ultimate limit state	<ul style="list-style-type: none"> • Stress at ultimate 	<ul style="list-style-type: none"> • Stress at ultimate 	<ul style="list-style-type: none"> • Stress at ultimate 	<ul style="list-style-type: none"> • Stress at ultimate 	<ul style="list-style-type: none"> • Stress at ultimate
Resistance & load factors	$f_{pr} = f_{pe} + 105$ $f_{pr} \leq f_{py}$	$f_{pr} = f_{pe} + 70 + \frac{f'_c}{100f_p}$ $f_{pr} \leq f_{py}$ and $f_{pr} \leq f_{pe}$ $f_{pr} \leq f_{pe} + 400$ $f_{pe} > 0.5 f_{pu}$	$f_{pr} = f_{pe} + 70 + \frac{f'_c}{100f_p}$ $f_{pr} \leq f_{py}$ and $f_{pr} \leq f_{pe}$ $f_{pr} > 0.5 f_{pu}$	$f_{pr} = f_{pe} + 70 + \frac{f'_c}{100f_p}$ $f_{pr} \leq f_{py}$ and $f_{pr} \leq f_{pe}$ $f_{pr} > 0.5 f_{pu}$	$f_{pr} = f_{pe} + 70 + \frac{f'_c}{100f_p}$ $f_{pr} \leq f_{py}$ and $f_{pr} \leq f_{pe}$ $f_{pr} > 0.5 f_{pu}$
Minimum bonded reinforcement	$A_s = 0 \dots$	$N_y / 0.5 f_y$ or $0.004 A$ <small>here is larger</small>	$N_y / 0.9$ $1.4D+1.7L$	$\phi = 0.9$ $1.4D+1.7L$	$\phi = 0.9$ $1.4D+1.7L$
			$0.004 A$	$0.004 A$	$0.004 A$

A_p area of unbonded prestressed steel

N_c tensile force in the concrete under load of $D+1.2L$

A is the area of that part of the cross section between flexural tension face and centroid of gross section

*stress after transfer limited to $0.70 f_{pu}$ at anchorages and couplers

** (... computations based on the transformed cracked section and on bilinear moment deflection relationships show that immediate and long-term deflections comply with code limits)

***ACI-ASCE 423-69 recommended that bonded reinforcement must be provided for crack control $A_s = N_y / 0.5 f_y$

CHAPTER 3

EXPERIMENTAL PROGRAM

3.1 Introduction

The overall objective of this experimental program was to investigate the minimum amount of non prestressed bonded reinforcement required to provide a ductile behavior in lightly prestressed members. The data were then used to develop and validate a model for predicting the flexural response of these members.

Eleven simply supported beams were tested. In the first series, seven beams had 50 MPa nominal concrete strength. The second series consisted of four beams with 100 MPa nominal concrete strength to assess the influence of concrete strength. All beams had identical geometric configuration, and a constant span-to-depth ratio of 14.25. The initial prestress was, $0.6f_{pu}$ in all beams. Other variables were the amount of unbonded prestressed reinforcement, and amount of non prestressed bonded reinforcement.

The beams were subjected to two point loading to create a test region with constant moment and zero shear between the point loads. Three deformation controlled tests were conducted. The remainder of the tests were gravity load tests in order to assess the impact effects associated with the "sudden" increase in deflection when the cracking load was reached.

The beams were designed in such a manner that some specimens failed in a brittle manner while others failed in a ductile manner. Thus, the boundary between brittle and ductile failure was bracketed.

The details of each specimen, the material properties, fabrication, instrumentation, and test procedure are described in this Chapter. The detailed test results and analysis are given in Chapter 4.

3.2 Test Specimens

3.2.1 Beams Designation

The 11 specimens were divided into two groups according to their concrete strength. The 50 MPa strength set is designated by letter "R" and numbered according to the order of testing, e.g., R-1. The 100 MPa set was designated by two letters "RH" and numbered according to the order of testing, e.g., RH-1.

3.2.2 Details of Specimens

Figure 3.1 shows the typical geometry and reinforcement arrangement. The amount of reinforcement and concrete strength is listed in Table 3.1. Note that the ends of the beam, outside of the point loads, had supplementary reinforcement to prevent shear failure. The test section is the constant moment region between the two point loads.

3.3 Materials

3.3.1 Concrete

Two mix designs were used in the program- one for intermediate strength concrete (target strength of 50 MPa concrete at 28 days), and one for high strength concrete (target strength of 100 MPa concrete at 28 days).

Normal Type 10 Portland cement was used. Local sand and aggregate were used to cast the beams. Mix designs are given in Table 3.2.

All beams were cast in the structural laboratory at the University of Alberta using a horizontal pan mixer capable of producing a 0.2 cubic metre batch.

Concrete test cylinders and modulus of rupture beams were cast at the same time from the same batch as the specimens. Cylinders were nominally 152 mm in diameter and 305 mm long for the 50 MPa concrete beams, and 100 mm diameter and 200 mm long for 100 MPa concrete beams. Modulus of rupture beams were 152 x 152 x 914 mm. Six concrete cylinders and two modulus of rupture beams were tested at the same time as the test specimens. Three cylinders were used to determine the compressive strength, and three were used to determine split cylinders strength. These tests were carried out in accordance with CSA A23.2 (CSA 1994). The concrete strengths are given in Table 3.3.

Typical stress-strain curves for both types of concrete are shown in Figs. 3.2 and 3.3.

3.3.2 Prestressed Reinforcement

All prestressed beams were reinforced with 9 mm diameter seven-wire stress relieved prestressing strand with static $f_{py} = 1778$ MPa except beam RH-1 where 13 mm diameter seven-wire stress relieved prestressing strand with static $f_{py} = 1620$ MPa was used. Some wires were clipped to reduce the effective area of the steel to more closely match the desired area. Properties are presented in Table 3.4.

The stress-strain curves for these strands are shown in Fig. 3.4. Tension tests for the prestressed reinforcement were done in accordance with ASTM A370-92.

3.3.3 Nonprestressed Bonded Reinforcement

The supplementary nonprestressed bonded reinforcement used in all specimens consisted of 6 mm diameter deformed steel bars (cross-sectional area of 29.15 mm^2). These bars were from the same heat, and had an ultimate strength of 645 MPa with no well defined yield point. The 0.2 % offset static yield stress was 460 MPa.

The typical stress-strain curve for the reinforcement is shown in Fig. 3.5. Tension tests for the nonprestressed reinforcement were done in accordance with ASTM A370-92.

3.4 Fabrication

The specimens were fabricated in the I. F. Structural Laboratory at the University of Alberta. Forms were made of plywood. The forms were oiled before casting the concrete. Reinforcing cages were assembled with tie wire. Prestressed reinforcement was greased (premium lubricating grease with RF-7) and encased inside plastic tubes having a 12.7 mm inside diameter and 15.875 mm outside diameter.

The concrete was vibrated using a hand held pencil vibrator. One batch of concrete was enough to cast one specimen with companion cylinders and modulus of rupture beams. The side forms were stripped twenty-four hours after casting. The beams were then cured with wet burlap and plastic sheets for approximately ten days. They were then allowed to cure uncovered in the laboratory until the time of testing. The test cylinders were always subjected to the same curing conditions as the beams in order to get a good estimate of the actual properties of the concrete in the beams.

Figure 3.6 shows specimens prior to casting.

3.5 Prestressing

The prestressing operation was carried out one day prior to testing. Fig 3.7 shows prestressing set up for both ends of the beam.

Prestressing force was applied using hydraulic jack that reacted against the beam, stresses were distributed through 125x125x25 mm steel bearing plates. The force and elongation of the tendon during the prestressing was monitored on the data acquisition system, readings were taken every 5 kN

increment in prestressing force. When the prestressing force reached 5kN higher than required, wedges were set. The jack force was released slowly allowing the complete engagement of the wedges. The loss of tendon elongation associated with the seating of the anchorage was ranged between 5 to 7 mm.

The jacking force was applied for the second time, and shim plates were inserted between the load cell and the bearing plate locking into place the required tendon force.

3.6 Test Set-up and Instrumentation

The specimens were tested in the load frame shown in Figs. 3.8, 3.9, and 3.10. In the stroke controlled tests, the loads were applied with hydraulic jacks pulling on the tension rods from below the strong floor. In the gravity load tests, hydraulic jacks were used to pick up the initial portion of the dead weights. The additional dead weights (50 pound calibrated weights) that were required to bring the specimen to failure were applied by hand.

The loads were applied through 80 x 80 mm steel bearing plates that were plastered to the top of the beam. There were rollers at each load and support location that prevented horizontal restraint. The adjustable wheel support was manually adjusted to keep the load at mid span of the beam.

Gravity loads were made up of three large steel beams with additional steel plates and 35 mm diameter reinforcing bars as needed. The dead weight assembly was supported by hanger rods, which transferred the weight to the specimen as two concentrated loads. Additional load was provided by standard 50 lb weights. See Fig. 3.11.

Electronic load cells were used to measure the loads and reactions. Load cells of 20 kip capacity were used to measure reactions and applied loads in the stroke control tests while 10 kip capacity tension load cells were used to measure the applied gravity loads. The force at each end of the tendon was measured with 40 kip capacity centre hole load cells located between the end bearing plate and the stressing chucks.

Vertical deflections were measured with cable transducers attached to the bottom of the specimen at mid-span and at the loading point locations. Also, cable transducers were used to measure the horizontal span change between support reactions and load points. The load and support points could move horizontally during the test.

All load cells and cable transducers were calibrated before and after the test program.

Cracks were measured with a microscope graduated to 0.001 inches. During the test, cracks were monitored and measured at most load steps. Measurement locations were at strand level, nonprestressed reinforcement level, and at the bottom of the beam and were marked to ensure measurements were taken at the same location each time.

A Demec gauge was used to measure concrete strain. Demec points with a 250 mm gauge length were located on both sides of the beam, as shown in Fig. 3.12.

All electronic readings were recorded using a Fluke data acquisition system. Demec gauge readings were recorded manually.

3.7 Test Procedure

3.7.1 Stroke Control Testing Procedure

After the test specimen was aligned, all instrumentation was checked. The initial readings of load cells, cable transducers, and Demec gauges were taken prior to the start of loading.

The loads in the hydraulic jacks were manually controlled. Care was taken to apply the loads at a constant rate using two separate hydraulic jacks, one for each point load. Load increments of 0.5 kN per jack were applied. The magnitude of the load was held constant while a set of reading was taken. Close to the cracking load, the data acquisition system was set to take readings at approximately two seconds intervals in order to capture the cracking load. After cracking, readings were taken at deflection increments of 5 mm until the failure occurred. The cable transducer under the south point load and the south load cell were connected to the data acquisition system that allowed monitoring of the load-deflection curve in real time during the test.

Tests were terminated when the maximum tendon force reached 98 % of the measured breaking strength of the tendon, or after crushing of the concrete.

3.7.2 Gravity Loading Test Procedure

After the test specimen was aligned, all instrumentation was checked. The initial readings of load cells, cable transducers, and Demec gauges were taken prior to start of loading.

The steel beams (gravity load) were gradually lifted up off their support, transferring their weight to the specimen, by means of two hydraulic jacks located on top of the two point loads. After the weight of the steel beams was supported completely by the specimen, supports for the steel beams were removed to allow for large deflection. The hydraulic system was then closed and kept closed until the end of the test. It's important to note that the total suspended weight right after closing the hydraulic system was less than the cracking load. Readings were taken during lifting the steel beams at 1 kN intervals.

Standard 50 lb weights were added at a constant rate. As the loads were applied, readings were taken automatically by the Fluke data acquisition system. Demec readings were taken at 200 lb load increments.

The overall behavior of each specimen was also monitored during the course of each test by plotting the north point load versus central deflection. Loads, deflections, and span length change were monitored continuously on the data acquisition screen. Each test took approximately three hours to complete.

3.8 Test Results

Detailed test results are given in Appendix A. Table 3.6 gives summary of the most important data: The ultimate deflection, loads and reactions along with Δf_{pr} and the cracking and ultimate moments.

As in all structural experiments the observed reactions and loads do not precisely satisfy statics. This is due to small differences in calibration factors before and after the testing, and normal minor experimental error.

In order that the free body diagram of the specimens satisfies statics exactly, adjustments to the load, reactions, and horizontal dimensions were made using the method of least squares. This is similar to adjusting a surveying traverse to eliminate the error of closure.

The standard error of a length measurement was 1 mm per metre. The accuracy of each load cell was taken as 0.005 times the capacity of the load cell. It was found that the maximum correction in either the load or support reaction in all tests was 1.89%. Moments have also been adjusted to include the effect of the beam and loading apparatus self weight.

The test results after adjustment of loads and reactions are reported in Table 3.6. Actual readings for loads and reactions are presented in the Appendix A.

Graphs of applied load vs mid-span deflection, load vs increase in strand stress, crack width vs increase in strand stress and other information are presented in Chapter 4, where they are discussed in detail.

Table 3.1 Specimens Properties

Series	Specimen #	Concrete Strength f'_c [MPa]	Prestressed Reinforcement A_p [mm^2]	P _p %	f_{ps} [MPa]	A_s [mm^2]	Non prestressed Reinforcement A_s [mm^2]	ρ_s %	Method of Testing
Intermediate Strength Concrete Series	R-1	49.22	47.14	0.15	1111	0.00	0.00	0.00	Stroke Control
	R-2	52.03	47.14	0.15	1128	29.15	0.07	0.07	Stroke Control
	R-3	52.74	47.14	0.15	1128	58.30	0.13	0.13	Stroke Control
	R-4	48.50	39.29	0.12	1112	0.00	0.00	0.00	Gravity Load
	R-5	51.20	39.29	0.12	1116	29.15	0.07	0.07	Gravity Load
	R-6	48.35	0.00	0.00	0.00	58.30	0.13	0.13	Gravity Load
	R-7	49.05	0.00	0.00	0.00	87.45	0.20	0.20	Gravity Load
High Strength Concrete Series	RH-1	118.38	99.00	0.31	1098	0.00	0.00	0.00	Gravity Load
	RH-2	117.99	47.14	0.15	1111	29.15	0.07	0.07	Gravity Load
	RH-3	119.25	47.14	0.15	1114	58.30	0.13	0.13	Gravity Load
	RH-4	123.38	47.14	0.15	1115	87.45	0.20	0.20	Gravity Load

Table 3.2 Concrete Mix Designs

Constituents	Specimens	
	High Strength Concrete [≈ 100 MPa]	Intermediate Strength Concrete [≈ 50 MPa]
Cement [kg/m ³]	520	380
Water [kg/m ³]	55	170
Coarse aggregate [kg/m ³]	1080	1000
Fine aggregate [kg/m ³]	695	815
Silica Fume [kg/m ³]	110	0
Superplasticizer [l/m ³]	18	0
W/(C+SF)	0.21	0.45

Notes:

1. Concrete mixes were designed based on 2 % air content.
2. Silica Fume Slurry had 49 % solids by weight.
3. Superplasticizer used was SPN 2000 which had 31 % solids by weight.
4. Maximum aggregate size is 14 mm
5. Quantities based on saturated surface dry aggregates

Table 3.3 Concrete Strength

Specimen	Compression*	Split *	Modulus of Rupture **
	[MPa]	[MPa]	[MPa]
R-1	49.22	4.30	3.75
R-2	52.03	4.45	4.02
R-3	52.74	4.31	3.67
R-4	48.50	4.11	3.85
R-5	51.20	4.35	3.71
R-6	48.35	4.20	3.82
R-7	49.05	4.25	3.93
RH-1 ^	118.38	6.72	5.60
RH-2 ^	117.99	6.70	5.24
RH-3 ^	119.25	6.69	5.17
RH-4 ^	113.38	6.67	5.50

* Average of three tests

** Average of two tests

^ 100 x 200 mm cylinders

Table 3.4 Reinforcement Properties

Reinforcement Type	Diameter [mm]	Nominal Area [mm ²]	Static Yield Stress [MPa]	Dynamic Yield Stress [MPa]	Ultimate Stress [MPa]	Modulus of Elasticity [MPa]
Nonprestressed Reinforcement	6.1	29.15	460	485	645	200000
Prestressed Reinforcement	9	55	1778	1832	2021	204000
Prestressed Reinforcement	13	99	1607	1651	1904	198000

Note:

Some strands had one wire clipped (i.e. cut) so the effective area = $(6/7) \times \text{nominal area}$
Some strands had two wires clipped (i.e. cut) so the effective area = $(5/7) \times \text{nominal area}$

Table 3.5 Test Results

Specimen #	North Load [kN]	South Load [kN]	North Reaction [kN]	South Reaction [kN]	Total Load [kN]	M_{α} [kN.m]	M_u [kN.m]	Max Deflection [mm]	Δf_p [MPa]	M_u/M_{α}
R-1	18.419	17.896	18.261	18.054	36.31	14.97	17.24	64.958	740.37	1.15
R-2	19.902	21.203	20.291	20.814	41.10	16.21	19.41	20.616	341.94**	1.20
R-3	30.407	27.353	29.487	28.273	57.76	16.28	26.78	60.772	706.21	1.64
R-4	14.448	14.572	14.485	14.535	29.02	14.05	14.07	1.99	7.94*	1.00
R-5	16.181	15.919	16.104	15.996	32.1	15.00	15.41	19.015	254.00**	1.03
R-6	15.408	17.41	16.033	16.785	32.81	9.63	15.99	118.058	—	1.66
R-7	12.669	8.921	11.539	10.051	21.59	9.82	11.53	63.587	—	1.17
RH-1	33.588	34.827	33.91	34.505	68.41	25.49	31.05	77.318	497.88	1.22
RH-2	22.777	22.103	22.576	22.304	44.88	20.85	20.91	1.805	3.63*	1.00
RH-3	21.851	24.499	22.643	23.707	46.35	20.89	21.87	16.559	236.1**	1.05
RH-4	30.925	29.94	30.629	30.236	60.86	21.12	27.75	70.499	608.78	1.31

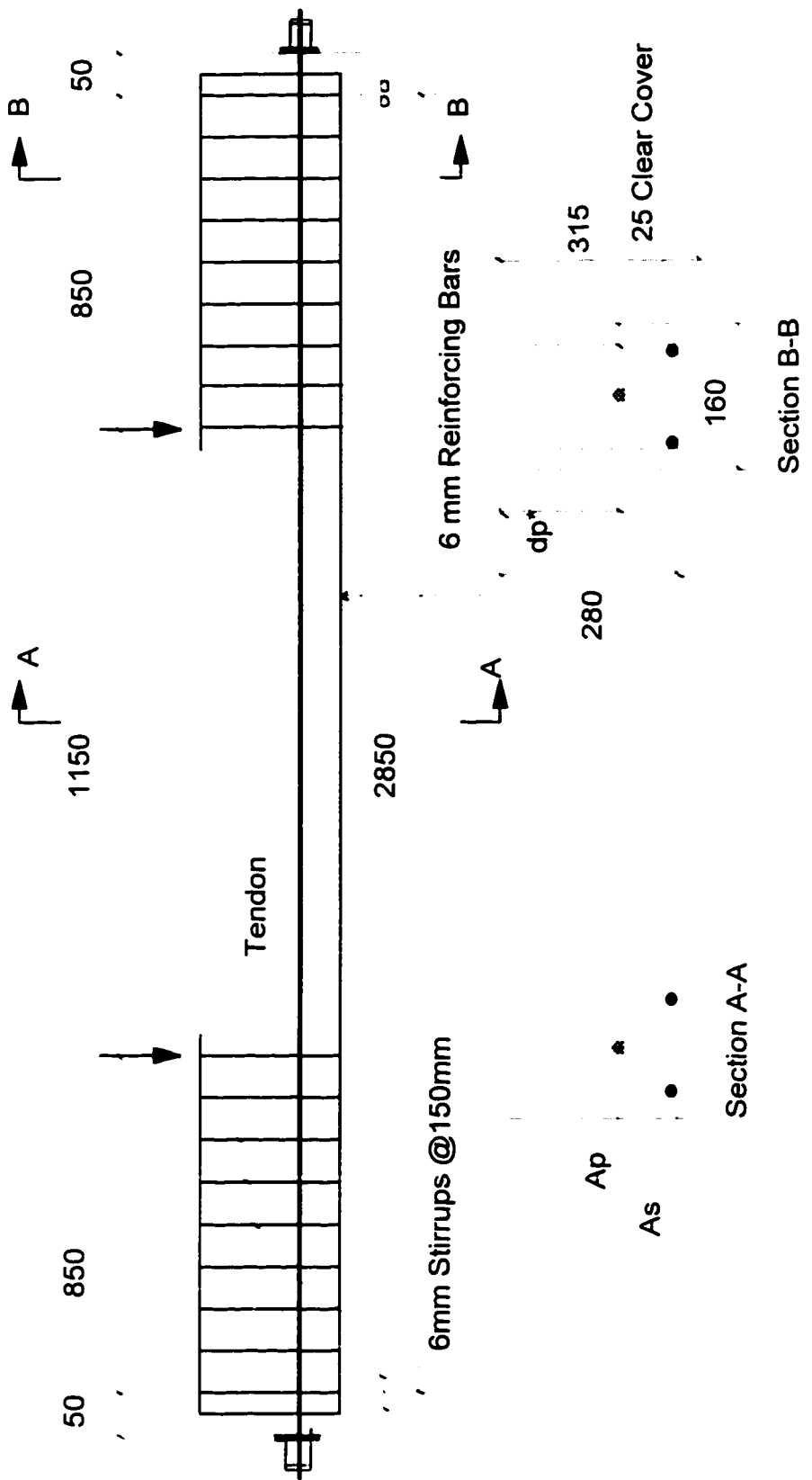
* Beams failed suddenly at cracking

** Last reading recorded before fracturing of the nonprestressed bonded reinforcement.

- Loads reported do not include self weight of beam and loading apparatus.

- Loads reported after corrections to satisfy statics are being made.

- Moments reported include the effect of self weight of the beam and loading apparatus



* Note: $d_p=200$ mm for all specimens except RH-1, $d_p=190$ mm

Figure 3.1 Test Specimen

all dimensions are in millimetre

**Figure 3.2 Typical Stress-Strain Curve for Intermediate strength Concrete
Nominal [50 MPa]**

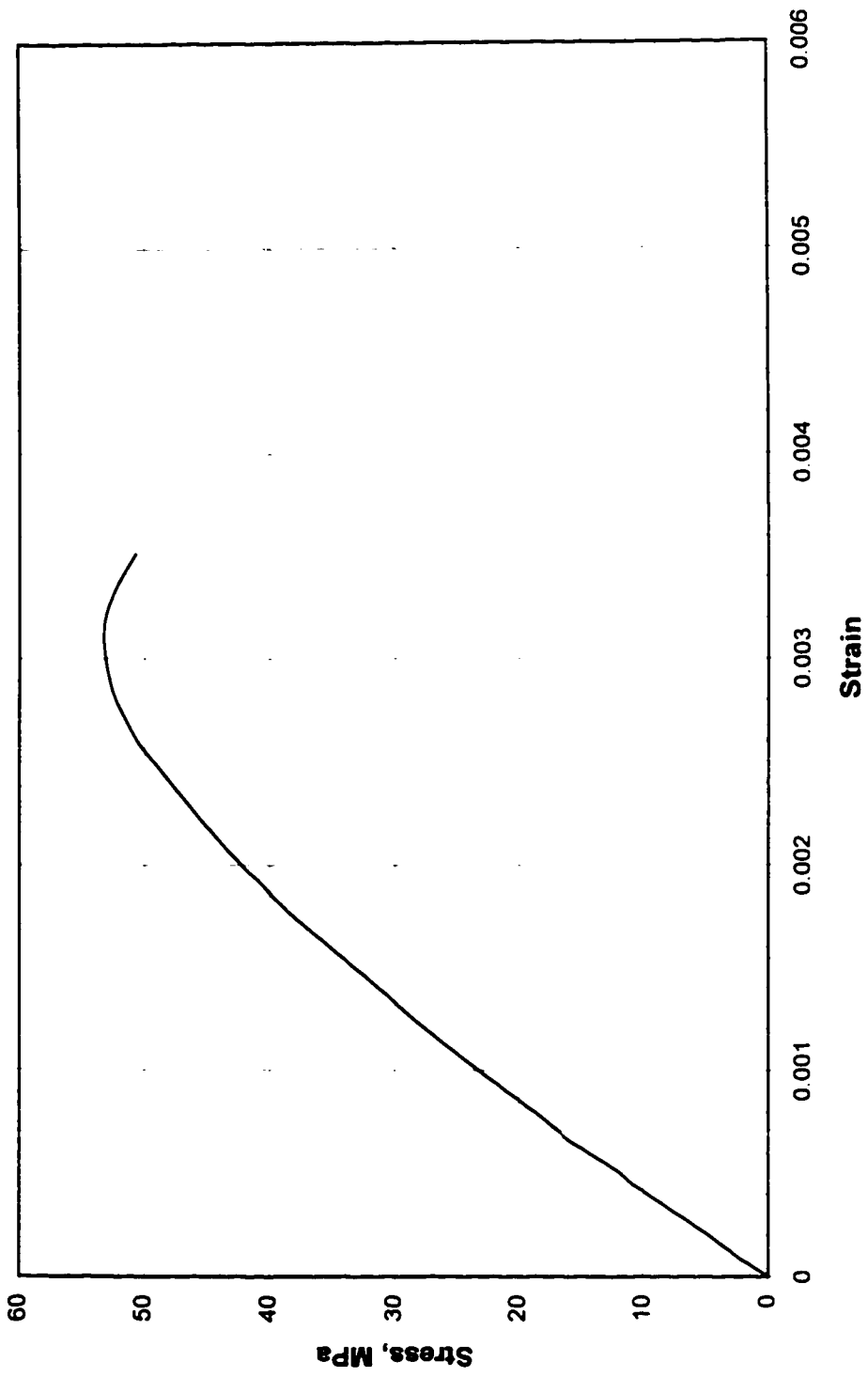


**Figure 3.3 Typical Stress-Strain Curve for High Strength Concrete
Nominal [100 MPa]**

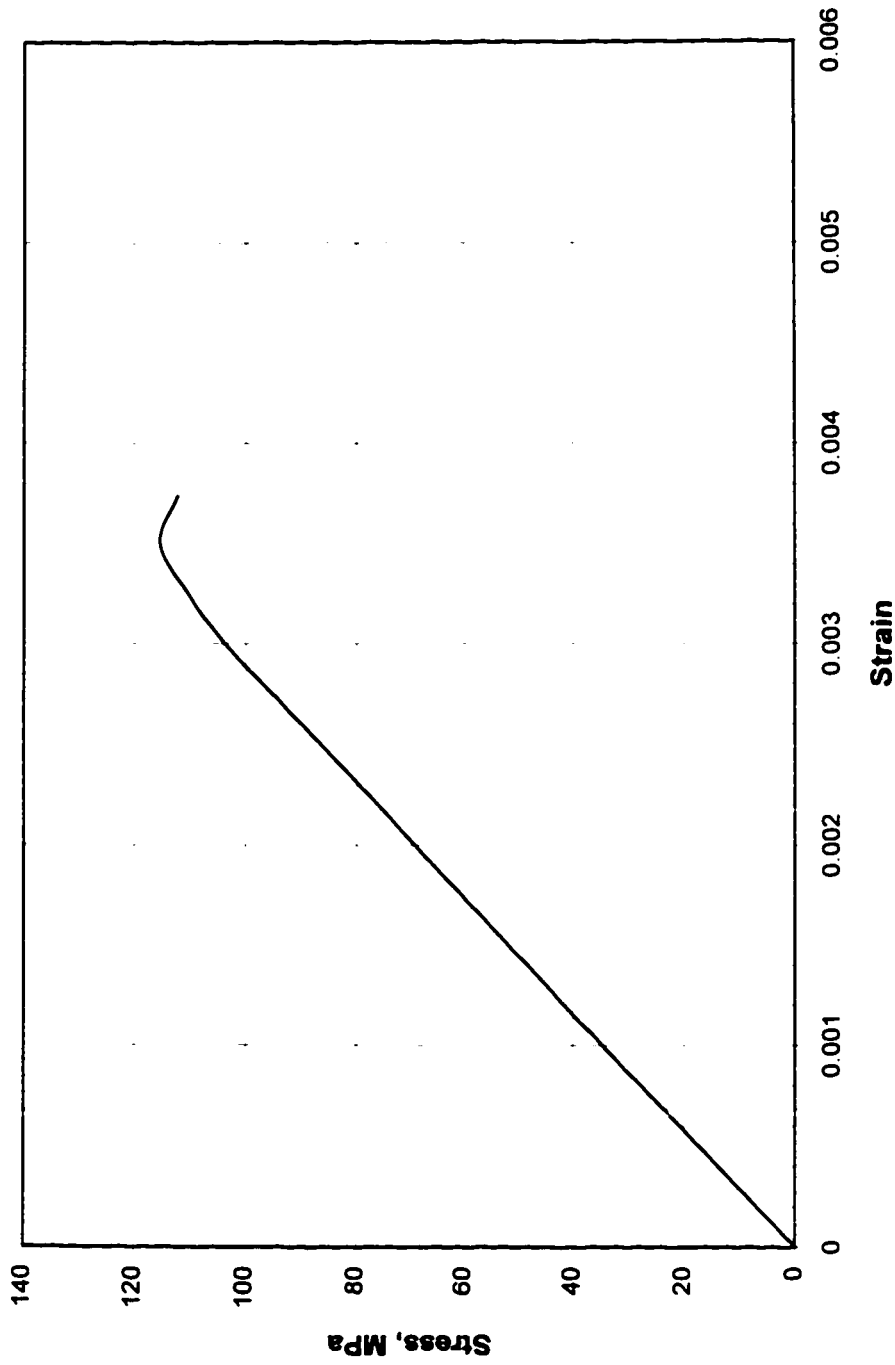


Figure 3.4 Typical Stress-Strain Curves for Prestressed Reinforcement

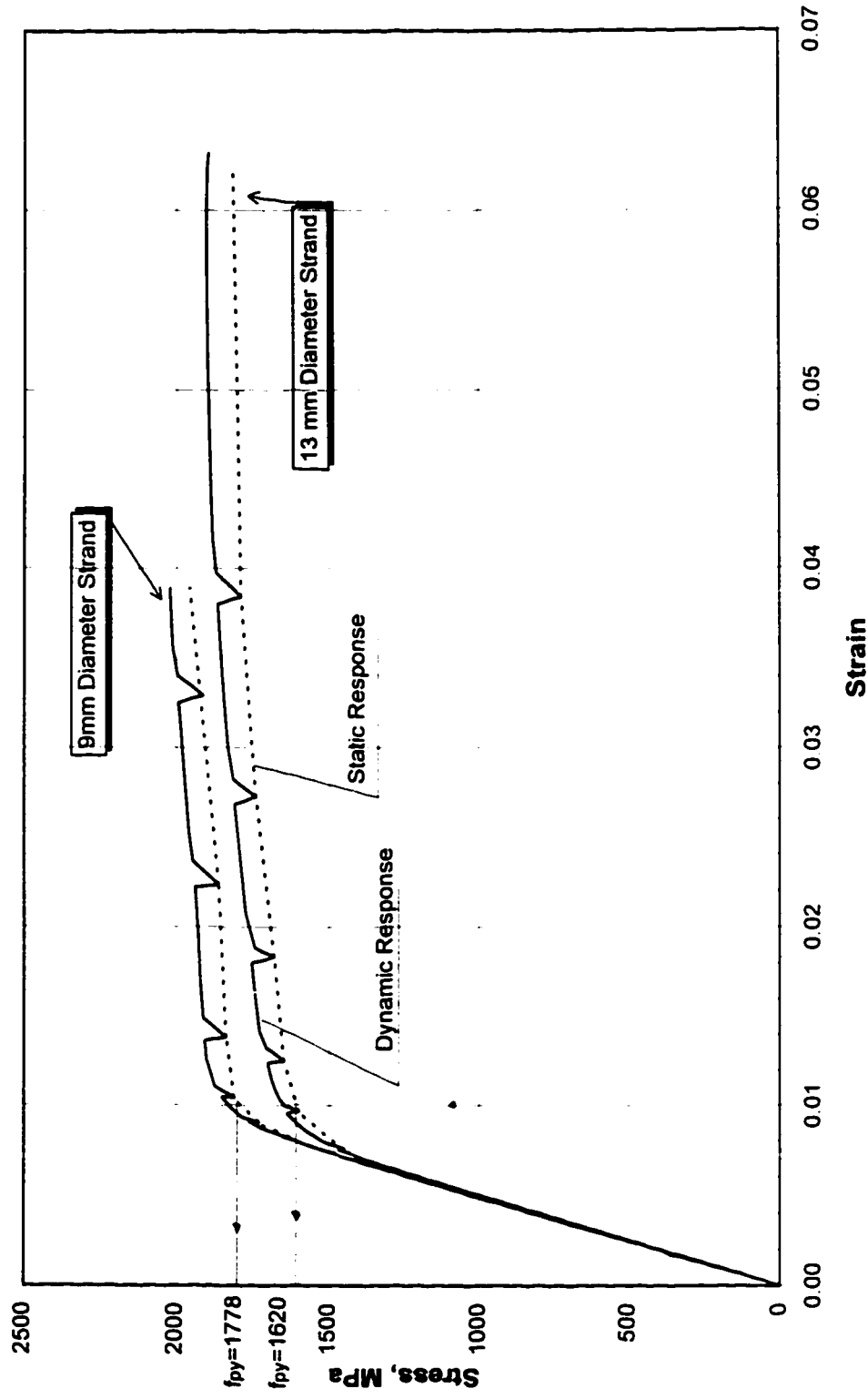


Figure 3.5 Typical Stress-Strain Curve for Nonprestressed Bonded Reinforcement

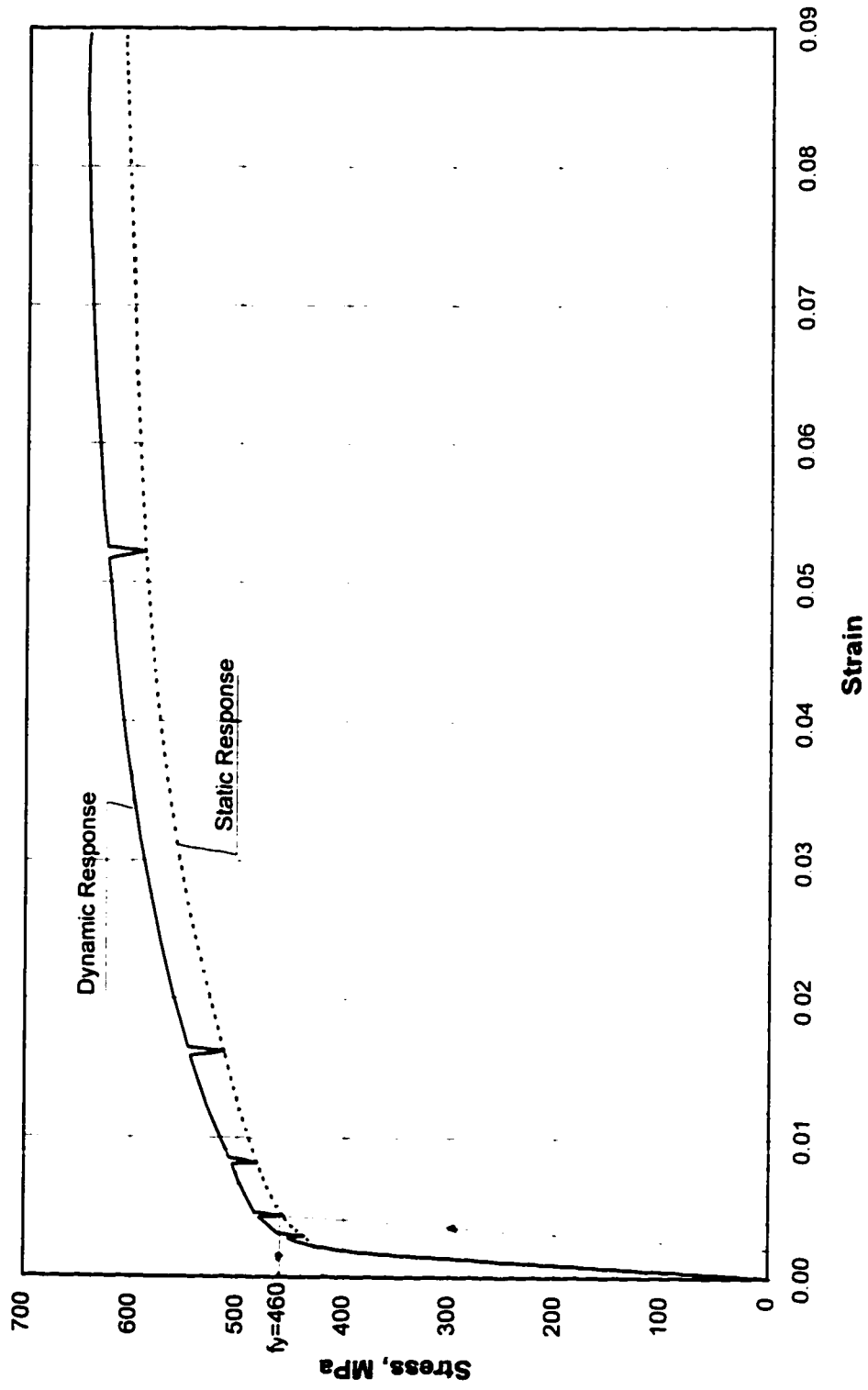




Figure 3.6 View of Reinforcing Steel Cages in the Wooden Forms

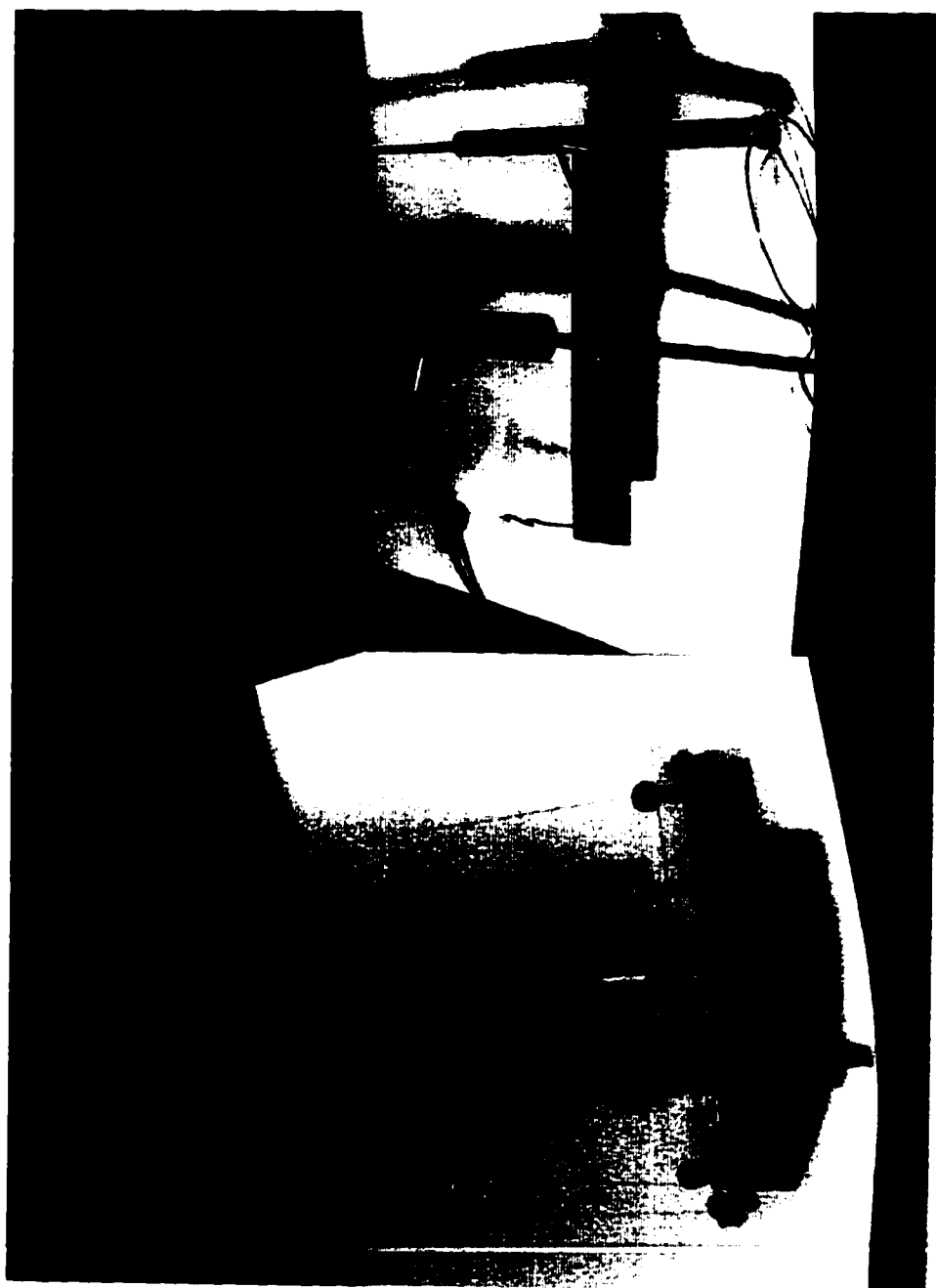


Figure 3.7 Prestressing Set-up at Both Ends of the Beam



Figure 3.8 Stroke Control Test Set-up

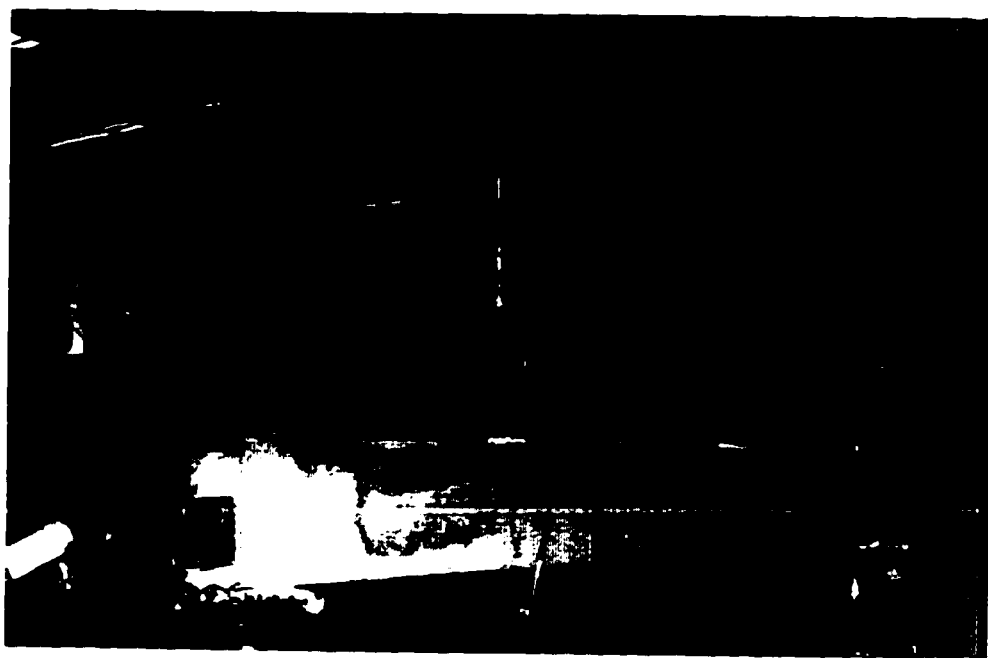


Figure 3.9 Gravity Load Control Test Set-up

Figure 3.10 Gravity Load Test Set-Up

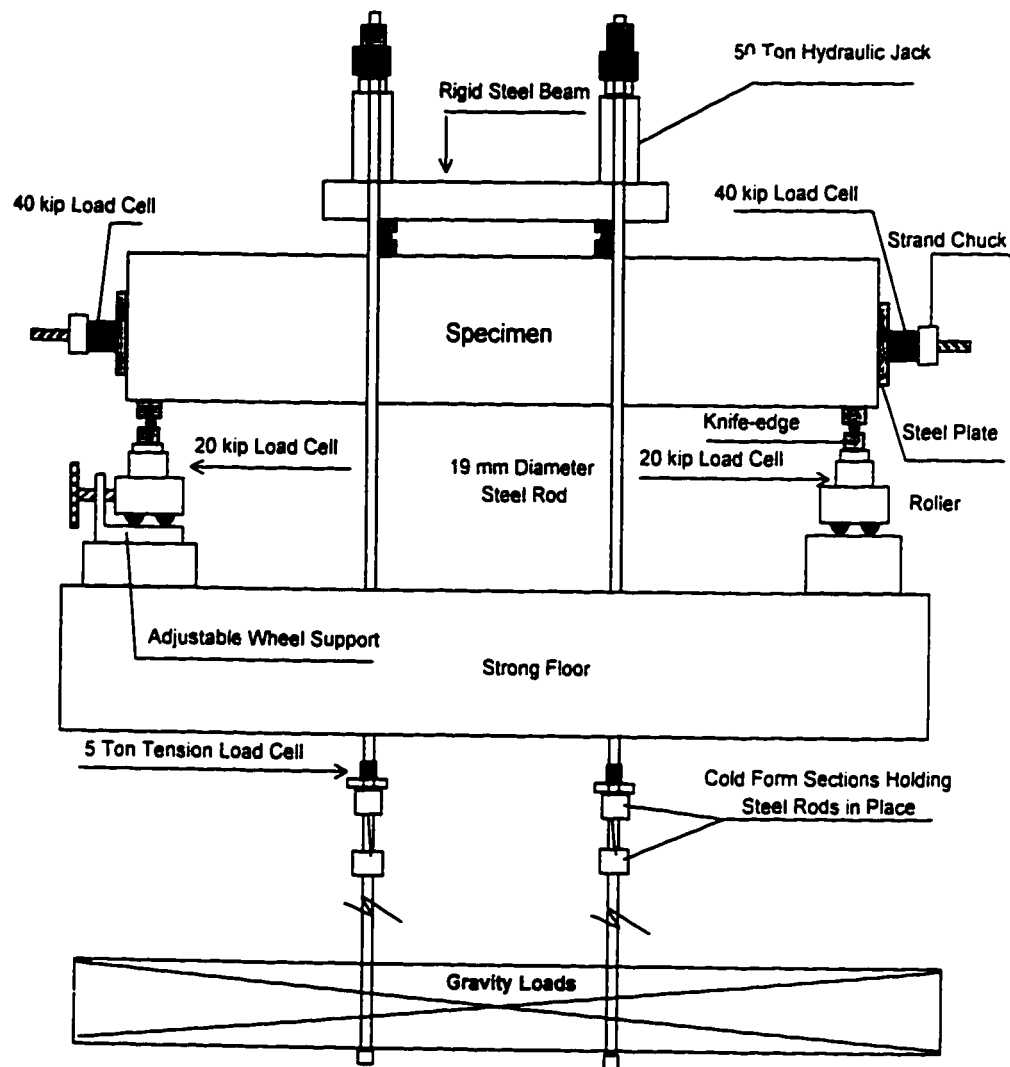
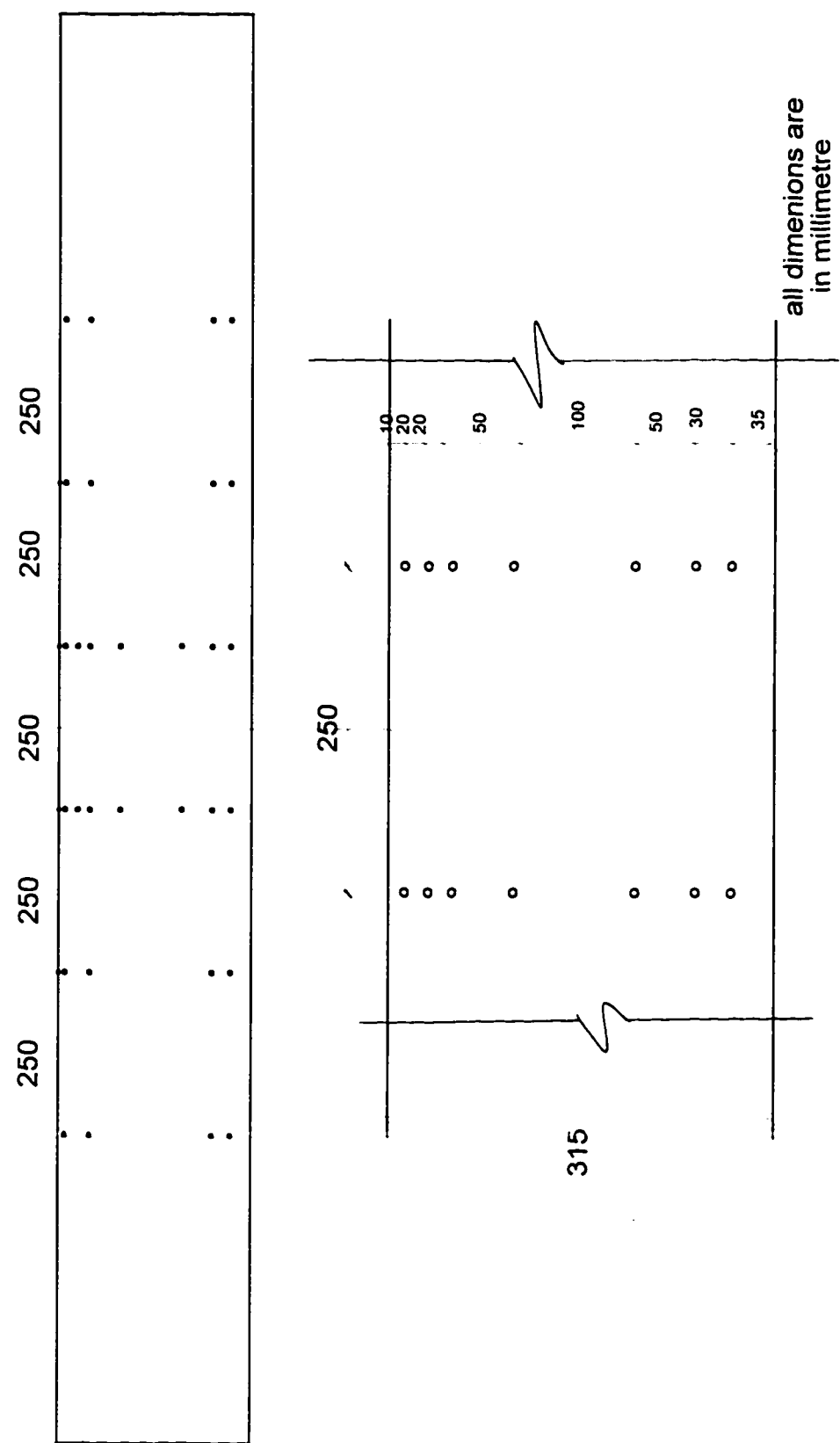




Figure 3.11 View of the Gravity Loads Used in the Test

Figure 3.12 Demec Gage Point Layout



CHAPTER 4

ANALYSIS

4.1 Introduction

This chapter presents a detailed analysis of the test results along with the development of an analytical model that predicts the flexural response of unbonded prestressed concrete members. An idealized response diagram is given in Fig. 4.1. The load-deflection curves have distinct regions associated with different physical phenomenon, such as: cracking of concrete, yield of reinforcement, and crushing of concrete. The phenomenon associated with each region of the load-deflection curve is discussed and a prediction model is developed. Appropriate values for the parameters in the model are established from the test results. The effect of concrete strength, strain hardening, and amount of nonprestressed bonded reinforcement are assessed with the prediction model and the experimental results.

Code requirements for minimum bonded reinforcement, and code predictions for M_{cr} and M_u are evaluated.

In addition, two equations for prediction of the tendon stress at failure using a collapse mechanism are presented.

4.2 Load-Deflection Relationship

Experimental load-deflection curves for all specimens are given in Appendix B. Selected curves are presented in Figs. 4.2 through 4.8. These figures present the curves for specimens that were similar except for the variation of one parameter. The effect of the parameter is readily apparent.

From a study of the experimental curves, the schematic plot of load-deflection shown in Fig. 4.1 for various loading stages was developed. Stage a-b represents the first stage of the applied load-deflection curve where the members behaved as a linearly elastic uncracked section. At cracking, two distinctly trends were observed depending upon the method of testing. Beams tested with the stroke control method followed the b-c trend line with a drop in load at cracking. Beams tested with the gravity load method followed the b-d trend line with an increase in deflection at cracking. This drop in load or increase in deflection is due to the reduction in stiffness of the member after cracking. The amount of nonprestressed bonded reinforcement provided, and the concrete strength influence the drop in load and increase in deflection.

With increasing load, the response curve follows c-e or d-e as appropriate. Point e on the curve represents yielding of the nonprestressed bonded reinforcement. Point f represents yielding of the prestressed reinforcement. And finally point g represents crushing of the concrete. After failure, beams tested with the stroke control method are still able to carry some load and follow the line g-h-i.

Beams R-4 and RH-2 failed at cracking (point b). Beams R-3 and RH-4 failed by crushing of the concrete after yielding the tendon (point g). Other specimens failed somewhere between points b and g due to strain localization that ruptured the bonded reinforcing bars. The position along the response curve where the specimen fails depends on parameters such as concrete strength, amount of nonprestressed bonded reinforcement, and amount of unbonded prestressed reinforcement.

Figure 4.2 presents the load versus deflection curves for beams R-1, R-2, and R-3, which have varying amounts of nonprestressed bonded reinforcement. All beams in this figure were tested in stroke control mode. Beam R-1, which had no bonded reinforcement, had an ultimate strength 18% greater than the cracking load, and appears to be ductile. It required almost 30 mm of deflection after cracking to sustain the cracking load. If this beam had been tested under gravity loads, this beam might have failed due to impact in a brittle manner at cracking. Beam R-2 which had $A_s = 0.00116A$ ($\rho = 0.00065$) is obviously ductile but there was a single flexural crack and the bonded reinforcement ruptured before the tendon yielded. Beam R-3 which had $A_s = 0.00232A$ ($\rho = 0.0013$) was ductile. The tendon yielded before the concrete crushed. A23.3-94 requires a minimum bonded reinforcement of $A_s = 0.004A$ to insure ductile behavior. Figure 4.2 clearly shows that ductility can be achieved with significantly less bonded reinforcement.

Figure 4.3 presents the load versus deflection curves for beams R-4, and R-5. The test specimens have the same amounts of unbonded prestressed

reinforcement and varying amounts of bonded nonprestressed reinforcement. These beams were tested with gravity loads. Beam R-4 was brittle but beam R-5 was ductile in that additional load after cracking was required to produce failure. It is evident that an area of bonded reinforcement as small as 0.00116A can prevent a sudden collapse when the cracking load is reached, but this is very close to the limiting value.

Figure 4.4 shows beams with the same amount of bonded reinforcement but different amounts of unbonded prestressed reinforcement. Beam R-2 which is clearly ductile, had $\rho_p=0.0015$ ($\omega_p=0.0315$). On the other hand, R-5 which can be described as barely ductile, had $\rho_p=0.0012$ ($\omega_p=0.0269$). These tests show that even a small reduction in effective prestress can produce a significant loss in strength and ductility. Thus, the reduction in effective prestress in existing structures due to corrosion can have serious consequences.

Figure 4.5 shows two beams that had similar reinforcement but different concrete strengths. Beam RH-3 which had 119.25 MPa concrete strength, had a higher cracking load, but less ultimate strength and ductility than beam R-3 which had 52.74 MPa concrete strength. Since both beams had the same reinforcement, RH-3 should have had an ultimate strength slightly greater than R-3. Beam R-3 had several cracks, while RH-3 had a single crack. The bonded reinforcing bars prematurely ruptured in beam RH-3. The higher concrete strength in RH-3 produced very short bond lengths and hence significant strain localization in bonded reinforcement. When the ductility of the reinforcing bars was exhausted at the crack, the bars ruptured. This required little member

deflection and hence there was little increase in tendon stress in RH-3. In beam R-3, the concrete tensile strength was lower, and the bonded reinforcement was sufficient to allow the development of several flexural cracks. This in turn, produced larger deflections, larger increase in tendon stress, and hence greater member strength and ductility. One can conclude that higher concrete strength may require additional reinforcement to get desirable member response.

Figure 4.6 shows the response of beam RH-1 and the response of specimen R3 tested by Ospina et al. (1997). The beams had the same reinforcement and concrete strength of 118.38 MPa and 108.5 MPa respectively. Beam R3 was tested using the stroke control method while RH-1 was tested with gravity loads. The difference in response is due to the difference in method of loading. This agrees with the previous discussion of Fig. 4.1. These beams show that one can have adequate strength and ductility in members without bonded reinforcement, even with high concrete strength, provided that there is sufficient prestressing. It worth noting that the sudden 38 mm deflection of RH-1 at cracking occurred slowly enough to eliminate major impact effects. (The time required to move from point a to point b in Fig. 4.6 was approximately two seconds).

Figure 4.7 shows a set of high strength concrete beams with the same amount of prestress but varying amounts of nonprestressed bonded reinforcement. Beam PH-4 ($A_s=0.00348A$) had approximately the minimum bonded reinforcement required by A23.3-94 ($A_s=0.004A$). This amount was enough to produce large ductility ($\delta/L=1/54$), three cracks, and yield of the tendon

before the beam failed by rupturing of the reinforcing bars. The more heavily reinforced beams attained greater ultimate load than those with less reinforcement. Additional bonded reinforcement improved member ductility. While member ductility was obscured by breakage of the reinforcing bar in beams RH-2 and RH-3, $A_s=0.00348A$ was enough to improve the ductility and permit yield of the tendon.

Figure 4.8 shows the results for beams R-6 and R-7. These members were nonprestressed and were designed to have predicted M_u/M_{cr} ratios of 1.00 and 0.67 respectively. These beams did not collapse at first cracking. They exhibited large deflection ($L/24$, and $L/44.6$) and had $M_{u_{real}}/M_{cr_{real}}$ ratio of 1.66 and 1.17 respectively. This occurred because strain hardening provided additional capacity that prevented a sudden collapse at cracking. This reserved capacity is proportionately smaller in prestressed members because the strain hardening influences only the bonded portion of the total reinforcement in the member. This figure shows that the influence of strain hardening on the ultimate strength of the nonprestressed members cannot necessarily be neglected.

From Fig. 4.2 and Fig. 4.7, it is evident that a nonprestressed bonded reinforcement index $\omega_s=\rho f_y/f_c$ greater than 0.01 was sufficient to prevent a large increase in deflection (gravity controlled) or drop in load (stroke controlled) for all concrete strengths tested.

4.3 Crack Patterns

Discussion of the observed crack patterns is warranted because the number and type of cracks gives an indication of the amount of bonded reinforcement present. This information is useful when assessing an existing structure.

In the tests, the first crack formed when the stress in the extreme concrete tension fibers reached a stress of $0.53\sqrt{f'_c}$ to $0.58\sqrt{f'_c}$. The mean stress at rupture was $0.55\sqrt{f'_c}$.

Figure 4.9 shows the crack pattern of all beams after failure. Figure 4.10 shows the two extreme types of crack behavior. Figure 4.10 (a) shows the crack development in beam R-3 which had a modest amount of bonded reinforcement ($\rho=0.0013$). Cracks were marked with black felt marker at each load step. The number written beside tick marks indicates the applied load in kN when the crack reached the tick mark. Four flexural cracks formed by the time the load reached 40 kN. The flexural cracks grew slowly with increasing load and branched or bifurcated as failure was approached. The photograph was taken when the load was 95% of the failure load.

Figure 4.10 (b) shows the crack development in beam RH-1 which had no bonded reinforcement. In this case the first crack occurred at a load of 55 kN. The crack was large and severely bifurcated. These typical photographs suggest that if one sees large bifurcated cracks in a structure, it will have zero or low amounts of bonded reinforcement. In all of the prestressed members tested, some bifurcation of the cracks occurred before failure. In members similar to

those tested, absence of crack bifurcation may be taken as an indication that the failure is not imminent. These observations may be useful when assessing an existing structure

4.4 Failure Modes

All beams failed in flexure. Failure was initiated by: rupture of the bonded non prestressed reinforcement, or yielding of the unbonded prestressed reinforcement. Either of these two events would lead to larger deflections and finally crushing of the concrete compression zone due to excessive deformation.

Figure 4.11 shows a view of the specimens after failure.

Beam R-1 failed by yielding of the prestressed reinforcement followed by initial crushing of concrete accompanied by increasing deflection under constant load. Beam R-2, failed by rupture of the non prestressed bonded reinforcement (6 mm bar) prior to yield of the prestressed reinforcement. Beam R-3, failed by crushing of concrete and rupture of the non prestressed bonded reinforcement after the unbonded prestressed reinforcement had yielded. Due to the stroke controlled loading procedure used, these three specimens were able to carry load after the peak load was reached.

Beams R-4, and RH-2 failed without any warning in a catastrophic manner at cracking.

Beams R-5, and RH-3 both failed by rupture of the non prestressed bonded reinforcement before the tendon reached yield.

Beam RH-4 followed the same trend as beam R-3 and failed by rupturing the non prestressed bonded reinforcement after yielding of the unbonded prestressed reinforcement.

Beam RH-1 failed in violent manner due to crushing of the concrete in the compression zone. While the ultimate failure was explosive, it occurred at a load greater than the cracking load and after significant deflection was developed ($\delta/L=1/36.5$).

Beams R-6, and R-7 had no prestressed reinforcement. These beams failed by rupture of the non prestressed bonded reinforcement.

4.5 Extreme Compression Fiber Strain Measurements

Demec points with a 250 mm gage length were used to measure the concrete strain distribution in the constant moment region. The maximum concrete strain reached in the top fiber of the beam was calculated assuming a linear strain distribution through the section. Plots of the variation in concrete strain along the member at the extreme compression fiber are given in Fig. 4.12.

The extreme concrete fiber strain tends to be non-uniform along the length of the member. As failure is approached, the strains grow rapidly at the governing failure crack.

The concrete compression strains at failure for all test specimens are given in Table 4.1. Only beam R-3 and RH-1 were governed by concrete crushing before the reinforcing bars ruptured. Hence, only these two specimens can be used to assess the maximum compression strain capacity of the concrete. The values of ϵ_{cu} were 0.00330 and 0.00360 respectively.

It may be concluded that the maximum compression strain of 0.0035 specified in CSA A23.3-94 can be reached even for members with large deflections.

4.6 Increase in Tendon Stress at Failure

Tendon stress was measured by load cells placed at each end of the beam. Stress in the tendon was taken as the average of the two load cells dividing by the nominal area of the tendon. The tendon force was monitored during stressing, immediately before testing and throughout the test.

Before cracking, the stress in the prestressed reinforcement showed only a slight increase that ranged between 3.41 MPa and 6.92 MPa.

After cracking, a sudden increase in the tendon force was observed in the beams that exhibited large deflection and a wide crack. This increase in tendon stress ranged between 169.00 MPa and 280.25 MPa. In beams that were able to maintain the cracking load without additional member deflection, the tendon force increase at cracking was negligible. With further loading, additional deflection produced additional tendon stress.

In other beams that failed suddenly at cracking, it was not possible to measure the tendon force at the instant of failure. After failure the beam was supported by the safety equipment, so the tendon force measured after failure was not relevant.

Figures 4.13 and 4.14 represent the relationship between the applied load and the increase in tendon stress. These curves are similar to the load-deflection curves. Consequently, the increase in tendon stress and deflection are linearly

related up to yield, as shown in Fig. 4.15. This relationship has the same shape as the stress versus strain curve for the tendon.

Figure 4.16 shows that deflection is linearly related to the sum of the crack widths at the level of the tendon. Since the sum of the crack widths at the level of the tendon equals the change in tendon length, one can estimate the change in tendon stress from the member deflection. This is used in the prediction model that is developed in the following section.

4.7 Prediction of the Increase in Stress at Ultimate Using a Collapse Mechanism

Figure 4.17 shows a typical collapse mechanism to an unbonded prestressed member with one crack at mid-span. Unbonded prestressed members might develop more than one crack, especially when supplementary nonprestressed bonded reinforcement is present.

From the geometry in Fig. 4.17

$$\frac{\delta}{\Delta L/2} = \frac{L/2}{ad_p} \Rightarrow \Delta L = 4 \frac{\delta}{L} ad_p \quad (4.1)$$

$$\Delta \epsilon_p = \frac{\Delta L}{I_e} = \frac{\Delta f_p}{E_p} \Rightarrow \Delta L = \Delta f_p \frac{I_e}{E_p} \quad (4.2)$$

Solving eq. (4.1) and eq. (4.2)

$$\Delta f_p = 4 E_p \frac{ad_p}{I_e} \frac{\delta}{L} \quad (4.3)$$

where:

Δf_p = the increase in tendon stress that corresponds to a given deflection δ/L

l_e = the distance between the two anchorages

L = the distance between the supports

Experimental results from the literature review in chapter 2 showed that unbonded beams with or without nonprestressed bonded reinforcement had a deflection-to-span ratio at failure ranged between a minimum and maximum of 1/125 and 1/35 respectively. This deflection depends on the span-to-depth ratio, and the depth of the neutral axis, which in turn related to the amount of reinforcement provided in the member.

It is proposed that the limiting deflection at failure be taken as:

$$\frac{\delta}{L} = \frac{1}{100 - L/d_p} \quad (4.4)$$

with

$$\alpha d_p = (d_p - c) \quad (4.5a)$$

or

$$\alpha d_p = (d_p - (0.9 + \omega_p)c) \quad (4.5b)$$

For simpler calculation c could be taken as:

$$c = c_y \quad (4.6a)$$

The two equations for predicting increase in tendon stress at ultimate are thus:

$$\Delta f_p = 4E_p \frac{1}{100 - L/d_p} \frac{(d_p - c_y)}{l_e} \quad (4.7a)$$

$$\Delta f_p = 4E_p \frac{1}{100 - L/d_p} \frac{(d_p - (0.9 + \omega_p)c_y)}{l_e} \quad (4.7b)$$

For unbonded prestressed members with small amounts of supplementary bonded nonprestressed reinforcement ($\omega_s \leq 0.01$) where failure may be triggered by rupture of the bars, maximum deflection of $\delta/L = 1/150$ should be used.

Equations (4.7a) and (4.7b) give better predictions than either ACI 318-95 or CSA A23.3-94. Tables 4.2 and 4.3 compares the proposed equations with CSA and ACI for increase in tendon stress at ultimate and ultimate moment capacity respectively. The proposed equations has a mean test to predicted ratio close to 1.0 with smaller coefficient of variation to average test predicted ratio, standard deviation, and coefficient of variation. Both proposed equations (4.7a) and (4.7b) are about the same. Note that Tables include results from other investigators ($14 \leq L/d \leq 40$) and ($0.013 \leq \omega \leq 0.43$).

4.8 Prediction Model for Load-Deflection Relationship

The collapse mechanism represents a good model for predicting the load-deflection response of prestressed unbonded flexural members after cracking.

Before cracking, deflection was calculated using the elastic theory.

For the specimens tested:

$$\delta = \frac{Wl_1}{24EI} (3L^2 - 4l_1^2) - P \frac{eL^2}{8EI} \quad (4.8)$$

Where

W = the applied load

P = the strand force

l_1 = the distance from the reaction to the applied point load

The cracking load was obtained from the cracking moment:

$$M_{cr} = \left(\frac{P}{A} + \frac{Pe}{S} + 0.55\sqrt{f'_c} \right) S \quad (4.9)$$

Equations (4.7a) or (4.7b) can be used to easily predict the load-deflection response of the flexural members as follows:

1. choose a value of δ/L (δ_c/L to 1/50)
2. calculate c_y and $(\omega_p$ if Eq.(4.7b) is used)

$$c_y = \frac{A_p f_{py} + A_s f_y}{\alpha_1 \beta f'_c b} \quad \text{and} \quad \omega_p = \frac{\rho_p f_{pe}}{f'_c}$$

3. calculate the increase tendon stress corresponding to this deflection

$$\Delta f_p = 4E_p \frac{\delta (d_p - c_y)}{L l_e} \quad \text{or} \quad \Delta f_p = 4E_p \frac{\delta (d_p - (0.9 + \omega_p)c_y)}{L l_e}$$

$$\text{tendon stress } f_p = f_{pe} + \Delta f_p \leq f_{py}$$

4. calculate c

$$c = \frac{A_p f_p + A_s f_y}{\alpha_1 \beta f'_c b}$$

5. calculate M

$$M = A_p \times f_p (d_p - \beta_1 c/2) + A_s \times f_y (d - \beta_1 c/2)$$

$$\text{where } \beta_1 = 0.97 - 0.0025 f_c$$

$$\alpha_1 = 0.85 - 0.0015 f_c$$

6. calculate load W corresponding to M

Repeat these steps for different values of deflection.

For better response predictions one should use c rather c_y . To account for the part of the stress-strain curve for prestressing steel near and after yield, the Ramberg-Osgood equation can be used. These refined procedures will be followed:

- 1) choose a value of δ/L (δ_{cr}/L to $1/50$)
- 2) calculate tendon stress corresponding to this deflection as follows:
 - a) initial strain in the pretressing steel

$$\varepsilon_p = \frac{f_{pe}}{E_p}$$

- b) change in strain due to the elongation in the tendon corresponding to the chosen deflection

$$\Delta\varepsilon_p = \frac{\Delta L}{l_e} = \frac{4(d_p - (0.9 + \omega_p)c)\delta}{l_e} \quad \text{which is an equation in terms of } c$$

- c) total prestressing steel strain

$$\varepsilon_p = \varepsilon_{pi} + \Delta\varepsilon_p = \frac{f_{pe}}{E} + \frac{4(d_p - c)\delta}{l_e} \frac{L}{L}$$

- d) tendon stress corresponding to this strain using Ramberg-Osgood equation

$$f_p = 204000\varepsilon_p \left[0.0205 + \frac{0.9795}{\left[1 + (113\varepsilon_p)^{10.25} \right]^{(1/30.25)}} \right]$$

which is an equation in terms of c

- 3) solve the previous equation for f_p and c such that

$$\text{Tension force} = \text{Compression force}$$

$$A_s \times f_y + A_p \times f_p = \alpha_1 \beta_1 b c f_c$$

4) calculate moment $M = A_p \times f_p (d_p - \beta_1 c/2) + A_s \times f_y (d - \beta_1 c/2)$

5) calculate load W corresponding to M

A complete set of test and predicted load-deflection curves is presented in Appendix B along with selected tests from other researches. A complete example calculation is presented in Appendix C.

The figures in Appendix B. show that:

- the predictions are excellent for members without bonded reinforcement regardless of the amount of unbonded prestressed reinforcement
- for members with significant amount of bonded reinforcement ($\rho \geq 0.003$) the model slightly over estimate the loads and moments after cracking because the model assumes the bars yield but it requires somewhat more deflection to yield the bars
- the predictions are good for members with nonprestressed bonded reinforcement, but the loads and moments at ultimate are slightly under estimated because strain hardening of the bonded reinforcement was neglected

4.9 Comparison of Test Results with the Current Codes

Table 4.2 shows a comparison of the value of the tendon stress increases at ultimate (Δf_{pr}) obtained in the test program with (Δf_{pr}) as calculated using ACI 318-95 and A23.3-94.

Both ACI 318-95 and A23.3-94 either under estimate or over estimate the increase in tendon stress at ultimate, but the predicted ultimate capacity by both codes is in the acceptable range for most prestressed members.

All beams tested in this program had a combined reinforcement index less than 0.05 which is low compared with current practice. The amount of unbonded prestressed reinforcement was less than the minimum amount required in ACI 318-95 and CSA A 23.3-94. All of the beams that had a predicted $M_u / M_{cr} \approx 1.00$ had a test M_u greater than $1.2M_{cr}$. The procedure used to predict M_u and M_{cr} in ACI and CSA appear to be unnecessarily conservative.

It is obvious that ACI is unnecessarily conservative and does not account for several of the important variables when predicting f_{pr} . CSA is somewhat better since it based on a mechanism analysis but still does not account for L/d. Equations (4.6a) and (4.7b) should be considered for implementation in the codes.

Table 4.1 Measured vs Predicted Ultimate Moment Capacity

Series	Specimen No	ε_c	Mu (ACI) [kN.m]	Mu (CSA) [kN.m]	Mu Measured [kN.m]	Mu Measured Mu (ACI)	Mu Measured Mu (CSA)
Intermediate Strength Concrete Series	R-1	-0.002430	13.89	14.30	17.24	1.24	1.21
	R-2	-0.003180	17.89	18.03	19.41**	1.08	1.08
	R-3	-0.0033300	21.41	21.56	26.78	1.25	1.24
	R-4		11.81	12.02	14.07*	1.19	1.17
	R-5	-0.001510	15.90	15.64	15.41**	0.97	0.99
	R-6	-0.001210	11.02	11.14	15.99	1.45	1.45
	R-7	-0.001000	7.40	7.45	11.53	1.55	1.55
High Strength Concrete Series	RH-1	-0.003600	29.97	29.66	31.05	1.11	1.12
	RH-2		20.22	18.30	20.91*	1.03	1.14
	RH-3	-0.001620	23.89	21.96	21.87**	0.92	1.00
	RH-4	-0.001660	27.53	25.55	27.75	1.01	1.09

* The recorded moment is M_{cr} , since these beams failed suddenly at cracking

** Reinforcing bar fractured before tendon strength was fully mobilized

**Table 4.2 Comparison of Proposed Equations, CSA, and ACI
for Increase in Tendon Stress at Ultimate**

Author	Specimen No	L/d	Δf_{ps} test		f_{ps} (Eq.4.7a)		f_{ps} (Eq.4.7b)		f_{ps} CSA		f_{ps} ACI		Δf_{ps} test		f_{ps} (Eq.4.7a)		f_{ps} (Eq.4.7b)		f_{ps} CSA		f_{ps} ACI		
			[MPa]	[MPa]	[MPa]	[MPa]	[MPa]	[MPa]	[MPa]	[MPa]	[MPa]	[MPa]	[MPa]	[MPa]	[MPa]	[MPa]	[MPa]	[MPa]	[MPa]	[MPa]	[MPa]	[MPa]	
Daher [This Thesis]																							
R-1	14.25	740.37	538.20	541.36	452.46	402.12	1.38	1.37	1.64	1.84													
R-2	14.25	341.94	204.93	306.98	448.43	426.22	1.12	1.11	0.76	0.80													
R-3	14.25	706.21	525.59	529.67	441.85	421.19	1.34	1.33	1.60	1.68													
*R-4	14.25	7.94	545.65	548.52	458.72	463.01																	
R-5	14.25	254	308.58	310.48	453.76	483.37	0.82	0.82	0.56	0.53													
RH-1	14.25	497.88	501.71	505.53	421.78	433.41	0.99	0.98	1.18	1.15													
*RH-2	14.25	3.69	315.79	317.43	464.40	869.02																	
RH-3	14.25	236.14	313.23	315.09	460.63	875.81	0.75	0.75	0.51	0.27													
RH-4	14.25	608.78	542.66	546.33	456.21	835.08	1.12	1.11	1.33	0.73													
Chouinard [1989]																							
B1	15	386	367.56	361.67	205.54	145.56	1.08	1.09	1.93	2.72													
B2	15	402	315.41	307.61	282.21	144.85	1.27	1.31	1.42	2.78													
B3	15	332	269.01	248.67	231.74	142.95	1.28	1.34	1.43	2.32													
B4	15	252	246.07	239.40	220.16	156.00	1.02	1.05	1.14	1.62													
B5	15	193	202.65	195.77	181.32	156.71	0.95	0.99	1.06	1.23													
B6	15	183	157.45	149.37	140.88	156.71	1.16	1.16	1.23	1.17													
Ospina [1997]																							
R1	15	639.6	458.12	462.51	396.98	244.25	1.40	1.38	1.61	2.62													
R2	15	592	490.67	494.16	425.18	362.15	1.21	1.20	1.39	1.63													
R3	15	412.2	481.90	485.55	417.58	389.42	0.86	0.85	0.99	1.03													
R4	15	504.1	497.64	500.62	431.23	532.93	1.01	1.01	1.17	0.95													
R5	15	623.6	477.23	480.42	413.54	295.55	1.31	1.30	1.51	2.11													
R6	15	475.1	491.04	493.96	425.51	365.45	0.97	0.96	1.12	1.30													
R7	15	639.1	463.95	467.86	402.03	303.04	1.38	1.37	1.59	2.11													
R8	15	486.9	440.19	444.07	381.44	249.40	1.06	1.05	1.22	1.87													
Du and Tao [1985]																							
a1	19.09	498	404.50	408.32	319.29	251.18	1.23	1.22	1.56	1.98													
a2	19.09	526	352.50	354.85	278.25	177.91	1.49	1.48	1.89	2.96													
a3	19.09	356	277.27	273.25	218.86	136.69	1.28	1.30	1.63	2.60													

Table 4.2 Comparison of Proposed Equations, CSA, and ACI for Increase in Tendon Stress at Ultimate, (Continued)

beams failed suddenly at cracking

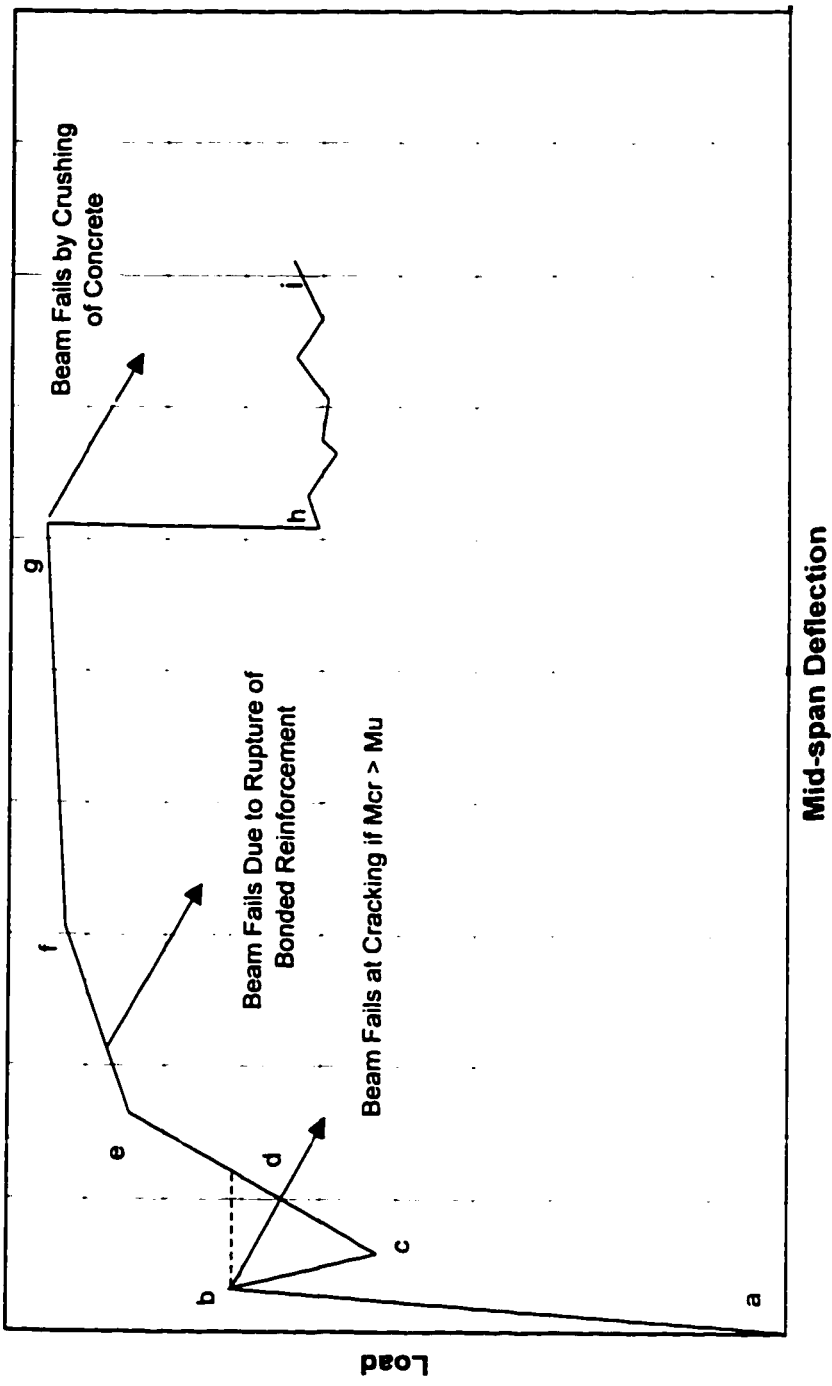
**Table 4.3 Comparison of Proposed Equations, CSA, and ACI
for Ultimate Moment Capacity**

Author	Specimen No	L/d	M _{test} [kN]	M _u (Eq. 4.7a) [kN]	M _u (Eq. 4.7b) [kN]	M _u CSA [kN]	M _u ACI [kN]	M _{test} (Eq. 4.7a) [kN]	M _u (Eq. 4.7b) [kN]	M _{test} Mu CSA	M _{test} Mu ACI
Daher [This Thesis]											
R-1	14.25	17.24	15.06	15.08	14.30	13.89	1.15	1.14	1.21	1.24	
R-2	14.25	19.41	16.76	16.78	18.03	17.89	1.16	1.16	1.08	1.09	
R-3	14.25	26.78	22.24	22.28	21.52	21.41	1.20	1.20	1.24	1.25	
*R-4	14.25	14.07	12.67	12.69	12.02	12.08	1.11	1.11	1.17	1.16	
R-5	14.25	15.41	14.57	14.58	15.64	15.90	1.06	1.06	0.99	0.97	
RH-1	14.25	31.05	29.10	29.17	27.70	28.09	1.07	1.06	1.12	1.11	
*RH-2	14.25	20.91	16.95	16.96	18.30	20.22	1.23	1.23	1.14	1.03	
RH-3	14.25	21.87	20.62	20.64	21.96	23.89	1.06	1.06	1.00	0.92	
RH-4	14.25	27.75	26.32	26.36	25.55	27.53	1.05	1.05	1.09	1.01	
Chouinard [1989]											
B1	15	45.50	41.75	41.61	37.63	36.29	1.09	1.09	1.21	1.25	
B2	15	63.30	55.78	55.61	55.03	52.34	1.13	1.14	1.15	1.21	
B3	15	81.10	68.21	68.01	67.67	66.67	1.19	1.19	1.20	1.22	
B4	15	98.00	84.80	84.68	84.32	84.35	1.16	1.16	1.16	1.16	
B5	15	105.50	96.40	96.29	96.04	97.39	1.09	1.09	1.10	1.08	
B6	15	120.20	107.04	106.92	106.80	109.40	1.12	1.12	1.13	1.10	
Ospina [1997]											
R1	15	26.01	22.10	22.18	21.06	18.51	1.18	1.17	1.24	1.41	
R2	15	12.49	12.23	12.26	11.58	10.99	1.02	1.02	1.08	1.14	
R3	15	28.49	28.83	28.90	27.71	27.57	0.99	0.99	1.03	1.03	
R4	15	22.34	21.07	21.11	20.22	21.33	1.06	1.06	1.10	1.05	
R5	15	21.36	19.60	19.64	18.83	17.44	1.09	1.09	1.13	1.22	
R6	15	16.37	15.82	15.85	15.18	14.64	1.03	1.03	1.08	1.12	
R7	15	41.62	35.20	35.29	33.87	31.96	1.18	1.18	1.23	1.30	
R8	15	49.74	46.00	46.11	44.34	40.98	1.08	1.08	1.12	1.21	
Du and Tao [1985]											
a1	19.09	31.10	26.24	26.28	25.29	24.61	1.19	1.18	1.23	1.26	
a2	19.09	46.80	39.35	39.39	38.10	36.59	1.19	1.19	1.23	1.28	
a3	19.09	63.60	53.72	53.62	52.33	50.77	1.18	1.18	1.22	1.25	
a4	19.09	38.30	30.60	30.66	29.71	29.23	1.25	1.25	1.29	1.31	

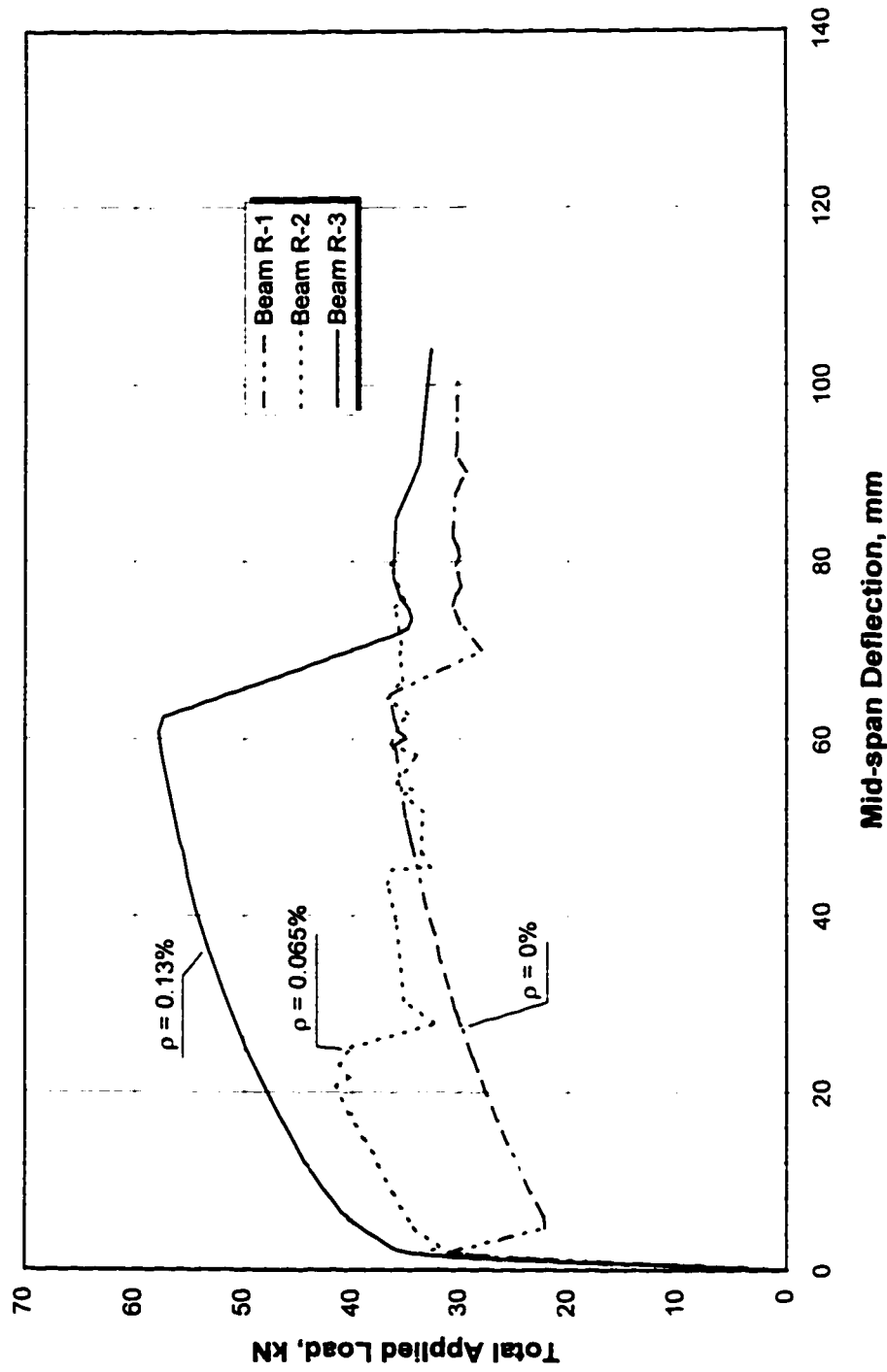
**Table 4.3 Comparison of Proposed Equations, CSA, and ACI
for Ultimate Moment Capacity, (Continued)**

Author	Specimen No	L/d	M _u test [kN]	M _u (Eq. 4.7a) [kN]	M _u (Eq. 4.7b) [kN]	M _u CSA [kN]	M _u ACI [kN]	M _{test} Mu (Eq. 4.7a)	M _{test} Mu (Eq. 4.7b)	M _{test} Mu CSA	M _{test} Mu ACI
Du and Tao [1985]	a5	19.09	51.20	44.80	44.88	43.87	43.37	1.14	1.14	1.17	1.18
	a6	19.09	72.40	67.51	67.38	66.53	66.47	1.07	1.07	1.09	1.09
	a7	19.09	41.50	37.86	37.91	37.32	37.86	1.10	1.10	1.11	1.10
	a8	19.09	59.40	54.16	54.24	53.52	54.05	1.10	1.10	1.11	1.10
	a9	19.09	102.50	88.75	88.62	88.18	90.01	1.15	1.16	1.16	1.14
	b1	19.09	30.30	27.72	27.76	26.58	26.76	1.09	1.09	1.14	1.13
	b2	19.09	50.40	43.01	43.08	41.38	40.36	1.17	1.17	1.22	1.25
	b3	19.09	61.00	61.08	61.08	59.19	57.54	1.00	1.00	1.03	1.06
	b4	19.09	38.40	33.52	33.58	32.45	32.62	1.15	1.14	1.18	1.18
	b5	19.09	53.40	49.35	49.43	48.16	48.10	1.08	1.08	1.11	1.11
Park [1981]	b6	19.09	75.80	73.06	73.10	71.84	71.40	1.04	1.04	1.06	1.06
	b7	19.09	42.50	40.38	40.43	39.67	41.30	1.05	1.05	1.07	1.03
	b8	19.09	63.10	57.25	57.33	56.42	57.36	1.10	1.10	1.12	1.10
	b9	19.09	89.70	91.62	91.74	90.68	92.40	0.98	0.98	0.99	0.97
	1	40	42.80	36.40	35.90	35.02	35.03	1.18	1.19	1.22	1.22
	2	40	45.70	41.97	41.92	39.42	38.29	1.09	1.09	1.16	1.19
	3	40	21.90	20.28	20.30	18.73	18.89	1.08	1.08	1.17	1.16
	4	30	44.00	38.25	37.83	36.91	36.75	1.15	1.16	1.19	1.20
	5	30	47.70	43.87	43.85	41.60	41.08	1.09	1.09	1.15	1.16
	6	30	20.80	21.20	21.22	19.87	22.01	0.98	0.98	1.05	0.94
	7	20	44.10	38.26	37.58	37.28	35.93	1.15	1.17	1.18	1.23
	8	20	47.40	45.66	45.59	43.86	40.78	1.04	1.04	1.08	1.16
	9	20	20.60	21.92	21.92	21.04	21.95	0.94	0.94	0.98	0.94

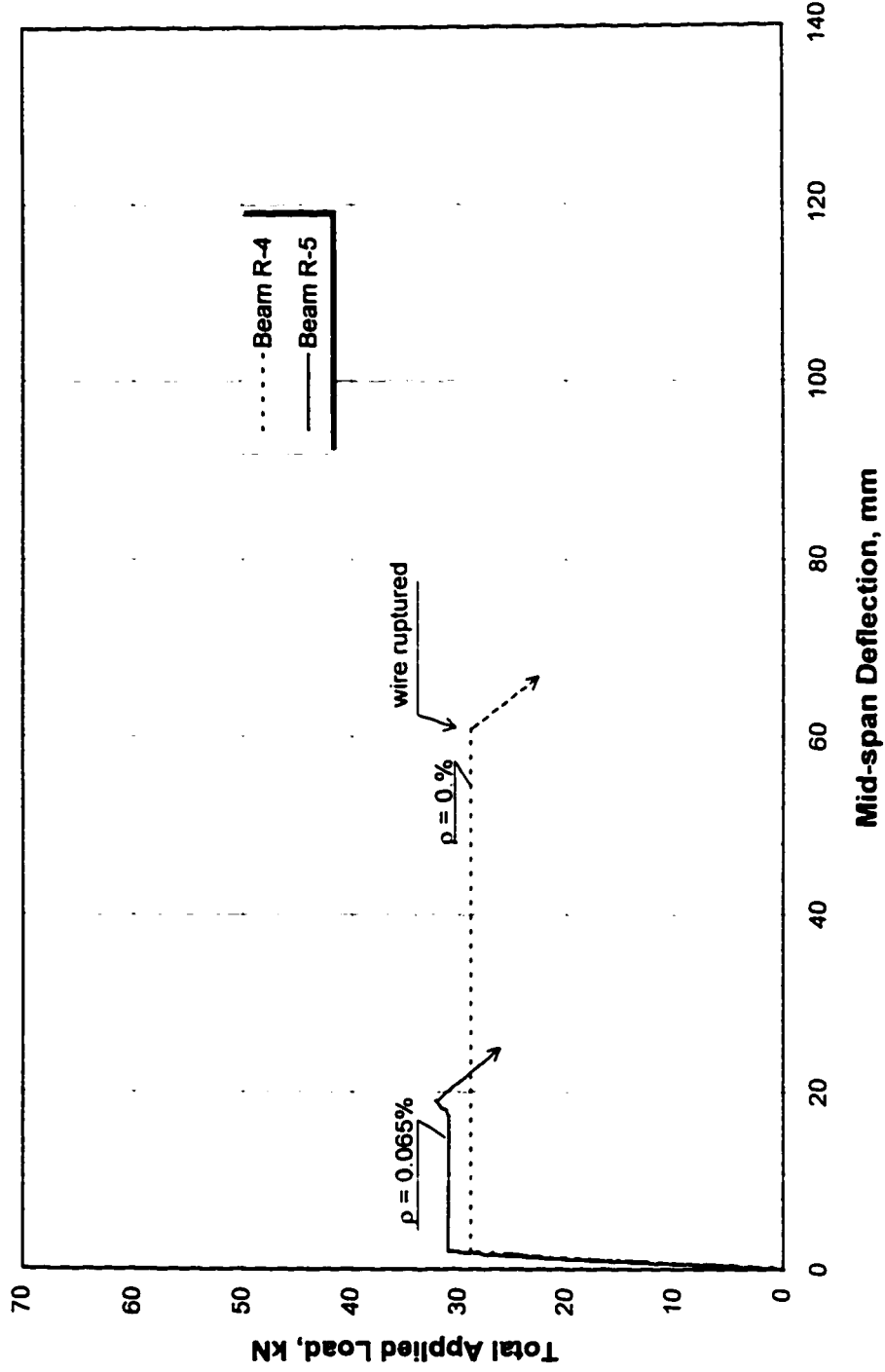
Figure 4.1 Idealized Member Response for Lightly Prestressed Unbonded Concrete Flexural Members



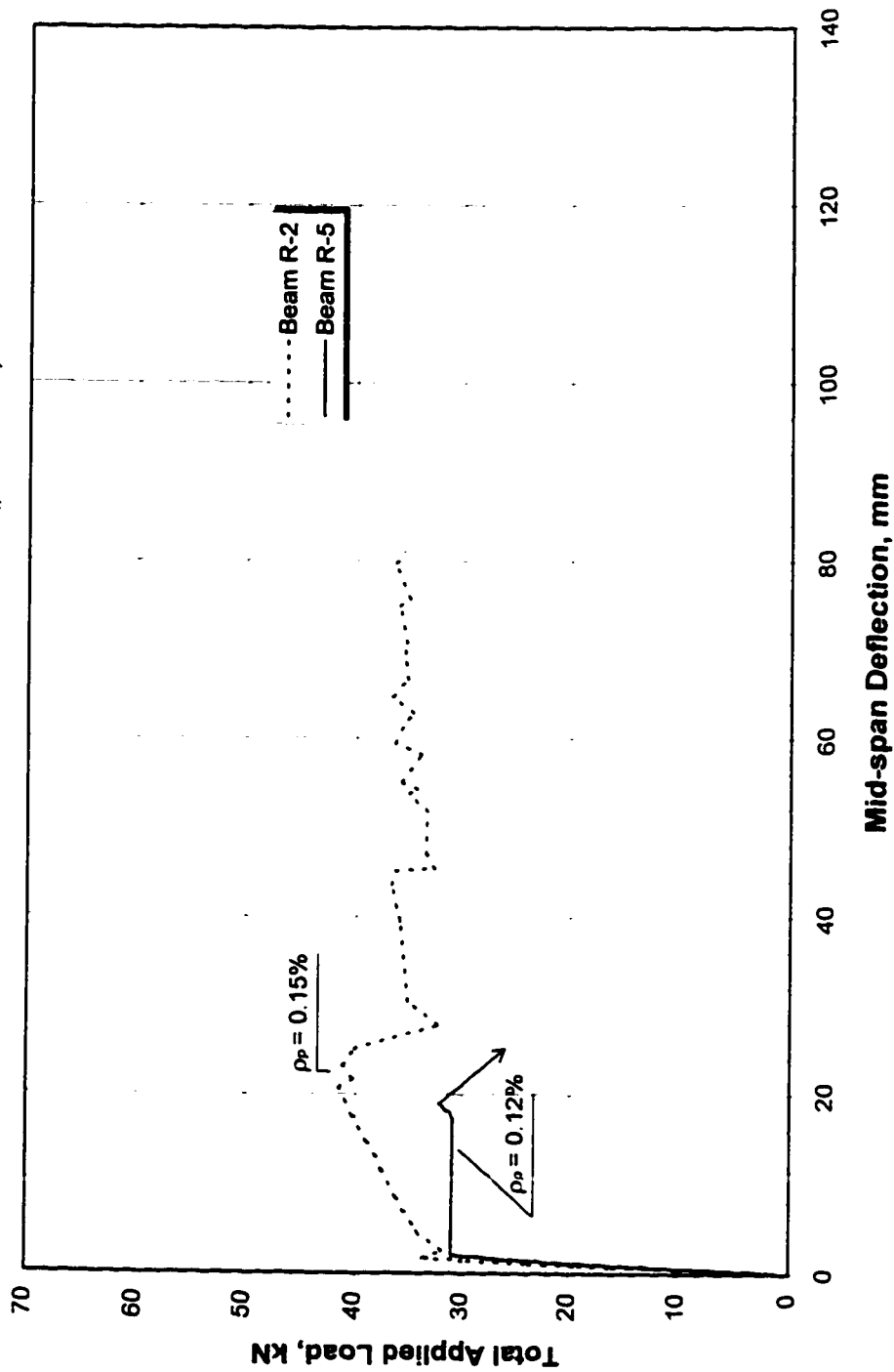
**Figure 4.2 Total Applied Load vs Mid-span Deflection
Beams R-1, R-2, and R-3 ($\rho_p=0.15\%$)**



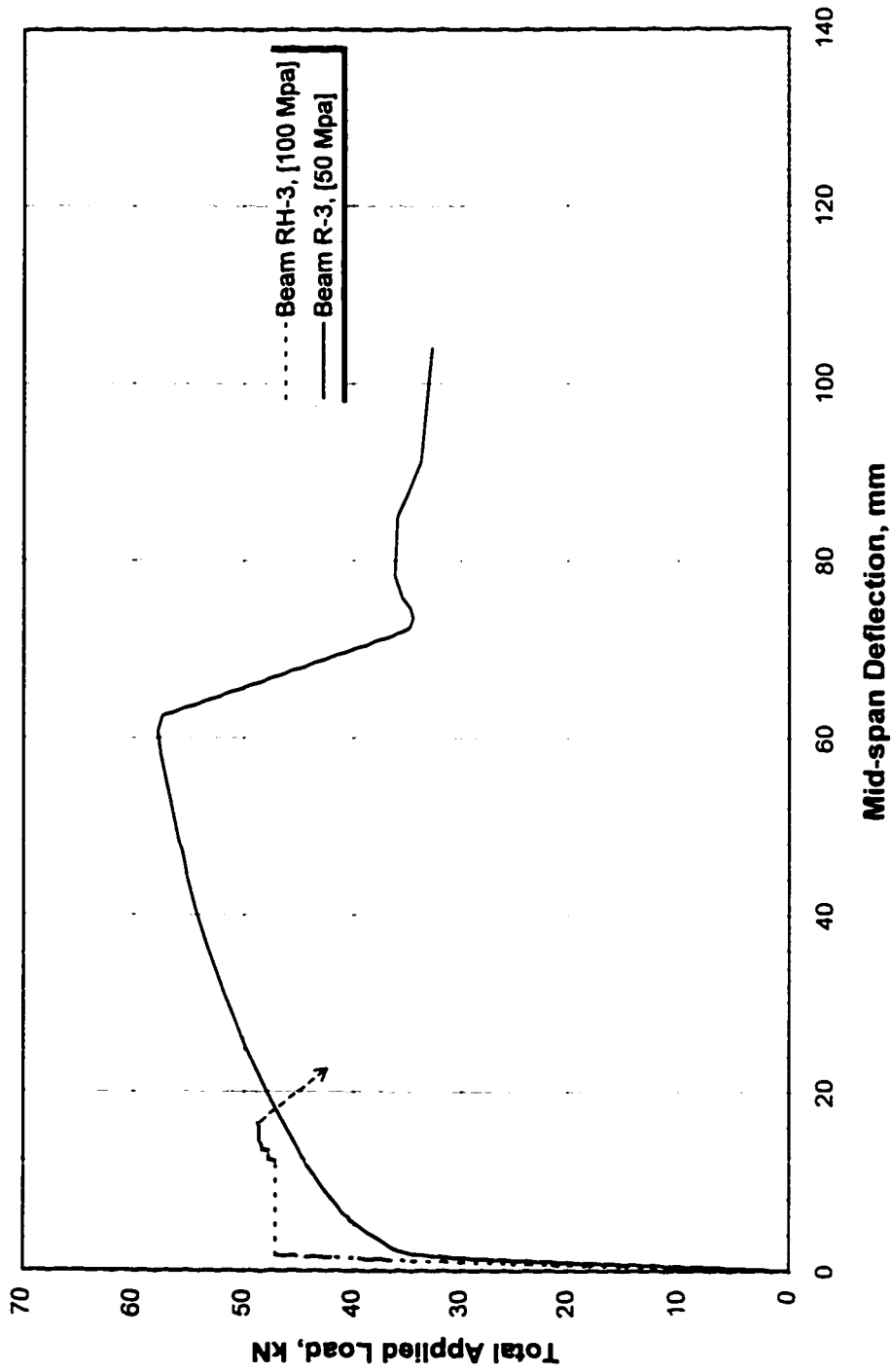
**Figure 4.3 Total Applied Load vs Mid-span Deflection
Beams R-4, and R-5 ($p_r=0.12\%$)**



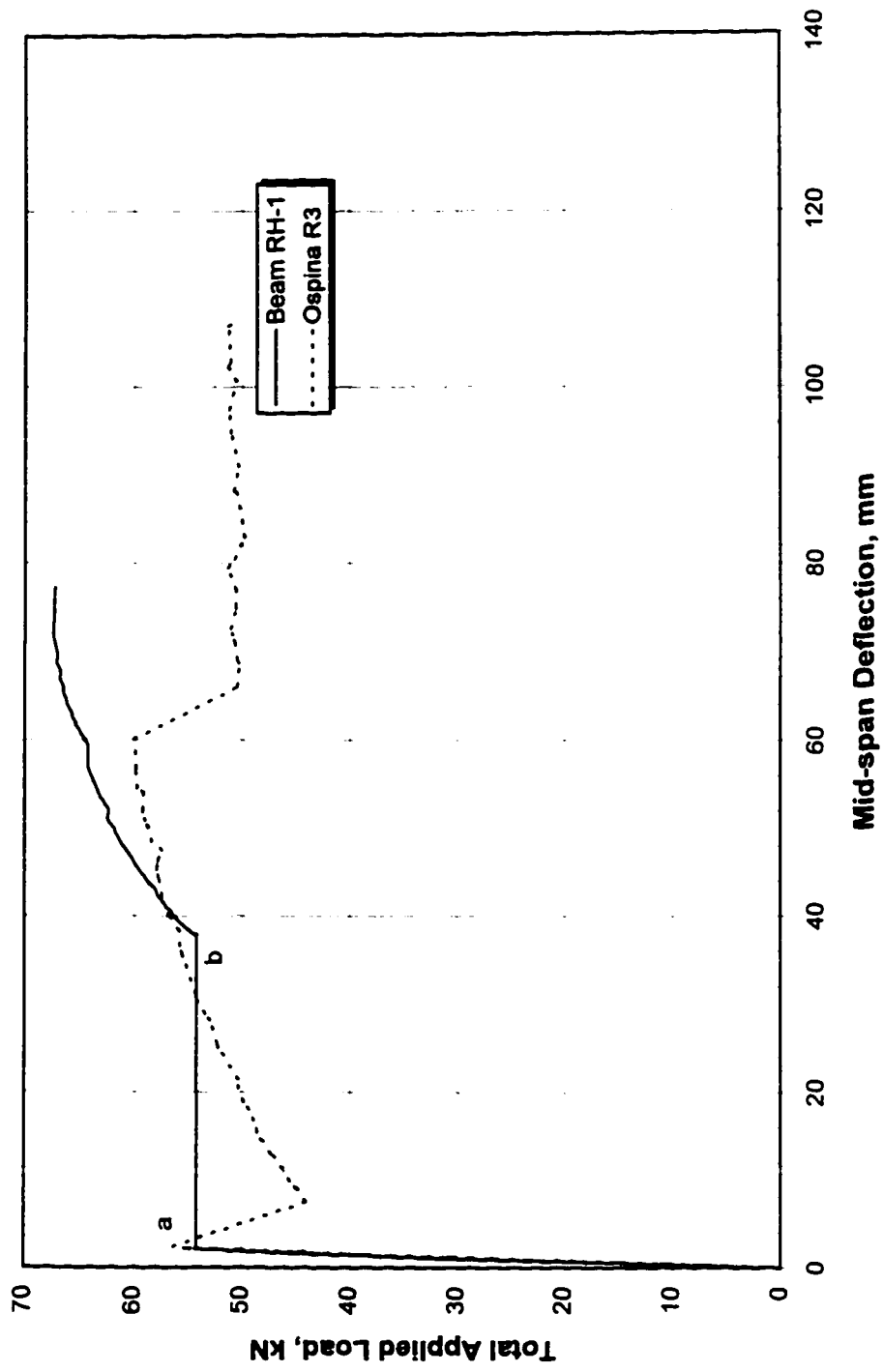
**Figure 4.4 Total Applied Load vs Mid-span Deflection
Beams R-2 and R-5 ($\rho=0.065\%$)**



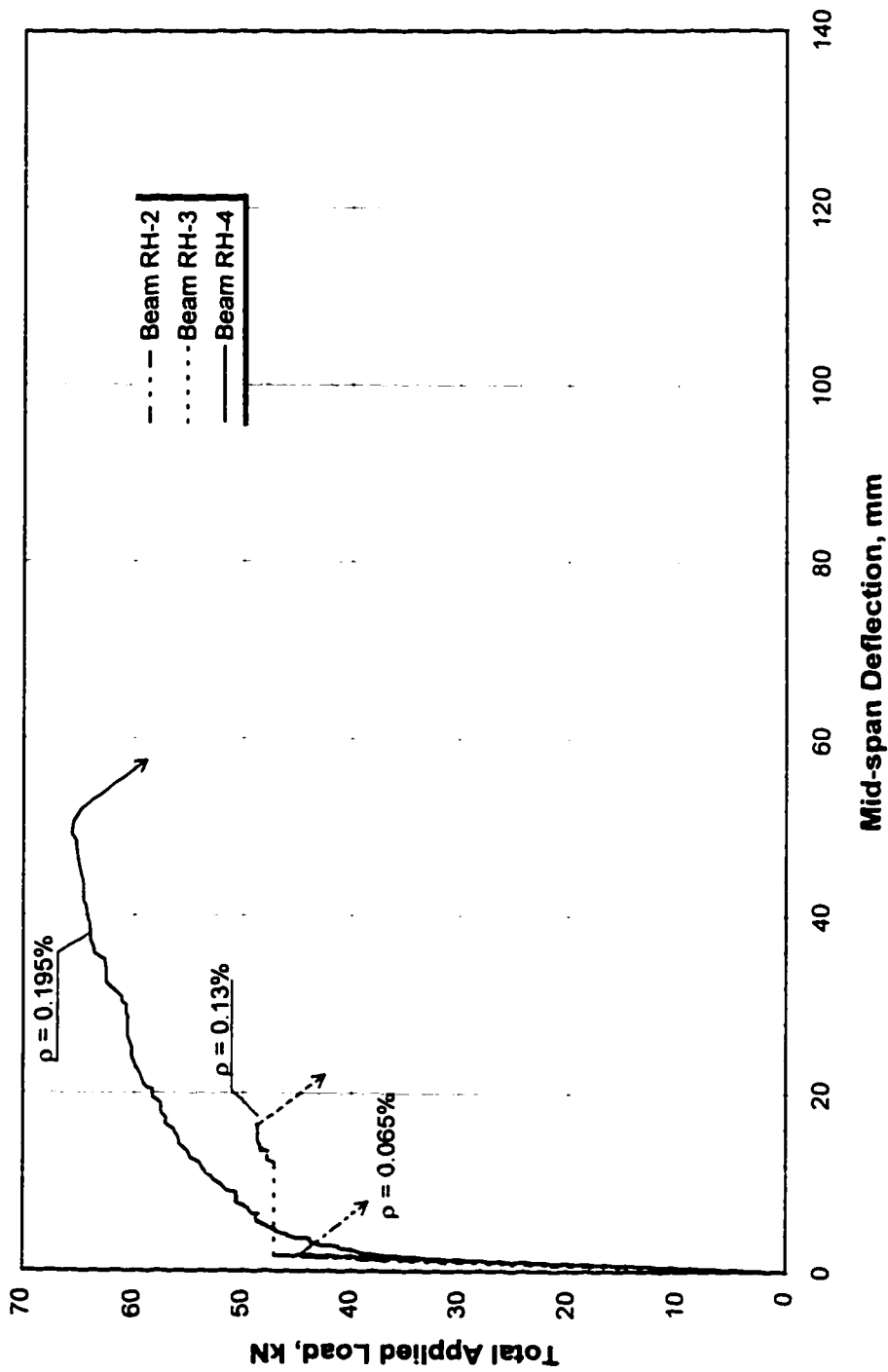
**Figure 4.5 Total Applied Load vs Mid-span Deflection
Beams R-3 and RH-3 ($\rho_p=0.15\%$, $\rho=0.13\%$)**



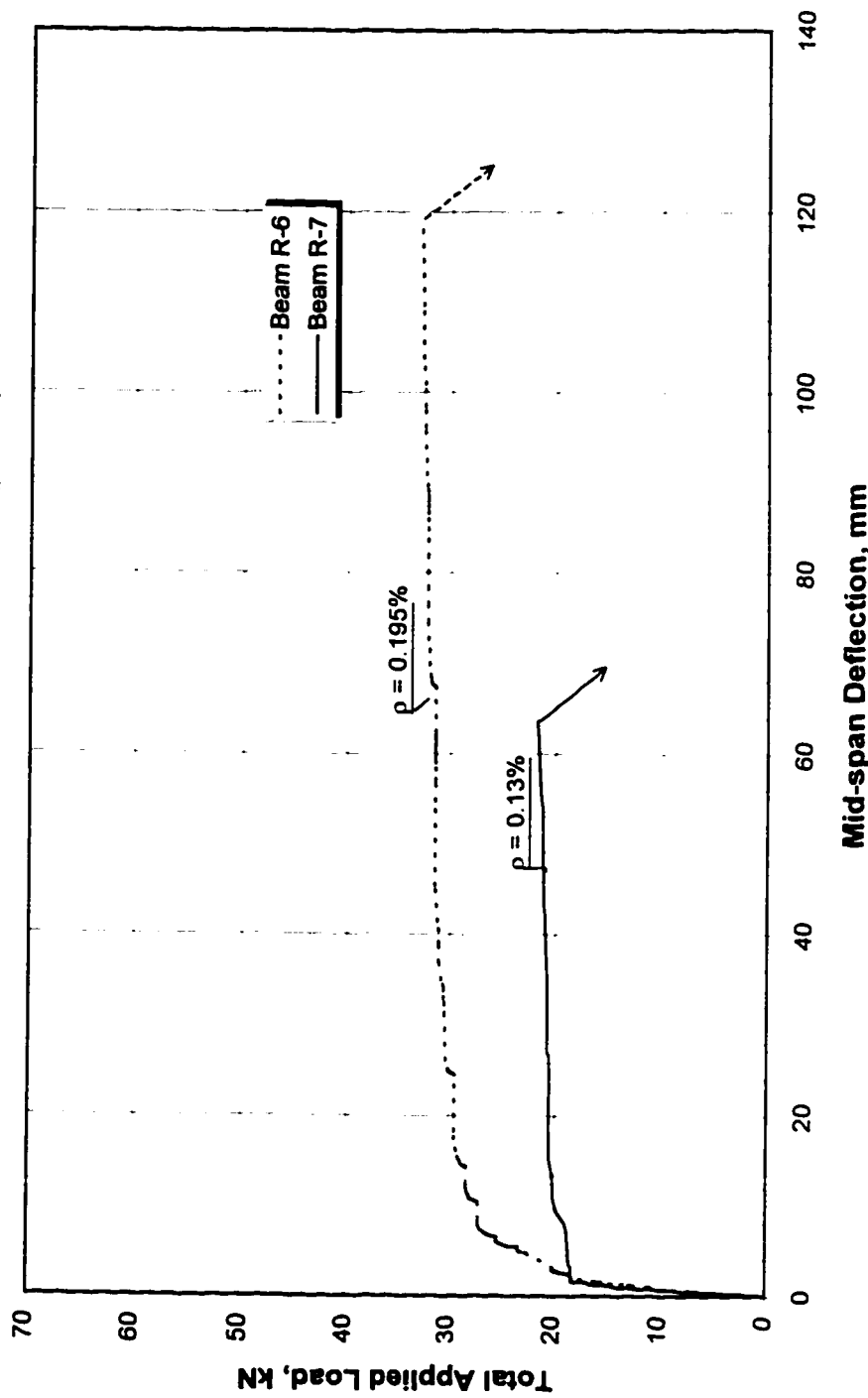
**Figure 4.6 Total Applied Load vs Mid-span Deflection
(Ospina R3) & Beam RH-1 ($\rho_p=0.3\%$, $p = 0\%$)**

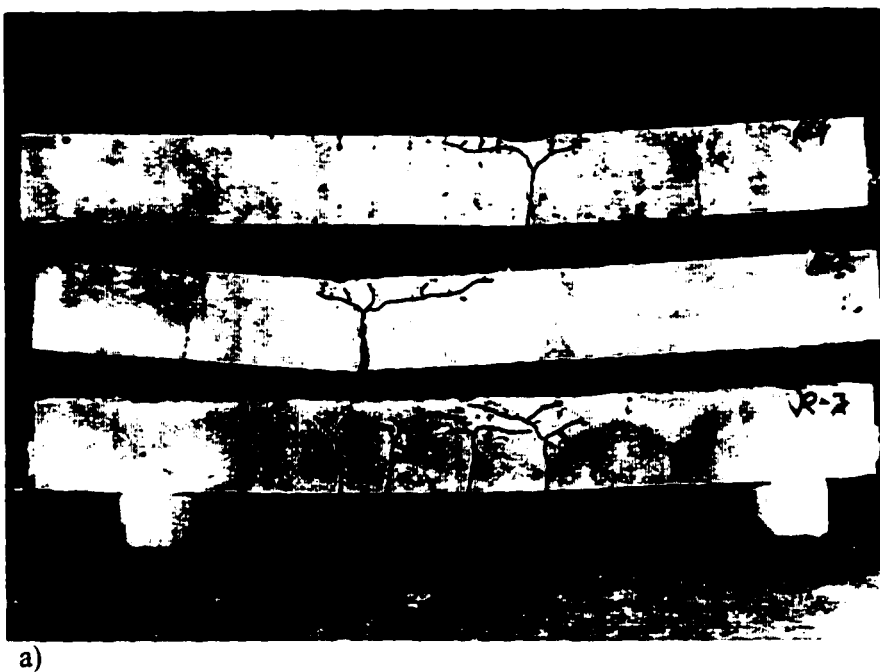


**Figure 4.7 Total Applied Load vs Mid-span Deflection
Beams RH-2, RH-3, and RH-4 ($\rho_p=0.15\%$)**

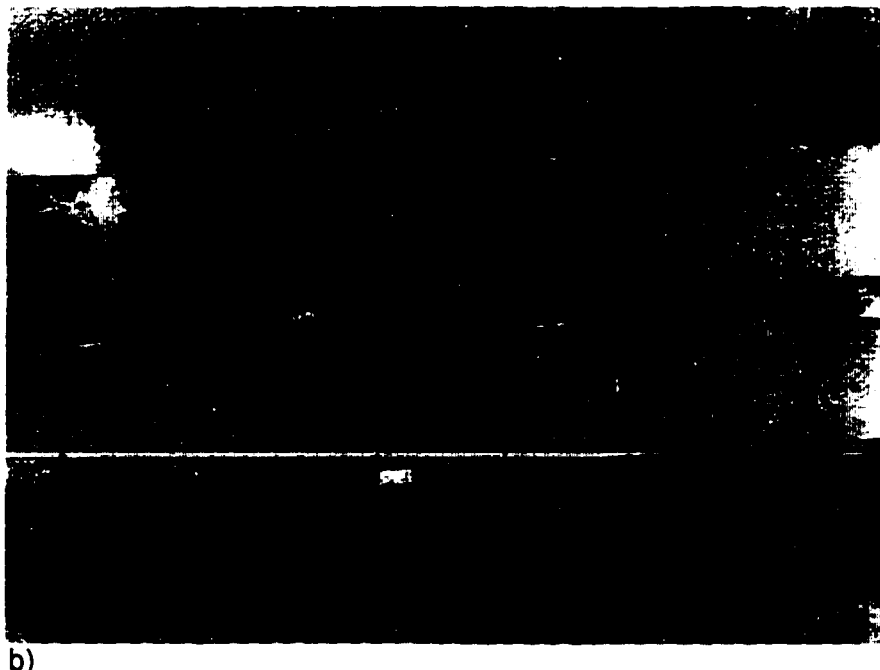


**Figure 4.8 Total Applied Load vs Mid-span Deflection
Beams R-6 and R-7 ($\rho_p=0\%$)**





a)

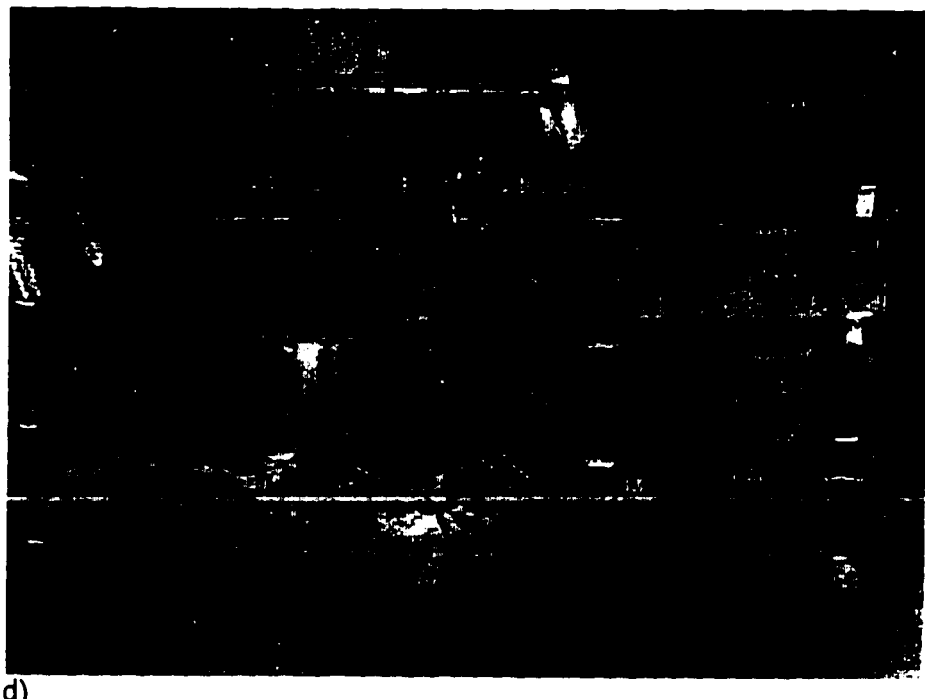


b)

Figure 4.9 Crack Pattern



c)



d)

Figure 4.9 Crack Pattern (Continued)

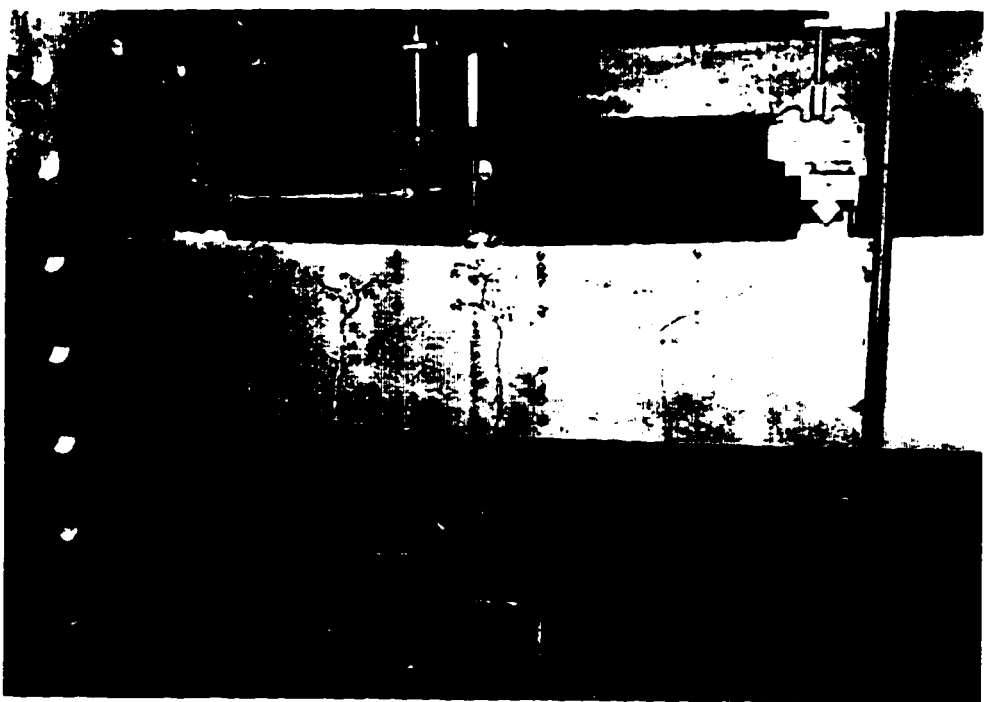
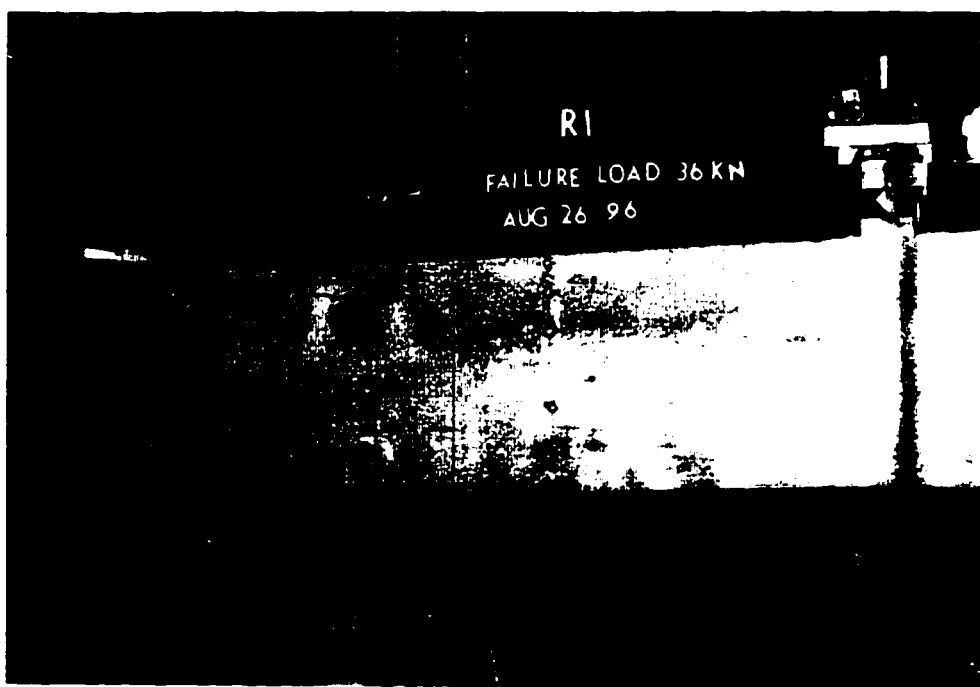


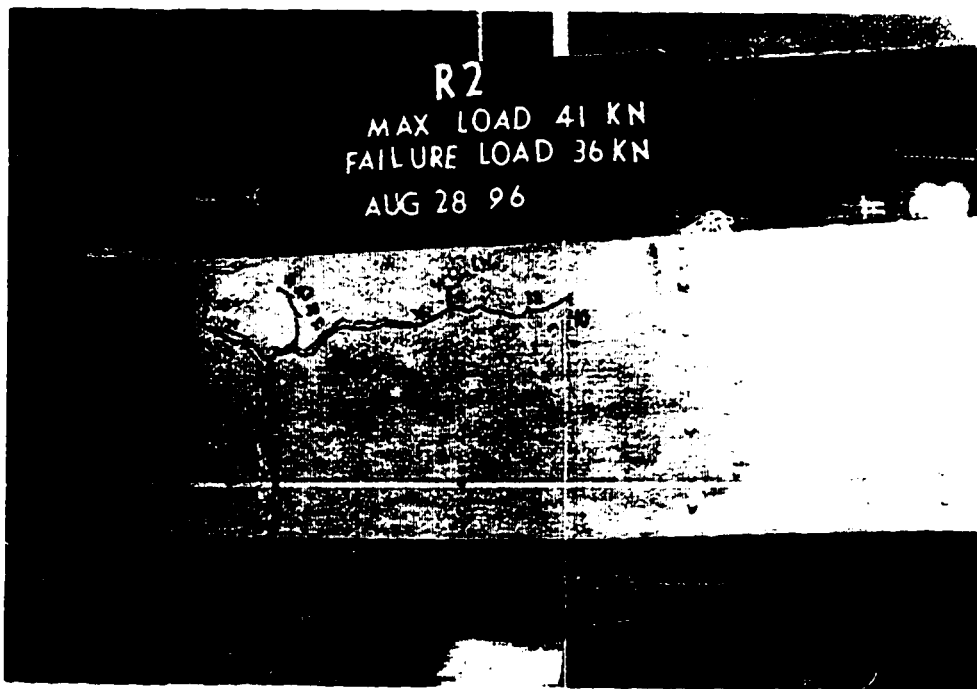
**Figure 4.10 (a) Crack Development of Specimen R-3
at 95% of the Load**



**Figure 4.10 (b) Crack Development of Specimen RH-1
at Cracking Load**

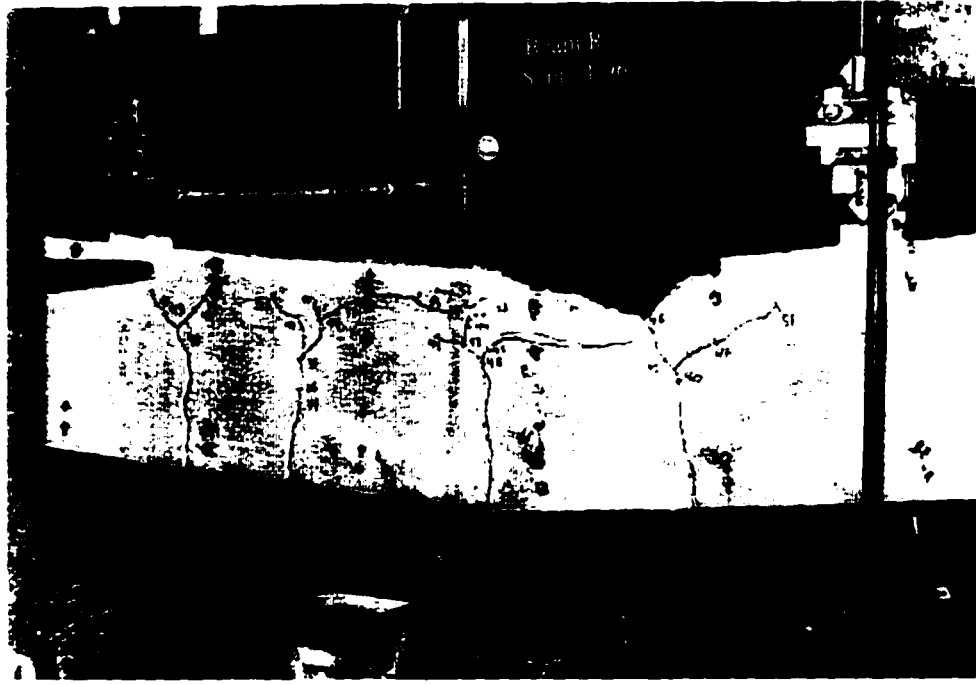


a) R-1 Yielding of prestressed reinforcement followed by
Initial crushing of concrete and tension failure



b) R-2 Rupture of nonprestressed reinforcement

Figure 4.11 Failure Modes



c) R-3 Yielding of the reinforcement followed by
crushing of concrete



d) R-4 Sudden collapse, Tension failure

Figure 4.11 Failure Modes (Continued)

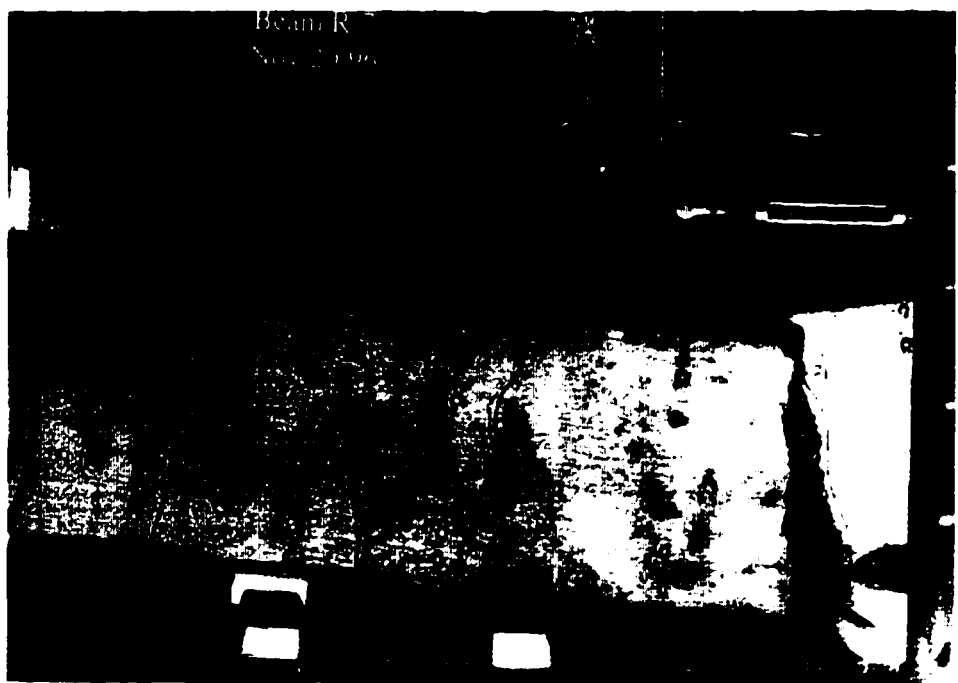


e) R-5 Tension failure



f) R-6 Tension failure with excessive cracking

Figure 4.11 Failure Modes (Continued)

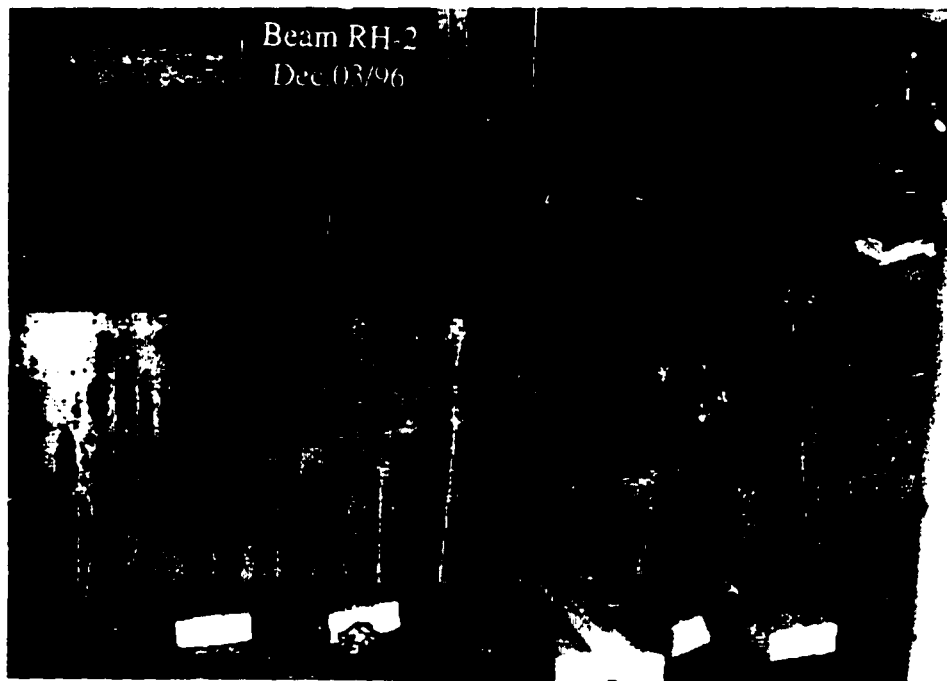


g) R-7 Tension failure

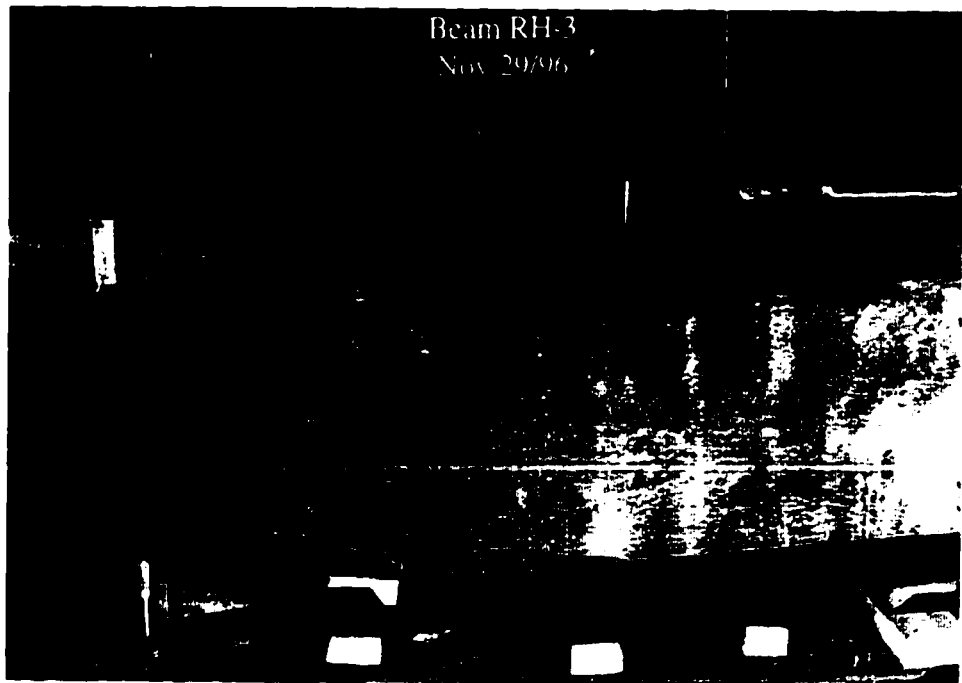


h) RH-1 Compression failure

Figure 4.11 Failure Modes (Continued)



i) RH-2 Sudden collapse, Tension failure



j) RH-3 Tension failure

Figure 4.11 Failure Modes (Continued)



k) RH-4 Tension failure

Figure 4.11 Failure Modes (Continued)

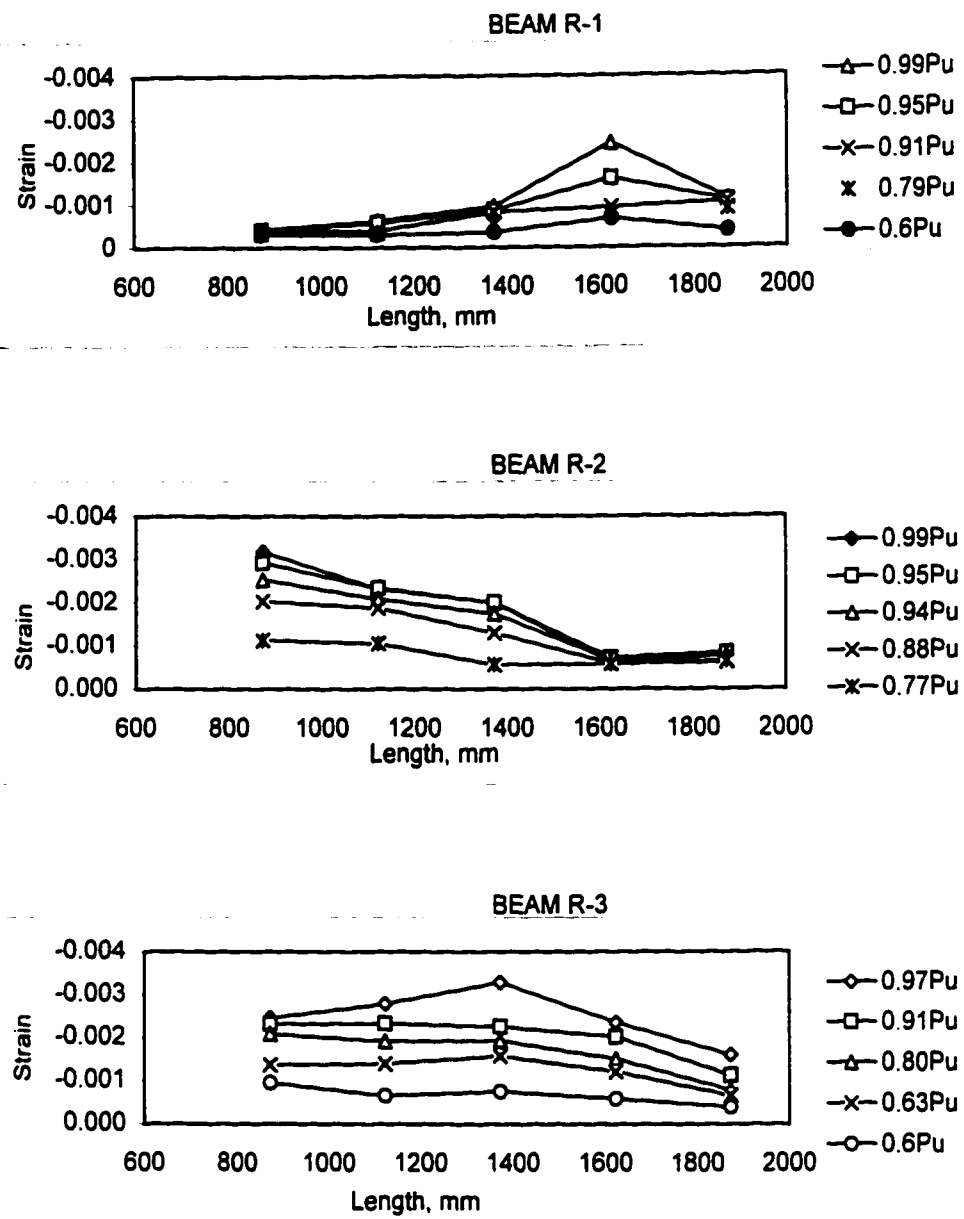


Figure 4.12 Distribution of Concrete Strain in the Extreme Compression Fibers Along the Flexural Span

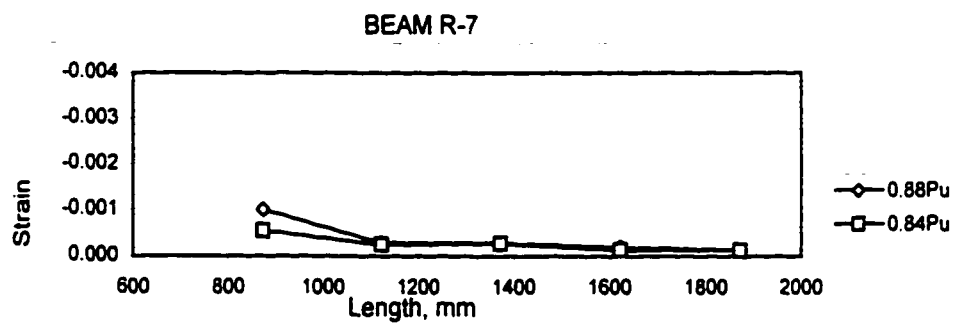
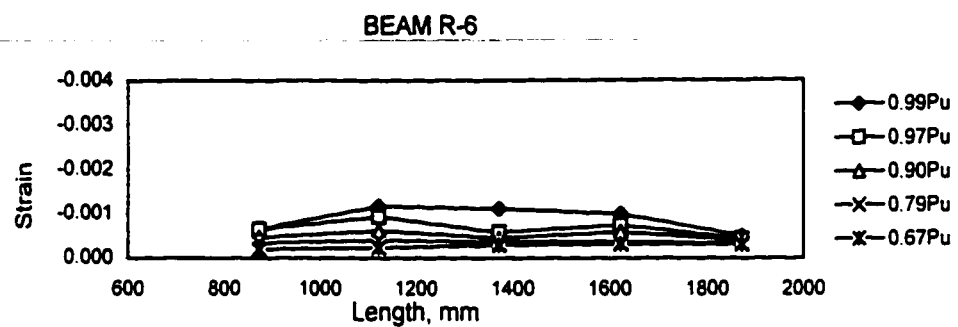
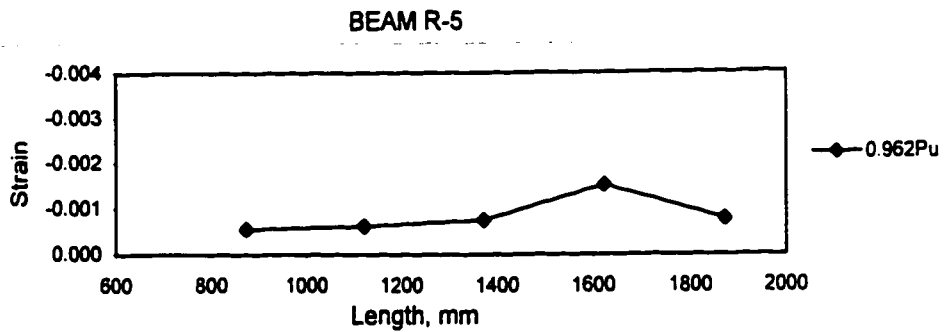


Figure 4.12 Distribution of Concrete Strain in the Extreme Compression Fibers Along the Flexural Span (Continued)

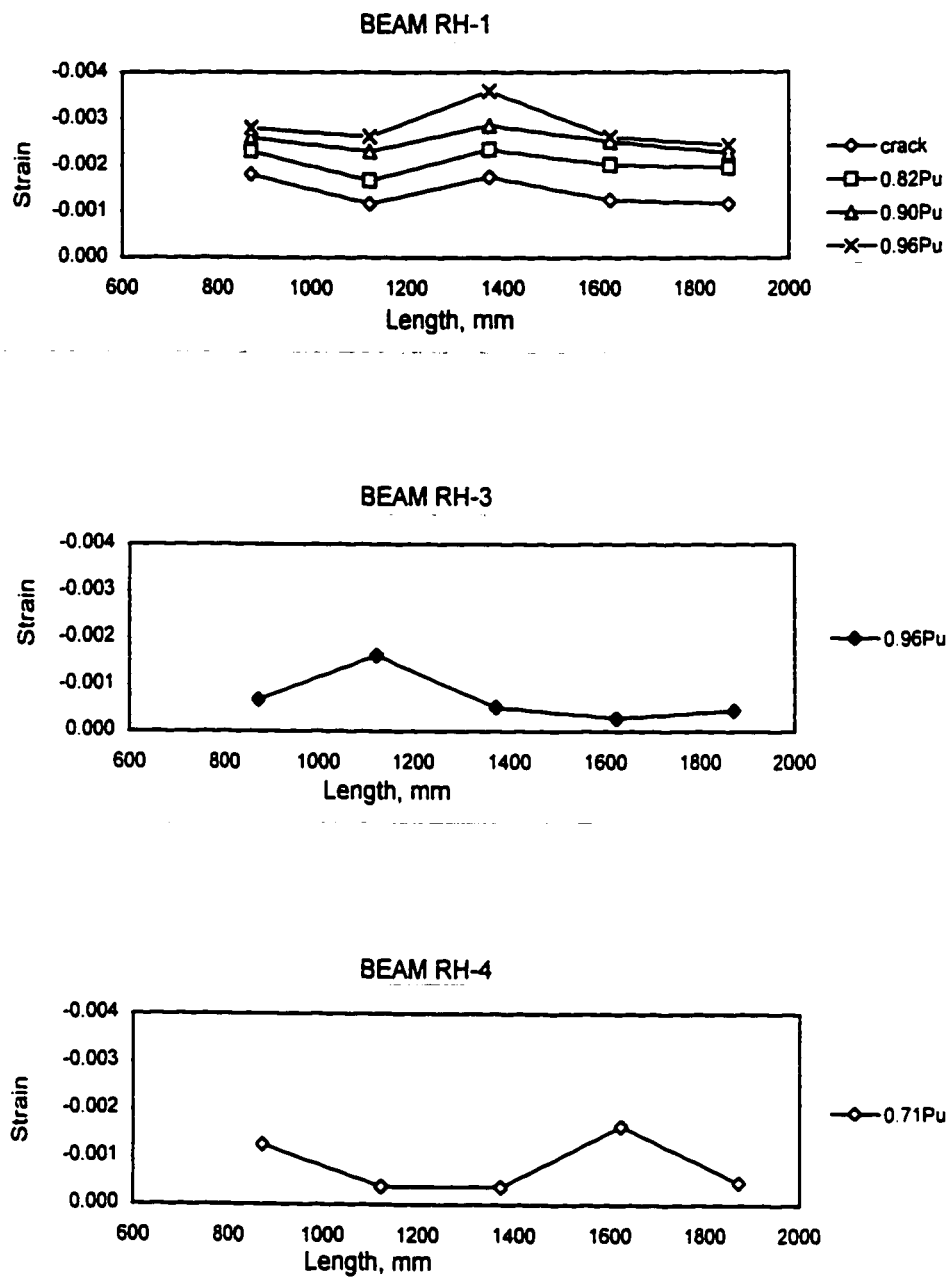
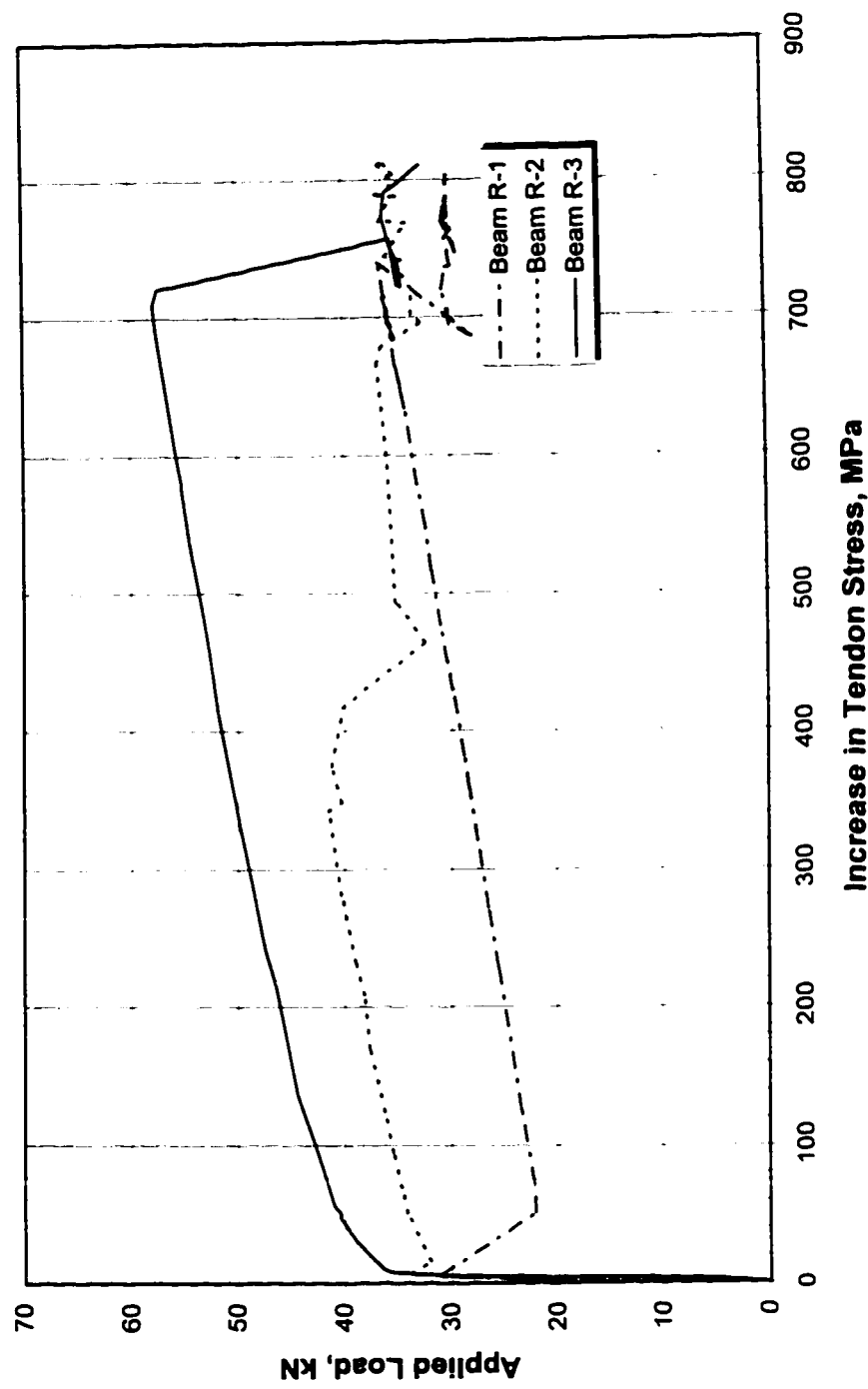


Figure 4.12 Distribution of Concrete Strain in the Extreme Compression Fibers Along the Flexural Span (Continued)

**Figure 4.13 Applied Load vs Increase in Tendon Stress
R-1, R-2, and R-3**



**Figure 4.14 Applied Load vs Increase in Tendon Stress
RH-2, RH-3, and RH-4**

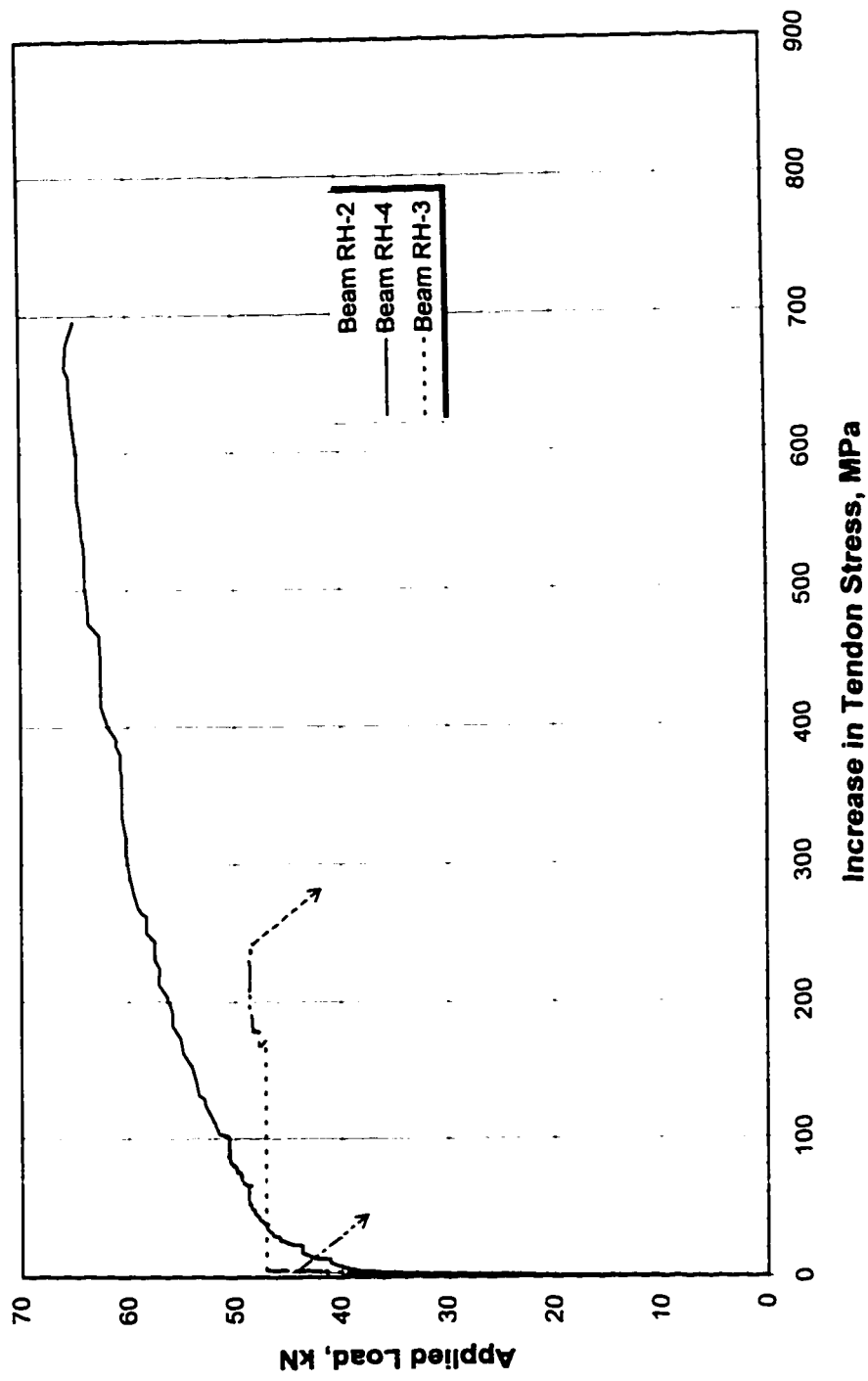


Figure 4.15 Increase in Tendon Stress vs Mid-span Deflection

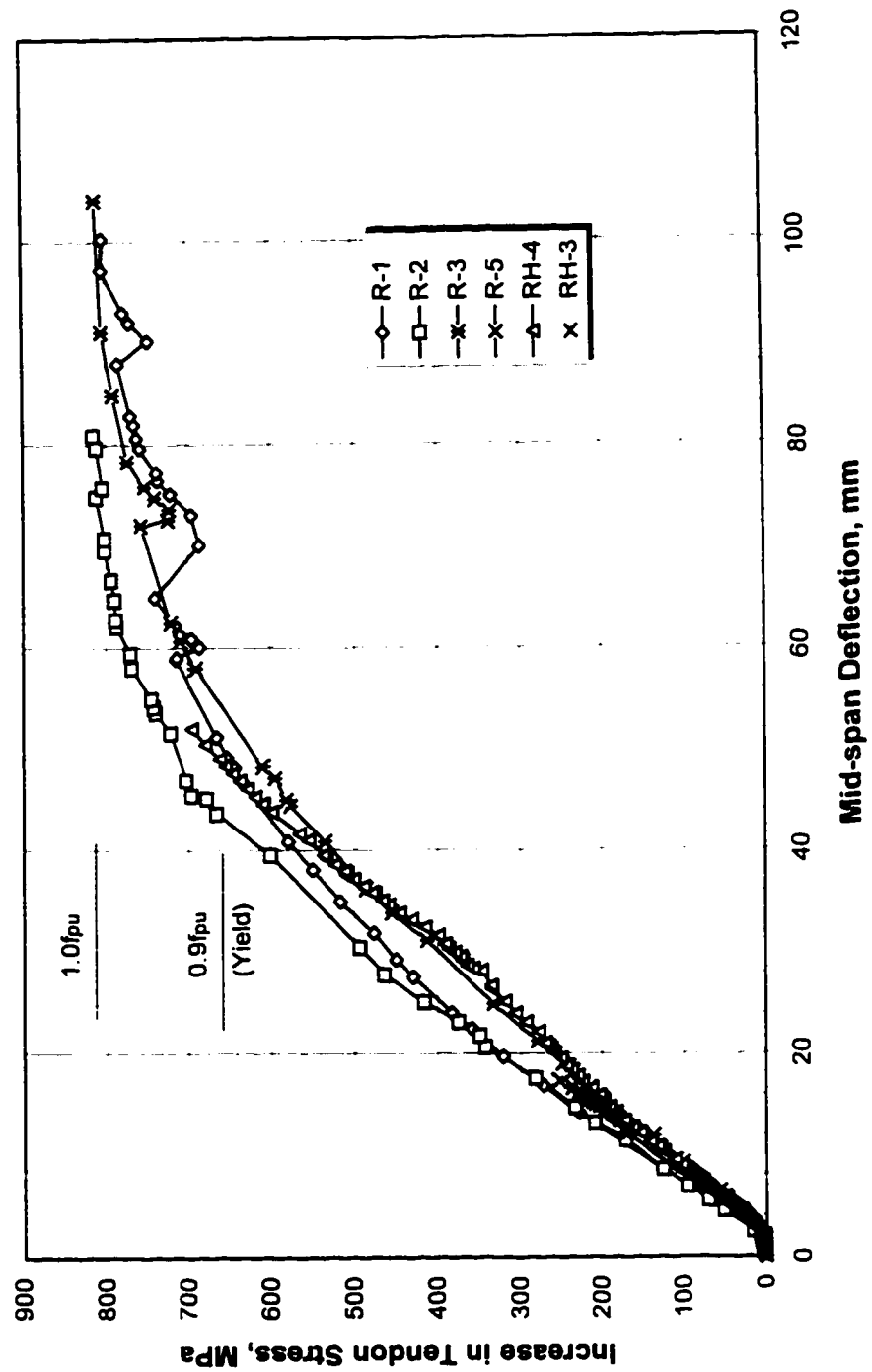
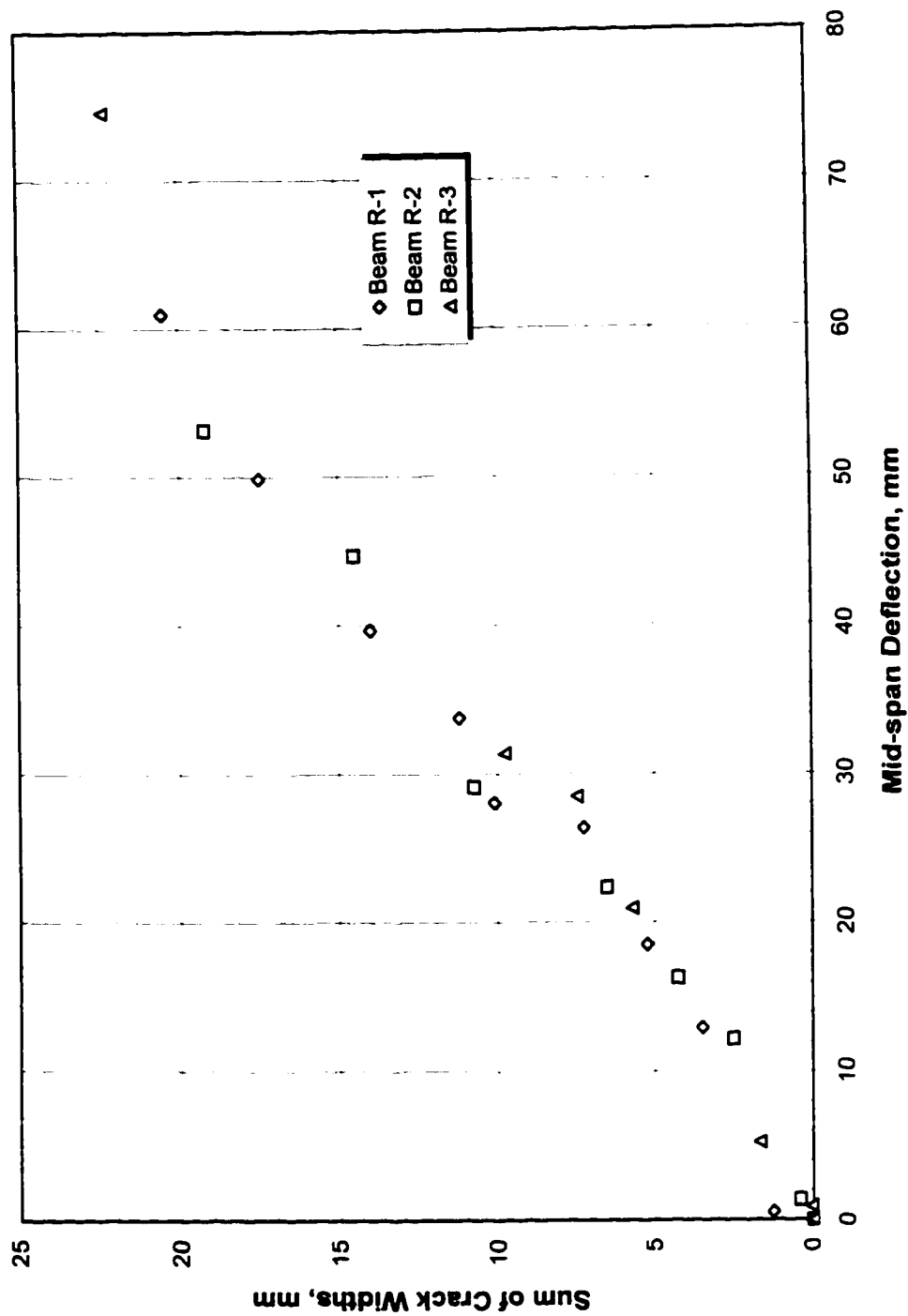


Figure 4.16 Sum of Crack Widths vs Deflection



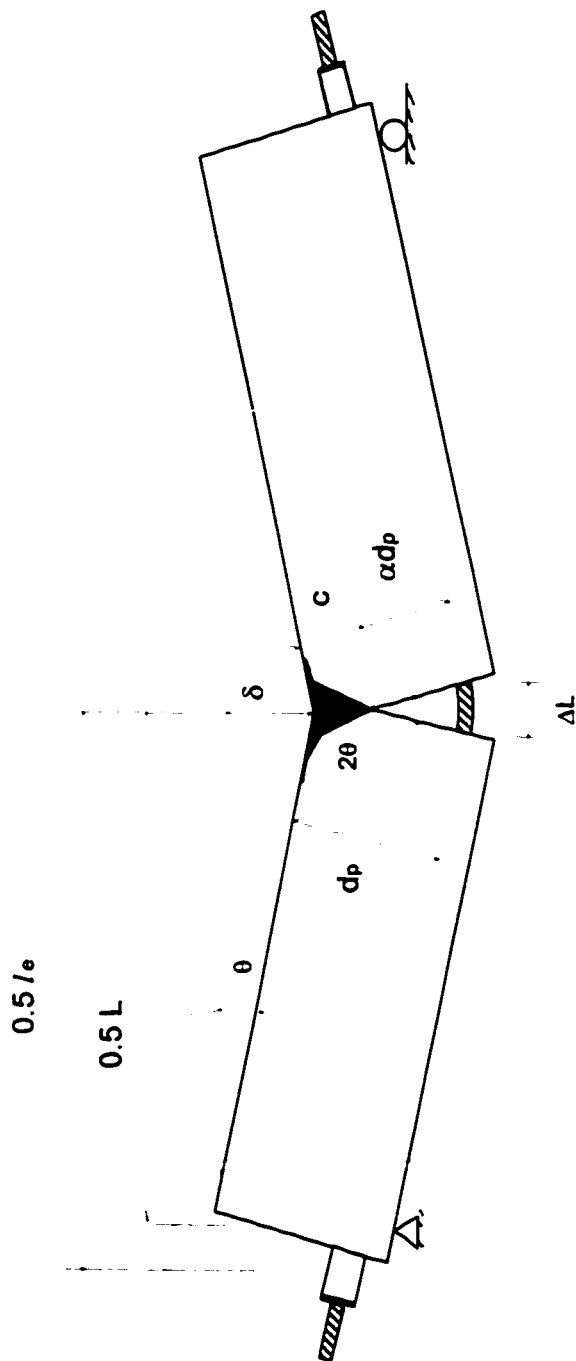


Figure 4.17 Typical Collapse Mechanism for Unbonded Prestressed Member

**Figure 4.18 Predicted and Actual Total Applied Load vs Mid-span Deflection
Beam R-1 ($\rho_p=0.15\%$, $\rho=0\%$)**

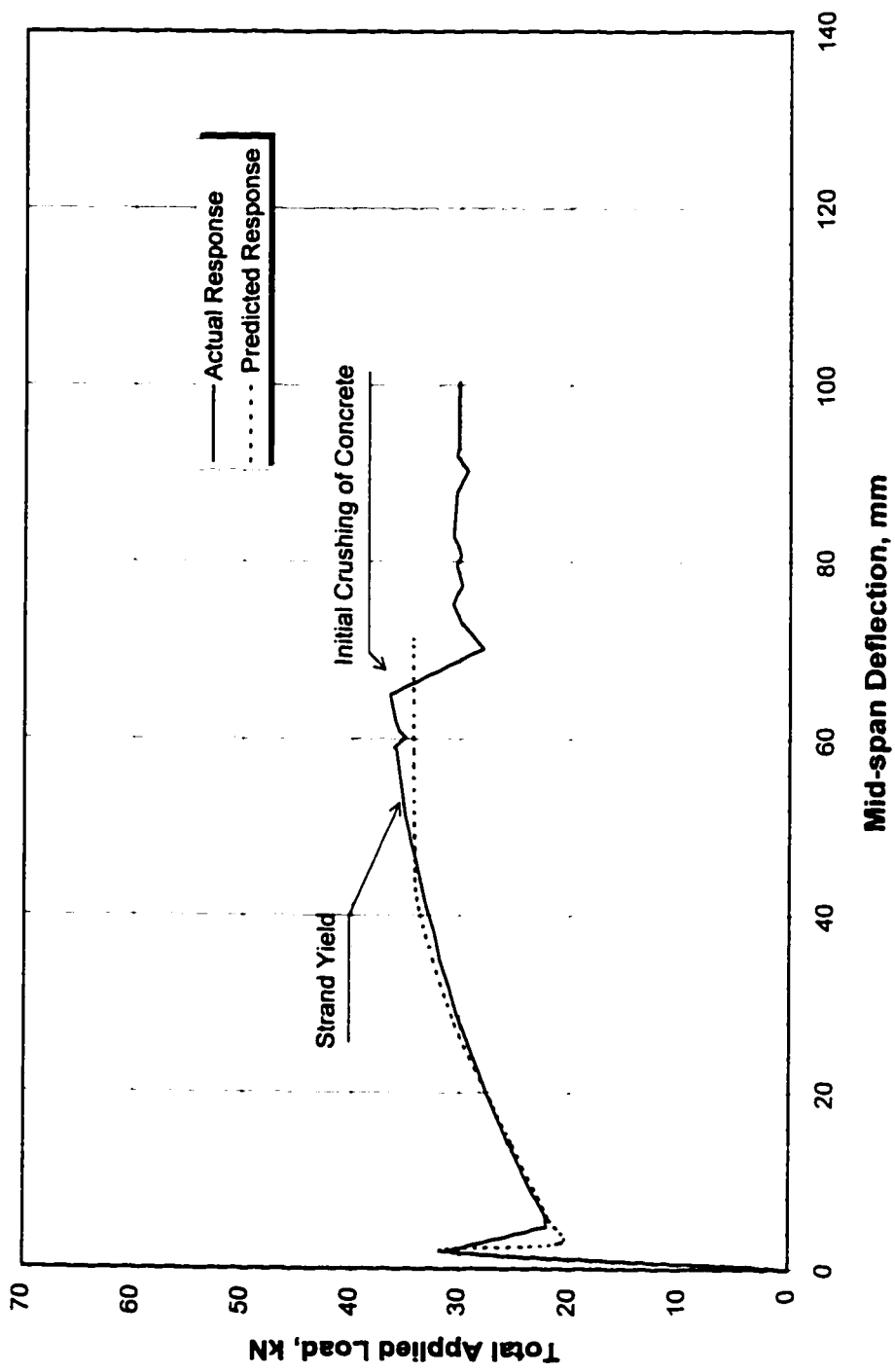
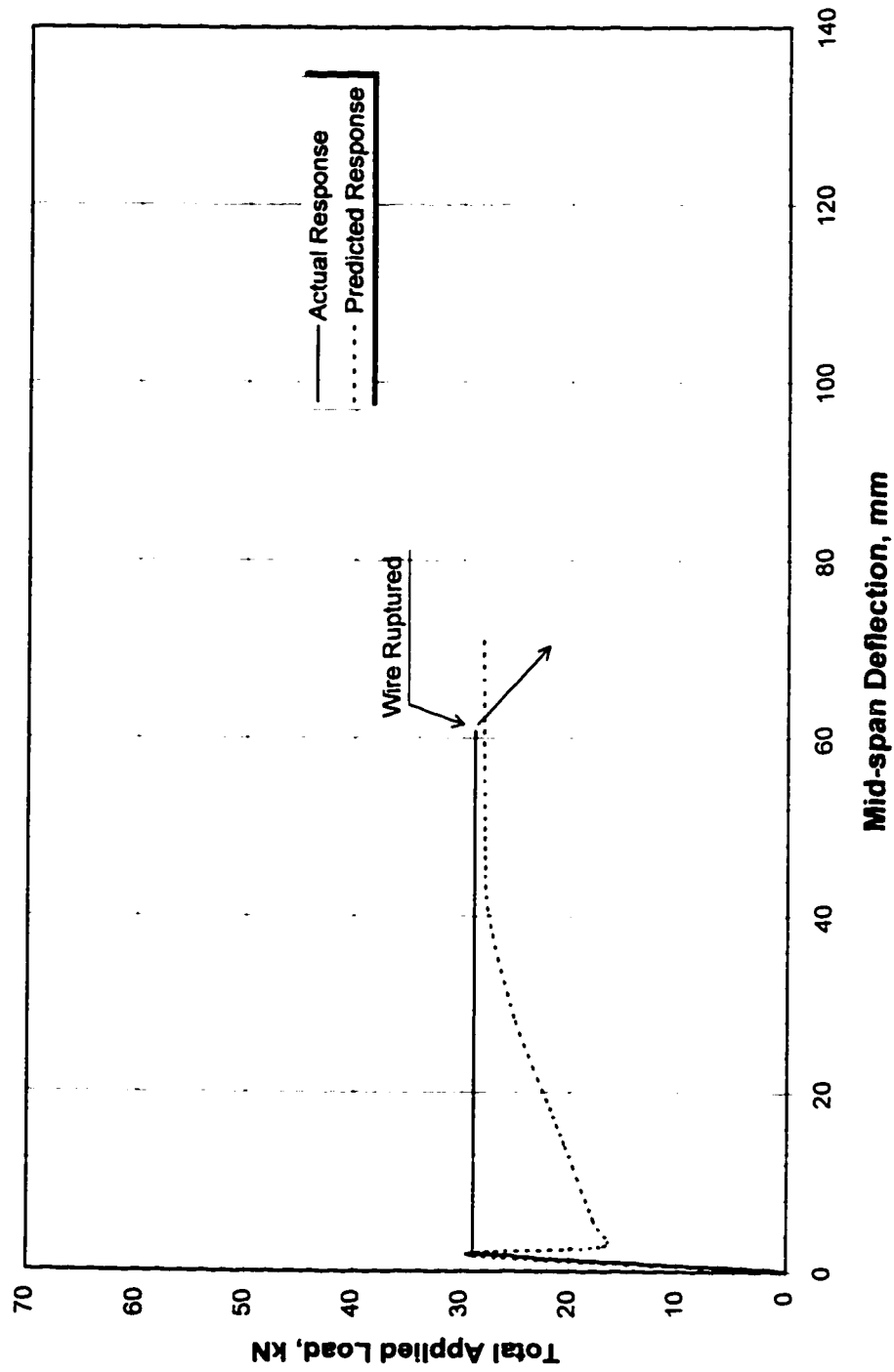


Figure 4.19 Predicted and Actual Total Applied Load vs Mid-span Deflection
Beam R-4 ($\rho_p = 0.12\%$, $\rho = 0\%$)



CHAPTER 5

CONCLUSIONS

5.1 Summary

Tests were conducted on 11 simply supported lightly prestressed concrete beams, with varying nonprestressed bonded reinforcement, unbonded prestressed reinforcement, and concrete strength. Nine beams were lightly prestressed and two beams were lightly reinforced. Three beams were tested with a stroke controlled testing procedure, while the remainder were tested using gravity loads. The later tests are more representative of the actual loading in practice. Gravity controlled loading captures any impact loads that might occur due to the sudden increase in deflection at cracking.

All beams had a span length of 2.85 m and span-to-depth ratio of 14.25. Testing was performed with two concentrated loads (1.15 m apart) in order to create a region of constant moment and zero shear. All beams had a nominal initial stress in the prestressed reinforcement of 1116 MPa ($0.6f_{pu}$). Concrete strengths ranged from 48.5 MPa to 123.4 MPa.

Experimental results including load-deflection curves, increase in tendon stress during loading, crack patterns, and concrete strains have been presented. Based on these results, a model for predicting the flexural response of lightly prestressed members with unbonded tendons was developed. The model was validated against all the prestressed beams tested in this project as well as

beams reported in the literature. The validation data set included 49 members from 5 researches with lightly and heavily reinforced specimens and span to depth ratios ranging from 14.25 to 40. The test results were used to evaluate the provisions of A23.3-94 and ACI 318-95.

5.2 Conclusions

Analysis of test results obtained in this study together with evaluation of results obtained by others on the behaviour of unbonded prestressed members has led to the following conclusions.

1. Ductile member response can be achieved by providing a certain minimum amount of unbonded prestressing and no bonded reinforcement. The tests indicate that a minimum $\omega_p=0.027$ produced ductile behavior. The amount of prestressing corresponding to this minimum ω_p is less than half that suggested by current codes. The parameter ω_p is a better indicator of ductility than p_p because it takes into account the influence of concrete strength.
2. The presence of even small amounts of bonded reinforcement reduced the amount of prestressing required to produce ductile behavior. The tests indicate that a minimum $\omega_s=0.01$ produced ductile behavior. The amount of bonded reinforcement corresponding to this minimum ω_s is less than half that suggested by current codes for intermediate strength concrete. The parameter ω_s is a better indication of ductility than p because it takes into account the influence of concrete strength.

3. A rational mechanical model was developed for predicting the response of unbonded prestressed members. The model can predict the ultimate load and whether the member will be brittle or ductile. The predictions of the model are more accurate than those of ACI 318-95 and CSA A23.3-94.
4. The change in tendon stress was found to be proportional to the sum of the crack widths in the span, which in turn was proportional to the deflection at midspan.
5. A midspan deflection corresponding to $\delta/L = 1/(100 - L/d_s)$ and a simple mechanism analysis gives a good estimate of the tendon stress at ultimate.
6. Strain hardening of the bonded reinforcement had a significant effect on member behavior and, in general should be taken into account when predicting the response of concrete members.
7. In prestressed concrete members with small amounts of bonded reinforcement, strain hardening of the bonded reinforcement has little effect on member behavior. In this case, strain hardening of bonded reinforcement may be neglected when predicting the member response of prestressed concrete members.
8. If a structure has bifurcated flexural cracks, it is an indication that there is little or no bonded flexural reinforcement present.
9. Current code minimum reinforcement requirements will ensure ductile member failure.
10. When assessing existing structures, the use of current code minimum reinforcement requirements as an indicator of brittle failure is too

conservative. Actual strength and ductility can be assessed using the model presented in Section 4.8.

11. For the same cross-sectional dimensions, the higher the concrete strength, the more non prestressed bonded reinforcement needed to prevent load loss or excessive deflection, at first cracking. The minimum bonded reinforcement required was 0.1% for 50 MPa nominal strength concrete and 0.175 % for 100 MPa concrete, which can expressed as $\omega_s = 0.01$.
12. The larger the cracking moment the greater the amount of non prestressed bonded reinforcement required to provide crack distribution.
13. In the gravity controlled tests, the "sudden" increase in deflection associated with reaching M_{cr} was sufficiently "slow" that large impact forces were not generated. In a real structure, impact should not be of concern.

5.3 Recommendations for Future research

On the basis of this investigation, it is recommended that the following changes to CSA A23.3-94 be studied:

1. The minimum bonded reinforcement requirements should be a function of the concrete strength.
2. The minimum bonded reinforcement requirements of $\rho = 0.2\%$ should be replaced by a minimum reinforcement index $\omega_s = 0.012$ but $\rho \nleq 0.1\%$.
3. The minimum ratio of M_r / M_{cr} should be reduced to 1.1 for prestressed concrete members and 1.0 for reinforced concrete.

Further study of the behaviour of lightly reinforced prestressed beams, one way slabs, and two-way slabs is recommended. The proposed prediction

model should be tested with more slender members, inverted T-beams, and indeterminate members. Tests relative to one-way and two-way shear behavior should also be conducted.

REFERENCES

1. Abeles, P. W., and Bardhan-Roy, B. K., "Prestressed Concrete Designer's Handbook", 3rd ed., London, 1981.
2. ACI 318-63, "Building Code Requirements for Reinforced Concrete", American Concrete Institute, Detroit, 1963.
3. ACI 318-71, "Building Code Requirements for Reinforced Concrete", American Concrete Institute, Detroit, 1971.
4. ACI 318-77, "Building Code Requirements for Reinforced Concrete", American Concrete Institute, Detroit, 1977.
5. ACI 318-83, "Building Code Requirements for Reinforced Concrete", American Concrete Institute, Detroit, 1983.
6. ACI 318-89, "Building Code Requirements for Reinforced Concrete", American Concrete Institute, Detroit, 1989.
7. ACI 318-95, "Building Code Requirements for Reinforced Concrete", American Concrete Institute, Detroit, 1995.
8. ACI-ASCE Committee 323 (now 423): "Tentative Recommendations for Prestressed Concrete", Journal of the American Concrete Institute, Proceedings V. 54, January 1958.
9. ACI-ASCE Committee 423: "Tentative Recommendations for Concrete Members Prestressed With Unbonded Tendons", Journal of the American Concrete Institute, Proceedings V. 66, No. 2, February 1969.
10. ACI-ASCE Committee 423: "Tentative Recommendation for prestressed Concrete Flat Plates", Journal of the American Concrete Institute, Proceedings V. 71, No. 2, February 1974.
11. Burns, N. H., Charney, Finley A.; and Vines, Wendell R., "Tests of One-Way Post-Tensioned Slabs With Unbonded Tendons", PCI Journal, V. 23, No .5, Sept.-Oct. 1978, pp. 66-83.
12. Burns, N.H., and Pierce, D.M., "Strength and Behaviour of Prestressed Concrete Members with Unbonded Tendons", PCI Journal, V. 12, No. 5, Sept.-Oct. 1967, pp. 15-29. 1967.

13. CSA-A135, "Prestressed Concrete", Canadian Standards Association, Rexdale, Ontario. 1962
14. CSA-A23.3-73, "Design of Concrete Structures for Buildings", Canadian Standards Association, Rexdale, Ontario.
15. CSA-A23.3-M77, "Design of Concrete Structures for Buildings", Canadian Standards Association, Rexdale, Ontario. 1977.
16. CAN3-A23.3-M84, "Design of Concrete Structures for Buildings", Canadian Standards Association, Rexdale, Ontario. 1984.
17. CAN-A23.3-94, "Design of Concrete Structures for Buildings", Canadian Standards Association, Rexdale, Ontario. 1994.
18. Chakrabarti, P.R., and Whang, T.P., "Study of Partially Prestressed Beams With Unbonded Post-Tensioning", Proceedings, ASCE, 1989, pp. 189-200.
19. Chen, R., "The Strength and Behaviour of Post-Tensioned Prestressed Concrete Slabs With Unbonded Tendons", M.Sc. Thesis, University of Texas, Austin, USA.
20. Chouinard, K. L., "Tendon Stress at Ultimate in Unbonded Partially Prestressed Concrete Beams", M. Sc. Thesis, Department of Civil Engineering Queen's University, Kingston, Ontario, 1989.
21. Cooke, N.I., Park, R., and Yong, P., "Flexural Strength of Prestressed Concrete Members With Unbonded Tendons", PCI Journal, V. 26, No. 6, Nov.-Dec. 1981, pp. 52-80.
22. Du, G., and Tao, X., "Ultimate Stress in Unbonded Tendons of Partially Prestressed Concrete Beams", PCI Journal, V. 30, No. 6, Nov.-Dec. 1985, pp. 72-91.
23. Elzanaty, A., and Nilson, A. H., "Flexural Behavior of Unbonded Post-Tensioned Partially Prestressed Concrete Beams", M. Sc. Thesis, Department of Structural Engineering, School of Civil and Environmental Engineering, Cornell University, Ithaca USA. 1982.
24. Gebre-Michael, Z., "Behaviour of Post-Tensioned Concrete Slabs With Unbonded Tendon Reinforcement", M.Sc. Thesis, University of Texas, Austin, USA. 1970

25. Harajli, M. H., and Kanji, M., "Ultimate Flexural Strength of Concrete Members Prestressed with Unbonded Tendons", ACI Journal, Proceedings V. 88, No. 6, Nov.-Dec. 1991, pp. 663-671.
26. Hemakom, R., "Behaviour of post-Tensioned Concrete Slabs with Unbonded Tendons", M.Sc. Thesis, University of Texas, Austin, USA. 1970.
27. Ivanyi, G., Buschmeyer, W. and Winter G., "Biegeversuche an mittig vorgespannten Zweifeldträgern (Bending tests on two-span beams with central prestressing)", Institute of Structural Concrete, University of Essen, Germany. 1987.
28. Kesner, K., and Poston, R.W., "Unbonded Post-Tensioned Concrete Corrosion: Myths, Misconceptions and Truths", Concrete International, July 1996, pp. 27-32.
29. Mattock, A.H.; Yamazaki, J.; and Kattula, B.T., "Comparative Study of Prestressed Concrete Beams, with and without Bond", ACI Journal, Proceedings V. 68, No. 2, Feb. 1971, pp. 116-125.
30. Ospina, C., Rogowsky, D.M., and Alexander, S.D.B., "Minimum prestressed requirement for Members With Unbonded Tendons and No Bonded Reinforcement", Technical Report, University of Alberta, 1997.
31. Pannell, F. N., "Ultimate Moment Resistance of Unbonded Prestressed Concrete Beams", Magazine of Concrete Research, V. 21, No. 66, Mar. 1969, pp. 43-54.
32. Schupack, M., "Corrosion Protection for Unbonded Tendons", Concrete International, Feb. 1991, pp. 51-57.
33. Tam, A., and Pannell, F. N., "The Ultimate Moment Resistance of Unbonded Prestressed Concrete Beams", Magazine of Concrete Research, V. 28, No. 97, Dec. 1976, pp. 203-208.
34. Warwaruk, J., Sozen, M.A., and Siess, C. P., "Investigation of Prestressed Reinforced Concrete for Highway Bridges, Part III: Strength and Behavior in Flexure of Prestressed Concrete Beams", Bulletin No. 464, University of Illinois Engineering Experiment Station, Urbana, USA., Aug. 1962.

APPENDIX A

TEST DATA

BEAM R-1

Scan #	Time h:mm:ss	South Reaction (kN)	North Reaction (kN)	South Load (kN)	North Load (kN)	S. Cable Force (kN)	N. Cable Force (kN)	Mid-span Deflection (mm)	Load point Span Change (mm)	Reaction Span Change (mm)
1	94202	0.00	0.00	0.00	0.00	52.16	52.60	0.00	6.69	150.40
2	100201	1.99	2.02	2.00	2.08	52.18	52.63	0.27	6.70	150.43
3	101256	3.98	3.93	4.04	3.97	52.20	52.65	0.44	6.82	150.38
4	102136	5.01	4.95	5.06	5.09	52.21	52.66	0.56	6.81	150.21
5	102208	6.18	6.19	6.20	6.31	52.24	52.67	0.66	6.82	150.21
6	102411	7.94	7.90	7.99	8.02	52.26	52.69	0.84	6.85	150.21
7	103327	10.34	10.34	10.46	10.52	52.29	52.72	1.08	6.89	150.35
8	103404	11.11	11.13	11.26	11.34	52.31	52.73	1.17	6.89	150.35
9	103515	11.87	11.90	11.99	12.13	52.32	52.73	1.27	6.90	150.35
10	104123	13.40	13.35	13.54	13.73	52.35	52.77	1.48	6.92	150.38
11	104151	13.89	13.83	14.03	14.04	52.36	52.77	1.55	6.93	150.38
12	104949	14.67	14.54	14.87	14.89	52.40	52.81	1.69	6.98	150.19
13	105544	15.13	15.09	15.26	15.33	52.43	52.85	1.83	7.02	150.19
14	105601	15.43	15.22	15.68	15.35	52.44	52.84	1.86	7.02	150.18
15	114410	11.16	10.79	11.46	10.65	54.38	55.23	4.72	7.34	148.31
16	114430	11.04	11.01	11.10	11.13	55.40	56.22	5.99	7.52	148.07
17	114526	11.63	11.40	11.87	11.55	57.95	58.69	8.58	7.70	146.52
18	121431	12.70	12.58	12.90	12.64	62.82	63.49	14.11	8.23	143.24
19	123756	13.04	13.11	13.22	13.29	64.82	65.62	16.84	8.47	141.67
20	124000	13.58	13.58	13.78	13.73	67.16	67.88	19.67	8.67	139.94
21	125349	13.97	13.99	14.09	14.21	68.89	69.68	22.41	8.89	138.43
22	125504	14.21	14.26	14.31	14.51	70.04	70.81	23.98	8.97	137.54
23	130656	14.75	14.76	14.89	14.99	72.21	73.02	27.55	9.21	135.74
24	130659	14.86	14.72	15.10	14.84	72.24	73.03	27.58	9.21	135.74
25	130911	15.01	14.99	15.19	15.21	73.18	73.99	29.24	9.40	134.84
26	132922	15.41	15.22	15.69	15.31	74.42	75.30	31.84	9.62	133.33
27	133557	15.74	15.69	15.97	15.89	76.31	77.17	34.92	9.83	131.82
28	135302	16.04	16.03	16.17	16.21	77.85	78.76	38.04	10.16	130.01
29	140436	16.45	16.39	16.62	16.49	79.20	80.19	40.85	10.39	128.50
30	142143	16.85	16.99	16.92	17.28	81.62	82.97	46.77	10.93	125.19
31	142217	17.04	17.07	17.20	17.30	82.04	83.41	48.16	11.06	124.59
32	142300	17.07	17.23	17.12	17.56	82.50	83.84	49.17	11.13	123.99
33	142435	17.37	17.31	17.58	17.48	83.11	84.41	51.21	11.29	123.01
34	145218	17.67	17.90	17.70	18.25	85.44	86.68	58.88	11.99	118.94
35	145225	18.03	17.76	18.42	17.76	85.39	86.68	59.04	12.00	118.88
36	151705	17.62	17.18	18.06	17.04	84.03	85.40	60.12	12.12	118.57
37	151738	17.94	17.50	18.51	17.22	84.48	85.86	60.94	12.19	117.99
38	151856	17.86	17.79	18.10	17.96	85.44	86.77	62.14	12.27	117.49
39	152935	17.93	18.17	18.01	18.52	86.66	87.89	64.96	12.55	116.14
40	153016	13.17	14.47	12.39	15.54	84.92	84.50	70.07	15.04	115.75
41	154058	14.86	14.73	15.14	14.81	84.44	85.89	73.04	15.62	115.49
42	154110	15.65	14.67	16.50	14.19	85.52	87.21	75.09	15.96	114.66
43	154116	14.59	15.09	14.44	15.87	86.27	87.94	76.42	16.22	114.30
44	154125	15.14	14.60	15.66	14.20	86.39	87.93	77.19	16.55	114.06
45	154134	15.31	14.78	15.82	14.59	87.26	88.97	79.63	16.99	113.46
46	154143	14.52	15.10	14.30	15.68	87.43	89.20	80.64	17.21	113.11
47	154204	15.02	14.92	15.27	15.03	87.55	89.35	81.94	17.40	112.55
48	154213	15.56	14.77	16.28	14.39	87.74	89.57	82.84	17.59	112.24
49	154257	14.89	15.13	14.90	15.47	88.36	90.37	87.95	18.56	110.44
50	154608	14.19	14.78	13.94	15.40	86.65	88.56	90.23	19.15	109.84
51	154622	15.43	14.60	16.17	14.21	87.75	89.62	92.04	19.48	109.24
52	154652	14.99	14.80	15.32	14.90	88.05	90.00	93.00	19.69	108.94
53	154720	14.69	15.12	14.59	15.65	89.21	91.31	97.18	20.43	107.43
54	154746	14.94	14.86	15.18	15.02	89.15	91.28	100.33	21.04	106.52

BEAM R-2

Scan #	Time h:mmss	South Reaction (kN)	North Reaction (kN)	South Load (kN)	North Load (kN)	S. Cable Force (kN)	N. Cable Force (kN)	Mid-span Deflection (mm)	Load point Span Change (mm)	Reaction Span Change (mm)
1	103057	0.00	0.00	0.00	0.00	52.58	53.79	0.00	107.60	150.80
2	103834	2.19	2.12	-2.09	2.09	52.61	53.81	0.15	107.60	150.79
3	103920	3.41	3.54	-3.65	3.65	52.63	53.82	0.27	107.60	150.79
4	104655	4.93	4.99	-5.11	5.11	52.66	53.84	0.43	107.60	150.79
5	104807	6.35	6.46	-6.60	6.60	52.68	53.85	0.57	107.60	150.80
6	104938	7.87	8.04	-8.21	8.21	52.70	53.85	0.71	107.60	150.79
7	111857	9.50	9.60	-9.76	9.76	52.73	53.89	0.86	107.60	150.79
8	112013	10.82	10.92	-11.07	11.07	52.76	53.91	0.98	107.60	150.79
9	112114	11.74	11.86	-12.04	12.04	52.78	53.92	1.07	107.60	150.79
10	113108	12.96	13.10	-13.40	13.40	52.81	53.94	1.21	107.60	150.79
11	113949	14.59	14.76	-14.99	14.99	52.86	53.99	1.41	107.60	150.79
12	115344	15.12	15.29	-15.50	15.50	52.91	54.03	1.53	107.60	150.41
13	115519	15.86	16.69	-17.33	17.33	52.92	54.08	1.64	107.60	150.41
14	115521	16.40	16.75	-17.05	17.05	52.93	54.05	1.67	107.60	150.41
15	115542	15.55	15.82	-16.07	16.07	53.51	54.39	2.49	107.60	150.19
16	122422	16.27	16.26	-17.38	17.38	55.39	55.82	4.52	107.60	149.27
17	122458	16.54	16.76	-17.72	17.72	56.29	56.67	5.52	107.60	148.67
18	122549	17.77	17.00	-16.63	16.63	57.54	57.83	6.88	107.60	148.06
19	122703	17.88	17.66	-17.56	17.56	58.92	59.18	8.50	107.60	147.16
20	124421	18.04	18.39	-18.85	18.85	61.03	61.43	11.47	107.59	145.35
21	124522	18.56	18.83	-19.04	19.04	62.89	63.18	13.43	107.59	144.44
22	124557	19.14	19.05	-19.01	19.01	64.00	64.31	14.69	107.60	143.77
23	125906	19.90	19.69	-19.25	19.25	66.28	66.65	17.58	107.60	141.98
24	125957	20.45	20.25	-20.04	20.04	69.15	69.46	20.62	107.60	140.19
25	131410	19.68	19.91	-20.20	20.20	69.41	69.86	21.75	107.60	138.74
26	131457	20.44	20.15	-20.07	20.07	70.68	71.03	23.11	107.60	138.74
27	131529	19.80	19.68	-19.70	19.70	72.63	72.98	25.08	107.60	137.53
28	131534	16.38	15.47	-14.94	14.94	74.98	75.16	27.77	107.60	135.75
29	131724	17.66	15.63	-15.49	15.49	76.21	76.70	30.44	107.60	134.55
30	133647	18.00	17.14	-16.33	16.33	81.20	81.77	39.49	107.59	129.41
31	133739	18.35	17.86	-17.61	17.61	84.40	84.78	43.61	107.59	127.00
32	133952	17.80	17.95	-18.17	18.17	84.65	85.04	45.12	107.60	126.09
33	141651	16.73	15.45	-14.67	14.67	82.50	82.75	45.43	105.62	125.49
34	141907	17.36	16.06	-14.57	14.57	83.63	83.41	46.94	104.71	125.49
35	141923	16.08	17.09	-18.25	18.25	87.18	87.20	51.65	104.87	122.98
36	141931	17.52	16.92	-17.26	17.26	88.10	87.99	53.67	105.53	121.87
37	141935	16.69	17.20	-17.58	17.58	88.17	88.15	54.22	104.88	121.57
38	141942	18.40	16.81	-15.85	15.85	88.34	88.23	55.04	104.44	121.50
39	141952	16.25	17.31	-18.79	18.79	89.50	89.36	58.07	102.93	119.77
40	142000	18.64	16.97	-16.09	16.09	89.59	89.39	59.47	103.50	119.17
41	142009	17.06	17.46	-18.06	18.06	90.55	90.07	62.13	104.19	117.92
42	142014	16.44	17.65	-18.73	18.73	90.46	90.25	62.77	104.50	117.38
43	142023	18.61	17.18	-16.57	16.57	90.59	90.21	64.72	104.60	116.77
44	142035	16.97	17.46	-18.21	18.21	90.84	90.37	66.65	104.28	115.56
45	142053	17.13	17.49	-18.15	18.15	91.19	90.76	69.59	103.83	114.35
46	142105	17.34	17.42	-18.45	18.45	90.99	90.96	70.73	103.45	113.76
47	142119	17.61	17.38	-17.66	17.66	91.76	91.12	74.81	103.57	111.94
48	142134	16.80	17.34	-18.15	18.15	91.38	90.78	75.73	102.97	111.49
49	142213	18.24	17.18	-16.85	16.85	91.76	91.11	79.71	102.42	109.84
50	142224	17.32	17.36	-17.80	17.80	91.93	91.25	80.91	103.10	109.24

BEAM R-3

Scan #	Time	South Reaction hmmss	North Reaction (kN)	South Load (kN)	North Load (kN)	S. Cable Force (kN)	N. Cable Force (kN)	Mid-span Deflection (mm)	Load point Span Change (mm)	Reaction Span Change (mm)
1	120955	0.00	0.00	0.00	0.00	52.87	53.47	0.00	6.15	150.19
2	122543	2.35	2.30	2.37	2.76	52.79	53.47	0.25	6.24	150.19
3	122601	3.63	3.70	3.58	3.79	52.80	53.47	0.36	6.27	150.19
4	122651	4.35	4.28	4.38	4.32	52.82	53.47	0.41	6.29	150.19
5	123141	5.86	5.84	6.00	5.62	52.84	53.49	0.51	6.33	150.19
6	123150	6.70	6.77	6.84	6.92	52.85	53.49	0.61	6.35	150.19
7	123210	7.86	7.79	7.88	7.92	52.88	53.50	0.72	6.37	150.19
8	123751	8.97	9.14	8.82	9.82	52.87	53.51	0.83	6.39	150.19
9	123803	10.09	10.22	9.94	10.82	52.85	53.51	0.91	6.39	150.18
10	123821	11.39	11.24	11.56	11.35	52.91	53.51	1.02	6.41	150.18
11	123857	12.18	12.05	12.25	12.22	52.92	53.52	1.10	6.42	150.19
12	124518	13.38	13.26	13.52	13.42	52.91	53.53	1.21	6.44	150.19
13	124536	13.97	13.88	14.02	14.12	52.96	53.53	1.27	6.45	150.19
14	124623	14.90	14.83	14.94	15.06	52.97	53.54	1.40	6.46	150.19
15	125300	15.73	15.53	15.86	15.68	53.01	53.55	1.51	71.65	150.19
16	125324	16.80	16.80	16.79	17.13	53.08	53.57	1.75	50.53	150.19
17	130023	17.64	17.05	17.95	17.34	53.11	53.63	2.05	53.36	150.19
18	130026	17.72	17.63	17.70	18.11	53.12	53.64	2.13	49.68	150.19
19	130040	18.49	17.60	19.07	17.25	53.25	53.67	2.46	50.13	150.19
20	132440	19.01	19.61	18.60	20.26	54.51	54.30	4.36	38.64	149.28
21	132647	20.18	19.76	20.45	19.97	55.57	54.94	5.64	40.22	148.67
22	132654	20.10	19.93	20.20	20.14	55.68	55.04	5.81	43.82	148.60
23	134050	20.87	19.84	21.57	19.43	55.87	55.46	6.37	7.14	147.42
24	134131	21.32	21.20	21.41	21.45	58.15	57.38	9.22	7.51	146.80
25	140745	22.50	21.21	22.87	21.53	59.76	59.11	11.84	7.74	145.35
26	141051	23.04	23.04	23.26	23.21	63.60	62.68	16.63	8.26	142.86
27	142949	23.20	23.37	23.16	24.24	64.89	63.78	18.69	8.46	141.44
28	143542	23.82	24.01	24.31	24.07	66.79	65.58	21.23	8.69	140.54
29	144346	24.31	24.83	24.75	25.07	69.36	68.00	24.87	9.01	138.43
30	150051	26.01	24.43	27.02	24.79	73.22	71.68	31.13	9.63	135.14
31	150115	26.20	25.87	25.88	26.73	75.21	73.71	33.84	9.83	133.63
32	150204	26.27	26.57	26.48	26.83	76.56	75.29	36.15	10.12	132.43
33	151011	26.89	27.04	27.36	27.12	78.99	77.45	40.83	10.54	130.30
34	151044	27.09	28.10	26.26	28.97	80.83	79.54	44.39	10.76	128.42
35	151053	27.64	27.33	27.82	27.44	81.19	79.64	44.97	10.83	128.19
36	151429	27.77	27.60	27.87	27.72	81.81	80.30	47.13	11.06	127.00
37	151438	28.32	27.31	28.99	26.93	82.64	80.86	48.25	11.15	126.40
38	153212	29.28	27.97	30.20	27.35	86.49	84.58	58.04	11.96	121.87
39	153221	28.20	29.50	27.40	30.42	87.28	85.65	60.72	12.22	120.67
40	153228	29.11	28.02	29.92	27.48	87.91	86.08	62.47	12.33	119.78
41	153649	17.68	17.61	17.77	17.73	89.85	87.54	72.01	12.98	115.50
42	154040	17.40	17.15	17.63	17.18	88.14	86.13	72.54	12.98	114.96
43	154645	16.75	18.26	15.78	18.69	87.99	86.15	73.57	13.20	114.96
44	154648	17.61	17.57	17.71	17.02	88.73	87.06	74.69	13.28	114.66
45	154651	18.47	16.89	19.63	15.87	89.27	87.68	75.82	13.35	114.36
46	154655	17.04	19.01	15.77	20.40	90.33	88.60	78.33	13.58	113.46
47	154720	16.32	19.40	14.24	21.67	91.11	89.44	84.89	14.34	111.04
48	154731	17.86	15.64	19.49	14.20	91.83	90.00	91.11	15.37	108.96
49	155410	17.25	15.13	18.85	13.79	92.19	90.29	104.08	17.37	105.32
50	155424	10.24	12.70	8.57	14.55	81.96	81.99	112.19	24.33	104.26
51	155435	10.31	12.62	8.75	14.36	81.92	81.88	112.19	24.13	104.29
52	160214	10.05	10.89	9.59	11.61	81.86	81.35	112.91	24.82	106.53

BEAM R-4

Scan #	Time h:mmss	South Reaction (kN)	North Reaction (kN)	South Load (kN)	North Load (kN)	S. Cable Force (kN)	N. Cable Force (kN)	Mid-span Deflection (mm)	Load point Span Change (mm)	Reaction Span Change (mm)
1	123852	0.00	0.00	0.00	0.00	43.29	44.06	0.00	22.76	155.60
2	124243	1.40	1.21	-0.64	0.32	43.31	44.07	0.18	22.77	155.60
3	124539	2.44	2.03	-1.85	1.04	43.32	44.09	0.29	22.77	155.59
4	124633	3.20	2.90	-2.55	2.03	43.33	44.09	0.39	22.79	155.60
5	124651	3.66	3.50	-2.89	2.66	43.33	44.10	0.45	22.80	155.60
6	124658	3.97	3.68	-3.30	2.79	43.32	44.10	0.47	22.80	155.60
7	124714	4.36	4.18	-3.62	3.36	43.34	44.10	0.51	22.81	155.59
8	124722	4.78	4.51	-4.17	3.58	43.34	44.10	0.55	22.81	155.60
9	124737	5.04	4.95	-4.24	4.20	43.36	44.11	0.58	22.82	155.59
10	124755	5.61	5.26	-4.99	4.33	43.36	44.11	0.62	22.83	155.59
11	124815	5.77	5.64	-5.01	4.87	43.36	44.12	0.65	22.84	155.60
12	124845	6.40	6.28	-5.62	5.56	43.39	44.12	0.71	22.85	155.59
13	124854	6.98	6.97	-6.08	6.41	43.38	44.12	0.78	22.86	155.59
14	124906	7.36	7.13	-6.68	6.29	43.40	44.13	0.82	22.86	155.59
15	124923	7.42	7.32	-6.64	6.60	43.41	44.13	0.84	22.86	155.59
16	124943	7.51	7.48	-6.67	6.81	43.42	44.13	0.85	22.86	155.59
17	125110	7.51	7.48	-6.66	6.81	43.40	44.13	0.85	22.87	155.59
18	130946	7.62	7.50	-6.81	6.79	43.47	44.13	0.89	22.87	155.60
19	131046	7.63	7.51	-6.80	6.79	43.46	44.14	0.90	22.87	155.60
20	131107	8.29	7.57	-8.02	6.35	43.46	44.14	0.93	22.87	155.59
21	131129	7.84	7.53	-7.12	6.69	43.46	44.14	0.95	22.87	155.59
22	131157	8.70	8.42	-8.25	7.56	43.47	44.14	0.99	22.89	155.59
23	131216	9.66	9.41	-8.94	8.75	43.48	44.15	1.11	22.90	155.59
24	131230	10.26	9.95	-9.56	9.29	43.50	44.16	1.18	22.91	155.59
25	131312	12.02	11.59	-11.39	10.83	43.49	44.17	1.36	22.93	155.59
26	131345	12.19	11.96	-11.42	11.26	43.51	44.18	1.39	22.94	155.59
27	131426	12.20	11.84	-11.59	10.95	43.51	44.18	1.41	22.94	155.59
28	131446	12.19	12.07	-11.45	11.40	43.51	44.18	1.41	22.94	155.59
29	133244	12.62	12.30	-11.94	11.53	43.61	44.21	1.53	23.15	155.18
30	133257	12.62	12.53	-11.79	11.90	43.62	44.21	1.54	23.15	155.18
31	133331	12.99	12.65	-12.34	11.77	43.53	44.22	1.57	23.16	155.18
32	133343	12.98	12.63	-12.36	11.77	43.55	44.21	1.57	23.16	155.18
33	133358	13.05	12.99	-12.25	12.35	43.57	44.22	1.59	23.16	155.18
34	133446	13.06	12.98	-12.25	12.36	43.58	44.23	1.60	23.17	155.19
35	133500	13.13	13.33	-12.14	12.92	43.58	44.24	1.65	23.17	155.18
36	133509	13.13	13.33	-12.14	12.92	43.59	44.25	1.67	23.18	155.18
37	133527	13.48	13.42	-12.68	12.81	43.60	44.28	1.73	23.19	155.00
38	133531	13.80	13.74	-13.03	13.12	43.61	44.29	1.75	23.20	155.00
39	133545	14.17	14.06	-13.38	13.43	43.62	44.30	1.77	23.21	155.01
40	133547	14.56	14.28	-13.73	13.74	43.63	44.30	1.79	23.23	155.02
41	133620	14.65	14.58	-14.08	14.05	43.62	44.31	1.79	23.24	155.01
42	133645	14.79	14.61	-14.43	14.36	43.63	44.32	1.80	23.25	155.00
43	133650	14.82	14.53	-14.48	14.41	70.11	71.23	60.81	28.86	120.33
44	133652	14.85	14.51	-14.48	14.41	69.42	70.28	60.15	28.88	120.33
45	133750	10.74	8.06	-14.48	14.38	60.51	59.57	121.17	42.97	98.37

BEAM R-5

Scan #	Time	South Reaction (kN)	North Reaction (kN)	South Load (kN)	North Load (kN)	S. Cable Force (kN)	N. Cable Force (kN)	Mid-span Deflection (mm)	Load point Span Change (mm)	Reaction Span Change (mm)
	hhmmss									
1	140010	0.00	0.00	0.00	0.00	43.58	44.11	0.00	23.34	157.41
2	140105	4.18	3.83	4.49	3.60	43.54	44.13	0.28	23.34	157.41
3	140112	4.76	4.23	5.20	3.87	43.52	44.13	0.32	23.34	157.41
4	140124	5.21	5.82	4.89	5.96	43.54	44.15	0.40	23.34	157.41
5	140132	6.23	5.97	6.48	5.88	43.52	44.15	0.47	23.34	157.40
6	140139	6.65	6.18	7.08	5.88	43.53	44.14	0.50	23.34	157.40
7	140145	6.70	6.65	6.87	6.53	43.52	44.15	0.53	23.33	157.41
8	140318	7.81	7.44	8.74	7.18	43.51	44.16	0.63	23.36	157.40
9	140328	9.96	9.82	10.22	9.71	43.51	44.18	0.88	23.41	157.40
10	140331	10.08	10.03	10.35	10.11	43.51	44.18	0.90	23.41	157.40
11	140335	10.23	10.28	10.29	10.65	43.50	44.17	0.92	23.41	157.40
12	140344	10.85	10.89	10.98	10.94	43.51	44.18	0.98	23.43	157.40
13	140401	11.11	11.26	11.19	11.38	43.52	44.19	1.03	23.44	157.40
14	140423	11.30	11.15	11.56	11.01	43.57	44.20	1.05	23.44	157.40
15	142053	11.47	11.45	11.62	11.48	43.52	44.20	1.13	23.57	157.40
16	142105	11.64	11.50	11.91	11.42	43.50	44.21	1.14	23.57	157.40
17	142125	11.73	11.85	11.81	11.96	43.52	44.20	1.16	23.57	157.40
18	142140	11.73	11.87	11.81	11.96	43.52	44.21	1.16	23.57	157.40
19	142205	12.08	11.96	12.34	11.87	43.55	44.21	1.18	23.57	157.40
20	142215	12.16	12.31	12.24	12.41	43.52	44.21	1.20	23.57	157.40
21	142217	12.15	12.31	12.23	12.42	43.53	44.20	1.20	23.57	157.40
22	142227	12.16	12.30	12.24	12.42	43.53	44.21	1.21	23.57	157.40
23	142229	12.16	12.31	12.24	12.42	43.53	44.20	1.21	23.57	157.40
24	142231	12.16	12.29	12.24	12.42	43.53	44.21	1.21	23.57	157.40
25	142234	12.16	12.32	12.24	12.42	43.52	44.20	1.21	23.57	157.40
26	142236	12.16	12.30	12.24	12.42	43.53	44.21	1.21	23.57	157.40
27	142239	12.16	12.30	12.24	12.42	43.53	44.20	1.21	23.57	157.40
28	142241	12.18	12.39	12.28	12.51	43.53	44.20	1.21	23.57	157.40
29	142243	12.23	12.44	12.27	12.61	43.55	44.21	1.22	23.57	157.40
30	142246	12.22	12.45	12.26	12.62	43.52	44.21	1.22	23.57	157.40
31	142248	12.25	12.48	12.29	12.64	43.52	44.20	1.22	23.57	157.40
32	142251	12.42	12.57	12.46	12.67	43.53	44.20	1.23	23.57	157.40
33	142253	12.36	12.54	12.43	12.64	43.54	44.21	1.23	23.57	157.40
34	142255	12.36	12.52	12.43	12.65	43.54	44.20	1.23	23.57	157.40
35	142258	12.36	12.51	12.44	12.64	43.54	44.22	1.24	23.57	157.40
36	142300	12.35	12.53	12.43	12.64	43.54	44.20	1.24	23.57	157.40
37	142303	12.36	12.52	12.43	12.64	43.53	44.20	1.23	23.57	157.40
38	142305	12.36	12.51	12.43	12.63	43.55	44.21	1.24	23.57	157.40
39	142307	12.35	12.52	12.42	12.63	43.55	44.21	1.24	23.57	157.40
40	142310	12.35	12.50	12.43	12.63	43.54	44.21	1.24	23.57	157.40
41	142312	12.35	12.52	12.42	12.63	43.55	44.22	1.24	23.57	157.40
42	142314	12.35	12.51	12.42	12.63	43.55	44.21	1.24	23.57	157.40
43	142317	12.40	12.66	12.44	12.83	43.54	44.20	1.24	23.57	157.40
44	142319	12.43	12.66	12.44	12.83	43.54	44.21	1.25	23.57	157.40
45	142322	12.43	12.65	12.45	12.83	43.54	44.21	1.25	23.57	157.40
46	142324	12.47	12.66	12.64	12.88	43.53	44.21	1.26	23.57	157.40
47	142326	12.56	12.75	12.64	12.88	43.54	44.21	1.26	23.57	157.40
48	142329	12.56	12.72	12.63	12.87	43.53	44.22	1.26	23.57	157.40
49	142331	12.57	12.73	12.63	12.86	43.55	44.21	1.26	23.57	157.40
50	142334	12.55	12.73	12.62	12.87	43.57	44.22	1.26	23.57	157.40
51	142336	12.57	12.74	12.62	12.86	43.55	44.21	1.26	23.57	157.40
52	142338	12.57	12.72	12.63	12.86	43.55	44.22	1.26	23.57	157.40
53	142341	12.57	12.73	12.63	12.86	43.55	44.21	1.26	23.57	157.40
54	142343	12.56	12.73	12.63	12.86	43.55	44.21	1.26	23.57	157.40
55	142345	12.56	12.75	12.63	12.86	43.54	44.21	1.26	23.57	157.40
56	142348	12.57	12.73	12.63	12.86	43.55	44.21	1.26	23.57	157.40

BEAM R-5 (continued)

Scan #	Time hrmmss	South Reaction (kN)	North Reaction (kN)	South Load (kN)	North Load (kN)	S. Cable Force (kN)	N. Cable Force (kN)	Mid-span Deflection (mm)	Load point Span Change (mm)	Reaction Span Change (mm)
57	142350	12.56	12.72	12.64	12.86	43.55	44.21	1.26	23.57	157.40
58	142353	12.70	12.82	12.71	13.05	43.54	44.22	1.28	23.57	157.40
59	142355	12.66	12.86	12.70	13.01	43.55	44.21	1.28	23.57	157.40
60	142357	12.78	12.95	12.84	13.11	43.55	44.21	1.28	23.57	157.40
61	142400	12.78	12.94	12.84	13.09	43.55	44.21	1.29	23.57	157.40
62	142402	12.78	12.97	12.85	13.09	43.53	44.22	1.29	23.57	157.40
63	142405	12.78	12.97	12.84	13.10	43.55	44.21	1.29	23.57	157.40
64	142407	12.78	12.95	12.84	13.14	43.55	44.22	1.29	23.57	157.40
65	142409	12.91	13.04	12.97	13.17	43.56	44.22	1.30	23.57	157.40
66	142412	12.90	13.05	12.99	13.18	43.55	44.22	1.30	23.57	157.40
67	142414	12.89	13.06	13.02	13.30	43.56	44.21	1.30	23.57	157.40
68	142417	13.00	13.17	13.06	13.32	43.56	44.21	1.31	23.58	157.40
69	142419	12.99	13.17	13.07	13.33	43.55	44.22	1.31	23.58	157.40
70	142421	12.99	13.20	13.06	13.32	43.56	44.21	1.31	23.58	157.40
71	142424	12.99	13.17	13.06	13.32	43.54	44.22	1.32	23.58	157.40
72	142426	12.99	13.39	12.93	13.69	43.56	44.21	1.33	23.58	157.40
73	142429	13.00	13.40	12.91	13.68	43.56	44.22	1.33	23.58	157.40
74	142431	13.00	13.41	12.92	13.68	43.54	44.22	1.33	23.58	157.40
75	142433	12.99	13.58	12.80	14.06	43.54	44.23	1.34	23.58	157.40
76	142436	13.00	13.60	12.89	13.93	43.56	44.21	1.34	23.58	157.40
77	142438	13.20	13.61	13.15	13.91	43.53	44.23	1.35	23.58	157.40
78	142440	13.21	13.64	13.12	13.90	43.54	44.21	1.36	23.58	157.40
79	142443	13.22	13.61	13.14	13.91	43.55	44.22	1.36	23.58	157.40
80	142445	13.21	13.61	13.14	13.91	43.56	44.22	1.36	23.58	157.40
81	142447	13.21	13.62	13.13	13.91	43.55	44.23	1.36	23.58	157.40
82	142450	13.22	13.61	13.14	13.91	43.55	44.23	1.37	23.58	157.40
83	142452	13.21	13.62	13.13	13.90	43.56	44.23	1.37	23.58	157.40
84	142455	13.43	13.72	13.47	14.07	43.56	44.22	1.38	23.58	157.40
85	142457	13.54	13.71	13.52	14.00	43.57	44.23	1.39	23.58	157.40
86	142459	13.46	13.81	13.49	14.00	43.56	44.22	1.40	23.58	157.40
87	142502	13.50	13.77	13.49	14.00	43.56	44.23	1.40	23.58	157.40
88	142504	13.50	13.77	13.49	13.99	43.56	44.22	1.40	23.58	157.40
89	142506	13.48	13.79	13.48	14.00	43.53	44.22	1.40	23.58	157.40
90	142509	13.50	13.78	13.50	14.05	43.52	44.22	1.40	23.58	157.40
91	142511	13.61	13.91	13.67	14.02	43.53	44.24	1.43	23.59	157.40
92	142513	13.62	13.95	13.80	14.01	43.53	44.23	1.43	23.59	157.40
93	142516	13.79	13.95	13.87	14.03	43.54	44.24	1.44	23.59	157.40
94	142518	13.78	13.93	13.90	14.04	43.53	44.23	1.44	23.59	157.40
95	142521	13.80	13.91	13.90	14.03	43.54	44.23	1.44	23.59	157.40
96	142523	13.76	13.92	13.89	14.03	43.53	44.24	1.44	23.59	157.40
97	142525	13.79	13.93	13.90	14.04	43.55	44.23	1.45	23.59	157.40
98	142528	13.79	13.90	13.90	14.03	43.54	44.24	1.45	23.59	157.40
99	142530	13.73	13.91	13.81	14.06	43.54	44.23	1.45	23.59	157.40
100	142532	13.71	13.90	13.80	14.06	43.54	44.24	1.45	23.59	157.40
101	142535	13.73	13.94	13.79	14.07	43.55	44.23	1.45	23.59	157.41
102	142537	13.73	13.91	13.80	14.07	43.55	44.24	1.45	23.59	157.40
103	142540	13.73	13.92	13.80	14.07	43.54	44.23	1.45	23.59	157.40
104	142542	13.73	13.92	13.80	14.07	43.52	44.24	1.45	23.59	157.40
105	142544	13.73	13.93	13.81	14.07	43.56	44.23	1.45	23.59	157.40
106	142547	13.73	13.91	13.80	14.07	43.50	44.24	1.45	23.59	157.40
107	142549	13.73	13.92	13.80	14.07	43.56	44.24	1.45	23.59	157.40
108	142551	13.73	13.93	13.80	14.07	43.57	44.23	1.46	23.59	157.40
109	142554	13.73	13.92	13.80	14.07	43.56	44.23	1.46	23.59	157.40
110	142556	13.73	13.91	13.80	14.06	43.57	44.24	1.46	23.59	157.40
111	142559	13.73	13.93	13.80	14.07	43.56	44.23	1.46	23.59	157.40
112	142601	13.73	13.92	13.80	14.07	43.57	44.24	1.46	23.59	157.40

BEAM R-5 (continued)

Scan #	Time hrmmss	South Reaction (kN)	North Reaction (kN)	South Load (kN)	North Load (kN)	S. Cable Force (kN)	N. Cable Force (kN)	Mid-span Deflection (mm)	Load point Span Change (mm)	Reaction Span Change (mm)
113	143334	13.73	13.91	13.80	14.07	43.60	44.26	1.55	23.62	157.40
114	143339	13.72	13.91	13.80	14.07	43.59	44.26	1.55	23.62	157.40
115	143344	13.72	13.91	13.80	14.07	43.60	44.25	1.55	23.62	157.40
116	143348	13.72	13.92	13.80	14.07	43.60	44.25	1.55	23.62	157.40
117	143353	13.73	13.91	13.80	14.07	43.62	44.26	1.55	23.62	157.40
118	143358	13.72	13.90	13.80	14.07	43.61	44.25	1.55	23.62	157.40
119	143403	13.73	13.91	13.80	14.07	43.61	44.26	1.55	23.62	157.40
120	143408	13.73	13.92	13.80	14.07	43.61	44.25	1.55	23.62	157.40
121	143412	13.72	13.91	13.80	14.07	43.59	44.26	1.55	23.62	157.40
122	143417	13.73	13.92	13.81	14.07	43.60	44.25	1.55	23.61	157.40
123	143422	13.73	13.91	13.80	14.07	43.61	44.26	1.55	23.62	157.40
124	143427	13.73	13.91	13.80	14.07	43.61	44.26	1.55	23.62	157.40
125	143432	13.72	13.91	13.84	14.07	43.61	44.26	1.55	23.62	157.40
126	143436	13.84	13.96	13.98	14.06	43.59	44.26	1.56	23.62	157.40
127	143441	13.84	13.97	13.98	14.07	43.60	44.25	1.56	23.62	157.40
128	143446	13.84	13.97	13.98	14.07	43.59	44.25	1.56	23.62	157.40
129	143451	13.85	13.95	13.99	14.10	43.62	44.26	1.56	23.62	157.40
130	143455	14.08	14.22	14.18	14.35	43.62	44.26	1.59	23.62	157.40
131	143500	14.04	14.21	14.15	14.34	43.59	44.25	1.59	23.62	157.40
132	143505	14.04	14.21	14.14	14.35	43.65	44.26	1.59	23.62	157.40
133	143510	14.03	14.21	14.14	14.34	43.63	44.26	1.59	23.62	157.40
134	143515	14.03	14.21	14.15	14.34	43.60	44.26	1.59	23.62	157.40
135	143519	14.04	14.21	14.15	14.34	43.61	44.25	1.59	23.62	157.40
136	143524	14.04	14.20	14.15	14.35	43.62	44.26	1.59	23.62	157.40
137	143529	14.04	14.22	14.14	14.35	43.60	44.26	1.59	23.62	157.40
138	143534	14.14	14.34	14.22	14.52	43.60	44.26	1.60	23.62	157.40
139	143538	14.18	14.38	14.25	14.53	43.60	44.25	1.60	23.62	157.40
140	143543	14.17	14.36	14.25	14.53	43.61	44.26	1.60	23.62	157.40
141	143548	14.16	14.38	14.25	14.53	43.62	44.26	1.61	23.62	157.40
142	143553	14.23	14.45	14.39	14.74	43.61	44.26	1.61	23.62	157.40
143	143558	14.31	14.55	14.40	14.72	43.61	44.27	1.62	23.62	157.40
144	143602	14.32	14.54	14.40	14.71	43.61	44.27	1.62	23.62	157.40
145	143607	14.32	14.54	14.40	14.71	43.60	44.28	1.62	23.62	157.40
146	143612	14.32	14.54	14.40	14.71	43.61	44.27	1.63	23.63	157.40
147	143617	14.39	14.55	14.52	14.73	43.61	44.27	1.63	23.63	157.40
148	143622	14.43	14.60	14.55	14.73	43.60	44.27	1.64	23.63	157.40
149	143626	14.44	14.58	14.56	14.62	43.60	44.28	1.64	23.63	157.40
150	143631	14.49	14.75	14.53	14.96	43.62	44.28	1.65	23.63	157.40
151	143636	14.49	14.76	14.53	14.98	43.62	44.28	1.65	23.63	157.40
152	143641	14.48	14.76	14.52	14.99	43.62	44.27	1.65	23.63	157.40
153	143646	14.48	14.79	14.53	14.97	43.61	44.28	1.65	23.63	157.40
154	143650	14.48	14.76	14.52	14.97	43.62	44.28	1.65	23.63	157.40
155	143655	14.48	14.76	14.52	14.97	43.63	44.28	1.66	23.63	157.40
156	143700	14.62	14.86	14.76	14.98	43.63	44.27	1.68	23.63	157.40
157	143705	14.65	14.81	14.74	14.95	43.63	44.28	1.68	23.63	157.40
158	143709	14.65	14.81	14.75	14.96	43.62	44.28	1.68	23.63	157.40
159	143714	14.64	14.83	14.75	14.95	43.62	44.29	1.68	23.64	157.40
160	143719	14.71	14.91	14.85	15.08	43.62	44.27	1.68	23.64	157.40
161	143724	14.80	14.97	14.90	15.10	43.63	44.28	1.69	23.64	157.40
162	143729	14.78	14.96	14.91	15.10	43.62	44.29	1.69	23.65	157.40
163	143733	14.79	14.96	14.90	15.10	43.63	44.29	1.69	23.65	157.40
164	143738	14.78	14.96	14.90	15.10	43.63	44.29	1.70	23.65	157.40
165	143743	14.79	14.96	14.90	15.10	43.64	44.29	1.70	23.65	157.40
166	143748	14.79	14.96	14.91	15.10	43.63	44.29	1.70	23.65	157.40
167	143753	14.78	14.96	14.90	15.10	43.63	44.29	1.70	23.65	157.40
168	143758	14.78	14.97	14.90	15.10	43.63	44.30	1.70	23.65	157.40

BEAM R-5 (continued)

Scan #	Time h:mmss	South Reaction (kN)	North Reaction (kN)	South Load (kN)	North Load (kN)	S. Cable Force (kN)	N. Cable Force (kN)	Mid-span Deflection (mm)	Load point Span Change (mm)	Reaction Span Change (mm)
169	143802	14.79	14.96	14.90	15.10	43.64	44.29	1.70	23.65	157.40
170	143807	14.84	14.94	15.07	15.04	43.63	44.29	1.71	23.65	157.40
171	143812	14.88	15.02	15.00	15.15	43.64	44.28	1.71	23.65	157.40
172	143817	14.86	15.13	14.93	15.30	43.64	44.30	1.72	23.65	157.40
173	143822	14.94	15.12	15.06	15.25	43.64	44.29	1.72	23.65	157.40
174	143826	14.94	15.11	15.07	15.25	43.64	44.29	1.72	23.65	157.40
175	143831	15.02	15.11	15.18	15.22	43.64	44.28	1.73	23.65	157.40
176	143836	15.01	15.13	15.17	15.22	43.64	44.29	1.73	23.66	157.40
177	143841	15.01	15.12	15.18	15.21	43.65	44.30	1.73	23.65	157.40
178	143846	15.01	15.12	15.18	15.21	43.64	44.30	1.73	23.66	157.40
179	143850	15.01	15.11	15.18	15.21	43.64	44.31	1.74	23.66	157.40
180	143855	15.02	15.18	15.16	15.30	43.64	44.30	1.74	23.66	157.40
181	143900	15.10	15.12	15.21	15.25	43.65	44.31	1.75	23.66	157.40
182	143905	15.04	15.17	15.22	15.24	43.64	44.29	1.75	23.66	157.40
183	143909	15.12	15.15	15.36	15.19	43.64	44.31	1.75	23.66	157.40
184	143914	15.15	15.17	15.36	15.20	43.64	44.31	1.76	23.66	157.40
185	143919	15.12	15.15	15.35	15.20	43.65	44.31	1.76	23.66	157.40
186	143924	15.13	15.17	15.41	15.12	43.63	44.30	1.76	23.66	157.40
187	143929	15.17	15.11	15.42	15.13	43.66	44.30	1.76	23.67	157.40
188	143933	15.18	15.15	15.39	15.15	43.66	44.30	1.76	23.67	157.40
189	143938	15.14	15.12	15.37	15.13	43.66	44.31	1.77	23.67	157.40
190	143943	15.13	15.16	15.35	15.20	43.66	44.31	1.77	23.67	157.40
191	143948	15.12	15.15	15.37	15.28	43.65	44.32	1.77	23.67	157.40
192	143952	15.30	15.47	15.43	15.61	43.65	44.31	1.79	23.68	157.40
193	143957	15.31	15.46	15.44	15.59	43.66	44.32	1.79	23.68	157.40
194	144002	15.31	15.46	15.44	15.59	43.66	44.31	1.80	23.68	157.40
195	144007	15.30	15.48	15.43	15.60	43.66	44.32	1.80	23.68	157.40
196	144012	15.30	15.46	15.44	15.60	43.67	44.32	1.80	23.68	157.40
197	144017	15.31	15.47	15.44	15.60	43.66	44.33	1.81	23.68	157.40
198	144021	15.30	15.46	15.43	15.60	43.67	44.31	1.81	23.68	157.40
199	144026	15.30	15.47	15.43	15.60	43.67	44.32	1.81	23.68	157.40
200	144031	15.30	15.46	15.44	15.60	43.67	44.33	1.82	23.69	157.40
201	144036	15.30	15.46	15.44	15.60	43.67	44.33	1.82	23.69	157.40
202	144041	15.30	15.47	15.43	15.60	43.68	44.33	1.83	23.69	157.40
203	144046	15.36	15.35	15.28	15.66	53.53	54.13	17.06	25.06	149.25
204	144051	15.26	15.49	15.42	15.61	53.39	54.09	17.06	25.06	149.25
205	144056	15.27	15.49	15.42	15.61	53.34	54.07	17.06	25.07	149.25
206	144101	15.26	15.50	15.42	15.61	53.31	54.05	17.06	25.07	149.25
207	144106	15.26	15.48	15.43	15.61	53.26	54.04	17.06	25.07	149.25
208	144111	15.27	15.49	15.42	15.61	53.25	54.03	17.06	25.08	149.25
209	144116	15.26	15.49	15.42	15.61	53.26	54.02	17.06	25.08	149.25
210	154222	15.27	15.51	15.42	15.61	53.05	53.81	17.31	25.15	149.25
211	81028	15.40	15.50	15.60	15.60	52.95	53.14	17.74	25.30	149.16
212	81538	15.57	15.76	15.77	15.86	53.02	53.21	17.97	25.31	149.09
213	82248	15.69	15.83	16.00	16.10	53.64	53.55	18.75	25.39	148.64
214	82315	15.83	16.12	16.03	16.22	53.72	53.57	19.02	25.39	148.64
215	82412	13.20	13.30	15.50	16.41	69.57	68.84	133.50	39.12	100.14
216	82732	13.12	12.78	15.61	16.13	68.04	68.22	133.51	39.12	100.14
217	84946	10.80	10.94	11.27	11.68	67.26	66.57	132.73	39.12	100.49

BEAM R-6

Scan #	Time h:mm:ss	South Reaction (kN)	North Reaction (kN)	South Load (kN)	North Load (kN)	S. Cable Force (kN)	N. Cable Force (kN)	Mid-span Deflection (mm)	Load point Span Change (mm)	Reaction Span Change (mm)
1	111547	0.00	0.00	0.00	0.00	0.00	0.00	0.00	19.07	158.31
2	111557	1.51	0.59	-2.32	0.00	0.00	0.00	0.18	19.11	158.30
3	111607	2.91	2.06	-3.51	1.50	0.00	0.00	0.30	19.15	158.30
4	111616	3.58	3.46	-3.67	3.47	0.00	0.00	0.50	19.20	158.30
5	111626	4.44	4.56	-4.32	5.13	0.00	0.00	0.68	19.24	158.30
6	111636	5.60	5.34	-5.79	5.23	0.00	0.00	0.94	19.28	158.30
7	111655	6.02	6.22	-5.99	6.64	0.00	0.00	1.12	19.30	158.30
8	111705	6.72	6.53	-6.88	6.50	0.00	0.00	1.26	19.32	158.30
9	111715	7.15	7.05	-7.23	7.19	0.00	0.00	1.33	19.33	158.31
10	111725	7.63	7.53	-7.84	7.59	0.00	0.00	1.45	19.36	158.30
11	114831	7.97	7.87	-8.15	7.85	0.00	0.00	1.62	19.41	157.71
12	115124	8.62	8.51	-8.83	8.48	0.00	0.00	1.73	19.42	157.70
13	115203	9.00	8.99	-9.12	9.05	0.00	0.00	1.90	19.46	157.70
14	115214	9.08	9.10	-9.19	9.18	0.00	0.00	2.18	19.45	157.70
15	115223	9.07	9.09	-9.18	9.17	0.00	0.00	2.23	19.46	157.70
16	115531	9.06	9.09	-9.17	9.17	0.00	0.00	2.38	19.48	157.70
17	115541	9.21	9.25	-9.31	9.33	0.00	0.00	2.40	19.48	157.70
18	115551	9.31	9.32	-9.44	9.38	0.00	0.00	2.43	19.48	157.70
19	115601	9.30	9.30	-9.44	9.36	0.00	0.00	2.43	19.48	157.70
20	115611	9.43	9.43	-9.58	9.49	0.00	0.00	2.46	19.49	157.70
21	115621	9.52	9.56	-9.62	9.66	0.00	0.00	2.51	19.50	157.70
22	115631	9.66	9.56	-9.72	9.72	0.00	0.00	2.54	19.51	157.70
23	115641	9.67	9.64	-9.82	9.69	0.00	0.00	2.62	19.51	157.70
24	115651	9.81	9.74	-9.97	9.79	0.00	0.00	2.69	19.51	157.70
25	115700	9.77	9.70	-9.95	9.73	0.00	0.00	2.73	19.52	157.70
26	115710	9.83	9.86	-9.94	9.93	0.00	0.00	2.78	19.53	157.70
27	115720	9.93	9.99	-10.03	10.10	0.00	0.00	2.86	19.54	157.70
28	115730	9.92	9.98	-10.02	10.09	0.00	0.00	2.91	19.54	157.70
29	115740	9.91	9.97	-10.02	10.08	0.00	0.00	2.94	19.56	157.70
30	115750	9.94	9.99	-10.02	10.07	0.00	0.00	2.97	19.60	157.70
31	115800	9.91	9.96	-10.02	10.07	0.00	0.00	2.98	19.60	157.70
32	115810	9.92	9.97	-10.02	10.06	0.00	0.00	3.00	19.60	157.70
33	115819	9.91	9.95	-10.02	10.06	0.00	0.00	3.01	19.60	157.70
34	115829	9.90	9.95	-10.01	10.05	0.00	0.00	3.02	19.60	157.70
35	115839	9.91	9.96	-10.01	10.05	0.00	0.00	3.03	19.63	157.70
36	115849	9.91	9.96	-10.01	10.05	0.00	0.00	3.04	19.63	157.70
37	115859	9.90	9.94	-10.01	10.04	0.00	0.00	3.04	19.63	157.69
38	123337	11.22	11.05	-11.54	10.94	0.00	0.00	4.71	19.88	157.10
39	123347	11.57	11.35	-11.99	11.07	0.00	0.00	4.82	19.90	157.10
40	123357	11.54	11.52	-11.76	11.54	0.00	0.00	4.88	19.91	157.06
41	123408	11.61	11.52	-11.85	11.51	0.00	0.00	4.93	19.91	157.04
42	123418	11.61	11.52	-11.85	11.52	0.00	0.00	4.96	19.92	157.02
43	123428	11.61	11.52	-11.85	11.52	0.00	0.00	4.99	19.92	157.01
44	123438	11.60	11.52	-11.85	11.52	0.00	0.00	5.01	19.93	156.94
45	123448	11.61	11.51	-11.85	11.52	0.00	0.00	5.03	19.93	156.80
46	123459	11.62	11.53	-11.85	11.51	0.00	0.00	5.05	19.94	156.80
47	124700	11.60	11.51	-11.85	11.52	0.00	0.00	5.33	19.97	156.80
48	124710	11.60	11.51	-11.85	11.51	0.00	0.00	5.34	19.97	156.80
49	124720	11.60	11.51	-11.85	11.51	0.00	0.00	5.34	19.97	156.80
50	124731	11.62	11.53	-11.84	11.51	0.00	0.00	5.34	19.97	156.80
51	124741	11.62	11.52	-11.85	11.52	0.00	0.00	5.34	19.97	156.80
52	124751	11.63	11.51	-11.87	11.54	0.00	0.00	5.34	19.97	156.80
53	124801	11.61	11.52	-11.85	11.52	0.00	0.00	5.35	19.97	156.80
54	124812	11.60	11.52	-11.85	11.51	0.00	0.00	5.35	19.97	156.80
55	124822	11.73	11.64	-11.97	11.62	0.00	0.00	5.37	19.97	156.80
56	124832	11.76	11.65	-12.00	11.66	0.00	0.00	5.38	19.97	156.80

BEAM R-6 (continued)

Scan #	Time h:mmss	South Reaction (kN)	North Reaction (kN)	South Load (kN)	North Load (kN)	S. Cable Force (kN)	N. Cable Force (kN)	Mid-span Deflection (mm)	Load point Span Change (mm)	Reaction Span Change (mm)
57	124842	11.74	11.67	-12.00	11.66	0.00	0.00	5.38	19.97	156.80
58	124853	11.76	11.65	-12.00	11.66	0.00	0.00	5.38	19.97	156.80
59	124903	11.75	11.66	-12.00	11.66	0.00	0.00	5.39	19.97	156.80
60	124913	11.90	11.75	-12.21	11.70	0.00	0.00	5.44	19.97	156.76
61	124924	12.03	11.83	-12.34	11.75	0.00	0.00	5.47	19.98	156.75
62	124934	12.13	11.94	-12.43	11.89	0.00	0.00	5.49	19.98	156.73
63	124944	12.22	12.07	-12.48	12.05	0.00	0.00	5.54	19.99	156.56
64	124955	12.20	12.09	-12.47	12.08	0.00	0.00	5.56	19.99	156.50
65	125005	12.35	12.16	-12.66	12.10	0.00	0.00	5.61	19.99	156.50
66	125015	12.46	12.26	-12.81	12.18	0.00	0.00	5.69	20.00	156.50
67	125026	12.57	12.38	-12.90	12.31	0.00	0.00	5.78	20.01	156.50
68	125036	12.66	12.52	-12.93	12.50	0.00	0.00	5.91	20.02	156.50
69	125046	12.65	12.52	-12.94	12.50	0.00	0.00	5.99	20.02	156.49
70	125057	12.65	12.52	-12.94	12.49	0.00	0.00	6.04	20.06	156.45
71	125107	12.65	12.52	-12.94	12.50	0.00	0.00	6.08	20.06	156.39
72	125721	12.65	12.52	-12.93	12.50	0.00	0.00	6.46	20.11	156.20
73	125731	12.65	12.52	-12.94	12.49	0.00	0.00	6.46	20.11	156.20
74	125741	12.65	12.52	-12.94	12.49	0.00	0.00	6.47	20.11	156.20
75	125752	12.65	12.52	-12.93	12.50	0.00	0.00	6.47	20.11	156.20
76	125802	12.65	12.52	-12.93	12.50	0.00	0.00	6.48	20.11	156.19
77	125812	12.75	12.73	-13.05	12.84	0.00	0.00	6.57	20.12	156.13
78	125823	12.86	12.81	-13.07	12.87	0.00	0.00	6.61	20.12	156.11
79	125833	12.87	12.83	-13.06	12.88	0.00	0.00	6.63	20.12	156.10
80	125843	12.85	12.81	-13.08	12.84	0.00	0.00	6.65	20.13	156.09
81	125854	12.89	13.00	-13.05	13.09	0.00	0.00	6.71	20.13	155.90
82	125904	12.94	13.16	-12.98	13.38	0.00	0.00	6.82	20.15	155.90
83	125914	12.94	13.16	-12.99	13.38	0.00	0.00	6.87	20.16	155.89
84	125924	13.10	13.21	-13.25	13.35	0.00	0.00	6.95	20.17	155.89
85	125935	13.34	13.21	-13.49	13.31	0.00	0.00	7.12	20.18	155.82
86	125945	13.39	13.31	-13.78	13.25	0.00	0.00	7.38	20.22	155.60
87	125955	13.67	13.30	-14.07	13.16	0.00	0.00	7.80	20.28	155.29
88	130006	13.66	13.32	-14.08	13.17	0.00	0.00	8.16	20.32	155.21
89	130016	13.66	13.32	-14.08	13.16	0.00	0.00	8.40	20.33	154.99
90	131332	13.66	13.32	-14.08	13.17	0.00	0.00	10.32	20.44	154.08
91	131342	13.66	13.32	-14.08	13.16	0.00	0.00	10.33	20.44	154.08
92	131353	13.66	13.32	-14.08	13.17	0.00	0.00	10.34	20.44	154.07
93	131403	13.65	13.32	-14.08	13.17	0.00	0.00	10.35	20.44	154.07
94	131413	13.66	13.32	-14.08	13.17	0.00	0.00	10.36	20.44	154.06
95	131424	13.71	13.59	-14.06	13.43	0.00	0.00	10.47	20.44	153.99
96	131434	13.75	13.52	-14.08	13.47	0.00	0.00	10.49	20.45	153.97
97	131444	13.73	13.53	-14.08	13.46	0.00	0.00	10.52	20.45	153.94
98	131455	13.95	13.61	-14.41	13.43	0.00	0.00	10.66	20.45	153.78
99	131505	14.15	13.63	-14.68	13.33	0.00	0.00	10.84	20.47	153.77
100	131515	14.20	13.63	-14.82	13.29	0.00	0.00	11.15	20.49	153.47
101	131526	14.29	13.76	-14.76	13.51	0.00	0.00	11.58	20.53	153.40
102	131536	14.26	13.81	-14.77	13.57	0.00	0.00	12.12	20.58	153.12
103	131546	14.26	13.80	-14.77	13.58	0.00	0.00	12.58	20.62	152.83
104	131842	14.26	13.80	-14.77	13.57	0.00	0.00	14.30	20.77	151.91
105	131853	14.26	13.81	-14.77	13.58	0.00	0.00	14.33	20.77	151.91
106	131903	14.26	13.80	-14.77	13.57	0.00	0.00	14.36	20.77	151.91
107	131913	14.33	13.91	-14.83	13.68	0.00	0.00	14.42	20.78	151.88
108	131923	14.47	13.93	-15.06	13.62	0.00	0.00	14.51	20.78	151.66
109	131934	14.70	13.90	-15.42	13.47	0.00	0.00	14.73	20.80	151.66
110	131944	14.68	13.93	-15.42	13.47	0.00	0.00	14.93	20.82	151.61
111	131955	14.77	14.03	-15.47	13.61	0.00	0.00	15.24	20.85	151.35
112	132005	14.81	14.16	-15.45	13.83	0.00	0.00	16.11	20.90	150.85

BEAM R-6 (continued)

Scan #	Time hrm:mss	South Reaction (kN)	North Reaction (kN)	South Load (kN)	North Load (kN)	S. Cable Force (kN)	N. Cable Force (kN)	Mid-span Deflection (mm)	Load point Span Change (mm)	Reaction Span Change (mm)
113	132015	15.05	14.16	-15.81	13.69	0.00	0.00	17.46	20.98	150.15
114	132026	15.00	14.20	-15.81	13.69	0.00	0.00	18.21	21.04	149.82
115	132854	15.02	14.18	-15.81	13.69	0.00	0.00	24.45	21.55	145.92
116	132904	15.02	14.18	-15.81	13.69	0.00	0.00	24.47	21.55	145.92
117	132914	15.02	14.18	-15.81	13.69	0.00	0.00	24.49	21.55	145.92
118	132925	15.02	14.17	-15.81	13.69	0.00	0.00	24.51	21.55	145.93
119	132935	15.12	14.19	-16.21	13.49	0.00	0.00	24.61	21.55	145.92
120	132945	15.24	14.18	-16.17	13.55	0.00	0.00	24.63	21.56	145.93
121	132956	15.23	14.18	-16.17	13.55	0.00	0.00	24.68	21.57	145.93
122	133006	15.28	14.58	-15.95	14.19	0.00	0.00	24.91	21.58	145.92
123	133016	15.28	14.81	-15.83	14.56	0.00	0.00	26.12	21.71	145.55
124	133027	15.34	14.87	-15.86	14.66	0.00	0.00	31.15	22.06	143.15
125	133037	15.34	14.89	-15.87	14.65	0.00	0.00	32.21	22.16	142.60
126	133048	15.37	14.98	-15.90	14.75	0.00	0.00	32.88	22.23	142.30
127	133058	15.41	14.96	-15.91	14.75	0.00	0.00	33.74	22.30	141.70
128	133109	15.38	14.97	-15.90	14.75	0.00	0.00	34.23	22.35	141.40
129	133119	15.48	15.17	-15.88	14.99	0.00	0.00	34.96	22.43	141.10
130	133129	15.49	15.32	-15.86	15.24	0.00	0.00	36.90	22.55	139.90
131	133140	15.50	15.32	-15.86	15.24	0.00	0.00	38.98	22.72	139.00
132	133151	15.52	15.31	-15.87	15.24	0.00	0.00	40.37	22.83	138.10
133	133201	15.64	15.36	-16.07	15.19	0.00	0.00	41.41	22.90	137.50
134	133211	15.79	15.38	-16.34	15.15	0.00	0.00	45.38	23.28	135.41
135	133222	15.81	15.39	-16.34	15.15	0.00	0.00	54.74	23.90	131.39
136	133233	15.80	15.39	-16.33	15.15	0.00	0.00	57.00	24.17	130.28
137	133244	15.79	15.39	-16.34	15.15	0.00	0.00	58.18	24.28	129.68
138	133254	15.79	15.39	-16.33	15.15	0.00	0.00	58.95	24.32	129.38
139	133305	15.79	15.39	-16.33	15.15	0.00	0.00	59.52	24.35	129.07
140	133316	15.79	15.39	-16.33	15.15	0.00	0.00	59.97	24.38	128.78
141	133326	15.78	15.38	-16.33	15.15	0.00	0.00	60.38	24.39	128.77
142	133337	15.79	15.39	-16.34	15.15	0.00	0.00	60.68	24.41	128.47
143	133347	15.79	15.39	-16.33	15.15	0.00	0.00	61.01	24.44	128.43
144	133358	15.79	15.39	-16.33	15.15	0.00	0.00	61.30	24.48	128.17
145	133408	15.79	15.40	-16.33	15.15	0.00	0.00	61.57	24.51	128.16
146	133419	15.79	15.39	-16.33	15.15	0.00	0.00	61.85	24.54	127.87
147	133429	15.78	15.39	-16.33	15.15	0.00	0.00	62.11	24.57	127.86
148	133440	15.79	15.40	-16.33	15.15	0.00	0.00	62.33	24.59	127.78
149	134135	15.79	15.40	-16.33	15.15	0.00	0.00	67.20	24.97	125.45
150	134145	15.79	15.39	-16.33	15.15	0.00	0.00	67.26	24.98	125.45
151	134156	15.78	15.40	-16.33	15.15	0.00	0.00	67.32	24.98	125.45
152	134207	15.89	15.43	-16.48	15.14	0.00	0.00	67.44	24.99	125.39
153	134217	15.99	15.47	-16.66	15.13	0.00	0.00	67.63	25.01	125.16
154	134228	16.05	15.55	-16.78	15.12	0.00	0.00	67.93	25.04	125.15
155	134238	16.13	15.52	-16.84	15.09	0.00	0.00	68.42	25.11	124.85
156	134249	16.26	15.53	-17.05	15.03	0.00	0.00	69.71	25.25	124.25
157	134300	16.25	15.52	-17.06	15.03	0.00	0.00	71.18	25.36	123.65
158	134310	16.29	15.59	-17.09	15.10	0.00	0.00	72.51	25.49	123.04
159	134321	16.31	15.62	-17.10	15.15	0.00	0.00	74.50	25.65	122.14
160	134331	16.31	15.61	-17.10	15.16	0.00	0.00	76.44	25.82	121.23
161	134342	16.30	15.61	-17.09	15.16	0.00	0.00	78.25	26.04	120.56
162	134352	16.32	15.63	-17.09	15.16	0.00	0.00	79.99	26.14	119.73
163	134403	16.30	15.62	-17.09	15.16	0.00	0.00	81.81	26.36	118.85
164	134414	16.30	15.61	-17.10	15.16	0.00	0.00	83.49	26.51	118.24
165	134424	16.31	15.63	-17.09	15.16	0.00	0.00	84.72	26.60	117.64
166	134435	16.30	15.62	-17.09	15.16	0.00	0.00	85.76	26.69	117.34
167	134446	16.30	15.61	-17.10	15.16	0.00	0.00	86.55	26.77	117.00
168	134456	16.30	15.62	-17.10	15.15	0.00	0.00	87.23	26.83	116.68

BEAM R-6 (continued)

Scan #	Time hrmmss	South Reaction (kN)	North Reaction (kN)	South Load (kN)	North Load (kN)	S. Cable Force (kN)	N. Cable Force (kN)	Mid-span Deflection (mm)	Load point Span Change (mm)	Reaction Span Change (mm)
169	134507	16.30	15.61	-17.10	15.15	0.00	0.00	87.83	26.93	116.43
170	134518	16.29	15.61	-17.10	15.15	0.00	0.00	88.37	26.99	116.13
171	134529	16.30	15.61	-17.10	15.15	0.00	0.00	88.93	27.04	115.83
172	134539	16.36	15.65	-17.19	15.16	0.00	0.00	89.58	27.08	115.53
173	134550	16.42	15.70	-17.27	15.18	0.00	0.00	90.88	27.16	114.93
174	134600	16.41	15.68	-17.27	15.18	0.00	0.00	92.37	27.32	114.33
175	134611	16.43	15.74	-17.23	15.30	0.00	0.00	93.86	27.48	113.72
176	134622	16.42	15.78	-17.23	15.34	0.00	0.00	96.15	27.73	112.82
177	134632	16.41	15.77	-17.23	15.34	0.00	0.00	98.43	27.95	111.81
178	134643	16.42	15.78	-17.23	15.34	0.00	0.00	100.90	28.23	110.75
179	134653	16.51	15.84	-17.37	15.38	0.00	0.00	103.75	28.53	109.71
180	134704	16.51	15.87	-17.37	15.38	0.00	0.00	109.58	29.12	107.34
181	134715	16.67	15.86	-17.68	15.23	0.00	0.00	118.06	30.08	103.78

BEAM R-7

Scan #	Time hrmrss	South Reaction (kN)	North Reaction (kN)	South Load (kN)	North Load (kN)	S. Cable Force (kN)	N. Cable Force (kN)	Mid-span Deflection (mm)	Load point Span Change (mm)	Reaction Span Change (mm)
1	134403	0.00	0.00	0.00	0.00	0.00	0.00	0.00	23.14	161.31
2	134403	1.53	1.86	-1.31	2.10	0.00	0.00	0.18	23.18	161.31
3	134403	2.75	2.41	-3.07	2.23	0.00	0.00	0.30	23.20	161.31
4	134403	3.31	3.58	-3.11	3.94	0.00	0.00	0.42	23.23	161.31
5	134403	3.38	3.91	-3.03	4.34	0.00	0.00	0.45	23.23	161.31
6	134403	4.65	4.52	-4.75	4.53	0.00	0.00	0.59	23.27	161.31
7	134403	4.67	4.53	-4.77	4.51	0.00	0.00	0.60	23.27	161.30
8	134403	5.62	5.54	-5.68	5.60	0.00	0.00	0.75	23.30	161.30
9	134403	5.58	5.52	-5.64	5.58	0.00	0.00	0.75	23.30	161.30
10	134403	6.62	6.55	-6.68	6.64	0.00	0.00	0.87	23.33	161.30
11	134403	6.78	6.76	-6.81	6.89	0.00	0.00	0.90	23.33	161.31
12	134403	6.89	6.85	-6.95	6.98	0.00	0.00	0.95	23.34	161.31
13	134403	7.08	6.96	-7.18	7.04	0.00	0.00	0.98	23.34	161.31
14	134403	7.11	7.04	-7.18	7.13	0.00	0.00	1.02	23.35	161.31
15	134403	7.54	7.44	-7.63	7.53	0.00	0.00	1.13	23.36	161.31
16	134403	7.53	7.43	-7.63	7.51	0.00	0.00	1.19	23.39	160.96
17	134403	7.53	7.43	-7.63	7.51	0.00	0.00	1.19	23.39	160.95
18	134403	7.53	7.43	-7.63	7.51	0.00	0.00	1.19	23.39	160.95
19	134403	7.62	7.39	-7.83	7.38	0.00	0.00	1.20	23.39	160.96
20	134403	7.67	7.33	-7.92	7.26	0.00	0.00	1.20	23.39	160.96
21	134403	7.82	7.51	-8.05	7.47	0.00	0.00	1.22	23.39	160.96
22	134403	7.95	7.81	-8.08	7.84	0.00	0.00	1.23	23.39	160.96
23	134403	7.95	7.79	-8.08	7.85	0.00	0.00	1.24	23.39	160.96
24	134403	7.95	7.79	-8.08	7.85	0.00	0.00	1.24	23.39	160.96
25	134403	7.94	7.79	-8.08	7.84	0.00	0.00	1.24	23.39	160.96
26	134403	7.94	7.79	-8.08	7.84	0.00	0.00	1.24	23.39	160.96
27	134403	7.94	7.79	-8.08	7.84	0.00	0.00	1.25	23.39	160.96
28	134403	7.94	7.78	-8.08	7.84	0.00	0.00	1.25	23.39	160.96
29	134403	8.22	7.68	-8.61	7.47	0.00	0.00	1.26	23.40	160.95
30	134403	8.04	7.71	-8.30	7.65	0.00	0.00	1.26	23.40	160.96
31	134403	8.12	7.96	-8.26	8.02	0.00	0.00	1.27	23.40	160.96
32	134403	8.11	7.95	-8.25	8.01	0.00	0.00	1.27	23.40	160.96
33	134403	8.36	8.17	-8.51	8.21	0.00	0.00	1.31	23.40	160.96
34	134403	8.35	8.16	-8.51	8.21	0.00	0.00	1.32	23.40	160.95
35	134403	8.34	8.14	-8.51	8.17	0.00	0.00	1.43	23.42	160.89
36	134403	8.34	8.13	-8.51	8.17	0.00	0.00	1.43	23.42	160.89
37	134403	8.33	8.13	-8.51	8.17	0.00	0.00	1.43	23.42	160.90
38	134403	8.52	8.29	-8.73	8.35	0.00	0.00	1.45	23.42	160.90
39	134403	8.62	8.38	-8.82	8.40	0.00	0.00	1.48	23.42	160.69
40	134403	8.75	8.31	-9.08	8.20	0.00	0.00	1.48	23.42	160.90
41	134403	8.83	8.59	-9.05	8.60	0.00	0.00	1.50	23.43	160.90
42	134403	8.80	8.65	-8.95	8.71	0.00	0.00	1.50	23.43	160.90
43	134403	8.96	8.84	-9.09	8.93	0.00	0.00	1.53	23.44	160.90
44	134403	9.07	8.88	-9.23	8.91	0.00	0.00	1.55	23.44	160.89
45	134403	9.07	8.85	-9.27	8.86	0.00	0.00	1.57	23.44	160.89
46	134403	9.06	8.81	-9.27	8.83	0.00	0.00	1.57	23.44	160.89
47	134403	9.13	8.91	-9.33	8.92	0.00	0.00	1.59	23.44	160.90
48	134403	9.26	8.91	-9.57	8.88	0.00	0.00	1.61	23.45	160.88
49	134403	9.24	8.89	-9.53	8.82	0.00	0.00	1.62	23.45	160.87
50	134403	9.23	8.85	-9.53	8.82	0.00	0.00	1.63	23.45	160.86
51	134403	8.36	9.16	-8.35	10.00	0.00	0.00	3.09	23.58	160.66
52	134403	8.11	9.00	-8.79	9.74	0.00	0.00	3.50	23.60	160.66
53	134403	8.87	8.65	-8.95	9.66	0.00	0.00	4.20	23.66	160.33
54	134403	8.75	8.84	-9.29	9.36	0.00	0.00	5.04	23.74	159.80
55	134403	8.77	9.04	-9.34	9.36	0.00	0.00	5.99	23.80	159.49
56	134403	9.18	9.54	-9.37	9.40	0.00	0.00	6.65	23.83	159.10

BEAM R-7 (continued)

Scan #	Time h:mm:ss	South Reaction (kN)	North Reaction (kN)	South Load (kN)	North Load (kN)	S. Cable Force (kN)	N. Cable Force (kN)	Mid-span Deflection (mm)	Load point Span Change (mm)	Reaction Span Change (mm)
57	134403	9.47	9.02	-9.62	9.16	0.00	0.00	7.24	23.85	158.90
58	134403	9.54	9.24	-9.53	9.46	0.00	0.00	7.83	23.88	157.72
59	134403	9.51	9.19	-9.48	9.41	0.00	0.00	7.86	23.89	157.69
60	134403	9.48	9.70	-9.39	10.26	0.00	0.00	10.34	24.10	157.23
61	134403	9.66	10.09	-9.42	10.56	0.00	0.00	10.94	24.16	157.00
62	134403	9.75	10.02	-9.62	10.47	0.00	0.00	11.72	24.20	156.64
63	134403	9.77	9.95	-9.62	10.47	0.00	0.00	12.06	24.24	156.44
64	134403	10.01	10.08	-9.62	10.47	0.00	0.00	13.05	24.29	155.90
65	134403	9.85	10.19	-9.67	10.55	0.00	0.00	13.49	24.30	155.78
66	134403	9.72	10.15	-9.51	10.59	0.00	0.00	13.53	24.30	155.63
67	134403	9.66	10.06	-9.47	10.48	0.00	0.00	15.15	24.36	154.96
68	134403	9.94	10.54	-9.59	10.90	0.00	0.00	16.98	24.52	153.78
69	134403	9.92	10.66	-9.59	10.90	0.00	0.00	18.25	24.63	153.41
70	134403	9.97	10.36	-9.85	10.65	0.00	0.00	18.99	24.70	152.87
71	134403	10.01	10.45	-9.84	10.66	0.00	0.00	19.39	24.73	152.81
72	134403	10.01	10.45	-9.85	10.65	0.00	0.00	24.09	25.05	150.15
73	134403	10.03	10.39	-9.81	10.72	0.00	0.00	26.77	25.30	148.64
74	134403	10.01	10.47	-9.91	10.66	0.00	0.00	26.88	25.31	148.63
75	134403	10.15	10.48	-9.93	10.80	0.00	0.00	26.96	25.32	148.60
76	134403	10.18	10.45	-9.95	10.78	0.00	0.00	27.90	25.38	148.03
77	134403	10.18	10.48	-9.95	10.78	0.00	0.00	34.52	25.44	147.73
78	134403	10.20	10.48	-9.95	10.78	0.00	0.00	38.12	25.46	147.43
79	134403	10.40	10.33	-10.20	10.72	0.00	0.00	42.35	25.52	147.06
80	134403	10.53	10.35	-10.36	10.67	0.00	0.00	43.25	25.55	146.72
81	134403	10.57	10.39	-10.39	10.75	0.00	0.00	49.69	25.64	145.92
82	134403	10.57	10.42	-10.39	10.82	0.00	0.00	53.63	25.65	145.85
83	134403	10.62	10.45	-10.39	10.82	0.00	0.00	55.64	25.83	144.34
84	134403	10.69	10.52	-10.45	11.00	0.00	0.00	61.57	26.08	142.83
85	134403	10.72	10.73	-10.48	11.17	0.00	0.00	63.59	30.63	115.53
86	134403	10.74	-0.06	-10.51	11.25	0.00	0.00	130.17	30.63	115.52
87	134403	0.45	0.07	-10.53	11.26	0.00	0.00			

BEAM RH-1

Scan #	Time h:mm:ss	South Reaction (kN)	North Reaction (kN)	South Load (kN)	North Load (kN)	S. Cable Force (kN)	N. Cable Force (kN)	Mid-span Deflection (mm)	Load point Span Change (mm)	Reaction Span Change (mm)
1	123703	0.00	0.00	0.00	0.00	109.42	107.91	0.00	32.03	171.21
2	123747	2.31	2.63	2.31	2.63	109.39	107.91	0.11	32.04	171.22
3	123754	3.17	4.20	3.17	4.20	109.63	107.91	0.19	32.05	171.21
4	123802	4.04	4.78	4.04	4.78	109.63	107.91	0.25	32.06	171.21
5	123809	5.30	5.93	5.30	5.93	109.64	107.91	0.33	32.08	171.22
6	123815	5.83	6.13	5.83	6.13	109.64	107.91	0.35	32.09	171.21
7	123823	6.60	6.96	6.60	6.96	109.65	107.91	0.41	32.09	171.22
8	123827	6.74	7.23	6.74	7.23	109.65	107.92	0.43	32.09	171.21
9	124200	7.86	7.68	7.86	7.68	109.66	107.92	0.50	32.10	171.21
10	124208	8.19	8.77	7.76	8.66	109.68	107.92	0.54	32.10	171.21
11	124212	8.28	9.08	9.34	8.59	109.70	107.92	0.55	32.11	171.21
12	124218	10.11	10.39	9.82	10.49	109.65	107.91	0.66	32.13	171.22
13	124223	10.90	11.35	11.10	11.75	109.66	107.94	0.72	32.14	171.21
14	124227	11.98	12.08	11.83	12.60	109.65	107.93	0.79	32.16	171.21
15	124231	12.99	13.28	12.48	13.71	109.71	107.94	0.86	32.17	171.21
16	124234	13.84	13.91	13.73	14.44	109.74	107.95	0.91	32.18	171.21
17	124238	14.57	14.52	14.22	15.18	109.75	107.94	0.95	32.20	171.21
18	124243	16.15	16.01	15.09	16.81	109.77	107.94	1.07	32.23	171.21
19	124251	18.17	18.11	16.52	18.84	109.83	107.95	1.22	32.26	171.21
20	124257	18.37	18.62	18.53	18.76	109.85	107.94	1.25	32.27	171.21
21	124303	18.49	18.58	19.08	18.91	109.87	107.95	1.26	32.28	171.21
22	124311	18.47	18.59	19.01	18.91	109.87	107.95	1.27	32.28	171.21
23	124333	18.54	18.71	19.03	18.93	109.89	107.96	1.28	32.28	171.21
24	124720	19.57	19.73	19.29	20.41	109.90	107.98	1.40	32.32	171.21
25	124726	20.18	20.73	19.93	20.26	109.90	107.98	1.45	32.32	171.21
26	124732	21.28	22.28	21.54	21.38	109.93	107.97	1.53	32.34	171.21
27	124738	22.73	23.82	23.30	22.82	110.00	107.97	1.66	32.37	171.21
28	124747	24.67	24.25	25.10	25.26	110.07	107.98	1.77	32.40	171.21
29	124759	25.09	25.33	24.67	25.41	110.09	107.98	1.84	32.41	171.21
30	124807	25.31	25.50	25.86	25.70	110.10	107.98	1.86	32.42	171.21
31	124824	25.77	25.42	25.90	26.47	110.12	107.99	1.89	32.43	171.21
32	124832	25.79	25.45	25.60	26.58	110.15	107.99	1.90	32.43	171.21
33	124840	25.73	25.47	25.54	26.56	110.14	108.00	1.90	32.43	171.21
34	124851	25.90	25.39	25.55	26.66	110.14	107.99	1.91	32.43	171.21
35	124914	26.00	25.42	25.51	26.79	110.16	108.00	1.92	32.44	171.21
36	124934	25.98	25.41	25.44	26.78	110.18	108.00	1.92	32.44	171.21
37	125034	25.94	25.37	25.44	26.83	110.16	107.99	1.94	32.44	171.21
38	125219	25.91	25.36	25.39	26.80	110.17	108.00	1.95	32.44	171.21
39	125341	25.89	25.36	25.39	26.79	110.16	108.00	1.95	32.44	171.21
40	125430	25.89	25.36	25.39	26.82	110.17	108.01	1.96	32.44	171.21
41	125449	26.11	25.37	25.39	27.01	110.16	108.01	1.98	32.45	171.21
42	125557	26.56	25.59	25.33	27.77	110.15	108.01	2.00	32.47	171.21
43	125616	26.76	25.92	25.41	27.94	110.16	108.02	2.02	32.47	171.21
44	125625	26.86	25.99	25.70	27.97	110.18	108.01	2.03	32.47	171.21
45	125641	27.00	26.32	25.88	27.95	110.17	108.01	2.04	32.48	171.21
46	125654	27.26	26.51	26.40	28.11	110.19	108.01	2.06	32.49	171.21
47	125705	27.10	26.74	26.79	27.93	110.18	108.01	2.07	32.50	171.21
48	125715	27.33	27.00	26.97	27.70	110.20	108.02	2.08	32.50	171.21
49	125723	27.33	26.98	27.68	27.79	110.21	108.02	2.09	32.52	171.21
50	125734	27.29	26.98	27.63	27.75	110.20	108.01	2.09	32.52	171.21
51	125745	27.18	27.07	27.62	27.70	110.22	108.01	2.09	32.52	171.21
52	125756	27.16	27.09	27.63	27.66	110.22	108.01	2.10	32.52	171.21
53	125801	27.22	27.03	27.64	27.72	110.23	108.02	2.10	32.52	171.21
54	125809	27.20	27.04	27.62	27.71	110.23	108.01	2.10	32.52	171.21
55	125816	27.19	27.08	27.63	27.69	110.23	108.01	2.11	32.52	171.21
56	125819	27.22	27.06	27.65	27.71	110.24	108.01	2.11	32.52	171.21

BEAM RH-1 (continued)

Scan #	Time	South Reaction (kN)	North Reaction (kN)	South Load (kN)	North Load (kN)	S. Cable Force (kN)	N. Cable Force (kN)	Mid-span Deflection (mm)	Load point Span Change (mm)	Reaction Span Change (mm)
	hhmmss									
57	125824	27.19	27.07	27.64	27.70	110.24	108.02	2.11	32.52	171.21
58	125827	27.19	27.06	27.65	27.72	110.22	108.01	2.12	32.52	171.21
59	125832	27.14	27.07	27.65	27.70	110.22	108.02	2.12	32.52	171.21
60	125836	27.19	27.07	27.63	27.71	110.22	108.00	2.12	32.52	171.21
61	125839	27.25	26.99	27.65	27.75	110.23	107.99	2.13	32.52	171.22
62	125842	27.23	26.99	27.63	27.74	110.24	108.01	2.13	32.52	171.21
63	125844	27.15	27.07	27.62	27.70	110.25	107.98	2.13	32.52	171.21
64	125847	27.25	26.98	27.64	27.73	110.24	107.98	2.13	32.52	171.21
65	125849	27.15	27.08	27.62	27.71	110.24	107.99	2.14	32.52	171.21
66	125852	27.24	26.97	27.63	27.71	110.31	107.98	2.17	32.52	171.21
67	125854	27.25	26.95	27.64	27.74	110.33	108.01	2.19	32.53	171.21
68	125857	27.20	27.04	27.62	27.70	110.35	107.98	2.20	32.53	171.21
69	125859	27.31	26.93	27.64	27.73	110.37	107.99	2.21	32.53	171.21
70	125901	27.22	27.02	27.63	27.70	110.38	107.99	2.22	32.53	171.21
71	125904	27.27	27.00	27.63	27.70	110.38	108.02	2.23	32.53	171.21
72	125906	27.30	26.96	27.65	27.73	110.40	107.98	2.24	32.54	171.21
73	125909	27.20	27.03	27.62	27.69	110.40	107.98	2.26	32.54	171.21
74	125911	27.25	26.95	27.63	27.72	110.44	136.76	2.32	33.60	162.80
75	125914	27.19	27.05	29.64	27.64	138.66	135.22	37.78	36.19	155.28
76	125916	27.25	27.10	27.57	27.67	138.11	134.84	37.78	36.19	155.28
77	130041	27.27	27.01	27.58	27.73	136.70	133.17	37.78	36.18	155.28
78	131419	27.27	26.88	27.61	27.72	135.93	132.17	37.85	36.10	155.28
79	131422	27.24	26.91	27.62	27.68	135.93	132.17	37.85	36.10	155.28
80	131424	27.29	26.87	27.62	27.70	135.92	132.17	37.85	36.10	155.28
81	131427	27.25	26.90	27.63	27.68	135.91	132.17	37.85	36.10	155.28
82	131430	27.25	26.90	27.62	27.67	135.91	132.16	37.85	36.10	155.28
83	131432	27.29	26.87	27.62	27.71	135.91	132.16	37.85	36.10	155.28
84	131435	27.24	26.91	27.62	27.68	135.93	132.16	37.85	36.10	155.28
85	131437	27.27	26.91	27.62	27.69	135.92	132.16	37.85	36.10	155.28
86	131440	27.28	26.88	27.62	27.71	135.92	132.16	37.85	36.10	155.28
87	131442	27.24	26.91	27.62	27.67	135.91	132.16	37.85	36.10	155.28
88	131445	27.31	26.89	27.63	27.76	135.92	132.16	37.85	36.10	155.28
89	131448	27.40	27.01	27.59	27.93	136.08	132.58	37.91	36.10	155.28
90	131450	27.43	27.05	27.64	28.07	136.10	132.67	37.92	36.10	155.28
91	131453	27.61	27.04	27.74	28.19	136.07	132.82	38.03	36.10	155.28
92	131455	27.53	27.10	27.59	28.13	136.07	132.83	38.04	36.10	155.28
93	131458	27.59	27.07	27.66	28.37	136.09	133.23	38.07	36.13	155.28
94	131500	27.76	27.14	27.74	28.44	136.14	133.41	38.30	36.13	155.28
95	131503	27.67	27.20	27.64	28.42	136.16	133.42	38.31	36.13	155.28
96	131506	27.68	27.15	27.65	28.33	136.14	133.42	38.31	36.13	155.28
97	131508	27.76	27.11	27.66	28.41	136.16	133.42	38.31	36.13	155.28
98	131511	27.85	27.21	27.63	28.60	136.19	133.69	38.46	36.14	155.28
99	131513	27.88	27.21	27.55	28.65	136.20	133.73	38.47	36.15	155.28
100	131516	27.93	27.15	27.58	28.67	136.21	133.72	38.47	36.15	155.28
101	131518	27.79	27.23	27.55	28.81	136.20	133.72	38.47	36.15	155.28
102	131521	27.90	27.15	27.58	28.65	136.20	133.71	38.48	36.15	155.28
103	131524	27.89	27.18	27.57	28.65	136.21	133.71	38.47	36.15	155.28
104	131526	27.79	27.22	27.60	28.61	136.19	133.70	38.48	36.15	155.28
105	131529	27.96	27.16	27.57	28.67	136.19	133.74	38.52	36.15	155.28
106	131531	27.95	27.30	27.75	28.73	136.37	134.13	38.66	36.17	155.28
107	131534	28.01	27.47	27.80	28.74	136.68	134.57	38.96	36.20	155.28
108	131537	28.09	27.40	27.92	28.80	136.66	134.56	38.96	36.20	155.28
109	131539	27.99	27.49	27.86	28.76	136.67	134.55	38.96	36.20	155.28
110	131542	28.05	27.43	27.86	28.80	136.67	134.54	38.96	36.20	155.28
111	131544	28.16	27.50	27.86	28.79	136.86	134.58	39.09	36.21	155.28
112	131547	28.05	27.62	28.10	28.74	136.88	134.63	39.09	36.21	155.28

BEAM RH-1 (continued)

Scan #	Time hhmmss	South Reaction (kN)	North Reaction (kN)	South Load (kN)	North Load (kN)	S. Cable Force (kN)	N. Cable Force (kN)	Mid-span Deflection (mm)	Load point Span Change (mm)	Reaction Span Change (mm)
113	131549	28.15	27.77	28.19	28.75	137.22	134.94	39.35	36.22	155.28
114	131552	28.15	27.74	28.38	28.73	137.21	134.93	39.35	36.22	155.28
115	131555	28.07	27.83	28.38	28.66	137.22	134.93	39.36	36.22	155.28
116	131557	28.18	27.71	28.40	28.74	137.20	134.92	39.36	36.23	155.28
117	131600	28.11	27.80	28.39	28.68	137.21	134.90	39.36	36.23	155.28
118	131602	28.21	27.94	28.40	28.83	137.84	135.43	39.80	36.25	155.26
119	131605	28.26	27.98	28.56	28.80	137.87	135.46	39.81	36.25	155.24
120	131607	28.42	28.14	28.62	28.99	138.44	136.08	40.28	36.27	154.98
121	131610	28.27	28.22	28.70	28.77	138.48	136.07	40.28	36.28	154.98
122	131613	28.46	28.21	28.77	28.86	138.74	136.20	40.48	36.29	154.98
123	131615	28.37	28.23	28.96	28.84	138.71	136.19	40.48	36.29	154.98
124	131618	28.30	28.35	28.91	28.77	138.71	136.16	40.48	36.29	154.98
125	131620	28.43	28.19	28.93	28.91	138.70	136.14	40.48	36.29	154.98
126	131623	28.35	28.24	28.95	28.86	138.67	136.13	40.48	36.29	154.98
127	131626	28.33	28.30	28.91	28.89	138.68	136.11	40.49	36.29	154.98
128	131628	28.42	28.24	28.94	28.88	138.66	136.10	40.49	36.29	154.98
129	131631	28.33	28.25	28.94	28.86	138.63	136.09	40.49	36.29	154.98
130	131645	28.56	28.54	28.91	28.78	139.48	136.82	41.05	36.34	154.67
131	131649	28.50	28.54	29.45	28.82	139.45	136.80	41.05	36.35	154.67
132	131718	28.50	28.86	29.43	28.64	140.15	137.39	41.63	36.42	154.37
133	131803	28.82	29.06	29.89	29.03	140.32	138.10	42.28	36.47	154.08
134	131806	28.77	29.02	29.99	29.00	140.32	138.09	42.29	36.47	154.08
135	131836	28.78	29.19	29.98	28.85	140.99	138.14	42.48	36.48	154.07
136	131935	28.73	29.21	30.33	28.82	140.81	138.13	42.56	36.49	154.07
137	132013	28.73	29.22	30.34	28.80	140.74	138.09	42.61	36.50	154.07
138	132115	28.89	29.20	30.34	28.97	141.18	138.43	42.94	36.51	153.77
139	132118	28.98	29.23	30.33	29.09	141.54	138.81	43.22	36.54	153.77
140	132121	28.99	29.26	30.24	29.13	141.49	138.81	43.22	36.54	153.77
141	132127	29.16	29.25	30.29	29.39	141.70	139.14	43.44	36.56	153.76
142	132136	29.38	29.34	30.19	29.73	142.02	139.63	43.81	36.59	153.47
143	132141	29.52	29.34	30.01	30.07	142.35	140.07	44.12	36.62	153.47
144	132206	29.70	29.48	29.92	30.43	142.64	140.81	44.75	36.67	153.17
145	132209	29.86	29.41	30.09	30.54	142.97	140.93	44.84	36.67	153.17
146	132223	30.07	29.50	30.08	30.81	143.39	141.48	45.31	36.72	152.87
147	132227	30.03	29.51	29.88	30.81	143.37	141.45	45.33	36.72	152.87
148	132247	30.17	29.55	29.88	30.97	143.46	141.64	45.56	36.75	152.86
149	132300	30.26	29.58	29.89	31.11	143.67	141.93	45.81	36.78	152.70
150	132306	30.33	29.55	29.86	31.18	143.64	141.96	45.87	36.79	152.57
151	132318	30.34	29.76	29.87	31.05	144.04	142.29	46.20	36.82	152.56
152	132324	30.39	29.85	30.22	31.12	144.57	142.60	46.58	36.87	152.27
153	132335	30.43	29.99	30.33	31.14	144.95	142.90	46.90	36.90	152.26
154	132338	30.46	29.99	30.50	31.14	144.89	142.85	46.91	36.90	152.26
155	132355	30.52	30.01	30.51	31.26	144.83	143.08	47.11	36.92	152.26
156	132407	30.62	30.11	30.53	31.23	145.31	143.41	47.47	36.96	151.96
157	132411	30.61	30.13	30.81	31.26	145.28	143.40	47.48	36.96	151.96
158	132429	30.61	30.28	30.70	31.24	145.51	143.61	47.84	36.99	151.96
159	132441	30.76	30.42	30.87	31.41	145.81	144.05	48.22	37.02	151.66
160	132447	30.85	30.33	30.95	31.53	145.82	144.09	48.31	37.03	151.66
161	132458	30.85	30.42	30.95	31.46	145.76	144.28	48.55	37.05	151.65
162	132504	30.86	30.47	31.10	31.47	146.16	144.34	48.64	37.06	151.65
163	132529	30.95	30.55	31.10	31.50	146.42	144.60	49.04	37.09	151.35
164	132553	31.06	30.66	31.23	31.53	146.84	145.03	49.51	37.12	151.05
165	132559	30.99	30.83	31.44	31.56	146.94	145.07	49.63	37.13	151.05
166	132620	31.02	30.76	31.44	31.57	147.15	145.25	49.92	37.16	151.05
167	132626	31.01	30.85	31.44	31.53	147.13	145.25	50.02	37.17	151.05
168	132638	31.41	30.85	31.51	32.13	147.50	145.90	50.53	37.22	150.75

BEAM RH-1 (continued)

Scan #	Time hrmms	South Reaction (kN)	North Reaction (kN)	South Load (kN)	North Load (kN)	S. Cable Force (kN)	N. Cable Force (kN)	Mid-span Deflection (mm)	Load point Span (mm)	Span Change (mm)	Reaction
169	132650	31.64	30.88	31.29	32.48	148.01	146.41	51.16	37.28	150.45	
170	132702	31.63	30.87	31.21	32.47	147.91	146.35	51.26	37.29	150.44	
171	132717	31.64	30.83	31.24	32.46	147.77	146.33	51.38	37.30	150.45	
172	132726	31.58	30.87	31.21	32.45	147.74	146.31	51.43	37.31	150.45	
173	132756	31.66	30.75	31.21	32.49	147.60	146.26	51.57	37.32	150.44	
174	132759	31.65	30.73	31.19	32.47	147.61	146.26	51.58	37.32	150.45	
175	132802	31.55	30.83	31.18	32.44	147.66	146.25	51.59	37.32	150.45	
176	132804	31.64	30.74	31.19	32.44	147.62	146.27	51.60	37.32	150.45	
177	132807	31.64	30.75	31.20	32.42	147.63	146.27	51.61	37.32	150.44	
178	132809	31.56	30.82	31.21	32.46	147.61	146.27	51.62	37.32	150.43	
179	132812	31.63	30.78	31.21	32.43	147.59	146.25	51.63	37.32	150.40	
180	132815	31.64	30.74	31.21	32.46	147.58	146.26	51.63	37.32	150.39	
181	132817	31.56	30.81	31.21	32.44	147.56	146.27	51.64	37.32	150.38	
182	132820	31.63	30.76	31.22	32.45	147.56	146.24	51.66	37.32	150.36	
183	132822	31.63	30.74	31.20	32.45	147.56	146.25	51.66	37.32	150.33	
184	132825	31.56	30.81	31.21	32.45	147.55	146.24	51.66	37.32	150.33	
185	132828	31.63	30.73	31.21	32.46	147.54	146.24	51.67	37.32	150.19	
186	132830	31.63	30.74	31.21	32.44	147.52	146.23	51.68	37.32	150.14	
187	132833	31.56	30.81	31.21	32.47	147.54	146.24	51.69	37.33	150.14	
188	132835	31.63	30.73	31.21	32.46	147.52	146.23	51.70	37.33	150.14	
189	132838	31.63	30.74	31.21	32.43	147.50	146.23	51.71	37.33	150.14	
190	132841	31.56	30.81	31.21	32.45	147.52	146.23	51.72	37.33	150.14	
191	132843	31.63	30.73	31.21	32.44	147.53	146.23	51.74	37.33	150.14	
192	132846	31.63	30.74	31.21	32.44	147.54	146.22	51.74	37.33	150.14	
193	132848	31.56	30.81	31.21	32.47	147.41	146.23	51.75	37.33	150.14	
194	132851	31.62	30.73	31.21	32.49	147.44	146.23	51.77	37.33	150.14	
195	132854	31.62	30.75	31.21	32.47	147.55	146.23	51.77	37.33	150.14	
196	132856	31.57	30.81	31.20	32.48	147.55	146.24	51.79	37.33	150.14	
197	132859	31.62	30.74	31.21	32.43	147.52	146.24	51.80	37.33	150.14	
198	132902	31.64	30.74	31.21	32.46	147.51	146.23	51.80	37.33	150.14	
199	132904	31.56	30.81	31.21	32.45	147.50	146.23	51.81	37.33	150.14	
200	132909	31.63	30.74	31.21	32.43	147.52	146.23	51.82	37.34	150.14	
201	132915	31.61	30.74	31.21	32.43	147.50	146.21	51.83	37.34	150.14	
202	132920	31.56	30.80	31.21	32.46	147.47	146.21	51.85	37.34	150.14	
203	132925	31.62	30.74	31.21	32.46	147.42	146.20	51.87	37.34	150.14	
204	132930	31.61	30.74	31.19	32.47	147.43	146.21	51.89	37.35	150.14	
205	132936	31.57	30.81	31.21	32.47	147.48	146.21	51.91	37.35	150.14	
206	132941	31.64	30.74	31.21	32.47	147.47	146.20	51.93	37.35	150.14	
207	132946	31.60	30.76	31.21	32.45	147.48	146.20	51.95	37.35	150.14	
208	132951	31.57	30.80	31.21	32.43	147.46	146.20	51.96	37.35	150.14	
209	132957	31.64	30.73	31.21	32.42	147.47	146.20	51.97	37.35	150.14	
210	133002	31.60	30.76	31.21	32.46	147.44	146.20	51.99	37.35	150.14	
211	133007	31.57	30.80	31.21	32.45	147.43	146.20	52.01	37.35	150.14	
212	133012	31.64	30.73	31.21	32.42	147.42	146.19	52.02	37.35	150.14	
213	133018	31.57	30.82	31.21	32.44	147.42	146.19	52.03	37.35	150.15	
214	133023	31.58	30.77	31.19	32.45	147.42	146.19	52.05	37.35	150.14	
215	133028	31.63	30.75	31.20	32.43	147.46	146.17	52.08	37.35	150.14	
216	133034	31.57	30.79	31.20	32.45	147.46	146.18	52.09	37.35	150.14	
217	133039	31.59	30.77	31.21	32.45	147.44	146.33	52.11	37.37	150.13	
218	133044	31.79	30.74	31.19	32.50	148.09	146.66	52.49	37.39	149.84	
219	133049	31.67	30.93	31.28	32.63	148.05	146.66	52.52	37.40	149.84	
220	133055	31.76	30.82	31.18	32.68	148.02	146.67	52.52	37.40	149.84	
221	133100	31.96	30.77	31.17	32.87	148.22	146.97	52.78	37.42	149.84	
222	133105	31.86	30.87	31.09	32.86	148.21	146.95	52.80	37.42	149.84	
223	133110	31.89	30.85	31.12	32.87	148.19	146.97	52.84	37.42	149.84	
224	133116	32.03	30.77	31.11	33.03	148.47	147.14	53.02	37.43	149.84	

BEAM RH-1 (continued)

Scan #	Time h:mm:ss	South Reaction (kN)	North Reaction (kN)	South Load (kN)	North Load (kN)	S. Cable Force (kN)	N. Cable Force (kN)	Mid-span Deflection (mm)	Load point Span Change (mm)	Reaction Span Change (mm)
225	133121	31.94	30.93	31.12	32.99	148.60	147.24	53.17	37.45	149.54
226	133126	32.00	31.03	31.15	33.06	148.87	147.49	53.39	37.47	149.54
227	133131	32.07	30.95	31.24	33.01	148.82	147.45	53.43	37.47	149.54
228	133137	32.02	31.16	31.28	33.09	149.12	147.69	53.63	37.49	149.54
229	133142	32.06	31.12	31.42	33.05	149.04	147.70	53.69	37.49	149.48
230	133147	32.10	31.05	31.46	33.09	149.04	147.72	53.76	37.49	149.46
231	133152	32.11	31.19	31.43	33.10	149.36	148.00	53.98	37.52	149.23
232	133157	32.14	31.18	31.48	33.12	149.29	147.99	54.03	37.53	149.24
233	133203	32.20	31.12	31.48	33.18	149.52	148.01	54.21	37.54	149.24
234	133208	32.21	31.23	31.46	33.17	149.74	148.27	54.48	37.57	149.09
235	133213	32.16	31.32	31.62	33.12	149.79	148.29	54.57	37.58	148.93
236	133218	32.27	31.21	31.61	33.14	149.71	148.30	54.62	37.59	148.93
237	133224	32.19	31.55	31.58	33.12	150.61	148.88	55.28	37.68	148.63
238	133229	32.27	31.56	32.12	33.00	150.56	148.85	55.37	37.68	148.62
239	133234	32.29	31.48	31.95	33.06	150.50	148.84	55.44	37.69	148.62
240	133239	32.25	31.64	32.01	33.01	150.92	149.11	55.82	37.72	148.63
241	133244	32.26	31.67	32.04	33.00	150.91	149.09	55.87	37.72	148.33
242	133250	32.32	31.61	32.24	33.00	150.79	149.09	55.93	37.73	148.33
243	133255	32.33	31.82	32.24	32.90	151.61	149.71	56.55	37.76	148.27
244	133300	32.28	31.85	32.54	32.90	151.41	149.54	56.57	37.77	148.25
245	133305	32.42	31.80	32.45	32.97	151.61	149.68	56.78	37.78	148.02
246	133311	32.39	31.82	32.44	33.05	151.47	149.65	56.87	37.78	148.02
247	133316	32.43	31.85	32.43	33.10	151.65	149.82	57.07	37.80	148.02
248	133321	32.46	31.80	32.38	33.12	151.53	149.75	57.13	37.80	148.02
249	133326	32.41	31.85	32.41	33.10	151.47	149.74	57.19	37.81	148.02
250	133332	32.42	31.84	32.43	33.12	151.45	149.72	57.24	37.81	148.02
251	133337	32.45	31.80	32.41	33.13	151.41	149.71	57.29	37.81	148.02
252	133342	32.41	31.84	32.41	33.09	151.41	149.71	57.33	37.81	147.95
253	133347	32.43	31.83	32.42	33.10	151.31	149.72	57.39	37.82	147.72
254	133352	32.44	31.80	32.41	33.09	151.29	149.74	57.47	37.82	147.72
255	133358	32.41	31.84	32.41	33.10	151.30	149.74	57.53	37.83	147.72
256	133403	32.43	31.82	32.42	33.11	151.32	149.73	57.60	37.83	147.72
257	133408	32.44	31.80	32.41	33.11	151.29	149.74	57.66	37.84	147.72
258	133413	32.41	31.84	32.42	33.10	151.28	149.75	57.71	37.84	147.72
259	133419	32.43	31.82	32.42	33.09	151.26	149.74	57.75	37.84	147.72
260	133424	32.43	31.80	32.41	33.10	151.26	149.74	57.78	37.85	147.72
261	133429	32.41	31.84	32.41	33.10	151.26	149.73	57.79	37.86	147.72
262	133434	32.43	31.81	32.41	33.11	151.26	149.73	57.81	37.86	147.72
263	133439	32.43	31.81	32.41	33.10	151.25	149.74	57.82	37.86	147.72
264	133445	32.41	31.84	32.41	33.10	151.22	149.73	57.83	37.87	147.72
265	133450	32.43	31.81	32.42	33.10	151.20	149.73	57.84	37.88	147.72
266	133455	32.42	31.82	32.41	33.11	151.19	149.73	57.88	37.88	147.72
267	133500	32.42	31.83	32.41	33.09	151.20	149.76	57.92	37.88	147.72
268	133506	32.44	31.81	32.41	33.06	151.25	149.75	57.99	37.89	147.72
269	133511	32.42	31.83	32.41	33.09	151.23	149.79	58.06	37.89	147.72
270	133516	32.42	31.82	32.41	33.10	151.18	149.79	58.10	37.90	147.70
271	133524	32.43	31.82	32.41	33.07	151.17	149.80	58.14	37.92	147.56
272	133532	32.43	31.81	32.41	33.09	151.14	149.79	58.20	37.92	147.42
273	133540	32.44	31.81	32.41	33.09	151.52	149.78	58.40	37.93	147.42
274	133548	32.44	31.81	32.41	33.11	151.42	149.77	58.42	37.93	147.42
275	133558	32.43	31.83	32.41	33.10	151.35	149.78	58.46	37.93	147.42
276	133608	32.42	31.83	32.41	33.07	151.30	149.77	58.50	37.94	147.42
277	133619	32.42	31.83	32.42	33.12	151.19	149.75	58.53	37.94	147.42
278	133629	32.43	31.81	32.40	33.09	151.17	149.77	58.55	37.94	147.42
279	133640	32.43	31.82	32.41	33.08	151.17	149.77	58.56	37.95	147.42
280	133650	32.42	31.83	32.41	33.10	151.06	149.77	58.57	37.95	147.42

BEAM RH-1 (continued)

Scan #	Time hrmms	South Reaction (kN)	North Reaction (kN)	South Load (kN)	North Load (kN)	S. Cable Force (kN)	N. Cable Force (kN)	Mid-span Deflection (mm)	Load point Span Change (mm)	Reaction Span Change (mm)
281	133701	32.43	31.81	32.41	33.12	151.05	149.76	58.58	37.95	147.42
282	133711	32.43	31.81	32.42	33.14	151.04	149.76	58.61	37.95	147.42
283	133722	32.42	31.82	32.41	33.13	150.95	149.76	58.63	37.96	147.42
284	133732	32.42	31.83	32.41	33.12	151.02	149.77	58.68	37.96	147.42
285	133743	32.43	31.82	32.41	33.12	151.06	149.76	58.75	37.97	147.42
286	133753	32.43	31.81	32.42	33.12	151.06	149.77	58.80	37.98	147.37
287	133804	32.43	31.82	32.41	33.12	151.02	149.77	58.83	37.98	147.34
288	133814	32.41	31.84	32.42	33.11	150.99	149.77	58.86	37.98	147.30
289	133825	32.42	31.82	32.40	33.13	150.96	149.78	58.89	37.98	147.12
290	133835	32.42	31.83	32.41	33.11	150.96	149.77	58.93	37.99	147.12
291	133846	32.43	31.81	32.40	33.11	150.92	149.79	58.96	37.99	147.12
292	133856	32.43	31.83	32.41	33.12	151.42	149.82	59.16	38.01	147.12
293	133907	32.43	31.83	32.39	33.13	151.32	149.80	59.17	38.01	147.12
294	133917	32.42	31.84	32.41	33.14	151.27	149.76	59.19	38.01	147.12
295	133928	32.43	31.83	32.40	33.13	151.21	149.78	59.21	38.01	147.12
296	133938	32.43	31.83	32.40	33.14	151.17	149.77	59.23	38.01	147.12
297	133949	32.42	31.83	32.40	33.14	151.14	149.79	59.25	38.02	147.12
298	133959	32.41	31.84	32.41	33.13	151.12	149.79	59.28	38.02	147.12
299	134010	32.43	31.81	32.40	33.13	151.09	149.80	59.30	38.02	147.12
300	134020	32.43	31.83	32.41	33.12	151.06	149.80	59.33	38.02	147.12
301	134031	32.43	31.82	32.40	33.12	151.01	149.81	59.34	38.02	147.12
302	134041	32.43	31.83	32.41	33.12	151.02	149.87	59.39	38.03	147.12
303	134052	32.43	31.82	32.41	33.10	150.98	149.86	59.40	38.04	147.12
304	134102	32.43	31.81	32.41	33.12	150.97	149.83	59.41	38.03	147.12
305	134113	32.44	31.81	32.41	33.12	150.93	149.83	59.43	38.04	147.12
306	134123	32.43	31.82	32.41	33.09	150.93	149.82	59.44	38.04	147.12
307	134134	32.61	31.90	32.41	33.10	151.66	150.38	59.96	38.08	146.82
308	134144	32.60	31.90	32.41	33.13	151.58	150.31	59.97	38.08	146.82
309	134155	32.68	32.05	32.42	33.14	152.06	150.74	60.36	38.12	146.68
310	134205	32.68	32.05	32.41	33.05	151.98	150.65	60.38	38.12	146.52
311	134216	32.84	32.16	32.41	33.13	152.56	151.18	60.88	38.18	146.52
312	134226	32.87	32.19	32.41	33.12	152.59	151.26	61.09	38.19	146.47
313	134237	32.86	32.19	32.41	33.08	152.48	151.23	61.14	38.19	146.42
314	134247	33.08	32.39	32.42	33.12	153.11	151.95	61.79	38.24	146.17
315	134258	33.03	32.36	32.42	33.12	153.00	151.79	61.88	38.25	146.14
316	134308	33.03	32.36	32.41	33.14	152.90	151.77	61.95	3. 5	145.92
317	134319	33.21	32.52	32.41	33.13	153.56	152.32	62.60	38.32	145.73
318	134329	33.18	32.52	32.42	33.10	153.42	152.19	62.65	38.32	145.61
319	134340	33.19	32.54	32.42	33.15	153.64	152.31	62.86	38.34	145.61
320	134350	33.20	32.53	32.42	33.12	153.52	152.24	62.93	38.35	145.61
321	134401	33.19	32.51	32.42	33.12	153.44	152.12	62.94	38.35	145.61
322	134411	33.36	32.54	32.41	33.38	153.75	152.51	63.31	38.38	145.34
323	134421	33.35	32.54	32.32	33.43	153.65	152.43	63.36	38.38	145.31
324	134432	33.43	32.77	32.32	33.42	154.35	153.06	64.06	38.47	145.00
325	134442	33.54	32.67	32.43	33.51	154.36	153.01	64.28	38.50	145.00
326	134453	33.54	32.76	32.62	33.44	154.86	153.26	64.77	38.53	144.70
327	134503	33.44	32.95	32.59	33.46	154.85	153.23	64.94	38.58	144.70
328	134514	33.62	32.87	32.80	33.53	155.17	153.44	65.34	38.62	144.70
329	134524	33.60	32.91	32.81	33.54	154.94	153.36	65.43	38.62	144.60
330	134535	33.56	33.05	32.78	33.49	155.25	153.47	65.68	38.65	144.40
331	134545	33.64	32.87	32.87	33.54	155.03	153.36	65.75	38.65	144.40
332	134556	33.57	32.93	32.80	33.55	154.89	153.35	65.83	38.65	144.40
333	134606	33.57	32.92	32.80	33.54	154.80	153.36	65.91	38.66	144.40
334	134617	33.61	33.25	32.82	33.36	155.97	154.12	66.92	38.72	143.80
335	134627	33.61	33.20	33.37	33.37	155.71	153.96	67.00	38.73	143.80
336	134638	33.63	33.18	33.35	33.36	155.59	153.97	67.15	38.74	143.79

BEAM RH-1 (continued)

Scan #	Time hhmmss	South Reaction (kN)	North Reaction (kN)	South Load (kN)	North Load (kN)	S. Cable Force (kN)	N. Cable Force (kN)	Mid-span Deflection (mm)	Load point Span Change (mm)	Reaction Span Change (mm)
337	134648	33.59	33.23	33.33	33.38	155.59	154.02	67.33	38.75	143.79
338	134659	33.60	33.20	33.33	33.37	155.52	154.03	67.46	38.76	143.80
339	134709	33.62	33.20	33.35	33.36	155.55	154.04	67.59	38.78	143.63
340	134720	33.59	33.22	33.32	33.38	155.48	154.07	67.69	38.79	143.49
341	134730	33.60	33.20	33.34	33.38	155.47	154.10	67.82	38.80	143.49
342	134741	33.96	33.20	33.35	33.84	156.26	155.01	68.71	38.90	143.19
343	134751	33.83	33.29	33.19	33.76	156.10	154.84	68.85	38.91	143.20
344	134802	33.84	33.26	33.32	33.70	156.10	154.80	68.98	38.92	143.19
345	134812	33.84	33.25	33.34	33.66	156.04	154.80	69.12	38.94	142.89
346	134823	33.82	33.26	33.34	33.70	155.98	154.85	69.24	38.95	142.90
347	134833	33.83	33.25	33.34	33.80	156.22	155.31	69.78	39.05	142.87
348	134844	33.86	33.32	33.34	33.81	156.24	155.74	70.28	39.10	142.59
349	134855	34.07	33.34	33.43	34.09	156.95	156.72	71.61	39.22	141.99
350	134905	34.00	33.44	33.33	34.07	157.02	157.17	72.60	39.34	141.69
351	134916	34.02	33.31	33.38	34.00	157.17	158.01	74.13	39.55	141.10
352	134926	34.05	33.28	33.35	34.06	157.17	158.22	75.24	39.67	140.80
353	134936	33.99	33.34	33.34	34.09	157.16	158.38	75.98	39.83	140.50
354	134947	33.98	33.36	33.34	34.03	157.20	158.44	76.58	39.93	140.20
355	134957	34.00	33.30	33.35	34.04	157.24	158.68	77.32	39.98	140.17

BEAM RH-2

Scan #	Time hrmms	South Reaction (kN)	North Reaction (kN)	South Load (kN)	North Load (kN)	S. Cable Force (kN)	N. Cable Force (kN)	Mid-span Deflection (mm)	Load point Span Change (mm)	Reaction Span Change (mm)
1	142323	0.00	0.00	0.00	0.00	51.93	52.80	0.00	25.19	166.08
2	142352	3.34	3.31	-3.24	-3.25	51.94	52.82	0.25	25.22	166.08
3	142401	5.19	5.04	-5.14	-4.88	51.93	52.82	0.41	25.24	166.08
4	142409	7.39	7.18	-7.33	-6.98	51.93	52.82	0.56	25.27	166.08
5	142423	9.95	9.97	-9.73	-9.94	51.95	52.84	0.76	25.30	166.08
6	142431	11.07	11.20	-10.76	-11.26	51.94	52.85	0.83	25.31	166.08
7	142533	11.43	11.36	-11.27	-11.32	51.92	52.86	0.87	25.33	166.08
8	142659	13.32	13.26	-13.17	-13.06	51.92	52.86	0.99	25.35	166.08
9	142710	14.69	14.73	-14.49	-14.76	51.93	52.87	1.09	25.37	166.08
10	142720	15.96	15.61	-15.97	-15.41	51.93	52.87	1.17	25.39	166.08
11	142731	17.10	16.82	-17.06	-16.67	51.94	52.89	1.24	25.41	166.08
12	142744	17.84	17.63	-17.75	-17.58	51.94	52.89	1.31	25.42	166.09
13	142829	17.92	17.64	-17.89	-17.52	51.94	52.90	1.34	25.43	166.08
14	143629	18.98	18.31	-19.28	-17.99	51.98	52.92	1.45	25.46	166.08
15	143639	19.02	18.32	-19.24	-17.96	51.97	52.92	1.45	25.46	166.09
16	143649	18.97	18.31	-19.25	-17.97	51.98	52.91	1.45	25.46	166.09
17	143659	19.02	18.33	-19.27	-18.00	51.98	52.92	1.46	25.46	166.08
18	143708	19.06	18.53	-19.18	-18.17	51.98	52.92	1.46	25.46	166.09
19	143718	19.07	18.50	-19.26	-18.25	51.98	52.92	1.46	25.46	166.08
20	143728	19.12	18.69	-19.23	-18.50	51.98	52.92	1.47	25.46	166.09
21	143738	19.19	18.84	-19.23	-18.73	51.98	52.92	1.48	25.46	166.08
22	143748	19.18	18.89	-19.22	-18.76	51.98	52.95	1.48	25.46	166.08
23	143758	19.24	19.07	-19.19	-19.06	51.98	52.92	1.48	25.46	166.08
24	143807	19.27	19.06	-19.20	-19.09	51.97	52.92	1.48	25.46	166.08
25	143817	19.53	19.07	-19.89	-19.03	51.98	52.92	1.50	25.46	166.09
26	143827	19.55	19.25	-19.67	-19.12	51.98	52.95	1.50	25.46	166.08
27	143837	19.49	19.19	-19.59	-19.10	51.98	52.95	1.50	25.46	166.08
28	143847	19.54	19.21	-19.59	-19.11	51.98	52.93	1.50	25.47	166.08
29	143857	19.64	19.33	-19.77	-19.11	51.98	52.93	1.51	25.47	166.08
30	143907	19.73	19.27	-19.92	-19.13	51.98	52.93	1.51	25.47	166.08
31	143914	19.89	19.33	-20.04	-19.15	51.98	52.93	1.52	25.47	166.08
32	143921	19.87	19.34	-20.02	-19.24	51.97	52.93	1.52	25.47	166.09
33	143929	19.95	19.54	-20.03	-19.39	51.98	52.93	1.53	25.47	166.08
34	143936	19.95	19.55	-20.04	-19.44	51.98	52.96	1.53	25.47	166.08
35	143944	20.10	19.62	-20.22	-19.42	51.99	52.93	1.53	25.47	166.09
36	143951	20.08	19.62	-20.23	-19.44	51.99	52.93	1.53	25.47	166.08
37	143958	20.13	19.63	-20.21	-19.43	51.98	52.92	1.54	25.47	166.09
38	144006	20.13	19.63	-20.24	-19.41	51.99	52.93	1.54	25.47	166.08
39	144013	20.28	19.72	-20.52	-19.52	51.99	52.93	1.55	25.47	166.08
40	144020	20.32	19.73	-20.56	-19.45	51.98	52.96	1.55	25.47	166.08
41	144028	20.29	19.71	-20.45	-19.47	51.99	52.93	1.55	25.47	166.09
42	144035	20.28	19.71	-20.47	-19.46	51.98	52.93	1.55	25.47	166.09
43	144042	20.29	19.71	-20.50	-19.45	52.00	52.93	1.55	25.47	166.09
44	144050	20.32	19.73	-20.50	-19.44	51.99	52.93	1.55	25.47	166.08
45	144716	20.28	19.72	-20.49	-19.47	52.05	52.97	1.58	25.53	166.08
46	144720	20.28	19.71	-20.49	-19.45	52.04	52.94	1.58	25.53	166.08
47	144723	20.27	19.71	-20.49	-19.46	52.04	52.94	1.58	25.53	166.08
48	144725	20.28	19.71	-20.49	-19.45	52.04	52.94	1.58	25.53	166.08
49	144728	20.27	19.71	-20.47	-19.46	52.03	52.94	1.58	25.53	166.08
50	144733	20.27	19.71	-20.48	-19.45	52.05	52.94	1.58	25.53	166.08
51	144738	20.27	19.71	-20.47	-19.44	52.05	52.95	1.58	25.53	166.09
52	144743	20.28	19.71	-20.47	-19.46	52.05	52.94	1.58	25.53	166.08
53	144747	20.28	19.71	-20.48	-19.46	52.05	52.95	1.58	25.53	166.08
54	144752	20.29	19.72	-20.48	-19.45	52.05	52.94	1.58	25.53	166.08
55	144757	20.28	19.71	-20.47	-19.45	52.05	52.95	1.58	25.53	166.09
56	144802	20.29	20.12	-20.23	-19.83	52.05	52.95	1.60	25.53	166.08

BEAM RH-2 (continued)

Scan #	Time hrmms	South Reaction (kN)	North Reaction (kN)	South Load (kN)	North Load (kN)	S. Cable Force (kN)	N. Cable Force (kN)	Mid-span Deflection (mm)	Load point Span Change (mm)	Reaction Span Change (mm)
57	144807	20.28	20.11	-20.28	-20.14	52.05	52.94	1.60	25.53	166.08
58	144812	20.33	20.41	-20.13	-20.54	52.05	52.98	1.60	25.53	166.08
59	144817	20.35	20.41	-20.16	-20.58	52.05	52.95	1.60	25.53	166.09
60	144822	20.35	20.38	-20.08	-20.55	52.06	52.95	1.60	25.53	166.08
61	144826	20.42	20.47	-20.06	-20.83	52.05	52.95	1.61	25.53	166.09
62	144831	20.38	20.62	-20.01	-20.94	52.05	52.95	1.61	25.53	166.08
63	144836	20.42	20.63	-20.13	-20.87	52.06	52.96	1.61	25.53	166.08
64	144841	20.55	20.70	-20.24	-20.93	52.05	52.94	1.62	25.53	166.08
65	144846	20.67	20.73	-20.47	-20.90	52.05	52.95	1.63	25.53	166.08
66	144851	20.68	20.72	-20.46	-20.94	52.05	52.95	1.63	25.53	166.08
67	144856	20.96	20.76	-20.81	-20.79	52.06	52.95	1.64	25.53	166.09
68	144901	20.95	20.75	-20.79	-20.80	52.05	52.95	1.64	25.53	166.08
69	144906	21.01	20.78	-20.97	-20.79	52.05	52.95	1.65	25.53	166.08
70	144911	21.01	20.81	-20.99	-20.79	52.06	52.95	1.65	25.53	166.08
71	144916	21.07	20.84	-21.03	-20.90	52.05	52.97	1.65	25.53	166.08
72	144920	21.12	20.88	-21.07	-20.86	52.06	52.98	1.66	25.53	166.08
73	144925	21.16	20.99	-20.97	-21.01	52.06	52.98	1.66	25.53	166.08
74	144930	21.14	20.99	-20.99	-21.05	52.06	52.98	1.66	25.53	166.08
75	144935	21.12	21.01	-21.00	-21.15	52.06	52.96	1.66	25.53	166.08
76	144940	21.20	21.12	-21.02	-21.31	52.06	52.95	1.67	25.53	166.08
77	144945	21.14	21.14	-20.98	-21.29	52.06	52.96	1.67	25.53	166.09
78	144950	21.21	21.14	-20.97	-21.29	52.06	52.96	1.67	25.53	166.08
79	144955	21.20	21.20	-21.03	-21.31	52.05	52.96	1.67	25.53	166.08
80	145000	21.18	21.21	-20.95	-21.36	52.06	52.96	1.67	25.53	166.08
81	145005	21.22	21.28	-20.97	-21.39	52.05	52.95	1.67	25.53	166.08
82	145009	21.21	21.25	-21.02	-21.34	52.06	52.96	1.68	25.53	166.09
83	145014	21.23	21.21	-21.00	-21.38	52.07	52.96	1.68	25.53	166.09
84	145019	21.27	21.33	-20.99	-21.51	52.06	52.98	1.68	25.53	166.08
85	145024	21.23	21.34	-20.99	-21.55	52.06	52.96	1.68	25.53	166.08
86	145029	21.25	21.31	-20.99	-21.53	52.06	52.98	1.68	25.53	166.08
87	145034	21.34	21.39	-21.09	-21.53	52.06	52.96	1.69	25.53	166.08
88	145039	21.36	21.38	-21.13	-21.61	52.06	52.96	1.69	25.53	166.08
89	145044	21.38	21.39	-21.14	-21.52	52.06	52.97	1.69	25.53	166.08
90	145049	21.53	21.46	-21.33	-21.56	52.06	52.96	1.71	25.53	166.08
91	145053	21.50	21.43	-21.38	-21.59	52.07	52.96	1.71	25.53	166.08
92	145058	21.58	21.52	-21.52	-21.62	52.06	52.96	1.72	25.53	166.08
93	145103	21.63	21.54	-21.52	-21.65	52.07	52.99	1.72	25.53	166.08
94	145108	21.77	21.66	-21.61	-21.77	52.06	52.98	1.72	25.54	166.08
95	145113	21.69	21.89	-21.65	-21.99	52.07	52.96	1.72	25.54	166.08
96	145118	21.81	21.81	-21.64	-21.96	52.07	52.97	1.73	25.54	166.08
97	145123	21.80	21.78	-21.64	-21.92	52.07	52.97	1.73	25.54	166.08
98	145128	21.92	21.97	-21.60	-22.19	52.06	52.97	1.75	25.54	166.09
99	145133	21.88	21.96	-21.67	-22.20	52.07	52.97	1.75	25.54	166.08
100	145137	21.94	21.97	-21.57	-22.34	52.07	52.97	1.75	25.54	166.08
101	145142	21.95	22.12	-21.63	-22.41	52.07	52.97	1.75	25.54	166.08
102	145147	21.94	22.33	-21.50	-22.63	52.07	52.97	1.77	25.54	166.09
103	145152	21.95	22.29	-21.54	-22.69	52.07	52.97	1.77	25.54	166.08
104	145157	21.99	22.30	-21.58	-22.72	52.06	52.97	1.77	25.54	166.08
105	145202	22.04	22.47	-21.54	-22.87	52.07	52.97	1.77	25.54	166.08
106	145207	22.00	22.43	-21.52	-22.90	52.06	52.97	1.77	25.54	166.08
107	145212	22.16	22.44	-21.87	-22.87	52.07	52.97	1.78	25.54	166.08
108	145217	22.18	22.47	-21.86	-22.80	52.07	52.97	1.78	25.54	166.08
109	145222	22.44	22.47	-22.12	-22.76	52.06	52.98	1.81	25.55	166.08
110	145227	22.40	22.54	-22.09	-22.81	52.07	53.00	1.81	25.55	166.08
111	145231	22.40	22.51	-22.05	-22.78	52.06	52.98	1.81	25.55	166.08
112	145236	22.36	22.52	-22.09	-22.80	52.08	52.98	1.81	25.55	166.09

BEAM RH-2 (continued)

Scan #	Time hrmmss	South Reaction (kN)	North Reaction (kN)	South Load (kN)	North Load (kN)	S. Cable Force (kN)	N. Cable Force (kN)	Mid-span Deflection (mm)	Load point Span Change (mm)	Reaction Span Change (mm)
113	145241	22.34	22.52	-22.08	-22.80	52.08	52.97	1.81	25.55	166.08
114	145246	22.35	22.51	-22.11	-22.81	52.06	53.01	1.81	25.55	166.08
115	145812	14.44	3.11	-28.21	-6.53	45.70	45.45	111.61	55.84	111.30

BEAM RH-3

Scan #	Time hrmrss	South Reaction (kN)	North Reaction (kN)	South Load (kN)	North Load (kN)	S. Cable Force (kN)	N. Cable Force (kN)	Mid-span Deflection (mm)	Load point Span Change (mm)	Reaction Span Change (mm)
1	122028	0.00	0.00	0.00	0.00	51.39	52.48	0.00	22.16	164.30
2	122142	5.36	5.81	-5.04	6.21	51.41	52.52	0.26	22.18	164.30
3	122153	6.55	6.56	-6.56	6.65	51.42	52.52	0.33	22.19	164.29
4	122200	7.98	8.19	-7.82	8.49	51.41	52.52	0.41	22.21	164.29
5	122209	9.71	9.30	-9.99	9.17	51.42	52.53	0.52	22.23	164.29
6	122225	10.03	9.84	-10.16	9.86	51.42	52.54	0.57	22.24	164.29
7	122318	11.04	10.41	-11.48	10.16	51.45	52.55	0.64	22.25	164.29
8	122720	12.13	11.53	-12.54	11.33	51.48	52.57	0.73	22.25	164.29
9	122730	13.82	13.86	-13.89	14.05	51.48	52.58	0.84	22.28	164.29
10	122735	15.19	13.93	-16.06	13.27	51.48	52.58	0.90	22.29	164.29
11	122740	15.44	13.90	-16.52	13.06	51.48	52.58	0.91	22.30	164.29
12	122750	16.35	15.53	-16.98	15.36	51.49	52.59	1.00	22.30	164.29
13	122759	16.75	16.24	-17.11	16.15	51.49	52.60	1.05	22.32	164.29
14	122809	17.17	16.98	-17.32	17.17	51.50	52.61	1.09	22.33	164.29
15	122819	17.32	17.02	-17.62	17.03	51.52	52.61	1.10	22.33	164.29
16	122828	17.47	17.03	-17.77	17.01	51.52	52.62	1.11	22.33	164.29
17	122838	17.47	17.02	-17.87	16.97	51.51	52.60	1.11	22.33	164.29
18	123022	17.50	17.02	-17.85	16.96	51.52	52.62	1.13	22.34	164.29
19	123032	17.50	17.03	-17.85	16.96	51.53	52.62	1.13	22.34	164.29
20	123041	17.49	17.02	-17.85	16.96	51.53	52.62	1.13	22.34	164.29
21	123051	17.43	17.02	-17.73	16.95	51.53	52.62	1.13	22.34	164.29
22	123101	17.47	17.03	-17.80	16.98	51.53	52.62	1.14	22.34	164.29
23	123111	17.55	17.00	-17.95	16.92	51.53	52.63	1.14	22.34	164.29
24	123120	17.57	17.00	-18.01	16.87	51.52	52.63	1.14	22.34	164.29
25	123130	17.57	17.00	-18.00	16.87	51.53	52.62	1.14	22.34	164.29
26	123140	17.50	16.99	-17.91	16.91	51.53	52.63	1.14	22.34	164.29
27	123149	17.51	17.00	-17.91	16.91	51.53	52.63	1.14	22.34	164.29
28	123159	17.51	17.00	-17.90	16.91	51.53	52.63	1.14	22.34	164.29
29	123209	17.51	16.99	-17.92	16.89	51.53	52.63	1.14	22.34	164.29
30	123218	17.50	17.01	-17.92	16.88	51.53	52.63	1.14	22.34	164.29
31	123228	17.50	16.99	-17.92	16.87	51.53	52.63	1.14	22.34	164.29
32	123238	17.50	17.00	-17.92	16.87	51.53	52.63	1.14	22.34	164.29
33	123247	17.50	17.00	-17.92	16.87	51.53	52.63	1.14	22.34	164.29
34	123257	17.50	17.00	-17.92	16.87	51.53	52.63	1.14	22.34	164.29
35	123306	17.62	17.04	-18.11	16.87	51.53	52.63	1.14	22.34	164.29
36	123316	17.64	17.12	-18.16	16.98	51.54	52.63	1.15	22.34	164.29
37	123326	17.68	17.20	-18.05	17.11	51.53	52.63	1.15	22.35	164.29
38	123335	17.69	17.23	-18.10	17.10	51.53	52.63	1.15	22.35	164.29
39	123345	17.65	17.18	-18.11	17.06	51.54	52.63	1.15	22.35	164.29
40	123355	17.80	17.25	-18.28	17.07	51.53	52.63	1.16	22.35	164.29
41	123404	17.78	17.25	-18.24	16.97	51.54	52.63	1.16	22.35	164.29
42	123414	17.83	17.38	-18.31	17.25	51.54	52.63	1.16	22.35	164.29
43	123424	17.85	17.37	-18.30	17.23	51.54	52.64	1.16	22.35	164.29
44	123433	17.96	17.36	-18.51	17.16	51.54	52.63	1.17	22.35	164.29
45	123443	17.92	17.37	-18.41	17.17	51.54	52.63	1.17	22.35	164.29
46	123453	17.98	17.40	-18.53	17.20	51.54	52.63	1.17	22.36	164.29
47	123502	18.10	17.46	-18.69	17.17	51.54	52.64	1.17	22.36	164.29
48	123512	18.15	17.41	-18.68	17.16	51.54	52.63	1.17	22.36	164.29
49	123522	18.04	17.52	-18.53	17.33	51.54	52.63	1.18	22.36	164.29
50	123531	18.02	17.50	-18.53	17.41	51.54	52.63	1.18	22.36	164.29
51	123541	18.17	17.53	-18.72	17.30	51.53	52.63	1.18	22.36	164.29
52	123550	18.20	17.55	-18.94	17.26	51.54	52.64	1.18	22.36	164.29
53	123600	18.24	17.60	-18.74	17.41	51.54	52.63	1.18	22.36	164.29
54	123610	18.21	17.64	-18.74	17.40	51.54	52.63	1.18	22.36	164.29
55	123619	18.21	17.61	-18.74	17.40	51.54	52.64	1.18	22.36	164.29
56	123629	18.22	17.73	-18.72	17.57	51.54	52.64	1.19	22.36	164.29

BEAM RH-3 (continued)

Scan #	Time h:mm:ss	South Reaction (kN)	North Reaction (kN)	South Load (kN)	North Load (kN)	S. Cable Force (kN)	N. Cable Force (kN)	Mid-span Deflection (mm)	Load point Span Change (mm)	Reaction Span Change (mm)
57	123639	18.27	17.72	-18.76	17.54	51.54	52.64	1.19	22.36	164.29
58	123648	18.23	17.78	-18.72	17.60	51.54	52.64	1.19	22.36	164.29
59	123658	18.33	17.86	-18.76	17.72	51.54	52.63	1.20	22.36	164.29
60	123708	18.33	17.82	-18.80	17.67	51.54	52.64	1.20	22.36	164.29
61	123717	18.33	17.82	-18.79	17.67	51.54	52.64	1.20	22.36	164.29
62	123727	18.33	17.82	-18.79	17.67	51.54	52.64	1.20	22.36	164.29
63	123737	18.47	17.81	-18.98	17.67	51.54	52.64	1.20	22.36	164.29
64	123746	18.43	17.91	-18.92	17.73	51.55	52.64	1.20	22.37	164.29
65	123756	18.60	17.89	-19.03	17.78	51.54	52.64	1.21	22.36	164.29
66	123806	18.48	18.01	-19.02	17.76	51.55	52.64	1.21	22.36	164.29
67	123815	18.59	17.94	-19.16	17.73	51.55	52.64	1.21	22.36	164.29
68	123825	18.56	18.02	-19.12	17.73	51.54	52.63	1.21	22.37	164.29
69	123835	18.60	17.96	-19.16	17.75	51.54	52.64	1.21	22.37	164.29
70	123844	18.75	18.08	-19.30	17.84	51.54	52.65	1.22	22.37	164.29
71	123854	18.77	18.13	-19.38	17.83	51.54	52.63	1.22	22.37	164.29
72	123903	18.77	18.08	-19.40	17.81	51.55	52.65	1.22	22.37	164.29
73	123913	18.80	18.11	-19.39	17.92	51.55	52.65	1.22	22.37	164.29
74	123923	18.78	18.09	-19.39	17.82	51.54	52.64	1.22	22.37	164.29
75	125225	18.99	18.75	-19.29	18.77	51.57	52.66	1.29	22.38	164.29
76	130744	20.12	19.54	-20.65	19.36	51.58	52.68	1.39	22.41	163.99
77	130754	20.12	19.55	-20.65	19.37	51.58	52.68	1.39	22.41	163.98
78	130803	20.12	19.54	-20.65	19.37	51.58	52.68	1.39	22.41	163.99
79	130813	20.12	19.54	-20.65	19.37	51.57	52.68	1.39	22.41	163.99
80	130822	20.12	19.55	-20.65	19.37	51.57	52.68	1.39	22.41	163.99
81	130832	20.12	19.55	-20.65	19.36	51.57	52.68	1.39	22.41	163.99
82	130842	20.12	19.54	-20.65	19.36	51.61	52.68	1.39	22.41	163.99
83	130851	20.12	19.55	-20.65	19.36	51.59	52.68	1.39	22.41	163.99
84	130901	20.12	19.55	-20.65	19.36	51.55	52.68	1.39	22.41	163.99
85	130911	20.12	19.54	-20.65	19.37	51.56	52.68	1.39	22.41	163.99
86	130920	20.12	19.55	-20.64	19.36	51.58	52.68	1.39	22.41	163.99
87	130930	20.12	19.54	-20.64	19.37	51.57	52.68	1.39	22.41	163.99
88	130939	20.12	19.55	-20.64	19.37	51.58	52.68	1.39	22.41	163.98
89	130949	20.12	19.55	-20.65	19.37	51.58	52.68	1.39	22.41	163.98
90	130959	20.12	19.55	-20.64	19.36	51.59	52.68	1.39	22.41	163.99
91	131009	20.12	19.54	-20.65	19.36	51.59	52.69	1.39	22.41	163.99
92	131018	20.12	19.55	-20.65	19.36	51.58	52.69	1.39	22.41	163.99
93	131028	20.12	19.54	-20.65	19.36	51.59	52.68	1.39	22.41	163.98
94	131037	20.12	19.54	-20.65	19.37	51.57	52.69	1.39	22.41	163.99
95	131047	20.12	19.54	-20.65	19.37	51.58	52.68	1.39	22.41	163.98
96	131057	20.12	19.54	-20.65	19.36	51.58	52.68	1.39	22.41	163.99
97	131106	20.12	19.55	-20.65	19.36	51.58	52.68	1.39	22.41	163.99
98	131116	20.12	19.55	-20.65	19.36	51.58	52.68	1.39	22.41	163.99
99	131126	20.12	19.55	-20.65	19.37	51.57	52.68	1.39	22.41	163.98
100	131135	20.12	19.55	-20.55	19.37	51.56	52.67	1.39	22.40	163.99
101	131145	20.12	19.55	-20.65	19.37	51.55	52.67	1.39	22.41	163.99
102	131155	20.35	19.58	-20.91	19.37	51.57	52.68	1.41	22.41	163.99
103	131204	20.49	19.66	-21.19	19.33	51.56	52.69	1.41	22.41	163.99
104	131214	20.67	19.78	-21.46	19.30	51.58	52.68	1.42	22.41	163.98
105	131224	20.84	19.84	-21.49	19.52	51.58	52.69	1.43	22.41	163.98
106	131233	20.72	19.94	-21.44	19.57	51.58	52.69	1.43	22.41	163.99
107	131243	20.82	20.09	-21.43	19.84	51.58	52.69	1.43	22.41	163.99
108	131253	20.82	20.10	-21.46	19.82	51.57	52.69	1.43	22.41	163.99
109	131302	20.88	20.30	-21.43	20.09	51.57	52.69	1.44	22.41	163.99
110	131312	21.06	20.38	-21.69	20.08	51.58	52.69	1.45	22.41	163.98
111	131322	21.08	20.33	-21.72	20.06	51.58	52.69	1.45	22.41	163.99
112	131331	21.07	20.60	-21.86	20.26	51.57	52.69	1.46	22.41	163.99

BEAM RH-3 (continued)

Scan #	Time hhmmss	South Reaction (kN)	North Reaction (kN)	South Load (kN)	North Load (kN)	S. Cable Force (kN)	N. Cable Force (kN)	Mid-span Deflection (mm)	Load point Span Change (mm)	Reaction Span Change (mm)
113	131341	21.12	20.54	-21.70	20.33	51.57	52.69	1.46	22.41	163.99
114	131351	21.16	20.53	-21.69	20.47	51.59	52.69	1.46	22.41	163.99
115	131400	21.16	20.65	-21.67	20.51	51.58	52.68	1.46	22.41	163.99
116	131410	21.16	20.64	-21.67	20.51	51.58	52.69	1.46	22.41	163.98
117	131419	21.17	20.64	-21.67	20.50	51.57	52.69	1.47	22.41	163.99
118	131429	21.16	20.65	-21.67	20.50	51.57	52.69	1.47	22.41	163.99
119	132009	21.61	21.19	-22.06	21.10	51.59	52.70	1.52	22.43	163.99
120	132716	21.61	21.18	-22.06	21.10	51.59	52.71	1.55	22.46	163.98
121	132726	21.61	21.18	-22.06	21.10	51.59	52.71	1.55	22.46	163.99
122	132735	21.61	21.18	-22.06	21.10	51.59	52.71	1.55	22.46	163.99
123	132745	21.60	21.17	-22.06	21.10	51.59	52.71	1.55	22.46	163.99
124	132755	21.61	21.17	-22.06	21.10	51.59	52.71	1.55	22.46	163.99
125	132804	21.61	21.18	-22.11	21.08	51.59	52.70	1.55	22.46	163.99
126	132814	21.67	21.12	-22.12	21.09	51.58	52.71	1.56	22.46	163.99
127	132824	21.75	21.32	-22.22	21.23	51.59	52.71	1.56	22.46	163.99
128	132833	21.75	21.34	-22.20	21.25	51.59	52.71	1.56	22.46	163.99
129	132843	21.76	21.32	-22.20	21.24	51.59	52.71	1.56	22.46	163.98
130	132853	21.91	21.45	-22.40	21.29	51.59	52.72	1.56	22.46	163.98
131	132902	22.04	21.57	-22.71	21.46	51.59	52.71	1.57	22.46	163.99
132	132912	22.22	21.74	-22.70	21.64	51.59	52.72	1.58	22.46	163.99
133	132921	22.30	21.87	-22.83	21.75	51.59	52.71	1.59	22.46	163.99
134	132931	22.33	21.86	-22.82	21.78	51.60	52.72	1.59	22.46	163.99
135	132941	22.33	21.86	-22.84	21.77	51.60	52.72	1.59	22.46	163.99
136	132951	22.33	21.86	-22.84	21.78	51.60	52.72	1.59	22.46	163.99
137	133000	22.62	22.06	-23.18	21.91	51.59	52.72	1.62	22.46	163.99
138	133010	22.78	22.32	-23.43	22.18	59.86	60.15	12.01	23.49	158.53
139	133030	22.89	22.38	-23.46	22.27	59.69	59.97	12.21	23.50	158.30
140	133040	22.93	22.35	-23.47	22.27	59.69	59.96	12.26	23.51	158.30
141	133050	22.90	22.36	-23.46	22.28	59.69	59.96	12.29	23.51	158.30
142	133100	22.91	22.36	-23.45	22.27	59.69	59.97	12.32	23.51	158.30
143	133110	22.90	22.34	-23.45	22.27	59.71	59.97	12.35	23.51	158.30
144	133120	22.90	22.36	-23.46	22.27	59.71	59.98	12.38	23.52	158.30
145	133131	22.91	22.34	-23.45	22.27	59.71	59.98	12.41	23.52	158.29
146	133141	22.90	22.34	-23.45	22.27	59.72	59.99	12.43	23.52	158.29
147	133151	22.90	22.35	-23.46	22.27	59.75	59.99	12.46	23.52	158.30
148	133201	22.90	22.35	-23.46	22.27	59.74	60.00	12.48	23.53	158.29
149	134216	22.90	22.34	-23.45	22.28	60.23	60.38	13.23	23.57	157.94
150	134219	22.90	22.33	-23.45	22.27	60.23	60.38	13.24	23.57	157.94
151	134221	22.89	22.33	-23.46	22.27	60.23	60.38	13.24	23.57	157.94
152	134224	22.90	22.33	-23.45	22.27	60.22	60.38	13.24	23.57	157.94
153	134226	22.90	22.33	-23.45	22.27	60.24	60.38	13.24	23.57	157.94
154	134229	22.89	22.33	-23.45	22.27	60.25	60.38	13.24	23.57	157.94
155	134231	22.90	22.33	-23.46	22.27	60.26	60.39	13.24	23.57	157.94
156	134233	22.90	22.33	-23.46	22.27	60.25	60.39	13.25	23.57	157.94
157	134236	22.90	22.33	-23.46	22.27	60.25	60.39	13.25	23.57	157.94
158	134238	22.89	22.34	-23.46	22.28	60.25	60.39	13.25	23.57	157.94
159	134241	22.89	22.34	-23.45	22.27	60.24	60.39	13.25	23.57	157.94
160	134243	22.89	22.33	-23.45	22.26	60.25	60.39	13.25	23.57	157.94
161	134246	22.92	22.34	-23.70	22.28	60.25	60.39	13.26	23.57	157.91
162	134248	23.10	22.38	-23.76	22.17	60.25	60.39	13.28	23.58	157.91
163	134251	23.07	22.39	-23.68	22.26	60.25	60.39	13.29	23.58	157.91
164	134253	23.23	22.43	-24.11	22.24	60.26	60.41	13.32	23.58	157.78
165	134256	23.28	22.40	-24.00	22.13	60.29	60.42	13.37	23.58	157.70
166	134258	23.45	22.44	-24.16	22.08	60.34	60.45	13.46	23.59	157.70
167	134301	23.46	22.45	-24.26	22.11	60.53	60.52	13.65	23.60	157.64
168	134303	23.41	22.47	-24.26	22.12	60.76	60.63	13.84	23.62	157.40

BEAM RH-3 (continued)

Scan #	Time hhmmss	South Reaction (kN)	North Reaction (kN)	South Load (kN)	North Load (kN)	S. Cable Force (kN)	N. Cable Force (kN)	Mid-span Deflection (mm)	Load point Span Change (mm)	Reaction Span Change (mm)
169	134306	23.43	22.45	-24.30	22.08	60.89	60.74	13.98	23.64	157.40
170	134308	23.63	22.49	-24.59	22.03	61.17	61.11	14.34	23.70	157.10
171	134311	23.60	22.50	-24.57	22.04	61.50	61.49	14.69	23.74	157.08
172	134313	23.64	22.48	-24.59	22.04	61.73	61.72	14.95	23.77	156.80
173	134316	23.62	22.49	-24.58	22.04	61.92	61.88	15.16	23.79	156.79
174	134318	23.61	22.48	-24.56	22.04	62.09	62.07	15.36	23.80	156.67
175	134321	23.62	22.48	-24.57	22.05	62.24	62.22	15.55	23.81	156.50
176	134323	23.62	22.48	-24.57	22.04	62.39	62.36	15.72	23.82	156.49
177	134326	23.61	22.48	-24.57	22.04	62.52	62.51	15.91	23.83	156.33
178	134328	23.62	22.49	-24.57	22.06	62.67	62.69	16.13	23.84	156.19
179	134331	23.61	22.83	-24.60	22.24	62.88	63.24	16.56	23.87	155.87
180	134333	13.16	16.96	-38.07	23.00	68.47	66.26	117.66	41.47	116.74

BEAM RH-4

Scan #	Time hrmrss	South Reaction (kN)	North Reaction (kN)	South Load (kN)	North Load (kN)	S. Cable Force (kN)	N. Cable Force (kN)	Mid-span Deflection (mm)	Load point (mm)	Reaction Span Change (mm)	Span Change (mm)
1	135404	0.00	0.00	0.00	0.00	52.53	52.62	0.00	31.29	165.49	
2	135421	4.14	4.37	-3.88	-4.48	52.52	52.66	0.30	31.29	165.49	
3	135428	5.05	5.18	-4.84	-5.26	52.53	52.66	0.38	31.30	165.49	
4	135432	5.54	5.82	-5.22	-5.90	52.54	52.66	0.43	31.31	165.49	
5	135438	6.43	6.37	-6.34	-6.30	52.55	52.66	0.50	31.31	165.48	
6	135442	7.02	6.90	-6.97	-6.78	52.54	52.67	0.54	31.32	165.49	
7	135446	7.66	7.57	-7.57	-7.68	52.54	52.67	0.60	31.32	165.48	
8	135450	8.24	8.20	-8.09	-8.17	52.56	52.67	0.65	31.33	165.48	
9	135454	9.06	9.13	-8.84	-9.18	52.55	52.68	0.72	31.33	165.47	
10	135458	9.80	9.95	-9.53	-10.06	52.55	52.68	0.78	31.34	165.45	
11	135503	11.01	10.83	-10.92	-10.76	52.55	52.69	0.86	31.35	165.45	
12	135507	11.04	11.20	-10.78	-11.35	52.55	52.69	0.88	31.35	165.45	
13	135513	11.12	11.17	-10.92	-11.23	52.56	52.66	0.89	31.36	165.45	
14	135519	11.29	10.97	-11.36	-10.81	52.58	52.69	0.89	31.36	165.45	
15	135537	12.09	11.54	-12.31	-11.19	52.59	52.69	0.94	31.36	165.45	
16	135544	12.40	13.28	-11.69	-13.99	52.59	52.70	1.00	31.37	165.45	
17	135556	13.84	13.48	-13.96	-13.62	52.59	52.71	1.07	31.38	165.45	
18	135608	15.25	14.94	-15.28	-14.83	52.62	52.72	1.24	31.41	165.45	
19	135617	16.38	16.62	-16.05	-16.90	52.61	52.74	1.37	31.48	165.45	
20	135627	18.17	18.65	-17.65	-19.11	52.65	52.82	1.67	31.63	165.47	
21	135634	19.16	18.72	-19.36	-19.10	52.68	52.85	1.79	31.65	165.47	
22	135640	19.41	19.35	-19.28	-19.48	52.70	52.89	1.92	31.67	165.47	
23	135705	19.84	20.13	-19.47	-20.55	52.85	52.98	2.26	31.72	165.46	
24	135728	20.67	20.43	-20.65	-20.47	53.04	53.07	2.52	31.76	165.21	
25	140212	20.67	20.43	-20.61	-20.46	53.17	53.17	2.71	31.80	165.19	
26	140222	20.67	20.43	-20.62	-20.46	53.18	53.17	2.71	31.81	165.19	
27	140232	20.68	20.43	-20.62	-20.46	53.18	53.17	2.71	31.81	165.19	
28	140236	20.68	20.44	-20.61	-20.46	53.18	53.20	2.71	31.81	165.19	
29	140241	20.67	20.44	-20.61	-20.46	53.19	53.17	2.72	31.81	165.19	
30	140246	20.67	20.44	-20.61	-20.46	53.18	53.17	2.72	31.81	165.19	
31	140251	20.68	20.44	-20.61	-20.46	53.19	53.17	2.72	31.81	165.19	
32	140256	20.68	20.44	-20.62	-20.47	53.18	53.17	2.72	31.81	165.19	
33	140301	20.79	20.54	-20.76	-20.51	53.19	53.18	2.74	31.80	165.19	
34	140306	20.97	20.60	-21.00	-20.54	53.19	53.18	2.75	31.81	165.19	
35	140311	20.97	20.57	-21.00	-20.54	53.19	53.18	2.75	31.81	165.19	
36	140316	21.13	20.66	-21.22	-20.52	53.20	53.21	2.76	31.81	165.19	
37	140321	21.22	20.78	-21.36	-20.63	53.21	53.18	2.78	31.82	165.19	
38	140325	21.36	20.96	-21.51	-20.94	53.22	53.19	2.80	31.83	165.18	
39	140330	21.44	20.98	-21.59	-20.97	53.22	53.20	2.82	31.83	165.18	
40	140335	21.53	21.09	-21.60	-21.02	53.23	53.21	2.84	31.83	165.18	
41	140340	21.50	21.16	-21.63	-21.16	53.24	53.24	2.85	31.83	165.18	
42	140345	21.58	21.28	-21.70	-21.23	53.25	53.22	2.87	31.84	165.19	
43	140350	21.63	21.22	-21.64	-21.39	53.24	53.23	2.89	31.84	165.16	
44	140355	21.65	21.25	-21.62	-21.25	53.25	53.24	2.91	31.85	165.15	
45	140400	21.68	21.33	-21.72	-21.29	53.27	53.25	2.92	31.85	165.15	
46	140405	21.68	21.33	-21.76	-21.30	53.27	53.26	2.94	31.85	165.15	
47	140410	21.68	21.31	-21.73	-21.31	53.27	53.26	2.95	31.86	165.15	
48	140414	21.71	21.44	-21.70	-21.43	53.28	53.30	2.97	31.86	165.15	
49	140419	21.73	21.43	-21.68	-21.49	53.29	53.31	2.98	31.86	165.15	
50	140424	21.77	21.48	-21.82	-21.58	53.31	53.32	3.01	31.86	165.14	
51	140429	21.79	21.48	-21.78	-21.52	53.31	53.30	3.02	31.87	165.14	
52	140434	21.80	21.49	-21.74	-21.51	53.31	53.30	3.03	31.87	165.14	
53	140439	21.80	21.64	-21.73	-21.71	53.33	53.31	3.06	31.87	165.13	
54	140444	21.76	21.65	-21.77	-21.73	53.34	53.35	3.07	31.88	165.12	
55	140449	21.91	21.65	-21.92	-21.65	53.34	53.34	3.10	31.88	164.89	
56	140454	21.94	21.62	-21.87	-21.67	53.36	53.37	3.11	31.88	164.89	

BEAM RH-4 (continued)

Scan #	Time hrmss	South Reaction (kN)	North Reaction (kN)	South Load (kN)	North Load (kN)	S. Cable Force (kN)	N. Cable Force (kN)	Mid-span Deflection (mm)	Load point Span Change (mm)	Reaction Span Change (mm)
57	140459	22.10	21.65	-22.11	-21.64	53.38	53.38	3.13	31.89	164.89
58	140503	22.02	21.69	-22.14	-21.64	53.38	53.37	3.15	31.89	164.90
59	140509	22.00	21.72	-22.10	-21.62	53.39	53.39	3.17	31.89	164.89
60	140513	22.08	21.67	-22.08	-21.64	53.42	53.41	3.18	31.90	164.89
61	140518	22.10	21.64	-22.14	-21.67	53.39	53.42	3.20	31.90	164.89
62	140523	22.04	21.69	-22.08	-21.63	53.40	53.41	3.21	31.90	164.89
63	140715	22.06	21.68	-22.09	-21.64	53.52	53.50	3.35	31.91	164.88
64	141923	22.05	21.69	-22.08	-21.64	53.62	53.64	3.54	32.11	164.59
65	142432	22.23	21.73	-22.30	-21.62	53.66	53.67	3.59	32.11	164.58
66	142437	22.41	21.74	-22.63	-21.55	53.66	53.66	3.60	32.11	164.58
67	142442	22.42	21.74	-22.63	-21.54	53.65	53.67	3.60	32.11	164.59
68	142447	22.64	21.75	-22.94	-21.41	53.65	53.67	3.61	32.11	164.58
69	142452	22.68	21.81	-23.14	-21.37	53.66	53.67	3.62	32.11	164.58
70	142455	22.75	21.80	-23.12	-21.44	53.67	53.68	3.62	32.12	164.58
71	142457	22.71	21.81	-23.19	-21.36	53.68	53.67	3.63	32.12	164.59
72	142500	22.76	21.78	-23.14	-21.37	53.67	53.67	3.63	32.12	164.58
73	142502	22.71	21.81	-23.16	-21.38	53.68	53.68	3.63	32.12	164.58
74	142505	22.82	21.91	-23.16	-21.64	53.68	53.69	3.65	32.12	164.58
75	142507	22.79	21.95	-23.14	-21.61	53.69	53.69	3.65	32.12	164.58
76	142510	22.78	21.96	-23.11	-21.83	53.69	53.69	3.65	32.12	164.58
77	142512	22.85	22.12	-23.12	-21.89	53.69	53.69	3.67	32.12	164.58
78	142515	22.80	22.17	-23.07	-21.90	53.73	53.70	3.67	32.12	164.58
79	142517	22.84	22.14	-23.06	-21.91	53.75	53.70	3.68	32.12	164.59
80	142520	22.94	22.26	-23.07	-22.16	53.75	53.71	3.70	32.12	164.58
81	142522	22.86	22.33	-23.03	-22.16	53.77	53.71	3.70	32.12	164.58
82	142525	22.92	22.27	-23.08	-22.15	53.75	53.72	3.71	32.12	164.59
83	142527	22.88	22.31	-23.03	-22.15	53.77	53.72	3.72	32.13	164.58
84	142530	22.86	22.32	-22.95	-22.42	53.78	53.73	3.73	32.13	164.58
85	142532	22.95	22.47	-22.99	-22.45	53.80	53.73	3.75	32.14	164.58
86	142535	22.89	22.52	-22.95	-22.44	53.80	53.74	3.76	32.14	164.58
87	142537	22.94	22.47	-23.00	-22.44	53.81	53.75	3.77	32.14	164.58
88	142540	22.95	22.46	-22.99	-22.45	53.80	53.75	3.78	32.14	164.58
89	142542	22.92	22.65	-22.94	-22.76	53.82	53.77	3.79	32.14	164.58
90	142545	22.98	22.64	-22.88	-22.79	53.82	53.78	3.81	32.14	164.58
91	142547	22.92	22.71	-22.89	-22.79	53.83	53.79	3.82	32.15	164.58
92	142550	23.09	22.81	-23.07	-22.76	53.83	53.80	3.85	32.15	164.58
93	142552	23.13	22.69	-23.18	-22.74	53.81	53.81	3.87	32.16	164.58
94	142555	23.07	22.79	-23.14	-22.76	53.85	53.82	3.88	32.16	164.58
95	142557	23.14	22.71	-23.12	-22.75	53.85	53.83	3.89	32.16	164.58
96	142600	23.10	22.74	-23.15	-22.76	53.86	53.84	3.91	32.16	164.58
97	142602	23.08	22.77	-23.13	-22.75	53.87	53.85	3.92	32.17	164.58
98	142604	23.15	22.70	-23.15	-22.74	53.88	53.86	3.93	32.17	164.58
99	142612	23.12	22.72	-23.13	-22.75	53.90	53.88	3.97	32.18	164.58
100	142619	23.08	22.76	-23.13	-22.76	53.93	53.90	3.99	32.18	164.55
101	142627	23.06	22.78	-23.16	-22.77	53.91	53.91	4.01	32.18	164.54
102	142635	23.07	22.77	-23.15	-22.76	53.91	53.92	4.03	32.19	164.54
103	142642	23.21	22.81	-23.35	-22.66	53.94	53.94	4.05	32.19	164.53
104	142647	23.23	22.79	-23.52	-22.66	53.98	53.94	4.06	32.19	164.52
105	142652	23.49	22.75	-23.79	-22.46	53.97	53.96	4.10	32.20	164.51
106	142657	23.78	22.69	-24.18	-22.33	54.00	53.97	4.14	32.20	164.40
107	142702	23.75	22.72	-24.24	-22.30	54.05	53.99	4.17	32.21	164.29
108	142707	23.74	22.77	-24.27	-22.28	54.09	54.00	4.20	32.22	164.29
109	142712	23.80	22.79	-24.26	-22.40	54.14	54.00	4.24	32.23	164.29
110	142717	23.87	22.83	-24.25	-22.45	54.18	54.02	4.28	32.23	164.29
111	142722	23.83	22.97	-24.27	-22.65	54.22	54.05	4.33	32.24	164.29
112	142727	23.84	23.04	-24.26	-22.68	54.27	54.08	4.37	32.25	164.28

BEAM RH-4 (continued)

Scan #	Time h:mmss	South Reaction (kN)	North Reaction (kN)	South Load (kN)	North Load (kN)	S. Cable Force (kN)	N. Cable Force (kN)	Mid-span Deflection (mm)	Load point Span Change (mm)	Reaction Span Change (mm)
113	142732	23.93	23.04	-24.33	-22.72	54.29	54.10	4.41	32.26	164.27
114	142738	23.97	23.10	-24.22	-22.83	54.35	54.12	4.46	32.27	164.27
115	142742	23.92	23.13	-24.24	-22.87	54.40	54.15	4.49	32.27	164.24
116	142748	23.93	23.21	-24.24	-23.24	54.42	54.16	4.52	32.28	164.22
117	142753	23.92	23.14	-24.27	-22.72	54.47	54.21	4.57	32.28	164.20
118	142758	23.96	23.08	-24.23	-22.84	54.49	54.21	4.58	32.28	164.18
119	142803	23.87	23.09	-24.31	-22.84	54.51	54.24	4.61	32.29	164.08
120	142808	24.02	23.32	-24.27	-23.02	54.52	54.26	4.64	32.29	163.99
121	142813	24.09	23.25	-24.29	-23.05	54.56	54.27	4.68	32.29	163.99
122	142818	24.06	23.29	-24.39	-23.07	54.58	54.30	4.70	32.30	163.99
123	142823	24.07	23.43	-24.40	-23.12	54.61	54.33	4.74	32.31	163.99
124	142828	24.17	23.56	-24.27	-23.45	54.66	54.36	4.81	32.31	163.98
125	142833	24.19	23.54	-24.34	-23.49	54.70	54.40	4.85	32.32	163.98
126	142838	24.12	23.60	-24.35	-23.48	54.73	54.44	4.90	32.33	163.98
127	142843	24.10	23.74	-24.21	-23.69	54.76	54.47	4.95	32.34	163.98
128	142849	24.24	23.72	-24.26	-23.71	54.81	54.51	5.01	32.35	163.94
129	142854	24.24	23.74	-24.33	-23.71	54.83	54.54	5.05	32.35	163.93
130	142859	24.28	23.96	-24.32	-24.01	54.88	54.59	5.11	32.37	163.88
131	142904	24.25	23.96	-24.26	-23.97	54.91	54.62	5.16	32.37	163.81
132	142906	24.27	23.93	-24.25	-23.97	54.93	54.66	5.18	32.38	163.69
133	142909	24.29	23.91	-24.30	-24.00	54.95	54.67	5.20	32.38	163.69
134	142911	24.25	23.95	-24.26	-23.98	54.98	54.68	5.21	32.38	163.69
135	142914	24.30	23.90	-24.26	-23.98	54.99	54.69	5.23	32.39	163.69
136	142916	24.27	23.94	-24.30	-24.00	55.00	54.71	5.24	32.39	163.69
137	142919	24.26	23.94	-24.21	-23.96	55.01	54.72	5.25	32.39	163.69
138	142921	24.43	24.05	-24.37	-24.02	55.03	54.74	5.28	32.39	163.68
139	142924	24.39	24.04	-24.45	-24.06	55.05	54.75	5.30	32.40	163.69
140	142926	24.43	24.01	-24.39	-24.01	55.06	54.76	5.31	32.40	163.69
141	142929	24.40	24.01	-24.43	-24.03	55.08	54.76	5.33	32.40	163.69
142	142931	24.44	24.05	-24.54	-24.06	55.09	54.78	5.35	32.41	163.68
143	142934	24.54	24.01	-24.52	-24.04	55.13	54.80	5.38	32.41	163.69
144	142936	24.47	24.08	-24.56	-24.06	55.13	54.81	5.40	32.42	163.68
145	142939	24.50	24.06	-24.55	-24.05	55.16	54.82	5.42	32.42	163.68
146	142941	24.52	24.04	-24.49	-24.03	55.17	54.83	5.43	32.42	163.68
147	142944	24.45	24.09	-24.59	-24.06	55.18	54.85	5.45	32.42	163.68
148	142946	24.66	24.05	-24.69	-23.94	55.21	54.86	5.47	32.42	163.68
149	142949	24.46	24.10	-24.59	-23.97	55.24	54.88	5.49	32.43	163.65
150	142951	24.57	24.14	-24.79	-24.07	55.25	54.89	5.51	32.43	163.64
151	142954	24.70	24.06	-24.76	-24.01	55.27	54.90	5.54	32.43	163.63
152	142956	24.61	24.13	-24.71	-24.02	55.27	54.91	5.56	32.43	163.62
153	142959	24.62	24.11	-24.83	-24.06	55.32	54.93	5.58	32.44	163.62
154	143001	24.68	24.07	-24.73	-24.01	55.35	54.93	5.60	32.44	163.60
155	143004	24.58	24.15	-24.72	-24.03	55.35	54.95	5.61	32.44	163.60
156	143006	24.66	24.08	-24.79	-24.05	55.39	54.97	5.64	32.44	163.56
157	143014	24.68	24.08	-24.76	-24.05	55.45	54.98	5.69	32.45	163.39
158	143022	24.68	24.07	-24.76	-24.04	55.52	55.01	5.74	32.45	163.40
159	143029	24.67	24.07	-24.76	-24.05	55.53	55.05	5.78	32.46	163.38
160	143037	24.64	24.11	-24.76	-24.04	55.55	55.08	5.82	32.46	163.39
161	143045	24.61	24.13	-24.73	-24.04	55.55	55.10	5.85	32.46	163.39
162	143052	24.60	24.14	-24.77	-24.04	55.57	55.12	5.87	32.47	163.38
163	143100	24.60	24.14	-24.73	-24.04	55.59	55.13	5.89	32.47	163.39
164	143108	24.61	24.13	-24.72	-24.02	55.62	55.14	5.91	32.47	163.39
165	143115	24.65	24.10	-24.74	-24.03	55.65	55.16	5.93	32.47	163.38
166	143123	24.68	24.11	-24.70	-24.01	55.63	55.16	5.95	32.47	163.39
167	143131	24.69	24.10	-24.71	-24.02	55.66	55.17	5.97	32.48	163.39
168	143138	24.69	24.10	-24.69	-24.00	55.66	55.19	5.99	32.49	163.39

BEAM RH-4 (continued)

Scan #	Time hhmmss	South Reaction (kN)	North Reaction (kN)	South Load (kN)	North Load (kN)	S. Cable Force (kN)	N. Cable Force (kN)	Mid-span Deflection (mm)	Load point (mm)	Reaction Span Change (mm)	Span Change (mm)
169	143146	24.64	24.11	-24.68	-24.02	55.70	55.21	6.01	32.50	163.39	
170	143154	24.61	24.12	-24.67	-24.01	55.75	55.21	6.02	32.49	163.39	
171	143201	24.60	24.14	-24.68	-24.02	55.77	55.23	6.04	32.50	163.35	
172	143209	24.61	24.13	-24.70	-24.03	55.76	55.24	6.05	32.50	163.34	
173	143709	24.66	24.08	-24.79	-24.04	55.91	55.42	6.23	32.53	162.49	
174	143715	24.62	24.13	-24.74	-24.02	55.91	55.41	6.23	32.53	162.49	
175	143717	24.66	24.08	-24.78	-24.04	55.91	55.42	6.24	32.53	162.49	
176	143720	24.63	24.11	-24.73	-24.03	55.88	55.42	6.24	32.53	162.49	
177	143722	24.64	24.09	-24.74	-24.04	55.90	55.42	6.24	32.53	162.49	
178	143727	24.62	24.13	-24.74	-24.01	55.90	55.41	6.24	32.53	162.49	
179	143732	24.63	24.11	-24.76	-24.03	55.90	55.41	6.24	32.53	162.49	
180	143737	24.65	24.09	-24.75	-24.02	55.91	55.41	6.25	32.53	162.49	
181	143742	24.65	24.12	-24.69	-24.02	55.95	55.41	6.25	32.53	162.49	
182	143747	24.62	24.12	-24.77	-24.04	55.94	55.43	6.25	32.53	162.49	
183	143753	24.63	24.11	-24.74	-24.02	55.94	55.42	6.26	32.53	162.49	
184	143758	24.66	24.07	-24.70	-24.02	55.94	55.43	6.26	32.53	162.49	
185	143803	24.64	24.11	-24.71	-24.04	55.94	55.42	6.26	32.53	162.49	
186	143808	24.62	24.12	-24.81	-23.99	55.94	55.42	6.26	32.53	162.49	
187	143813	24.41	24.09	-24.37	-24.18	55.96	55.43	6.27	32.53	162.49	
188	143818	24.69	24.08	-24.70	-24.01	55.95	55.43	6.27	32.53	162.49	
189	143823	24.88	24.16	-25.23	-23.94	55.95	55.43	6.30	32.53	162.49	
190	143828	24.91	24.17	-25.29	-23.83	55.98	55.44	6.31	32.53	162.49	
191	143833	24.93	24.12	-25.27	-23.82	55.96	55.44	6.32	32.53	162.49	
192	143838	25.03	24.05	-25.31	-23.80	56.00	55.46	6.33	32.53	162.48	
193	143843	24.99	24.08	-25.29	-23.82	56.01	55.47	6.35	32.54	162.48	
194	143848	24.91	24.16	-25.30	-23.80	56.02	55.46	6.36	32.54	162.48	
195	143853	24.96	24.09	-25.27	-23.81	56.03	55.46	6.37	32.54	162.48	
196	143858	25.04	24.05	-25.28	-23.81	56.05	55.48	6.38	32.54	162.47	
197	143903	24.94	24.14	-25.29	-23.84	56.04	55.47	6.39	32.54	162.48	
198	143908	25.00	24.29	-25.24	-24.04	56.04	55.49	6.41	32.54	162.47	
199	143913	25.03	24.22	-25.28	-24.02	56.01	55.49	6.42	32.54	162.46	
200	143918	25.05	24.23	-25.26	-24.11	56.06	55.50	6.45	32.55	162.46	
201	143924	25.00	24.34	-25.26	-24.16	56.08	55.60	6.61	32.57	162.46	
202	143929	25.01	24.34	-25.24	-24.14	56.12	55.62	6.65	32.58	162.46	
203	143934	25.12	24.36	-25.22	-24.23	56.14	55.64	6.69	32.59	162.46	
204	143939	25.06	24.42	-25.25	-24.26	56.17	55.65	6.72	32.59	162.46	
205	143944	25.03	24.44	-25.25	-24.24	56.18	55.68	6.74	32.59	162.46	
206	143949	25.05	24.39	-25.24	-24.24	56.19	55.68	6.75	32.59	162.46	
207	143954	25.09	24.37	-25.24	-24.25	56.21	55.69	6.77	32.59	162.46	
208	143959	25.06	24.42	-25.23	-24.24	56.23	55.71	6.78	32.59	162.46	
209	144004	25.02	24.43	-25.22	-24.26	56.23	55.74	6.79	32.59	162.46	
210	144009	25.05	24.38	-25.23	-24.25	56.26	55.73	6.91	32.60	162.46	
211	144014	25.11	24.36	-25.23	-24.25	56.28	55.76	6.82	32.60	162.46	
212	144019	25.06	24.39	-25.22	-24.25	56.27	55.76	6.83	32.60	162.46	
213	144024	25.02	24.43	-25.23	-24.24	56.28	55.75	6.84	32.60	162.46	
214	144029	25.06	24.39	-25.24	-24.25	56.30	55.76	6.85	32.60	162.46	
215	144034	25.10	24.35	-25.23	-24.25	56.31	55.78	6.86	32.60	162.46	
216	144040	25.06	24.41	-25.22	-24.25	56.31	55.78	6.87	32.61	162.46	
217	144045	25.02	24.44	-25.24	-24.26	56.32	55.78	6.88	32.61	162.46	
218	144050	25.06	24.39	-25.22	-24.25	56.31	55.80	6.88	32.61	162.46	
219	144055	25.10	24.36	-25.24	-24.25	56.32	55.81	6.89	32.61	162.46	
220	144100	25.07	24.38	-25.26	-24.26	56.32	55.82	6.90	32.61	162.46	
221	144105	25.02	24.43	-25.26	-24.25	56.32	55.81	6.91	32.61	162.46	
222	144110	25.05	24.39	-25.26	-24.24	56.33	55.81	6.91	32.61	162.46	
223	144115	25.10	24.36	-25.26	-24.26	56.33	55.83	6.92	32.61	162.46	
224	144120	25.08	24.41	-25.27	-24.25	56.34	55.82	6.93	32.61	162.46	

BEAM RH-4 (continued)

Scan #	Time hhmmss	South Reaction (kN)	North Reaction (kN)	South Load (kN)	North Load (kN)	S. Cable Force (kN)	N. Cable Force (kN)	Mid-span Deflection (mm)	Load point Span Change (mm)	Reaction Span Change (mm)
225	144125	25.04	24.45	-25.29	-24.37	56.34	55.85	6.93	32.61	162.46
226	144130	25.11	24.50	-25.29	-24.40	56.35	55.86	6.96	32.62	162.46
227	144135	25.22	24.49	-25.28	-24.47	56.37	55.86	6.98	32.62	162.46
228	144140	25.12	24.57	-25.27	-24.46	56.37	55.86	6.99	32.62	162.46
229	144145	25.15	24.61	-25.31	-24.51	56.39	55.88	7.01	32.62	162.46
230	144150	25.18	24.57	-25.27	-24.47	56.39	55.88	7.02	32.63	162.46
231	144155	25.22	24.55	-25.29	-24.49	56.42	55.91	7.04	32.63	162.46
232	144200	25.15	24.58	-25.51	-24.63	56.43	55.92	7.06	32.63	162.46
233	144206	25.26	24.64	-25.39	-24.52	56.45	55.91	7.08	32.63	162.46
234	144211	25.22	24.67	-25.39	-24.54	56.48	55.92	7.10	32.63	162.46
235	144216	25.25	24.65	-25.38	-24.56	56.48	55.95	7.11	32.64	162.46
236	144221	25.27	24.64	-25.40	-24.55	56.50	55.94	7.13	32.64	162.46
237	144226	25.26	24.65	-25.37	-24.72	56.51	55.97	7.14	32.64	162.46
238	144231	25.23	24.71	-25.37	-24.69	56.52	55.97	7.17	32.64	162.46
239	144236	25.28	24.61	-25.35	-24.46	56.54	55.99	7.18	32.64	162.46
240	144241	25.27	24.64	-25.42	-24.57	56.54	55.99	7.19	32.64	162.46
241	144246	25.30	24.53	-25.44	-24.47	56.55	56.00	7.20	32.64	162.46
242	144251	25.26	24.64	-25.44	-24.45	56.58	56.01	7.21	32.65	162.46
243	144256	25.31	24.74	-25.39	-24.65	56.59	56.04	7.23	32.65	162.46
244	144301	25.33	24.72	-25.42	-24.64	56.59	56.03	7.24	32.65	162.46
245	144306	25.34	24.73	-25.41	-24.70	56.61	56.05	7.25	32.65	162.46
246	144311	25.37	24.91	-25.40	-24.67	56.63	56.08	7.30	32.66	162.46
247	144317	25.28	24.92	-25.24	-25.11	56.65	56.12	7.33	32.66	162.46
248	144322	25.34	24.93	-25.30	-25.07	56.67	56.13	7.36	32.66	162.46
249	144327	25.32	24.99	-25.27	-25.05	56.68	56.14	7.38	32.67	162.46
250	144332	25.29	25.01	-25.27	-25.06	56.68	56.16	7.39	32.67	162.46
251	144337	25.33	24.98	-25.28	-25.04	56.72	56.18	7.41	32.67	162.46
252	144342	25.36	25.16	-25.21	-25.34	56.73	56.19	7.45	32.67	162.46
253	144347	25.35	25.13	-25.17	-25.35	56.75	56.24	7.47	32.67	162.46
254	144352	25.33	25.16	-25.19	-25.38	56.78	56.25	7.49	32.68	162.46
255	144357	25.32	25.17	-25.15	-25.34	56.78	56.27	7.52	32.68	162.46
256	144402	25.36	25.15	-25.16	-25.37	56.79	56.29	7.54	32.68	162.46
257	144407	25.35	25.17	-25.19	-25.36	56.81	56.30	7.56	32.68	162.46
258	144412	25.33	25.16	-25.19	-25.37	56.83	56.32	7.57	32.68	162.46
259	144417	25.34	25.16	-25.17	-25.34	56.83	56.34	7.59	32.69	162.46
260	144422	25.37	25.20	-25.19	-25.35	56.85	56.34	7.61	32.69	162.45
261	144427	25.34	25.18	-25.20	-25.35	56.86	56.35	7.62	32.69	162.44
262	144432	25.39	25.25	-25.17	-25.33	56.87	56.39	7.64	32.69	162.43
263	144437	25.38	25.23	-25.19	-25.39	56.88	56.41	7.66	32.70	162.43
264	144442	25.39	25.24	-25.21	-25.38	56.90	56.40	7.68	32.70	162.42
265	144448	25.38	25.24	-25.16	-25.38	56.91	56.43	7.70	32.70	162.42
266	144453	25.36	25.25	-25.17	-25.36	56.92	56.42	7.71	32.70	162.42
267	144458	25.38	25.28	-25.20	-25.38	56.92	56.44	7.73	32.70	162.41
268	144503	25.41	25.32	-25.20	-25.38	56.94	56.45	7.75	32.70	162.34
269	144508	25.37	25.21	-25.17	-25.33	56.95	56.46	7.77	32.70	162.20
270	144513	25.33	25.19	-25.21	-25.35	56.97	56.47	7.77	32.70	162.20
271	144518	25.34	25.18	-25.19	-25.35	56.97	56.48	7.78	32.70	162.20
272	144523	25.35	25.17	-25.17	-25.36	56.98	56.49	7.78	32.70	162.20
273	144528	25.35	25.18	-25.19	-25.36	56.99	56.50	7.79	32.71	162.20
274	144533	25.34	25.19	-25.19	-25.37	56.98	56.50	7.80	32.71	162.20
275	144538	25.35	25.20	-25.21	-25.35	56.97	56.51	7.81	32.71	162.20
276	144543	25.37	25.23	-25.22	-25.37	57.00	56.52	7.82	32.71	162.20
277	144548	25.36	25.18	-25.21	-25.36	57.00	56.54	7.83	32.71	162.20
278	144553	25.38	25.21	-25.19	-25.33	57.01	56.54	7.84	32.72	162.20
279	144558	25.38	25.25	-25.20	-25.36	57.02	56.55	7.85	32.72	162.20
280	144603	25.37	25.21	-25.19	-25.36	57.02	56.56	7.86	32.72	162.20

BEAM RH-4 (continued)

Scan #	Time h:mm:ss	South Reaction (kN)	North Reaction (kN)	South Load (kN)	North Load (kN)	S. Cable Force (kN)	N. Cable Force (kN)	Mid-span Deflection (mm)	Load point Span Change (mm)	Reaction Span Change (mm)
281	144608	25.37	-25.25	-25.19	25.39	57.03	56.55	7.87	32.72	162.20
282	144613	25.36	-25.23	-25.18	25.37	57.03	56.56	7.87	32.72	162.20
283	144618	25.35	-25.25	-25.20	25.38	57.04	56.56	7.88	32.72	162.20
284	144623	25.37	-25.22	-25.18	25.36	57.03	56.57	7.89	32.72	162.20
285	144629	25.36	-25.19	-25.18	25.35	57.04	56.57	7.90	32.72	162.20
286	144634	25.37	-25.25	-25.18	25.36	57.05	56.60	7.91	32.72	162.19
287	144639	25.39	-25.19	-25.23	25.38	57.05	56.59	7.92	32.72	162.20
288	144644	25.39	-25.18	-25.20	25.31	57.06	56.61	7.94	32.73	162.19
289	144649	25.33	-25.21	-25.17	25.36	57.07	56.60	7.94	32.73	162.19
290	144654	25.36	-25.18	-25.22	25.36	57.06	56.60	7.94	32.73	162.19
291	144659	25.36	-25.16	-25.21	25.37	57.07	56.62	7.94	32.73	162.19
292	144704	25.37	-25.18	-25.20	25.32	57.08	56.63	7.95	32.73	162.20
293	144709	25.37	-25.17	-25.20	25.32	57.08	56.64	7.96	32.73	162.19
294	144714	25.34	-25.16	-25.25	25.36	57.08	56.63	7.96	32.73	162.20
295	144719	25.34	-25.18	-25.25	25.36	57.08	56.63	7.97	32.73	162.20
296	144724	25.31	-25.19	-25.22	25.38	57.07	56.63	7.98	32.73	162.20
297	144729	25.33	-25.18	-25.21	25.34	57.09	56.64	7.99	32.73	162.20
298	144734	25.34	-25.15	-25.24	25.39	57.09	56.66	8.01	32.73	162.19
299	144739	25.35	-25.15	-25.22	25.36	57.09	56.67	8.01	32.73	162.19
300	144744	25.41	-25.21	-25.33	25.45	57.10	56.66	8.03	32.73	162.20
301	144749	25.40	-25.17	-25.19	25.30	57.10	56.68	8.03	32.74	162.19
302	144754	25.39	-25.23	-25.24	25.39	57.14	56.70	8.07	32.75	162.19
303	144759	25.42	-25.20	-25.22	25.35	57.15	56.69	8.08	32.75	162.19
304	144804	25.42	-25.19	-25.19	25.36	57.14	56.72	8.09	32.75	162.19
305	144810	25.45	-25.23	-25.23	25.36	57.17	56.72	8.12	32.75	162.19
306	144815	25.40	-25.18	-25.24	25.35	57.17	56.74	8.13	32.75	162.19
307	144820	25.45	-25.20	-25.16	25.36	57.20	56.77	8.16	32.75	162.17
308	144825	25.46	-25.21	-25.19	25.37	57.20	56.79	8.18	32.75	162.16
309	144830	25.37	-25.20	-25.21	25.35	57.21	56.79	8.19	32.76	162.15
310	144835	25.42	-25.22	-25.18	25.34	57.23	56.81	8.22	32.76	162.14
311	144840	25.42	-25.19	-25.20	25.37	57.25	56.84	8.24	32.76	162.12
312	144845	25.37	-25.17	-25.20	25.36	57.25	56.86	8.26	32.76	162.12
313	144850	25.40	-25.20	-25.17	25.36	57.27	56.87	8.29	32.76	162.11
314	144855	25.41	-25.19	-25.17	25.37	57.26	56.90	8.32	32.76	162.10
315	144900	25.38	-25.19	-25.19	25.36	57.27	56.90	8.34	32.76	162.08
316	144905	25.42	-25.23	-25.16	25.39	57.29	56.92	8.37	32.76	162.03
317	144910	25.39	-25.21	-25.20	25.40	57.30	56.93	8.39	32.76	161.93
318	144915	25.36	-25.21	-25.21	25.36	57.32	56.95	8.40	32.77	161.90
319	144920	25.38	-25.22	-25.19	25.39	57.32	56.96	8.42	32.77	161.90
320	144925	25.42	-25.23	-25.19	25.41	57.33	56.99	8.44	32.77	161.90
321	144930	25.40	-25.22	-25.21	25.40	57.34	56.99	8.45	32.77	161.90
322	144935	25.38	-25.20	-25.19	25.40	57.35	57.01	8.46	32.77	161.89
323	144940	25.38	-25.21	-25.18	25.40	57.36	57.02	8.47	32.78	161.90
324	144945	25.35	-25.21	-25.20	25.40	57.36	57.01	8.48	32.78	161.90
325	144951	25.38	-25.20	-25.16	25.41	57.37	57.03	8.49	32.78	161.90
326	144956	25.40	-25.24	-25.17	25.41	57.38	57.02	8.50	32.78	161.90
327	145001	25.39	-25.24	-25.18	25.41	57.40	57.03	8.51	32.78	161.90
328	145006	25.38	-25.22	-25.19	25.39	57.39	57.04	8.52	32.78	161.90
329	145011	25.37	-25.21	-25.18	25.39	57.40	57.05	8.53	32.78	161.90
330	145016	25.35	-25.20	-25.19	25.41	57.40	57.07	8.53	32.78	161.89
331	145021	25.35	-25.21	-25.20	25.40	57.40	57.06	8.54	32.78	161.90
332	145026	25.38	-25.20	-25.18	25.41	57.40	57.08	8.54	32.78	161.89
333	145031	25.38	-25.22	-25.17	25.40	57.43	57.07	8.55	32.78	161.90
334	145334	25.39	-25.22	-25.22	25.40	57.50	57.22	8.78	32.80	161.60
335	145339	25.47	-25.32	-25.20	25.41	57.53	57.22	8.80	32.80	161.60
336	145344	25.71	-25.84	-25.65	25.72	57.55	57.29	8.89	32.83	161.80

BEAM RH-4 (continued)

Scan #	Time hrmmss	South Reaction (kN)	North Reaction (kN)	South Load (kN)	North Load (kN)	S. Cable Force (kN)	N. Cable Force (kN)	Mid-span Deflection (mm)	Load point Span Change (mm)	Reaction Span Change (mm)
337	145349	25.93	-26.02	-25.80	26.02	57.87	57.72	9.44	32.90	161.29
338	145354	26.13	-26.70	-25.99	26.12	58.48	58.36	10.26	32.98	160.99
339	145357	26.17	-26.44	-26.07	26.16	58.76	58.50	10.59	33.00	160.85
340	145359	26.47	-26.96	-26.32	26.45	58.83	58.67	10.76	33.02	160.69
341	145402	26.42	-26.80	-26.20	26.43	59.26	59.08	11.22	33.08	160.35
342	145404	26.85	-27.22	-26.65	26.83	59.89	59.63	12.06	33.14	160.04
343	145407	27.25	-27.64	-27.00	27.44	60.25	60.19	12.65	33.23	159.66
344	145409	27.17	-27.49	-26.89	27.48	60.82	60.57	13.34	33.28	159.19
345	145412	27.76	-28.12	-27.53	27.73	61.23	61.07	14.18	33.35	158.89
346	145414	27.50	-27.79	-27.35	27.48	61.71	61.48	14.66	33.42	158.54
347	145417	27.96	-28.15	-27.74	27.93	62.02	61.78	15.28	33.47	158.29
348	145419	27.71	-27.92	-27.75	27.86	62.17	61.86	15.52	33.49	158.25
349	145422	28.05	-28.30	-27.85	28.29	62.28	62.02	15.84	33.52	157.99
350	145424	28.46	-28.72	-28.21	28.61	62.65	62.56	16.57	33.59	157.69
351	145427	28.49	-28.58	-28.27	28.65	63.20	63.09	17.19	33.68	157.25
352	145429	28.68	-28.84	-28.47	28.73	63.52	63.31	17.78	33.73	157.09
353	145432	28.45	-28.65	-28.58	28.60	63.93	63.56	18.34	33.77	156.70
354	145434	28.35	-28.60	-28.78	28.59	64.19	63.93	18.79	33.83	156.49
355	145437	29.06	-29.22	-28.82	29.29	64.45	64.29	19.52	33.89	156.15
356	145439	28.89	-29.07	-28.63	29.01	64.92	64.54	20.03	33.94	155.89
357	145442	28.72	-28.99	-28.44	29.01	65.12	64.73	20.40	33.99	155.59
358	145444	28.82	-29.05	-28.44	29.17	65.24	64.89	20.66	34.04	155.29
359	145447	28.82	-29.08	-28.52	29.16	65.45	65.06	21.02	34.08	155.29
360	145535	29.63	-29.84	-29.34	29.73	65.71	65.64	22.15	34.17	154.67
361	145538	29.81	-30.10	-29.51	30.21	66.46	66.31	23.07	34.25	154.22
362	145540	29.94	-30.29	-29.50	30.40	67.07	66.92	23.99	34.39	153.77
363	145543	29.83	-30.01	-29.55	30.10	67.68	67.49	25.09	34.48	153.14
364	145545	30.21	-30.39	-29.98	30.46	68.45	68.21	26.38	34.59	152.56
365	145548	29.80	-29.92	-29.62	30.01	68.58	68.15	26.67	34.61	152.54
366	145550	30.35	-30.41	-30.12	26.33	68.73	68.50	28.10	34.78	151.36
367	145553	29.72	-29.85	-29.66	25.88	68.76	68.66	28.35	34.78	151.35
368	145556	29.91	-30.05	-30.32	26.25	68.93	68.92	28.64	34.77	151.06
369	145558	30.21	-30.30	-30.48	26.59	69.52	69.50	29.17	34.80	150.75
370	145601	30.04	-30.12	-30.41	26.42	69.01	69.61	29.50	34.84	150.65
371	145604	30.14	-41.14	-30.53	26.59	69.93	69.90	29.93	34.87	150.46
372	145606	30.31	-30.50	-30.90	26.75	70.18	70.19	30.30	34.91	150.34
373	145609	30.31	-30.54	-30.75	26.81	70.57	70.66	30.76	35.01	149.84
374	145612	30.66	-30.90	-30.96	27.19	71.20	71.21	31.59	35.04	149.54
375	145614	30.97	-31.16	-31.56	27.47	71.78	71.90	32.42	35.08	149.18
376	145617	31.02	-31.18	-31.37	27.47	72.36	72.52	33.18	35.13	148.63
377	145619	30.85	-31.11	-31.38	27.30	73.01	73.07	33.79	35.24	148.30
378	145622	30.98	-31.03	-31.49	27.63	73.58	73.54	34.57	35.31	147.73
379	145625	30.92	-31.12	-31.32	27.48	73.88	73.82	35.02	35.33	147.73
380	145632	31.37	-31.62	-32.14	28.13	74.11	74.27	35.69	35.39	147.42
381	145635	30.99	-31.21	-31.33	27.56	74.32	74.35	35.77	35.41	147.13
382	145638	31.52	-31.73	-32.08	28.11	74.72	74.78	36.45	35.44	147.02
383	145640	31.42	-31.29	-32.34	28.42	75.11	75.30	37.11	35.51	146.52
384	145643	31.35	-31.26	-32.08	28.24	75.35	75.56	37.58	35.55	146.44
385	145645	31.12	-31.32	-31.64	28.18	75.53	75.54	37.63	35.56	146.23
386	145704	31.29	-31.52	-32.10	28.20	75.55	75.71	37.92	35.60	145.92
387	145706	31.28	-31.47	-32.14	28.33	76.02	76.12	38.55	35.67	145.61
388	145709	31.35	-31.51	-32.25	28.53	76.44	75.53	39.24	35.72	145.31
389	145711	31.97	-32.12	-31.61	27.99	76.63	75.58	39.52	35.75	145.22
390	145722	32.36	-32.62	-31.89	31.39	77.48	77.17	40.98	35.85	144.40
391	145725	32.16	-32.40	-32.13	28.46	77.87	77.63	41.63	35.91	143.95
392	145732	31.81	-31.89	-32.50	28.85	79.04	79.08	43.76	36.19	142.60

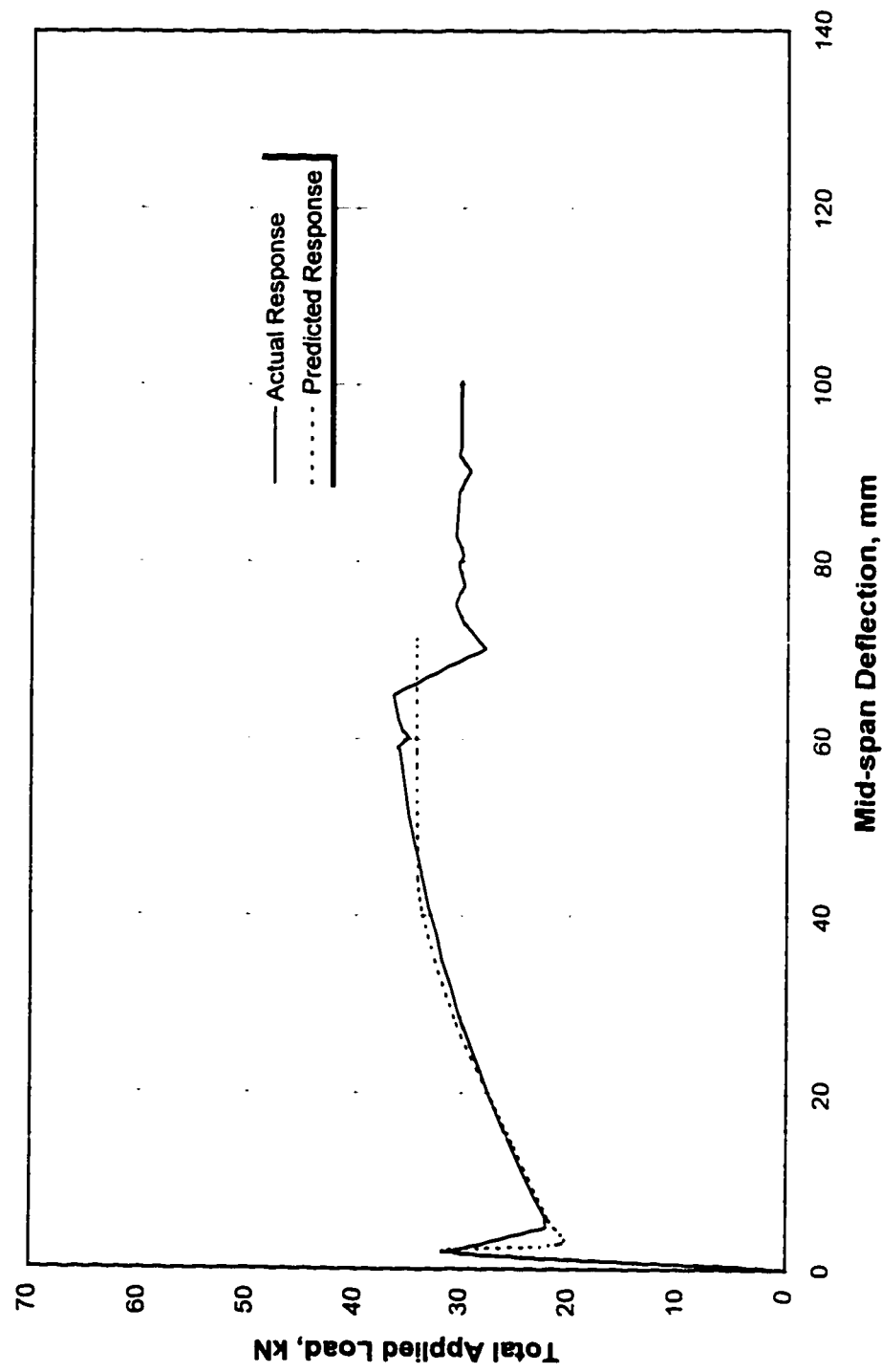
BEAM RH-4 (continued)

Scan #	Time hrmmss	South Reaction (kN)	North Reaction (kN)	South Load (kN)	North Load (kN)	S. Cable Force (kN)	N. Cable Force (kN)	Mid-span Deflection (mm)	Load point Span Change (mm)	Reaction Span Change (mm)
393	145735	31.87	-32.08	-32.64	28.94	79.40	79.56	44.56	36.24	142.27
394	145738	31.92	-31.92	-32.83	28.94	79.79	79.86	45.31	36.30	141.70
395	145740	31.97	-32.02	-32.96	29.17	80.20	80.25	46.08	36.38	141.35
396	145743	32.03	-32.23	-32.94	29.20	80.55	80.61	46.85	36.44	140.80
397	145746	32.02	-32.27	-33.12	29.29	80.90	80.95	47.60	36.50	140.50
398	145748	32.03	-32.25	-32.96	29.31	81.23	81.31	48.35	36.56	140.17
399	145751	32.23	-32.44	-33.32	29.49	81.43	81.62	49.02	36.63	139.60
400	145756	32.18	-32.05	-33.16	29.39	82.07	82.34	50.50	36.76	138.70
401	145801	32.07	-31.98	-32.51	28.71	82.71	83.02	52.07	36.95	137.98

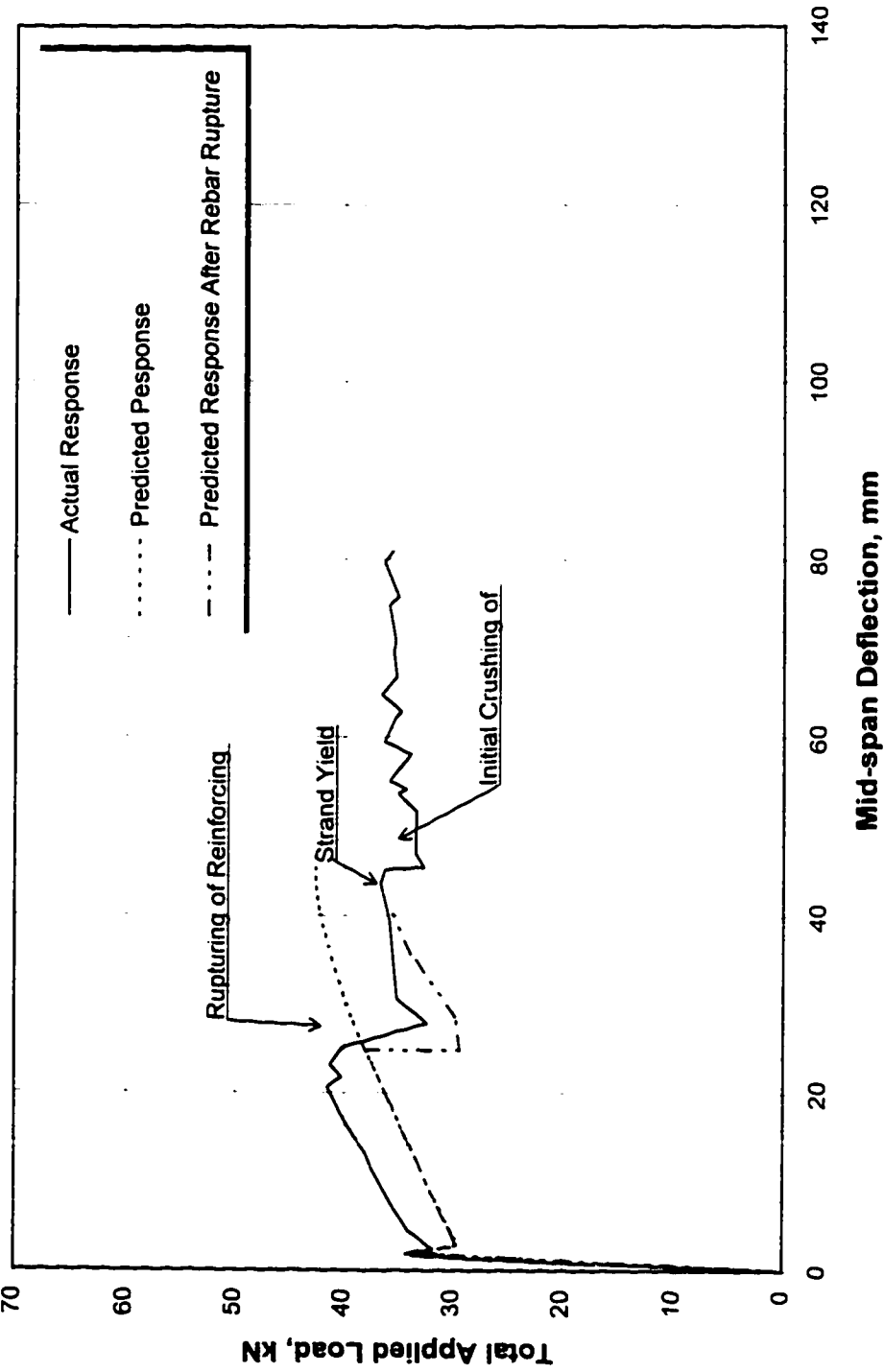
APPENDIX B

COMPLETE SET OF PREDICTED AND ACTUAL LOAD-DEFLECTION CURVES

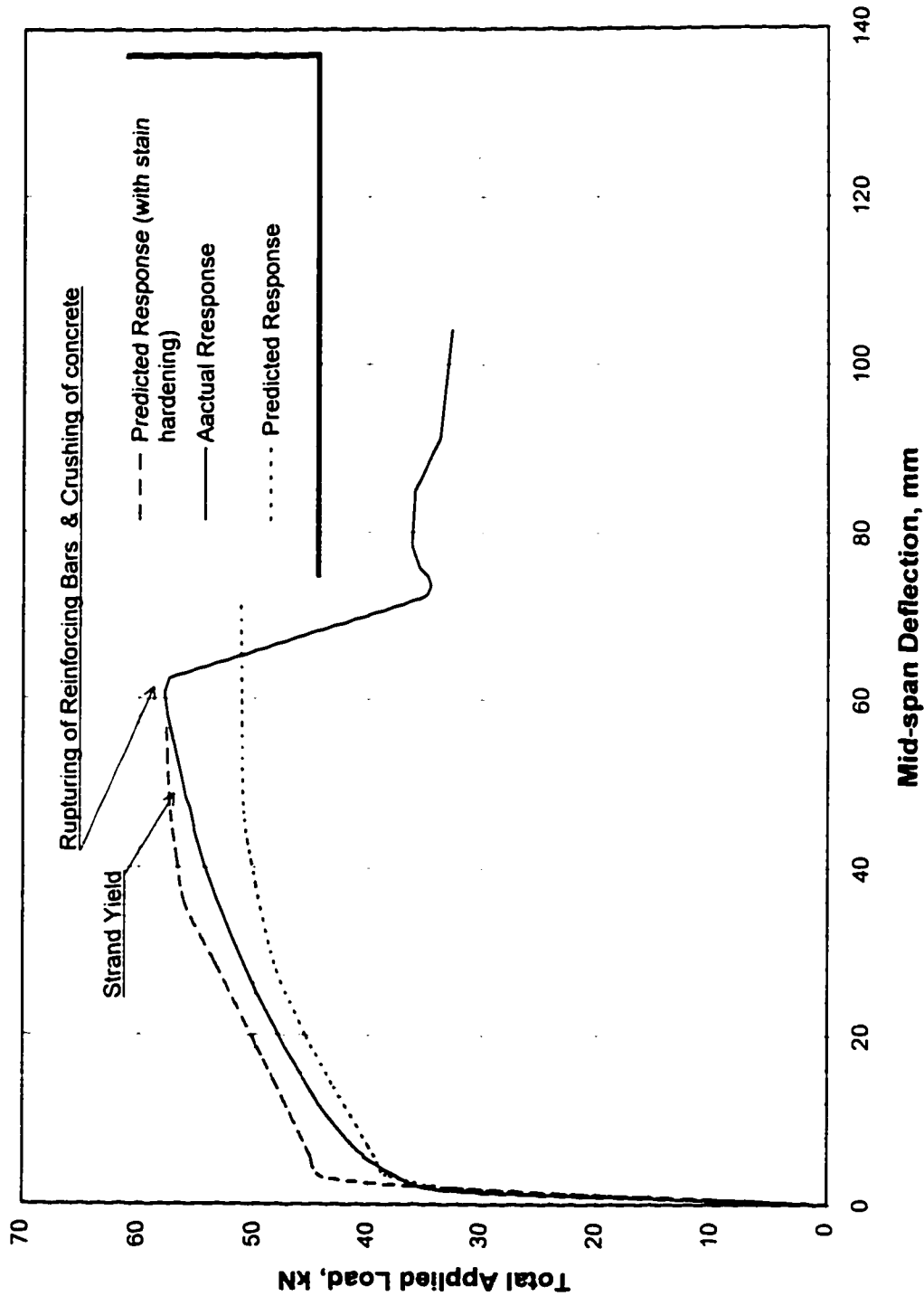
Total Applied Load vs Mid-span Deflection
Beam R-1 ($\rho_p=0.15\%$, $\rho=0\%$)



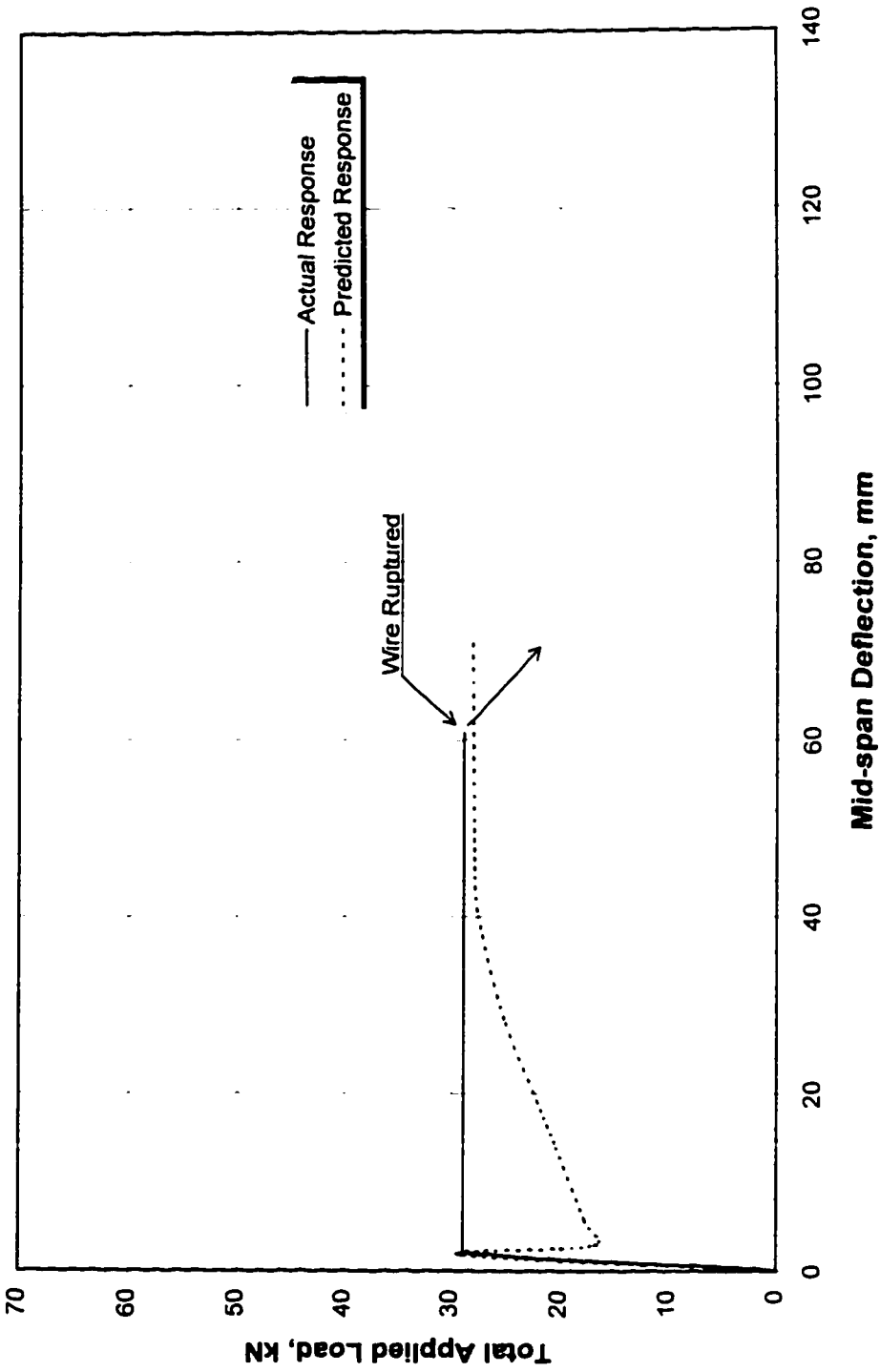
Total Applied Load vs Mid-span Deflection
Beam R-2 ($p_a=0.15\%$, $p=0.065\%$)



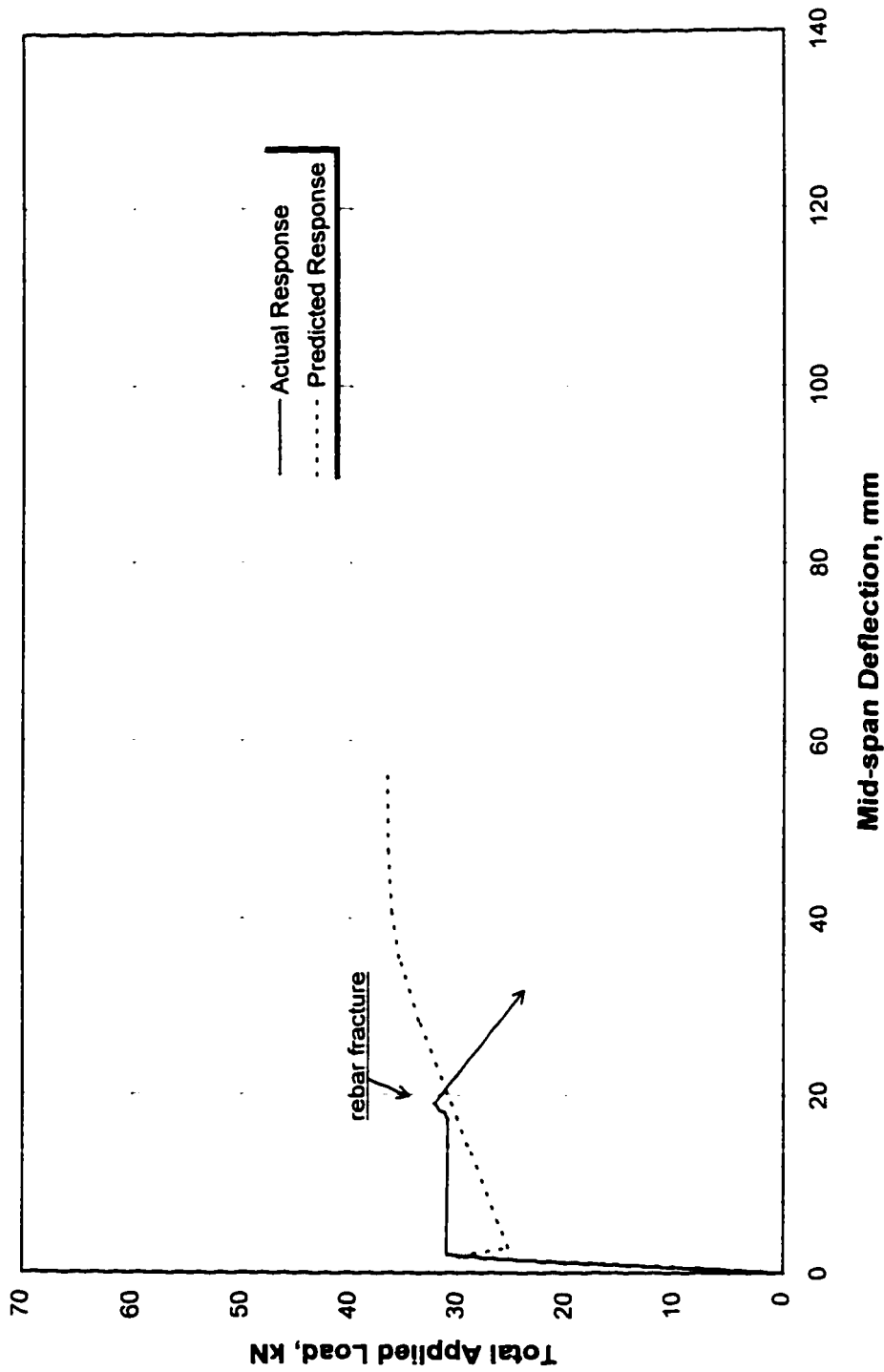
Total Applied Load vs Mid-span Deflection
Beam R-3 ($\rho_p=0.15\%$, $\rho=0.13\%$)



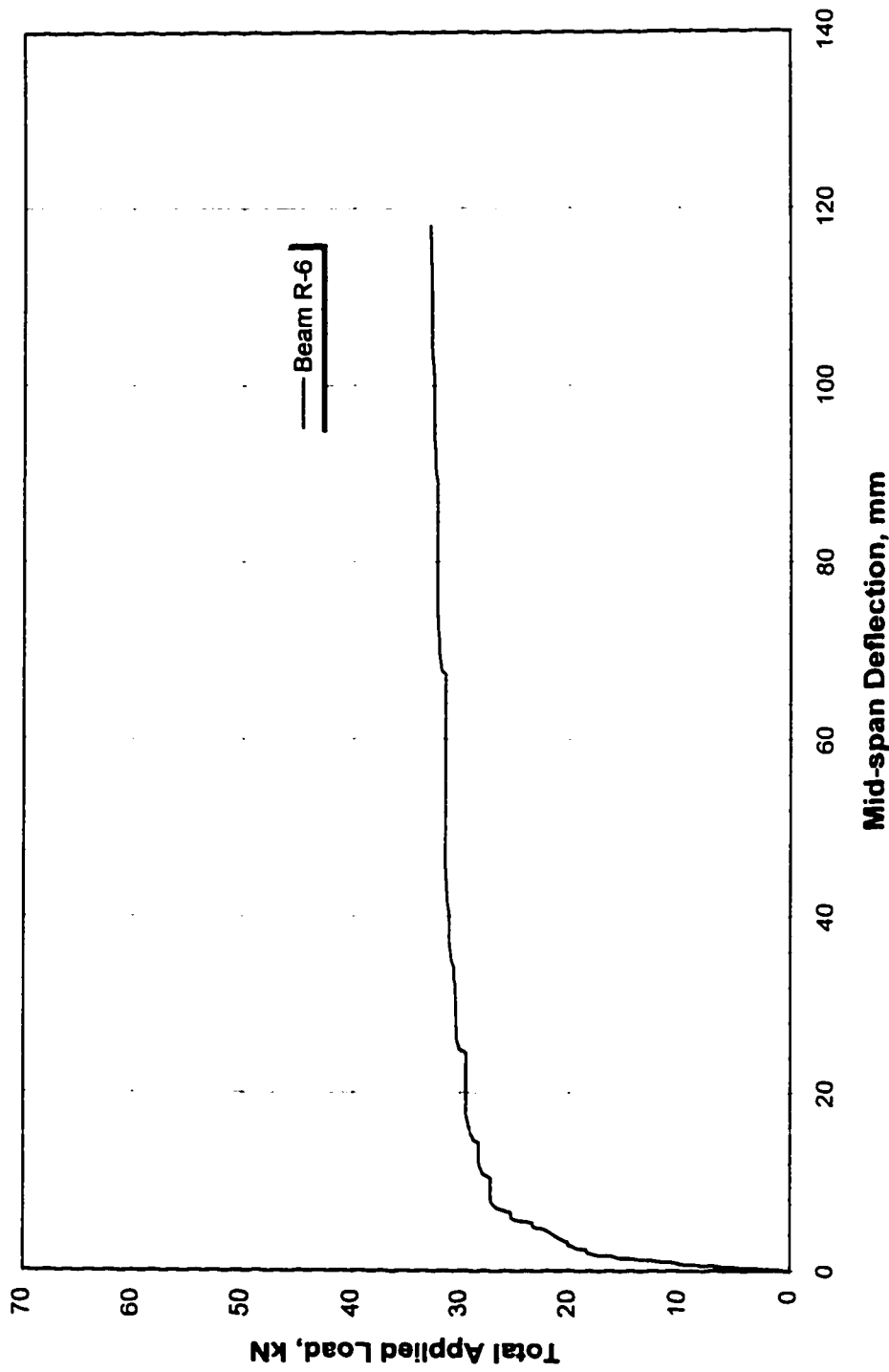
Total Applied Load vs Mid-span Deflection
Beam R-4 ($\rho_o = 0.12\%$, $\rho = 0\%$)



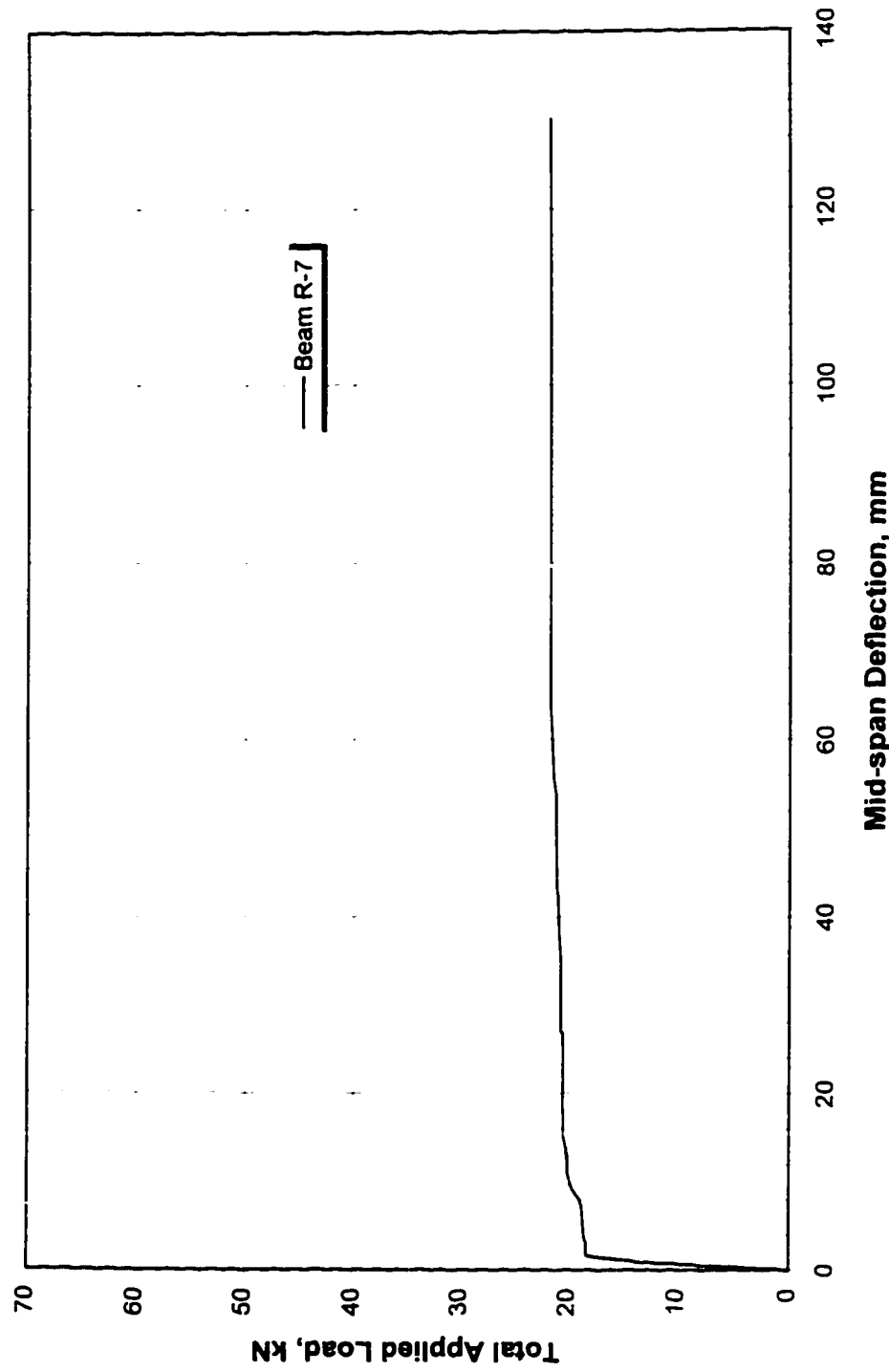
Total Applied Load vs Mid-span Deflection
Beam R-5 ($\rho_p=0.12\%$, $\rho=0.065\%$)



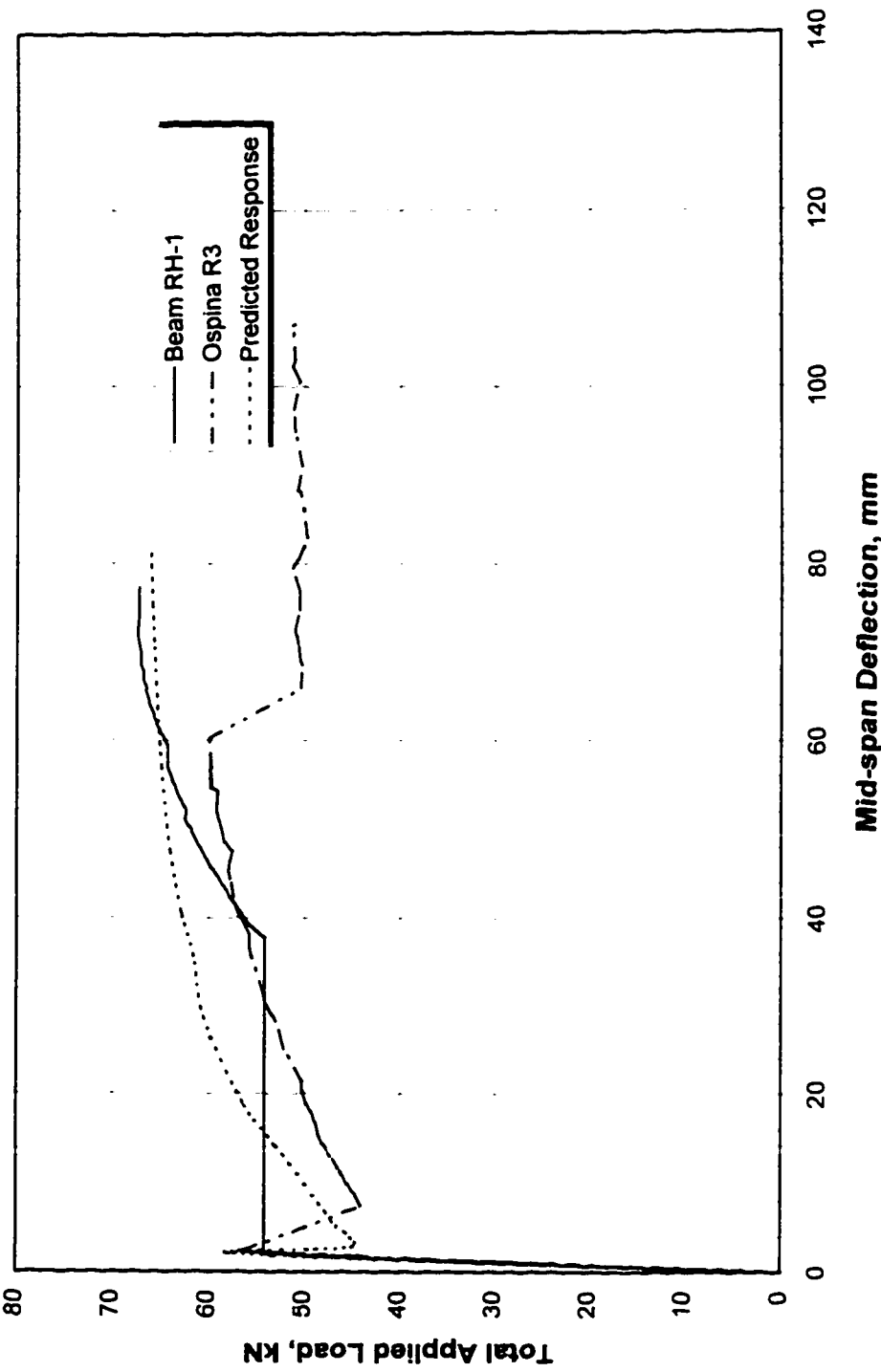
Total Applied Load vs Mid-span Deflection
Beam R-6, ($\rho_p=0\%$, $\rho=0.195\%$)



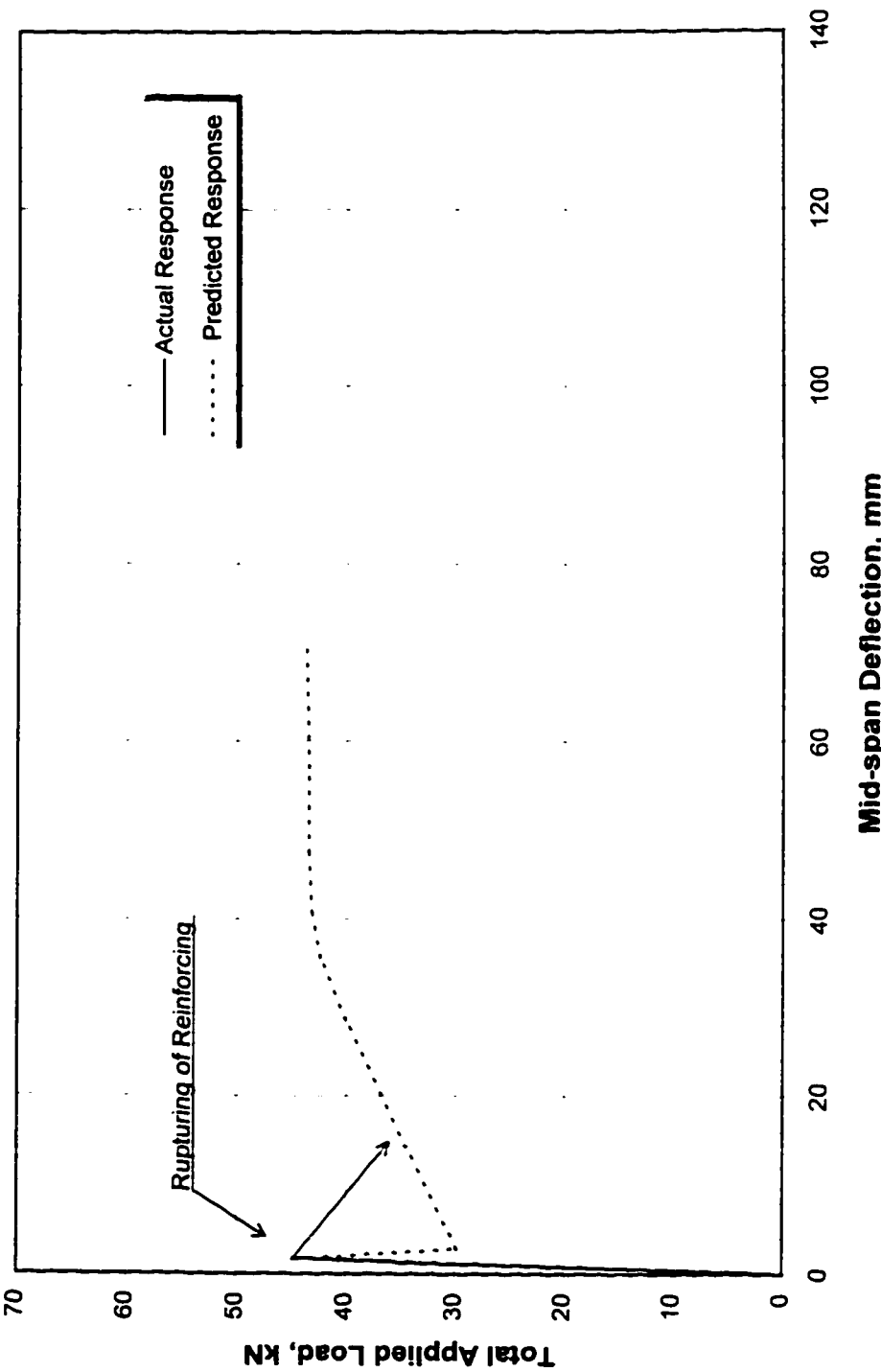
Total Applied Load vs Mid-span Deflection
Beams R-7 ($\rho_p=0\%$, $\rho_p=0.13\%$)



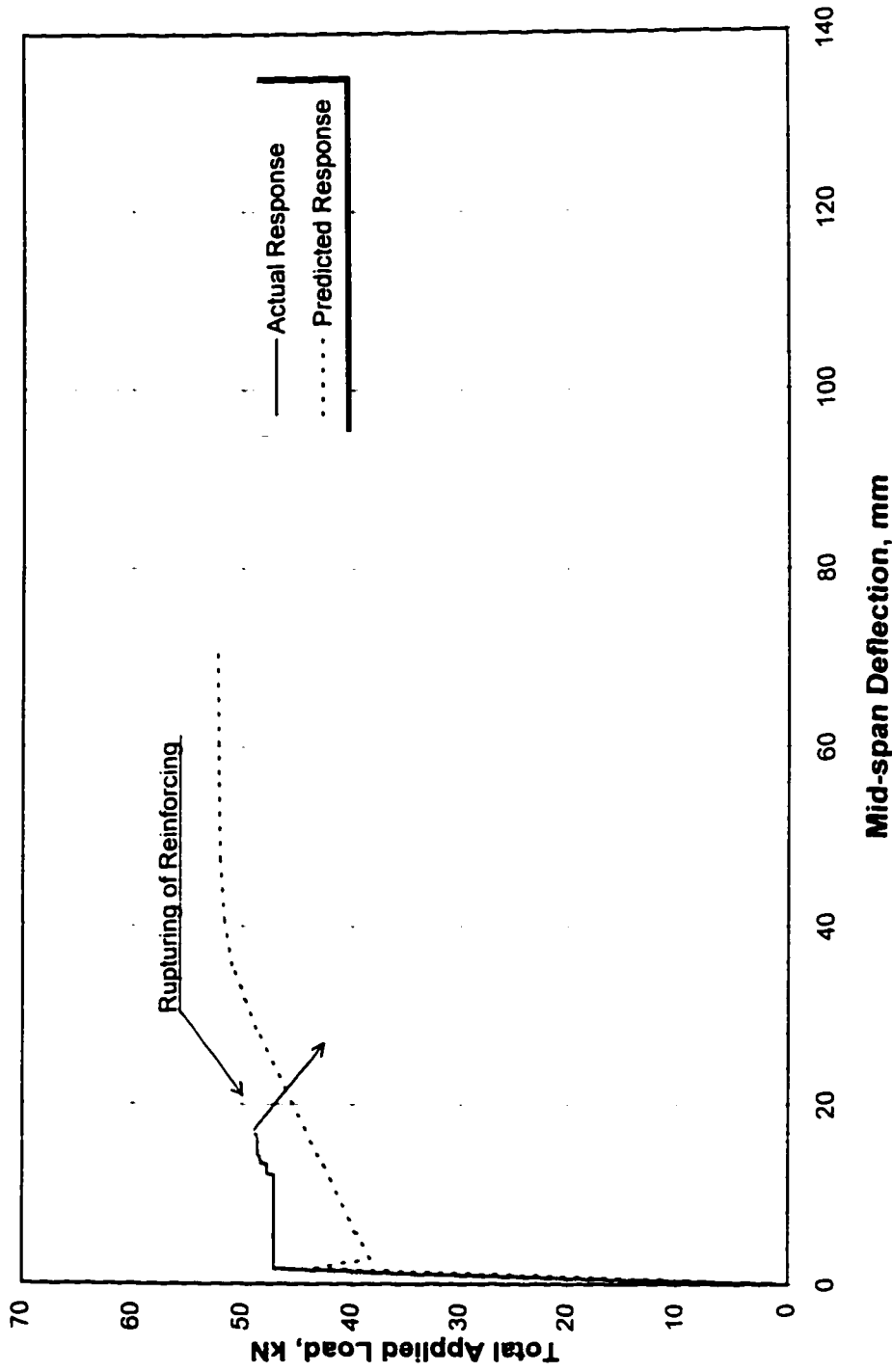
Total Applied Load vs Mid-span Deflection
Beam RH-1 ($\rho_o=0.3\%$, $\rho=0\%$)



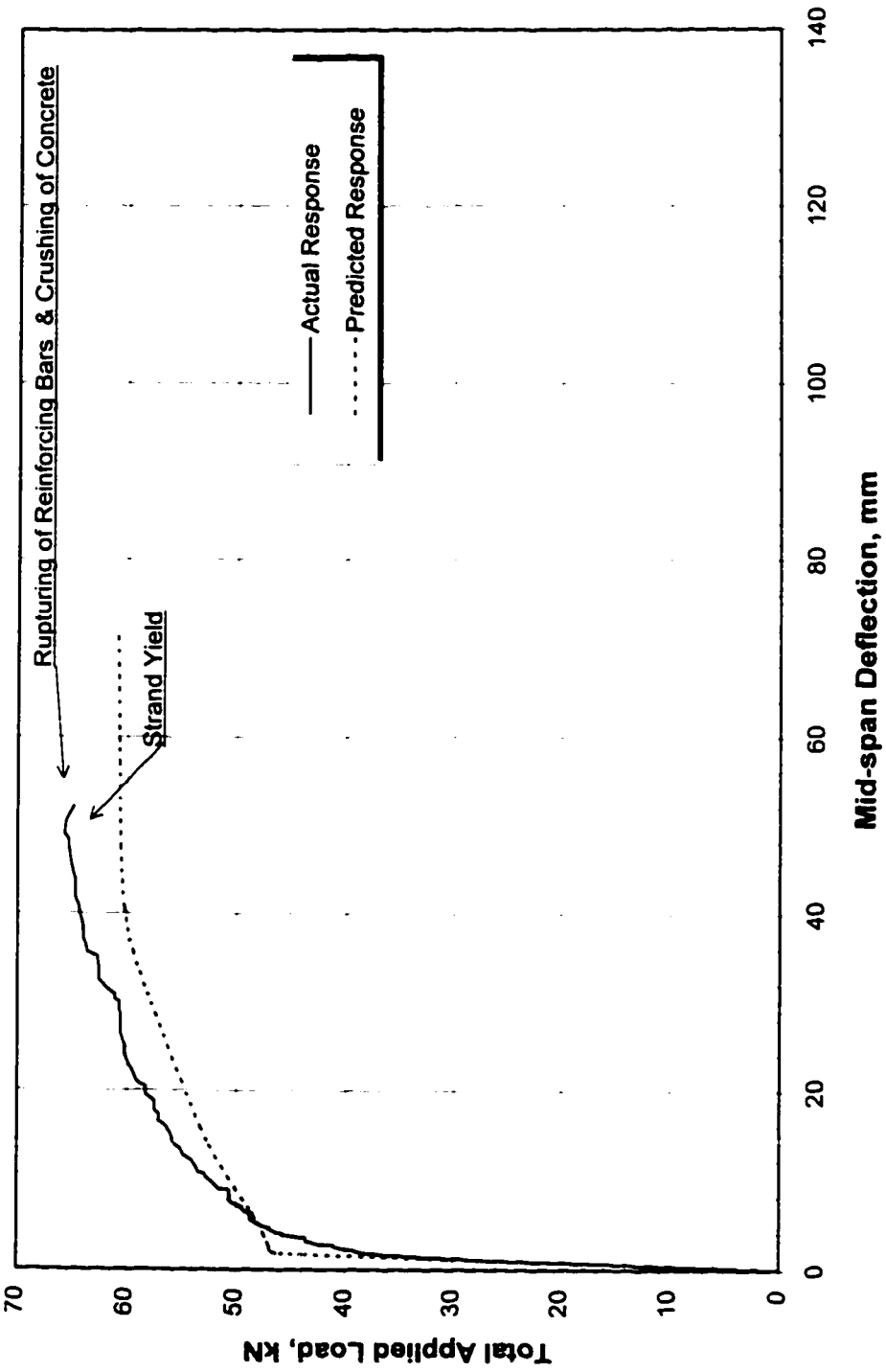
Total Applied Load vs Mid-span Deflection
Beam RH-2 ($p_a=0.15\%$, $p=0.065\%$)



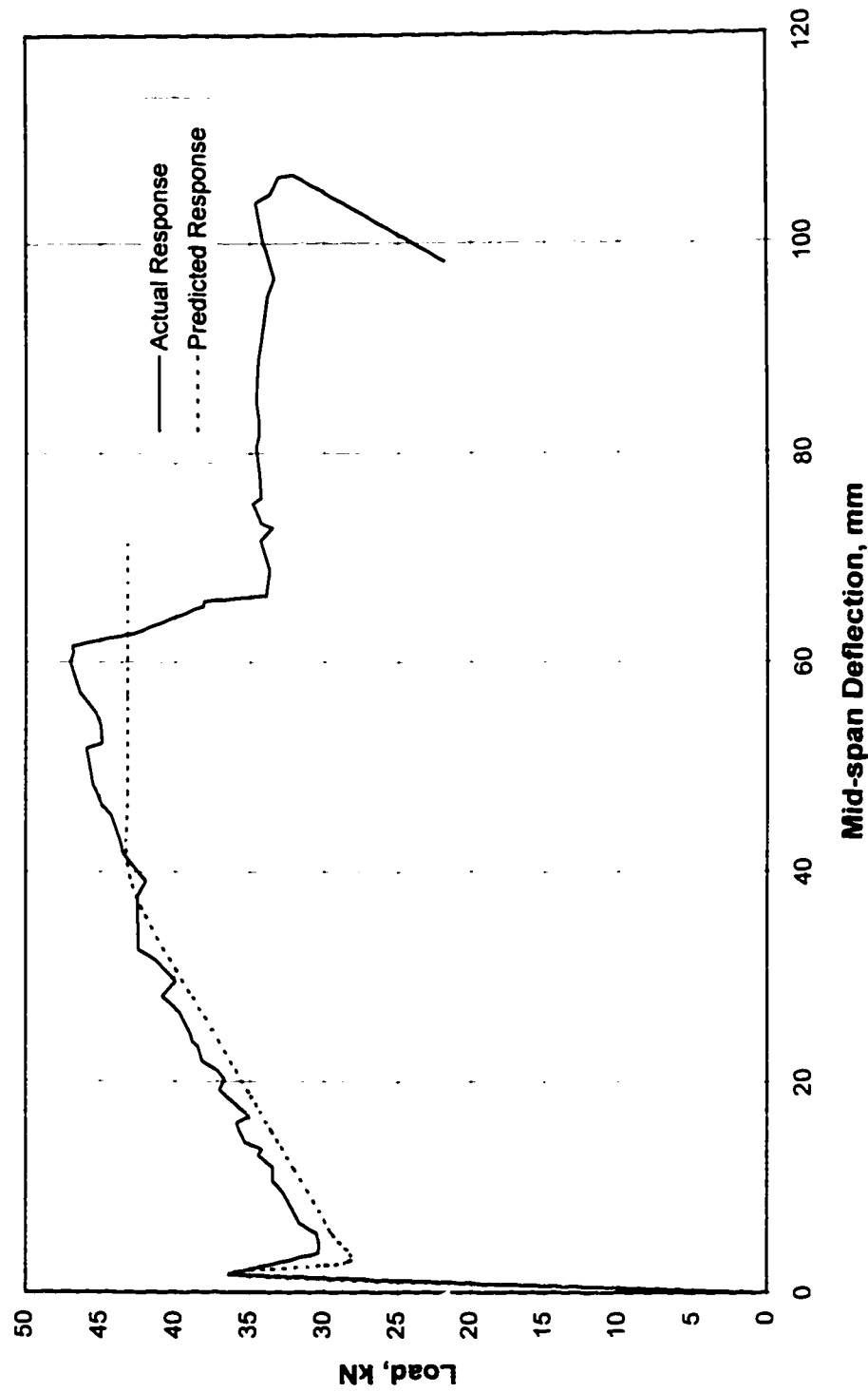
Total Applied Load vs Mid-span Deflection
Beam RH-3 ($p_p=0.15\%$, $p=0.13\%$)



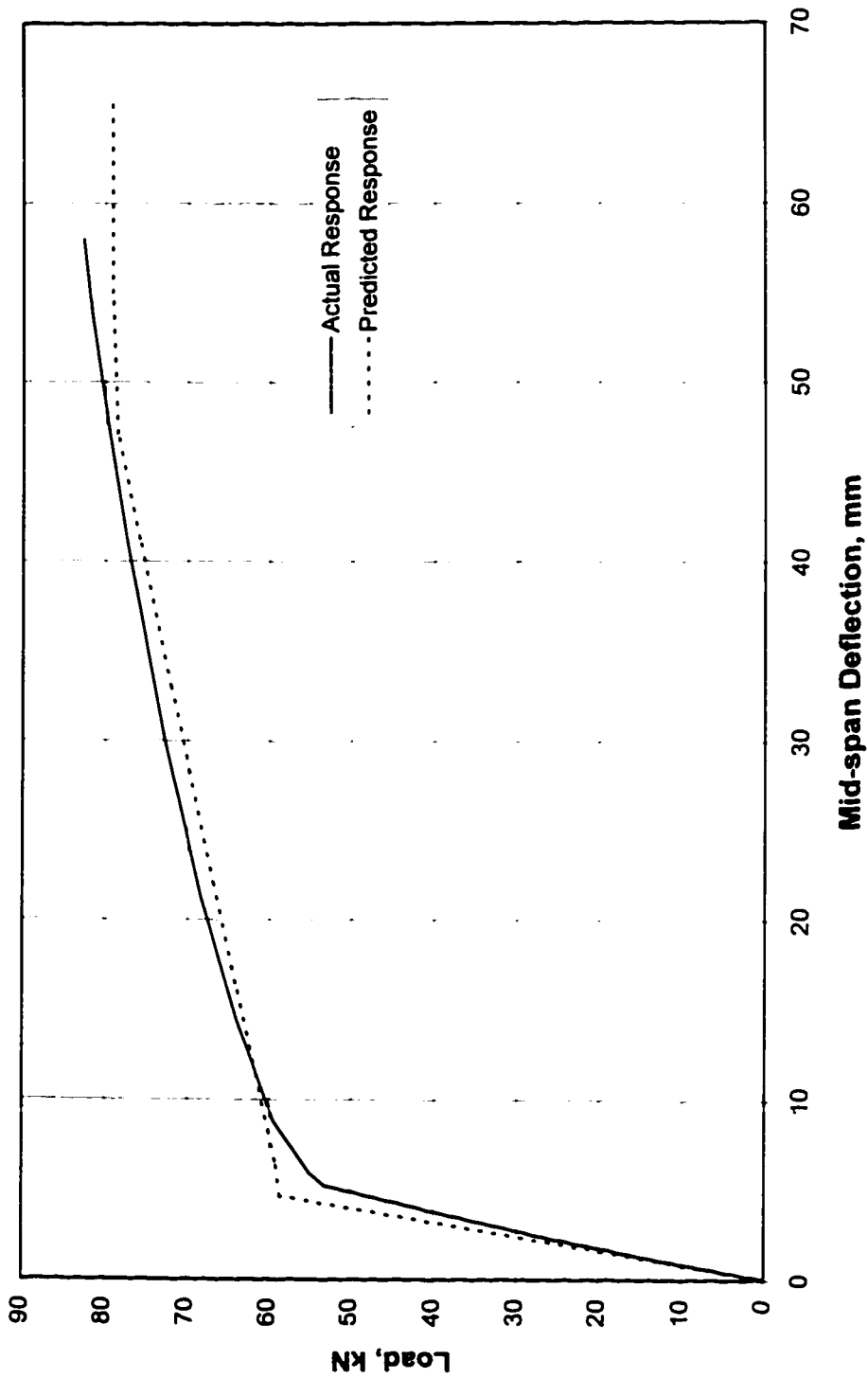
Total Applied Load vs Mid-span Deflection
Beam RH-4 ($\rho_p=0.15\%$, $\rho=0.195\%$)



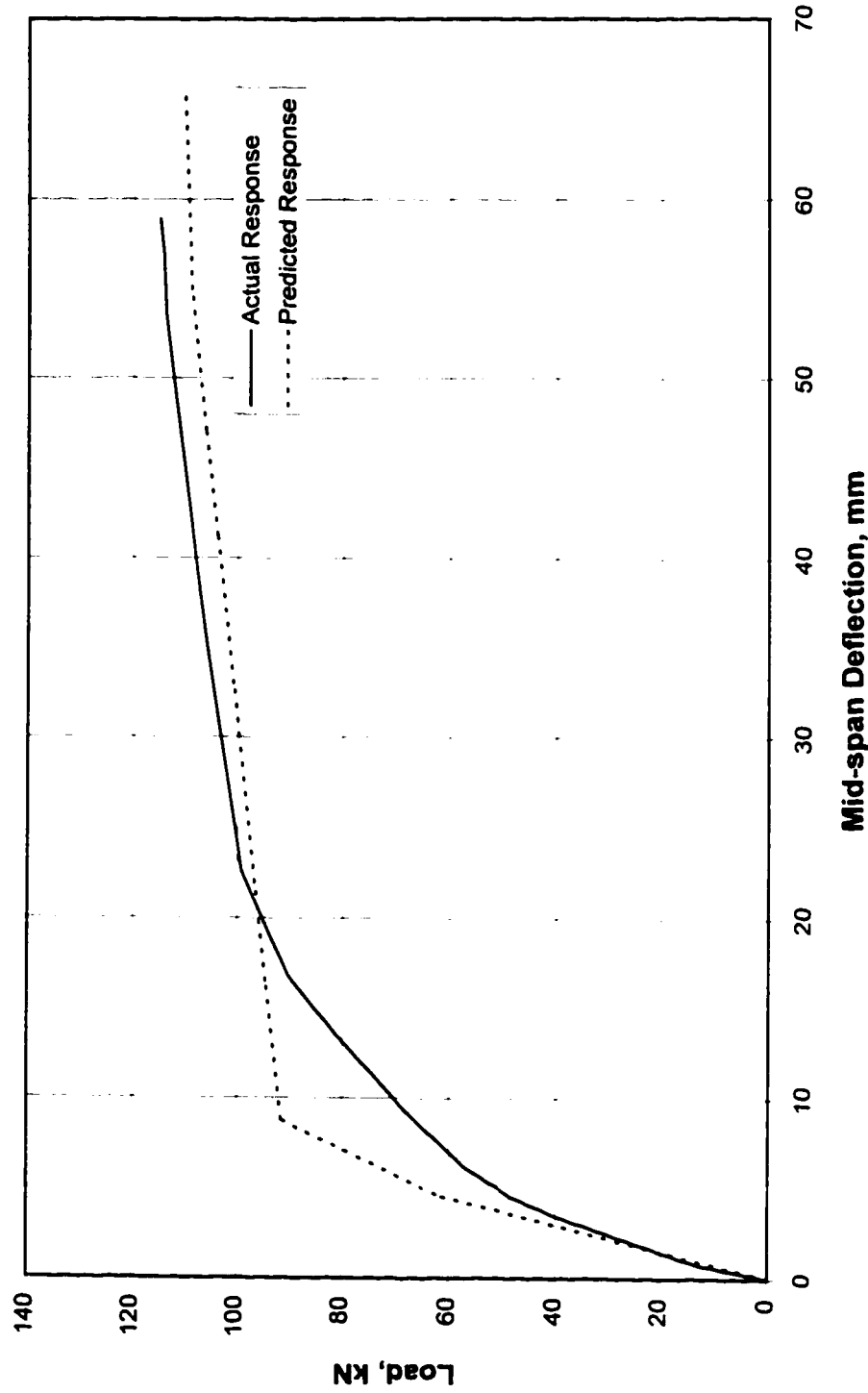
Comparison of Predicted and Actual Load-Deflection Curve
Beam R5 ($\rho_p = 0.0023$) (Ospina-1997)



Comparison of Predicted and Actual Load-Deflection Curve
Beam R1 ($p_p = 0.0042$)(Chouinard-1989)



**Comparison of Predicted and Actual Load-Deflection Curve
Beam R2 ($\rho_p = 0.0042$ & $\rho = 0.0057$) (Chouinard-1989)**



APPENDIX C

CALCULATIONS OF THE LOAD-DEFLECTION RESPONSE FOR BEAM

R-1

a) material and section properties

$$\begin{array}{lll}
 l_e = 3250 \text{ mm} & f_{py} = 1778 \text{ MPa} & l_1 = 850 \text{ mm} \\
 L = 2850 \text{ mm} & A_p = 47.14 \text{ mm}^2 & b = 160 \text{ mm} \\
 f_c = 49.22 \text{ MPa} & A_s = 0 \text{ mm}^2 & d_s = 280 \text{ mm} \\
 f_{pe} = 1111 \text{ MPa} & S = 2646000 \text{ mm}^3 & d_p = 200 \text{ mm} \\
 f_y = 460 \text{ MPa} & E_p = 204000 \text{ MPa} & E_c = 31500 \text{ MPa}
 \end{array}$$

$$\beta_1 = 0.97 - 0.0025 f_c = 0.847$$

$$\alpha_1 = 0.85 - 0.0015 f_c = 0.776$$

b) Determining the load and deflection corresponding to cracking moment.

$$M_{cr} = \left(\frac{P}{A} + \frac{Pe}{S} + 0.55\sqrt{f_c} \right) S$$

$$M_{cr} = \left(\frac{52372}{50400} + \frac{52372 \times 42.5}{2646000} + 0.55\sqrt{49.22} \right) 2646000 \times 10^{-6} = 15.19 \text{ kN.m}$$

$$\text{Load } W = \frac{2M}{l_1} = \frac{2 \times 15.19}{0.85} = 35.37 \text{ kN}$$

$$\delta_{cr} = \frac{Wb}{24E_c I} (3L^2 - 4l_1^2) - P \frac{eL^2}{8E_c I} = 1.89 \text{ mm}$$

Where l_1 is the distance between the reaction and the point load, equal

850 mm

c) Predicting the load-deflection curve using (cy and without Ramberg- Osgood formula

1) choose a value of $\delta/L = 1/1000$ $\Delta = 2.85 \text{ mm}$

2) calculate c_y

$$c_y = \frac{A_p f_{py} + A_s f_y}{\alpha_1 \beta_1 f'_c b} = \frac{47.14 \times 1778 + 0 \times 460}{0.776 \times 0.847 \times 49.22 \times 160} = 16.19 \text{ mm}$$

$$\omega_p = \frac{\rho_p f_{pe}}{f'_c} = \frac{0.00147 \times 1111}{49.22} = 0.033$$

3) calculate the increase tendon stress corresponding to this deflection as follows:

$$\Delta f_p = 4E_p \frac{\delta (d_p - (0.9 + \omega_p)c_y)}{L l_c} = \frac{4 \times 204000}{1000} \left(\frac{200 - 0.933 \times 16.19}{3250} \right) = 52.94 \text{ MPa}$$

4) tendon stress $f_p = f_{pe} + \Delta f_p \leq f_{py} = 1111 + 52.94 = 1163.94 \text{ MPa}$

5) calculate c

$$c = \frac{A_p f_p + A_s f_y}{\alpha_1 \beta_1 f'_c b} = \frac{1163.94 \times 47.14 + 0 \times 460}{0.779 \times 0.847 \times 49.22 \times 160} = 10.6 \text{ mm}$$

6) calculate M

$$M = A_p \times f_p (d_p - \beta_1 c/2) + A_s \times f_y (d - \beta_1 c/2)$$

$$M = 47.14 \times 1163.94 (200 - 0.847 \times 10.6/2) \times 10^{-6} + 0 = 10.73 \text{ MPa}$$

7) Calculate load W

$$W = \frac{2M}{l_i} = \frac{2 \times 10.73}{0.85} = 25.24 \text{ kN}$$

Repeat same steps for different values of deflection

δ/L	Moment [kN.m]	Load [kN]	Deflection [mm]	Load* [kN]
Cracking	15.19	35.73	1.89	31.25
1000	10.73	25.24	2.85	20.76
500	11.20	26.36	5.70	21.88
200	12.63	29.71	14.25	25.23
150	13.41	31.56	19.00	27.08
100	14.98	35.24	28.50	30.76
80	16.14	37.98	35.63	33.50
70	16.19	38.09	40.71	33.61
60	16.19	38.09	47.50	33.61

*dead load were subtracted to compare it with the actual response

c) Prediction using method 2 with c and Ramberg-Osgood formula instead of c_y

- 1) choose a value of $\delta/L = 1/50$
- 2) calculate tendon stress corresponding to this deflection

$$\varepsilon_p = \varepsilon_{p1} + \Delta\varepsilon_p = \frac{f_{pe}}{E} + \frac{4(d_p - c)}{l_c} \frac{\delta}{L}$$

$$\varepsilon_p = \frac{1111}{204000} + \frac{4(200 - 0.933c)}{3250} \frac{1}{50}$$

- 4) tendon stress corresponding to this strain using Ramberg-Osgood equation

$$f_p = 204000 \varepsilon_p \left[0.00205 + \frac{0.9795}{\left[1 + (113 \varepsilon_p)^{30.25} \right]^{(1/30.25)}} \right]$$

which is an equation in terms of c

- 5) solve the previous equation for f_p and c such that

$$\text{Tension force} = \text{Compression force}$$

$$A_s \times f_y + A_p \times f_p = \alpha_1 \beta_1 b c f_c$$

$$0 \times 460 + 47.14 \times f_p = 0.776 \times 0.847 \times 160 \times 49.22 \times c$$

by solving the two equations for f_p and c with EXCEL

$$f_p = 1809 \text{ MPa} \text{ and } c = 16.47 \text{ mm}$$

$$5) \text{ calculate moment } M = A_p \times f_p (d_p - \beta_1 c/2) + A_s \times f_y (d - \beta_1 c/2)$$

$$M = 47.14 \times 1809 (200 - 0.847 \times 16.43/2) \times 10^{-8} + 0 = 16.46 \text{ MPa}$$

7) Calculate load W

$$W = \frac{2M}{l_i} = \frac{2 \times 16.46}{0.85} = 38.73 \text{ kN.}$$

Repeat same steps for different values of deflection

δ/L	Moment [kN.m]	Load [kN]	Deflection [mm]	Load* [kN]
Cracking	15.19	35.73	1.89	31.25
1/1000	10.74	25.28	2.85	20.80
1/500	11.23	26.42	5.70	21.94
1/200	21.17	49.80	14.25	45.32
1/150	13.45	31.64	19.00	27.16
1/100	14.96	35.20	28.50	30.72
1/70	16.27	38.28	40.71	33.80
1/60	16.43	38.67	47.50	34.19
1/50	16.49	38.80	57.00	34.32
1/40	16.52	38.87	71.25	34.39

*dead load were subtracted to compare it with the actual response